DESIGN OF UNBRACED MULTI-STOREY STEEL FRAMES

BY

TAT SENG LOK

A THESIS SUBMITTED TO THE UNIVERSITY OF WARWICK,

ENGLAND, FOR THE DEGREE OF DOCTOR OF PHILOSOPHY

DECEMBER 1984

TO MY WIFE AND CHILDREN -

MONICA, JUSTIN AND REBECCA

SUMMARY

The thesis examines the behaviour and design of unbraced rigid-jointed multi-storey steel frameworks subjected to combined vertical and horizontal loading.

Design charts are presented which enable guidance to be given on whether the serviceability limit on sway or ultimate limit state under combined loading will be critical for the choice of sections in preliminary design. Parametric studies on forty-three multi-storey, multi-bay rectangular frameworks provide the verification of the Merchant-Rankine formula for the design of such frames.

An alternative semi-empirical expression based on the study of the deterioration of overall frame stiffness has been developed. Comparison with the parametric study indicated a significant improvement on the Merchant-Rankine approach to estimate the failure load of frameworks. The expression has then been used as the basis of an approximate optimization procedure for the design of frames to satisfy ultimate strength under combined loading.

An approximate hand method to trace the formation of plastic hinges has been developed. The method is applicable to single bay frames, and has also been extended to multi-bay frames. The latter are transformed into equivalent single bay frames.

A computer analysis program for semi-rigid connections has been presented using the matrix displacement method. The technique is reduced to an analysis of a rigid-jointed framework by repeated modification of the load vector alone. The analysis program has been used to investigate the sway deflection of unbraced frames and the determination of the effective length of braced columns.

CONTENTS

ACKNOWLEDGEMENT

The work described in this thesis was carried out in the Department of Engineering, University of Warwick, under the supervision of Dr. D. Anderson, whose advice and encouragement has been greatly appreciated.

The author wishes to thank Dr. R.H. Wood for his valuable suggestions and criticisms.

Thanks is also due to Mr. E.H. Roberts who supervised the author during a period of study at the Building Research Station, Watford.

The funds for this work was provided by the Science and Engineering Research Council and the Building Research Establishment in the form of a CASE studentship to whom the author is grateful.

DECLARATION

I declare that the research reported in this thesis is my own work. It has never been submitted previously in support for an application for any degree or qualification in other Academic Institution.

NOTATION

A	Cross-sectional area.
$\underline{A}$	Displacement transformation matrix.
a	Modifying factor.
a	Stiffness parameter. (EA/L)
b	Stiffness parameter. ($12EI/L^3$)
C	Total cost of a frame.
C	Constant.
C_f	Force coefficient.
c	Direction cosine.
	Stability function.
D	Constant.
	Connection dimension.
d	Value of the determinant.
	Stiffness parameter. ($-6EI/L^2$)
E	Young's modulus of elasticity.
	Constant.
e	Stiffness parameter. (4EI/L)
F	Total wind shear.
	Constant.
f	Stiffness parameter. (2EI/L)
f_y	Yield stress.
G_k	Characteristic dead load.
H	Horizontal wind load.
h	Storey height.

I_c	Column moment of inertia.
I_b	Beam moment of inertia.
I_1 , I_2	General term for moment of inertia.
i	Joint number.
	Constant.
j	Joint number.
	Constant.
$\underline{K}$	Overall stiffness matrix.
K	Dimensionless factor.
K_c	Stiffness of column. (I_c/h)
K_b	Stiffness of beam. (I_b/L)
k	Member stiffness matrix.
	Nominal stiffness of a member.
k_t	Distribution factor for the top joint.
k_b	Distribution factor for the bottom joint.
Σk_c	Sum of column stiffnesses.
k_1 , k_2 ,	Cost factors.
$\underline{L}$	Load vector.
L	Length of beam.
l	Effective length.
	Connection dimension.
M	General term for bending moment.
M_p	Plastic moment of resistance.
m	Number of bays.
N	Total vertical design load.
	Total number of members.
N_{pl}	Squash load $(A.f_y)$

n	Storey indicator.
	Stability function.
	Ratio of axial load to squash load.
o	Stability function.
P	Total vertical load.
	Column axial load.
P_e	Euler load. $(\pi^2 EI/h^2)$
P_c	Critical load.
Q	Equivalent eccentricity force.
Q_k	Characteristic imposed load.
q	Dynamic wind pressure.
R_b	Beam stiffness.
r	Ratio of bay width to storey height.
r_1 , r_2	Eccentricity parameter.
S	Spring stiffness.
	Section size of member.
S_1 , S_2	Statistical wind load coefficients.
s	Wind shear per bay.
$\bar{s}$	Cladding stiffness.
s_T	Total storey stiffness.
T	Connection dimension.
U	Ratio of restraining beam to column moments.
V	Vertical loading.
W	Total weight.
W_k	Characteristic wind load.
w	Load per unit length.
	Eccentricity parameter.

X	x-direction of overall coordinate system.
$\underline{X}$	Joint displacement vector.
Y	y-direction of overall coordinate system.
Z_p	General term for Plastic modulus.
α_i	Coefficient.
β	Deflection coefficient.
γ_f	Partial safety factor.
δ	Displacement.
ε	Parameter.
η	Distribution factor.
θ	Rigid-joint rotation.
θ'	Semi-rigid connection rotation.
λ	General term for load factor.
λ_e	Elastic failure load.
λ_c	Lowest elastic critical load.
λ_p	Rigid-plastic collapse load.
λ_f	Elastic-plastic failure load.
λ_{mr}	Merchant-Rankine failure load.
λ_{mrw}	Merchant-Rankine-Wood failure load.
λ_{det}	'Deteriorated' critical load.
λ_{expt}	Experimental failure load.
λ_{prop}	Proposed failure load.
λ_{cr}	Initial estimate of elastic critical load.
ν	Uniformly distributed wind load.
	Effective length ratio.
ρ	Ratio of axial load to Euler load.
τ	Eccentricity parameter.

ϕ_1, ϕ_2	Livesley's stability functions.
ψ	Coefficient in proposed expression.
Ω	Parameter.
Δ	Displacement.
	Increment.
	Permissible sway deflection.
Λ	Rate of change of failure load to total weight.

CHAPTER 1

INTRODUCTION

The purpose of methods for structural analysis is to enable an engineer to design safe and economical structures. Despite the complexity and variety of present-day structures, the design techniques in current use are generally sufficient to provide adequate safety. Improving knowledge of structural behaviour is mainly used to increase economy and reduce design time.

Many investigators have examined the various problems of analysis and design, particularly of steel framed buildings. The result is that today's engineer has at his disposal several well-tried methods by which he can design a specific structure. With the aid of computers, there is no doubt that analysis and design methods have become more sophisticated. The tendency has been to develop suitable computational methods to assess more accurately the overall behaviour of the structure from the onset of loading to collapse.

Nowadays, it is not only necessary for an engineer to be able to design a safe structure. He must also make use of available resources in the most economical manner. Optimum design techniques have been developed and used extensively in building structures, in an attempt to reduce cost and increase efficiency. With increasing competition, small savings in material and weight can influence the result of a tender.

This thesis presents some developments in design methods for plane unbraced multi-storey frames. To justify this research, previous papers that are relevant to the research are first discussed.

1.1 Elastic design of steel frameworks

The majority of present-day design methods for analysis and design are based on the early observations of Hooke regarding the properties of an elastic material. Since that time, a number of important contributions incorporating the principles of elasticity have been published. They include such analysis techniques as moment distribution by Cross(1) and the slope-deflection method. The moment distribution method in particular, enables the analysis and design of some redundant frameworks to be carried out with relative ease by hand. Due to the redundancy of the structure, though, the distribution of moments depends on the stiffness of each member in the structure, and initial estimates of member sizes must be made. Strictly, therefore, an iterative procedure is necessary. Further difficulty arises when a highly redundant structure such as a multi-storey unbraced frame has to be analysed.

To avoid such problems, BS.449(1969) permits what is known as the 'simple' method of design. Two approaches are available, for braced and unbraced structural steel frameworks respectively. The former approach assumes the beams to be simply-supported; these members are designed against failure from excessive bending and shear. The columns are designed to carry the reactions from the beams and moments due to eccentricities arising from the nominally

pinned connections. The combined stresses in the columns must not exceed certain permissible stresses. These are dependant on the yield stress of the steel and the susceptibility of the member to buckling. Sway loads are resisted by walls or bracings and transmitted by them to the foundations.

For unbraced frames, rigid joints are required to provide lateral stability. To avoid analysis of a redundant structure, the traditional procedure is to carry out a preliminary design based on the method described above for vertical loads and then to determine the additional forces and moments resulting from wind, using approximate analyses(3). The commonly-used procedure is the 'portal' method, in which the frame is rendered statically determinate by assuming points of contraflexure at mid-length of all members. At this stage of design, the connections are assumed rigid. As the frame is rendered statically-determinate, iteration is avoided. The total member forces under combined loading are obtained by using the principle of superposition.

An important criticism arising from this method is the contradictory assumptions of pinned and rigid joints used to obtain the combined stresses. Such assumptions are incompatible with the actual behaviour of a frame. Although the method has not found favour amongst some engineers, recent arguments have contested that the method provides sound economic construction. Certainly, the 'simple' method is still widely accepted as a suitable method for design.

The aim of the pre-war Steel Structures Research Committee(SSRC) was to evolve a rational method for the design of no-sway frames. It was recognised that the stresses developed in actual building frames have little or no relation to those calculated in the 'simple' method. The 'Recommendations for Design'(4,5) allowed the engineer to make use of the rigidity of the connection when selecting beam sizes, provided certain standard connections were used. This formed the basis for a 'semi-rigid' design method. The column design was based on a single chart. This relates the permissible major end-bending stress, for the worst conditions, to the axial stress and the slenderness ratio. The resulting designs showed reductions of beam sizes, but with corresponding increases in the column sizes due to the additional end moment. Although this is a more rational method for design, engineers failed to adopt this approach. Comparisons between 'simple' and 'semi-rigid' designs indicated no appreciable savings in weight. The design time was also increased due to the inherent complexities of 'semi-rigid' design.

Since the advent of computers, development in linear elastic structural analysis has accelerated. The computer is able to perform lengthy arithmetic and store hugh amounts of data with great speed and accuracy. Therefore, the slope-deflection method is no longer a tedious operation although it involves the solution of simultaneous equations. The matrix displacement method has been developed from this method. It utilizes matrix algebra, thus permitting a systematic procedure for analysis to be programmed. The unknown joint displacements can be obtained by solving the

simultaneous equations using standard Gaussian elimination techniques. This can be expressed as,

$$\underline{X} = \underline{K}^{-1} \underline{L} \qquad (1.1)$$

where $\underline{X}$ and $\underline{L}$ are the vectors of joint displacements and external applied loads respectively and $\underline{K}$ is the overall stiffness matrix.

Computer methods have enabled engineers to extend their design capability to larger and more innovative structures which would not have been possible previously. It must be realised though that early computer programs did not design structures. This still had to be carried out manually. The main function was to provide a rapid analysis of a given frame at a specific loading level, usually working load. Results from this analysis had to be checked to ensure that all stresses and displacements were satisfactory.

Early programs were usually based on small deflection, linear elastic theory, although Livesley(7) developed a program with the option of including secondary effects due to axial load. These are included by using stability functions. These functions depend on the ratio of axial force to the Euler load of a member, and the particular functions used by Livesley have the value unity for zero load. Repeated analysis is necessary because the axial forces in the members are initially unknown. The axial forces from the previous solution are therefore used to calculate the stability functions for the current iteration.

It is instructive at this stage to clarify the general load-deflection behaviour of the different methods of analyses. This is shown in figure (1.1). Curve(1) represents the linear elastic behaviour of an initially undeformed frame. Such behaviour is given by the slope-deflection or moment distribution methods of analysis. However, when the reduction in frame stiffness due to the compressive axial forces is considered, then the non-linear elastic response given by curve(2) is obtained. At any given load factor, λ the difference between this curve and the linear elastic curve(1) is a measure of the reduction in stiffness due to the compressive axial forces at λ . For the non-linear elastic response, the lateral deflection tends to infinity as the applied load approaches a value of λ_e . It is at this load level, known as the elastic failure load, that the frame stiffness becomes zero. This should not be confused with the lowest elastic critical load, λ_c . The elastic critical load is the load at which bifurcation of equilibrium occurs with the frame subjected to the loading shown in figure (1.1 (b)). The distinction is a fine one because λ_e and λ_c are virtually identical in value.

The main disadvantage of early computer programs was the size of the overall stiffness matrix. There are, however, certain special features of the stiffness matrix which can be used to reduce the storage of the actual number of elements. These are symmetry and the existence of many zero sub-matrices outside the irregular half band-width. Jennings(10) suggested a highly economical storage scheme which makes use of these properties. In this approach, only the elements which lie between the first

non-zero one and that on the leading diagonal, inclusive, for each row of the stiffness matrix are stored. Once this is completed, a rapid solution can be obtained by the method due to Jennings(10). This is based on the Gaussian elimination technique for the direct solution of linear simultaneous equations. A rapid solution is obtained as the method operates only on the economically-stored elements. Majid and Anderson(41) adopted such an approach for elastic analysis of very large frames.

The analysis and design methods outlined above do not consider economical distribution of building materials. This is in contrast to optimum design methods which attempt to produce structures which are not only safe but also economical. In such methods, the aim is often to maximise or minimise the value of a specified function (the 'objective function') by means of mathematical programming. Material weight is usually adopted as the objective function because it is easily quantified. Although cost is of more practical importance, it is often difficult to obtain a cost objective function. One such method for minimising the cost of a structure to sway deflection limitation has been proposed by Anderson and Islam(59). This is discussed in Section (1.5). The specific requirements to be satisfied in order for the design to be acceptable are known as constraints. Optimization is usually an iterative procedure because of the non-linearity of the objective function or constraints, and computer methods are often employed.

In optimum elastic design, the constraints are usually limitations on stress and deflection. In a method due to Moses(9), equilibrium equations are obtained, which relate the member

deformations to the bending moments and axial forces. The required constraints are then obtained by joint compatibility. These constraints, together with the function to be optimised are subsequently expanded in a linear first-order Taylor series about an initial trial design. A solution is found by the simplex method of linear programming operating on the linearised equations. The process is repeated in the region of the new design point until no reduction in weight is possible.

The optimum design program of Anderson(24) automatically formulates the design problem for pinned and rigid-jointed frames, with constraints obtained by the matrix force method of structural analysis. The optimization includes both strength and deflection constraints, and produces an optimum solution using piecewise linearisation in conjunction with the simplex algorithm. The method is restricted to relatively small frames due to the excessive demand on computer time and storage.

1.2 Plastic design

It was recognised through the work of the SSRC(4) that continuity in rigid-jointed steel frames results in a higher load-carrying capacity and should offer greater economy than 'simple' design. After extensive research, first at Bristol University and later at Cambridge, the rigid-plastic method was proposed by Baker(11) and Baker et al(12). The rigid-plastic design method is based on the state of the frame at collapse. A factor of safety is introduced by using factored loads in the design calculations. The fundamental conditions of rigid-plastic analysis

which must be satisfied are,

a)Equilibrium - The bending moment distribution must be in equilibrium with the externally applied loads.

b)Yield - The bending moment at any point must not exceed the plastic moment capacity of the member.

c)Mechanism - A state of collapse due to a sufficient number of plastic hinges must be obtained.

Referring to figure (1.1), rigid-plastic analysis is represented by the vertical axis from zero to λ_p . The deflection is assumed to be negligible until λ_p is reached. It is assumed that all members remain fully elastic except at the discrete points at which plastic hinges occur. Once such a hinge has formed, it is assumed that indefinite plastic deformation can take place at that point. The stiffness of the frame reduces when each hinge forms, and becomes zero when the mechanism is complete. Collapse then occurs, as indicated by the horizontal line at λ_p (curve 3) in figure (1.1).

The principal assumptions upon which the rigid-plastic theory is based are,

i)Changes in geometry are neglected.

ii)Buckling out-of-plane and local instability do not occur.

iii)Yielding is confined to the discrete plastic hinges.

iv)Strain hardening is neglected.

Separate column checks are necessary for condition (ii), while conditions (iii) and (iv) lead to reasonably accurate and safe results. Assumption (i), however, can be applied only to simple portal-type structures and structures not exceeding two storeys, where changes in geometry is minimal.

Iffland and Birnstiel(13) conducted an extensive survey of design methods on realistic frames up to a maximum of two storeys. This provides justification for the rigid-plastic method to be used for such frames. This fact is emphasised by the AISC code(14) which allows rigid-plastic design up to two storeys provided the frame can be shown to be sufficiently stiff. However, the effects of changes of geometry especially in tall unbraced slender structures are significant. They cause instability in the structure and cannot be neglected.

Several techniques can be employed to determine the rigid-plastic collapse load. Neal and Symmonds(15) developed a rapid upper bound method of analysis utilising 'combination' of mechanisms. However, the method is usually restricted to relatively small frames due to the excessive number of mechanisms to be investigated, particularly in non-rectangular frames.

Horne(16,17) proposed a direct method of plastic moment distribution which is akin to elastic moment distribution. The distribution of moment is arbitrary and checks are necessary to ensure that the yield condition is not violated.

A design in which the weak-beam, strong-column approach(18) was adopted showed significant savings in the weight of steel when applied to a four storey frame. The unbraced frame was designed for vertical loads only because wind loading was not critical. This is not surprising because for a relatively low unbraced framework, it is usual for the choice of sections to be governed by vertical loading rather than combined loading. The beams were designed plastically for simple beam collapse while the columns were designed elastically(19).

If instability effects in the frame are neglected, it is possible to determine λ_p by a succession of elastic analyses under increments of loading. The formation of plastic hinges is represented by inserting pins into the model of the structure. This method permits the designer to trace the linear elastic-plastic behaviour of the structure up to collapse, and is represented by curve(4) in figure (1.1). If necessary, the reduction in plastic moment capacity due to shear force and axial force can be included. As the above procedure requires iteration, it is not used in present-day manual design.

In one of earliest attempts on optimum plastic design, Heyman(64) applied the method of random steps to simple examples. It was assumed that the weight of a member is proportional to the product of its length and full plastic moment. The minimum weight was obtained by linear programming by considering all the possible rigid-plastic collapse mechanisms of the structure. The method was approximate and was suitable only for simple beams and portals.

Indeed, all the methods described so far require considerable expertise if used in hand calculation, particularly when larger frames are involved. For this reason, computer methods have been developed.

Methods of rigid-plastic analysis and design by computers have been proposed by Livesley(8) and Ridha and Wright(21). Both methods include an element of optimization. In design, Livesley utilised a search technique to proportion the members such that the frame satisfies the conditions (a) to (c) for rigid-plastic collapse. The frame is assumed to be subjected to concentrated loads only and hence there is a fixed number of points at which plastic hinges can occur. The moments at these hinge positions are expressed in terms of the applied loads and 'redundants'. The values of the redundants are determined by satisfying conditions (a) to (c). The unknown terms to be solved are the redundant forces.

The method due to Ridha and Wright makes use of the method of combination of mechanisms to generate a feasible design. To prevent collapse by specific mechanisms, virtual work equations are changed to an inequality. The set of inequalities is obtained by considering all possible mechanisms for the structure. Both computer methods appear to give economical designs but the computing time becomes excessively high for large or non-rectangular frames.

1.3 Elastic-Plastic design

A close approximation to the true behaviour of an unbraced frame is illustrated by curve(5) in figure (1.1). Throughout the range of loading, reduction in frame stiffness occurs due to the compressive axial forces in the columns. In addition, as the load gradually increases, parts of the structure are stressed beyond the elastic limit into the plastic range. In figure (1.1), it is assumed that plasticity is confined to discrete points at which plastic hinges occur. Spread of yield and the beneficial effects of strain hardening under increasing load are assumed to be negligible.

Whenever a hinge forms, the overall stiffness of the frame deteriorates which in turn results in a faster rate of increase of deflection than hitherto. The frame reaches collapse when the stiffness is reduced to zero due to the combined effects of compressive axial forces and plasticity. This is expressed mathematically by the determinant of the overall stiffness matrix becoming singular i.e. non-positive. Further, lateral deflection has to be balanced by a corresponding decrease in load if equilibrium is to be maintained. The peak load, which is lower than the rigid-plastic collapse load, is given by λ_f , and is known as the elastic-plastic failure load. To distinguish the 'collapse load' given by rigid-plastic theory, the 'failure load' is used in the text to indicate 'collapse' given by elastic-plastic theory.

Wood(26) illustrated this behaviour by reference to the 'deteriorated critical load'. This is obtained by studying the

non-linear elastic response [curve(2) in figure (1.1)], but with the plastic hinges replaced by real pins at the corresponding locations. Thus, the effect of progressive formation of plastic hinges in reducing the overall frame stiffness is illustrated by figure (1.2) Each horizontal line corresponds to a value of the 'deteriorated' critical load calculated from the pattern of plastic hinges that are currently present in the frame. At some load level, the 'deteriorated critical load' coincides with or falls below the rising load factor. The frame then has zero or negative stiffness and therefore collapses.

The concept of the 'deteriorated critical load' makes it clear that failure can occur long before a complete mechanism of hinges has formed. Indeed, the positions and load levels at which the plastic hinges form do not necessarily correspond to those obtained from a rigid-plastic analysis. The rigid-plastic collapse load provides an upper bound to the failure load and will be particularly unsafe for unbraced multi-storey frames with relatively high compressive axial loads. The design of such structures is usually governed by overall stability.

Several methods have been proposed with the aim of obtaining safe and economic designs for multi-storey unbraced frames. Heyman(27) adopted a weak-beam, strong-column ultimate load approach by assuming a pattern of plastic hinges which involved collapse in both beams and columns. As a safeguard against instability, it was suggested that up to working load, a frame should remain elastic and deflections should be limited. An approximate method was proposed to calculate the sway deflections.

Stevens(28) proposed a design method based on the collapse state of the structure. Maximum overload deformations are specified and used in formulating virtual work equations corresponding to collapse mechanism in the deformed frame. Member sections are then selected and the resulting design analysed by an approximate method. If the specified deformations are exceeded, then the procedure is repeated until a satisfactory design is obtained.

Holmes and Gandhi(31) and later Holmes and Sinclair-Jones(32) proposed a hand method for modifying the rigid-plastic method with an allowance for frame instability. The effects of compressive axial loads, point of contraflexure not occurring at mid-height of columns and the reduction of member stiffness due to the formation of plastic hinges are incorporated into the design method. Collapse is assumed to occur by beam, combined and sway mechanisms in the upper, middle and lower regions of the frame respectively. In the second paper, modified boundary conditions are included and the design calculations speeded up by reducing the number of iterations to determine the necessary magnification factors. Attempts to further reduce design time by using graphs were proposed. The results of the numerous designs were checked against a non-linear elasto-plastic design program of Majid and Anderson(42).

The methods described above depend on a predetermined pattern of plastic hinges which may not occur and there is no guarantee that deflections are within reasonable limits. When deflections were found excessive, no guidance was suggested to correct beam or column members. Securing elasticity at working load does not necessarily prevent early collapse. The application is restricted

to regular and rectangular frames and considerable experience is needed to design a specific structure.

A manual design method developed at Lehigh University(33) makes use of sway sub-assemblages to obtain lateral deflections under combined loads. The details of these sub-assemblages are also discussed in relation to preliminary design of unbraced frames by computer by Driscoll, Armacost and Hansell(43). Initial member sizes are obtained by considering vertical loads only. The appropriate sway sub-assemblage is then used to formulate equilibrium equations for each storey. These equations enable the bending moments due to the wind forces and the deformed shape to be estimated. Beam-type members are designed so that the combined collapse mechanism would only form when a specified level of combined loading was exceeded. A moment redistribution procedure is used to estimate the bending moments in the columns and sections for these members are then selected. Sway deflections are estimated by a slope-deflection method and the frame redesigned if necessary. Provisions which enable an engineer to obtain a safe design are given when insufficient restraints are provided about both axes of the columns. Collapse before a complete plastic mechanism has formed was recognised but the method involves the extensive use of charts.

Moy(74) proposed the storey stiffness concept for the design of multi-storey frames to satisfy strength and stiffness. The fundamental problem is the determination of the stiffness of each storey. Once this is determined, strength design follows by modifying the member stiffnessess in a sub-assemblage.

Sub-assemblages are used by assuming points of contraflexure at mid-length of all members except for the roof and ground floor region. The storey stiffness is taken as the sum of the stiffnesses of its sub-assemblages. For example, when column axial forces are less than half the Euler load in the intermediate sub-assemblages of an intermediate storey, consisting of 'm' columns, the total storey stiffness at a given load factor is,

$$s_T = \frac{12.E}{h^3} \sum_{i}^{m} \left[\frac{I_c}{1 + U.q} \right] - \frac{\lambda \Sigma P}{h}$$

where E = Young's modulus, I_c = column inertia,

P = column axial load, h = storey height.

U = ratio of beams' restraining moment to column moment taking the value as follows,

a)All storeys except for the top and bottom storey	2
b)Top storey	1
c)Bottom storey (pinned base)	1.5
d)Bottom storey (fixed base)	2 ≤

and $q = \frac{I_c}{h} \left[\frac{1}{\sum_1^n (a_i . I_{bi} / L_{bi})} \right]$

n = number of beams in a joint (≤ 2)

a_i = beam stiffness modifying factor taking the value corresponding to the conditions as follows,

e)Both ends rigid	1
f)Near end rigid, far end pinned	0.5
g)Near end pinned	0

and I_{bi} and L_{bi} are the beam inertia and length respectively.

Sway deflections and bending moments are determined from the

results of the storey stiffness. The effects of plastic hinges on the beam stiffness are accounted by the modifying factor 'a_i'. The column stiffness was assumed to be zero when a plastic hinge develops at the top end. When such hinges are found, reduction in storey stiffness is observed in the above equation. Under increments of load, the total bending moments and sway displacements are obtained by summing the moments and displacements existing at the previous load level and the incremental values. Maximum strength is assumed when any storey stiffness becomes zero or non-positive.

In a method due to Anderson and Islam(72), initial estimates of the secant stiffness of beams are made in a substitute Grinter frame analysis to determine the sway deflections. These displacements are used in conjunction with expressions developed from slope-deflection for the bending moments and joint rotations based on a limited frame. Several cases of plastic hinges occurring at prescribed positions in the limited frame were derived. These hinges usually occur at the leeward end of beams for frames under combined loading. A pattern of plastic hinges is initially assumed. The method proceeds from one limited frame to the next; the results obtained in the former being used in the latter limited frame. When the last limited frame has been analysed, the joint rotations are used to modify the secant stiffness of the beams in the substitute Grinter frame. The procedure is repeated until satisfactory convergence is achieved. Sway deflections are determined with allowance for the reduction in column stiffness due to compressive axial forces. Only one plastic hinge per beam is permitted in the method unless a satisfactory design load level has been attained.

Plastic hinges are not allowed in the columns below the design load level for combined loading.

More recently, Scholz(68) proposed an approximate method which relies on iteration between the rigid-plastic collapse load λ_p and the elastic critical load, λ_c . The basis of the method is the equivalent 'limiting frame'. Each group of 'limiting frames' is identified by a common curve which relates the rigid-plastic collapse load, λ_p and the elastic critical load, λ_c to the failure load, λ_f . Consequently, a family of curves for different groups of frames can be related to the two parameters, λ_c and λ_p. . The technique was compared with the results obtained from a non-linear elasto-plastic computer analysis program. Scholz also conducted model frame tests to further validate the approximate approach. The method may be modified for frames with semi-rigid connections, partially-braced frames, or for frames subjected to vertical loading alone.

The claim of the above methods as suitable for 'manual' application is unjustified, particularly in the design of multi-bay frames. Moy's method requires the determination of each sub-assemblage stiffness, which correspond in number to the number of columns in a storey. The method of Anderson and Islam involves the use of numerous expressions for each limited frame with a plastic hinge, and a separate analysis is required to determine the sway deflections. Furthermore, double hinges on the beams are not permitted, and several iterations are required to locate the position at which plastic hinges form. Scholz's method is significantly more complex due to the need to evaluate 'limiting

frame' parameters, apart from the rigid-plastic collapse load and the elastic critical load. However, they can all be programmed for use on desk-top computers.

Computer methods to assess the elastic-plastic behaviour of a frame are well documented, although necessarily complex. Jennings and Majid(36) used the matrix displacement method of Livesley(7) and developed a general program to analyse elastic-plastic frameworks subject to proportional loading. The method traces the history of plastic hinge formation from initial yielding to ultimate collapse. The formation of each plastic hinge causes a reduction in the frame stiffness. The 'modified' frame is reanalysed with a small increase in load, assuming the plastic hinges to be real pins sustaining the plastic moment capacity of the appropriate members. Failure occurs when the determinant is non-positive.

A similar program developed by Parikh(37) includes the effects of axial shortening and residual stresses by a modified slope-deflection method. Instead of tracing and inserting plastic hinges under increasing load, the plastic hinge pattern itself is taken as the variable. Several examples were shown and verified by comparison with frames designed by other investigators.

Davies(39,40) extended the elastic-plastic analysis method of Jennings and Majid to include hinge reversal and unloading, shakedown effects and the beneficial phenomenon of strain hardening.

Horne and Majid(38) proposed a complete elastic-plastic design method for general plane frames. Commencing with an initial set of sections, repeated cycles of elastic-plastic analysis and redesign are carried out until the frame satisfies the design criteria,

a)Beams must remain elastic at working load.

b)Plastic hinges are not allowed in columns until a certain load factor is reached.

c)A satisfactory collapse load factor must be attained.

In the course of the iterations, material is redistributed to those regions where it is most beneficial, thereby leading to economy in the final design.

The computer methods described above suffer as a result of the large amounts of storage and computer time demanded by repeated cycles of analysis and redesign. Majid and Anderson(41,42) took advantage of the symmetry of the overall stiffness matrix and the compact techniques of storage and solution proposed by Jennings(10), in order to analyse large frames more rapidly. They also proposed measures to ensure that the initial design was realistic, in order to avoid an excessive number of iterations. Even so, the computing time becomes extremely high for large frames. Further, no attempt was made to restrict deflection which may be the critical factor in design.

As a result, Horne and Morris(7) suggested an alternative method of design based on the rigid-plastic theory, but with allowance for changes in geometry of the structure. When such

effects are taken into account in an analysis, the behaviour is represented by the rigid-plastic 'drooping' curve(6) shown in figure (1.1). To preserve equilibrium, the applied loads must be reduced. The method depend on the assumption that the displacement of a point on the 'drooping' rigid-plastic curve(6) intersecting the elastic-plastic failure load can be established. It was assumed that the ratio of the sway deflection at such a point, to the intersection of curve(1) with the rigid-plastic collapse load curve(3) shown in figure (1.1), is some function of the number of storeys in a frame. A factor of 2.5 was proposed based on the study of a number of frames. This factor, which must be multiplied by the rigid-plastic collapse design load, is used as a common multiple applied to the linear elastic working load deflection of the trial frame. Sway deflections are obtained using the 'portal' method described in Section (1.1). In this way, instability effects are included in the design. The method is necessarily approximate due to the assumption of the empirical displacement amplification factor, derived from the studies of regular and rectangular frames only.

1.4 Merchant-Rankine formula

Computer-based methods discussed in the previous Section for the evaluation of the failure load of unbraced multi-storey steel frames are most appropriate. However, if suitable computational facilities and software are not available, then the intuitive Merchant-Rankine formula is an attractive alternative for the design of such frames. Such an approach may also be required to provide a check on a computer method and to satisfy the engineer

who wishes to maintain full control of the design process.

The formula relates the failure loads, denoted here by λ_{mr} to the lowest elastic critical load factor, λ_c and the rigid-plastic collapse load, λ_p ,

$$\frac{1}{\lambda_{mr}} = \frac{1}{\lambda_c} + \frac{1}{\lambda_p} \qquad (1.2)$$

Merchant's proposal is the result of the early work of Rankine(1866) on the failure load of isolated struts. In either of the extreme cases when λ_c or λ_p is large, equation (1.2) tends to the correct estimate of the failure load, namely λ_p or λ_c. In the practical range, frames collapse by an interaction of the effects of plasticity and elastic instability and therefore reasonable approximations to the failure load can be expected from equation (1.2).

Salem(45) conducted a series of experimental tests on a large number of single and two storey, one bay model frames. The bases were fixed and the joints were rigidly-connected by gusset plates. These models were fabricated from hollow tubular sections and in all cases the Merchant-Rankine load provided a safe estimate of the experimental failure load. Extreme care was taken to ensure that the sections used were properly heat-treated to relieve all the induced internal stresses.

Low(48) performed further model tests on three, five and seven storey miniature frames. The frames were fabricated entirely from rectangular sections, with some models subject to vertical loads

only, while others were tested under combined horizontal and vertical loads. For frames with low horizontal loads in relation to the vertical loads, equation (1.2) was very conservative, whilst for those with significant side loads, the formula gave close estimates of the failure load.

Ariaratnam(49) conducted a series of tests on four and six storey, single bay models with rectangular sections while the three and seven storey, single bay frames were fabricated from tubular sections. Attempts to reduce the effects of strain hardening and residual stresses on the specimens by annealing were reported. Ariaratnam demonstrated that the Merchant-Rankine formula can become unsafe when the frame is subject to side loads which are high in relation to the vertical loads. It was recognised, though, that these conditions are unlikely to be experienced in real structures.

In contrast, Adam's investigation(46) suggests that the Merchant-Rankine formula is unsafe when the ratio of the horizontal load to the simultaneously applied vertical load is low. The six storey, single bay frame examined by Adam in the studies was very slender indeed, with the storey height twice the single bay width. For such unusual and slender frames, the Merchant-Rankine failure load overestimated the accurate failure load obtained from a non-linear elasto-plastic analysis by as much as 22%.

It should be noted that all the experimental models and the evidence produced relate to single bay rectangular frames. None of the tests was conducted on a multi-bay or non-rectangular frame,

and no proposals for the evaluation of the two parameters λ_c and λ_p were given to assist practical design using the Merchant-Rankine formula.

Theoretical justification of the Merchant-Rankine formula was provided by Horne(25). It was shown that the expression gives a close approximation of the actual failure load on condition that the rigid-plastic mechanism and the lowest elastic critical mode were the same. Using a similar approach to Horne, Majid(47) showed that the formula can be derived by considering the linear and non-linear elastic behaviour, and the rigid-plastic failure load, as shown in figure (1.3). The basis of the derivation is the geometrical relationship indicated by curve(1) and curve(2).

From geometry, Majid assumed that a particular point (J) on the non-linear curve(2) could be obtained which is numerically equal to the rigid-plastic collapse load factor. From similar triangles, BDE and GOE,

$$\frac{\lambda_p}{\lambda_{mr}} = \frac{\Delta_p + \Delta_c}{\Delta_c} = 1 + \frac{\Delta_p}{\Delta_c} \qquad (1.3)$$

Similarly, by considering AOC and BOD

$$\frac{\Delta_p}{\Delta_c} = \frac{\lambda_p}{\lambda_c} \qquad (1.4)$$

Combining equations (1.3) and (1.4) results in the expression given by equation (1.2). An important development arising from this method is the estimation of the elastic critical load by a similar process utilising the geometrical layout given in figure (1.3).

Examples published by Majid appear to indicate a reasonable estimate of the failure load and the lowest elastic critical load.

An interaction formula similar to equation (1.2) was recommended by Lu(57),

$$\lambda_{LU} = \frac{3.4\lambda_c}{1 + 3\frac{\lambda_c}{\lambda_u}} \qquad (1.5)$$

where λ_c has been defined previously and λ_u is the ultimate load corresponding to failure of the columns with the frame prevented from swaying. This value is obtained from tables which relate the axial force to the larger column end-moment and the column slenderness ratio. The verification of the formula rests on extensive tests on models and full-scale pinned base portals. The design using such an expression is, however, suggested for frames not exceeding three storeys. Further, equation (1.5) does not consider the effects of horizontal loading and is therefore restricted to structures designed to support heavy vertical loads only.

In Section (1.2), mention was made of the recent extensive review of available design methods carried out by Iffland and Birnstiel(13). As a result of the interest expressed by the above authors in the Merchant-Rankine formula, further design studies were conducted. These consisted of 34 representative two storey, two bay frames with a wide range of parameters. The frames examined have such features as,

a)Fixed base,

b)Pinned base,

c)Symmetrical configuration (16 number in all),

d)Unsymmetrical configuration (18 number in all),

e)Vertical load acting alone,

f)High and low ratios of vertical to horizontal loading,

g)Horizontal loads applied from any of the two directions for the unsymmetrical frames,

h)Erection tolerance for symmetrical frames.

The results of the study showed that the Merchant-Rankine formula underestimated the failure loads obtained from a non-linear elasto-plastic analysis program in all the symmetrical frames. Unsafe cases arose in 4 out of the 18 unsymmetrical frames; three frames by 5% and only one by 10%. Based on the limited numerical studies above, the Merchant-Rankine formula has been proposed by Iffland and Birnstiel for inclusion in a revised American Specification.

Wood(50) recognised the generally conservative results given by the Merchant-Rankine formula for bare frames and has suggested a modified version, to account for the beneficial effects of strain hardening and minimal composite action,

$$\frac{1}{\lambda_{mrw}} = \frac{1}{\lambda_c} + \frac{0.9}{\lambda_p} \qquad (1.6)$$

The expression has since been included in European Recommendations(54) and in a draft British Code of Practice(55). In these documents, frames can be designed by equation (1.6) if $4 \leq \lambda_c/\lambda_p < 10$. For $\lambda_c/\lambda_p \geq 10$, the failure load is taken as λ_p.

whilst if $\lambda_c/\lambda_p < 4$, a more accurate method than equation (1.6) should be used. Plastic hinges developing in the columns below the specified load level applicable to frames under combined loading are not permitted. An exception is the comprehensive combined collapse mechanism where plastic hinges are allowed only at the base.

Early attempts to design frames using the Merchant-Rankine formula were somewhat hindered because of the difficulty involved in the calculation of the elastic critical load. Several approximate methods have since been published. Horne(51) and Bolton(52) adopt similar approaches. It is necessary in both these methods to obtain values of linear elastic deflection. The minimum storey deflection is used to determine the lowest elastic critical load. However, Bolton's method is potentially dangerous as it considers frame instability as a local phenomenon. The calculation is based on a single joint from a 'no-shear' frame and therefore the lowest elastic critical load can be missed, while Horne's approach will be conservative by no more than 20%.

Wood(50) introduced the method of stiffness distribution based on an equivalent substitute Grinter frame, to calculate λ_c . The basis of the Grinter frame is that for horizontal loads acting on the real frame, the rotations of all the joints at any level are approximately equal, and that each beam restrains a column at both ends. Beams are therefore bent into approximate double-curvature. Charts have been published which enables the engineer to speed up the design process with little loss in accuracy.

Williams(53) proposed a simplified design procedure which takes full account of λ_c without actually calculating λ_c in a trial design. It was shown by Williams that in a design situation (as opposed to an analysis), a lower bound on λ_c is all that is required to check the adequacy of the trial frame. Due to the condition that must be observed for use of the modified Merchant-Rankine formula, designs are permitted if the following are satisfied,

$$\lambda_c \geq 4\,\lambda_p$$
$$\lambda_{mrw} \leq \lambda_p \leq 1.15\,\lambda_{mrw} \qquad (1.7)$$

The factor of 1.15 is obtained by substituting the ratio $\lambda_c/\lambda_p=4$ into equation (1.6). With λ_{mrw} as the required load factor for collapse and λ_p being the rigid-plastic collapse load for the trial design, equation (1.6) can be rearranged to express λ_c in terms of λ_{mrw} and λ_p . A trial design is therefore adequate providing a lower bound value of the elastic critical load exceeds the minimum required value.

Williams suggested modifying the substitute Grinter frame into 'cells' to obtain a lower bound on λ_c. Each 'cell' is divided longitudinally at the beam level except at the top and the ground beam (if any). The beam stiffness is proportioned in the form of $\alpha_i R_{bi}$ and $(1-\alpha_i).R_{bi}$, where α_i is any coefficient between 0 and 1 and R_{bi} is the stiffness of the beam. The two portions of each beam are rigidly connected to a common roller at the far ends. By this arrangement, each 'cell' buckles independantly and therefore has its own critical load. The elastic critical load for

each 'cell' may be obtained very rapidly using the critical load charts due to Wood(50). If the lower bound value of λ_c is inadequate, then the engineer may be able to avoid altering his design simply by refining his choice of α values to obtain a closer lower bound value of λ_c for the actual frame.

Williams's design procedure in which only a lower bound may be required for λ_c has much merit as long as it is λ_c, rather than λ_p that is the more difficult to calculate. The evaluation of the rigid-plastic collapse load has been discussed above, in particular, the method of combining mechanisms due to Neal and Symmonds(15). In addition, standard textbooks(12,17,22) provide alternative procedures for calculating λ_p.

When one tries to calculate the rigid-plastic collapse load exactly, it is found that for relatively large frames, it is by no means an easy task. For this reason, it is convenient to alter Williams's procedure to avoid the need to calculate an exact value of λ_p. Using equation (1.6) under factored load conditions, the required value of λ_{mrw} is unity and the expression becomes,

$$\lambda_p = 0.9 \left[1 - 1/\lambda_c \right] \qquad (1.8)$$

where λ_p is now the MINIMUM required value of the load level for rigid-plastic collapse.

The designer has now to prove that the minimum value of the rigid-plastic collapse load factor is at least reached. A lower bound equilibrium approach can therefore be used, thus avoiding the

need for an 'exact' value of λ_p . This contrasts with the original proposal of Williams(53) in which the rigid-plastic collapse load was initially specified. As a result of the developments described above, the lowest elastic critical load can be obtained accurately and swiftly for a trial design.

The procedure given by equation (1.8) is therefore usually more convenient. This form of equation is particularly useful for tall unbraced frames, in which lateral stiffness, rather than strength is often the dominant criterion in design. If such frames are designed first to have adequate stiffness, then it will only be necessary to demonstrate that the factored load level for the ultimate limit state can at least be attained.

1.5 Deflection control

Relatively high load factors apply at the ultimate limit state, and these prevent significant plasticity at the working load. As a result, deflection calculations are usually based on elastic behaviour. While beam deflections can readily be determined by analysis of a limited frame(35), the problem has been horizontal deflection in multi-storey frames.

Design Recommendations(54,55) forbid excessive horizontal movement. The reasons for such action are to avoid discomfort and alarm to occupants, and cracking of plaster, glazing and end-wall panels. Restriction of sway also limits secondary 'P- Δ' effects which cause instability of the structure (28,29).

While the British code BS.449(1969) gives no recommendation for limiting deflection in multi-storey frames, recent design recommendations(54,55) have settled on a value of 1/300th of each storey height based on calculations of the bare frame.

Design studies on multi-storey frames have been carried out by Batten(34). The studies showed the sensitivity of frame weight to alternative design methods and forms of construction. The following parameters were also varied,

a)Building height,

b)Storey height,

c)Bay widths,

d)Location of braced bay,

e)Column splices,

f)Ratio of vertical to horizontal loading,

g)Deflection constraints,

h)Use of beam sections for columns and vice-versa.

Results from the studies provide guidance to designers on the choice of methods for designing a specific structure.

A number of approximate methods for the calculation of sway deflections are available for medium-rise frames. These methods are suitable for hand calculation, while some enable direct design to specified limits. Moy(58) proposed a satisfactory procedure which enables the engineer to alter the sections in a trial design if the need arose. This has the advantage that it provides guidance on what member section changes will be required if deflections in a

trial design are found to be excessive.

When the control of sway is likely to govern the choice of sections in a design, then the method of Anderson and Islam(59) is more appropriate. This direct method of design enables suitable sections to be selected to satisfy limits on sway. The method makes use of equations derived by considering sub-assemblages for the top, intermediate and lower regions of the frame. These sub-assemblages are shown for a 'regular' multi-storey frame in figure (1.4). The design equations were based on the following assumptions,

i) Vertical loads have a negligible effect on the horizontal displacements.

ii) A point of contraflexure occurs at the mid-height of each column, except in the bottom storey, and at the mid-length of each beam.

iii) The total horizontal shear is divided between the bays in proportion to their relative widths.

These assumptions render a frame statically determinate, except in the bottom storey, and enables each storey to be considered in isolation. The sub-assemblages, therefore, consists of an upper beam, lower beam and an internal column. Equations relating the sway deflection over a storey height to the inertias of the column and surrounding beams were then derived. Using equilibrium and compatibility, the inertias of the beams and external columns were expressed in terms of the inertia of an internal column. The need to select trial values was avoided by introducing an element of

optimization into the design. The cost function for a typical intermediate storey is assumed to be in the form,

$$C = \frac{m.r.h}{2}(k_1 I_1 + k_2 I_2) + (m-1)h.k_3 I_3 + 2h.k_4 I_4 \qquad (1.9)$$

where m = number of bays,

r = ratio of bay width to storey height,

h = storey height,

I_1, I_2, I_3 and I_4 are the inertias for the upper beam, lower beam, internal column and external column respectively.

k_1, k_2, k_3 and k_4 are the cost factors corresponding to I_1, I_2, I_3 and I_4 .

Once the optimum value for the inertia of an internal column is calculated, the inertias for other members are obtained by back-substitution. The weakness of the method lies in the difficulty of achieving in practice the ideal relationships between the inertias of the internal columns and those of the other members which are assumed in the derivation of the method. Selected inertias are often higher than those calculated because of the discontinuous range of available sections.

The charts of Wood and Roberts(60) are most convenient as a check for sway of a trial design. The analysis was based on a limited substitute frame which represents an individual storey of a multi-storey frame. This consists of a column with beams attached at the top and bottom ends. The far end of the lower beam was rigidly fixed while the far end of the top beam was fixed against rotation but free to sway. The single storey substitute frame is

shown in figure (1.5). Using the method of slope-deflection, a non-dimensional expression relating the sway angle to the joint stiffnesses was then obtained, given by,

$$\varphi = \frac{\Delta/h}{F.h/12E.K_c} = M.\left[1 + \frac{3(k_b + k_t - k_b.k_t)}{4-3k_b-3k_t+2k_b.k_t + \bar{s}(1-k_b.k_t/4)/3}\right]$$

where $k_t = \frac{K_c}{K_c + K_{bt}}$, $k_b = \frac{K_c}{K_c + K_{bb}}$

$K_c = I_c/h$, $K_{bt} = I_{bt}/L_t$, $K_{bb} = I_{bb}/L_b$

φ = sway angle, Δ/h,

F = total wind shear,

$\bar{s}$ = cladding stiffness,

$= \frac{S.h^2}{E.K_c}$,

S = spring stiffness (force per unit displacement),

E = Young's modulus of elasticity,

Δ = sway deflection,

M = $12/(12 + \bar{s})$,

L = length of beam,

h = height of column,

I_b = second moment of area of the attached beam,

and the suffices 't' and 'b' refers to the top and bottom beams attached to the column respectively.

To assist designers, Wood and Roberts presented their analysis in the form of charts. The charts are constructed by selecting values for φ , $\bar{s}$ and k_t and solving the above equation for k_b. For unclad and unbraced frames, $\bar{s}$ = 0. No guidance was given, however, to the

preferred choice of beam or column sections to be replaced when sway limits are unsatisfactory.

In the above methods, differential axial shortening of columns which can lead to significant additional sway is neglected. Such effects have been considered in multi-storey frames by Moy(62). He considered a frame subject to uniform horizontal loading with the floors assumed to be rigid and the cross-sections of columns varying linearly from the roof to the base level. At any level, 'z' measured above the foundation, the sway deflection is given by,

$$\delta_z = \frac{\nu}{2E.T_1}\left[B_z + \frac{C_z^2}{2} + \frac{D_z^3}{3} - \frac{E}{F}.\ln\left(1 - \frac{G_z}{H}\right)\right]$$

The expression was simplified in the form of a chart relating all the terms in the square bracket in the equation above to storey height measured from the ground. Each storey is considered at a time by selecting the corresponding coordinate at the top and bottom end of a column measured from the base. From these two values of 'z', the deflection coefficients βz are obtained on the appropriate curve on the chart. These two values of βz are substituted into the following equation to give δ_{z1} and δ_{z2}, where generally,

$$\delta_z = \frac{\nu H^4}{E.T_1} \cdot \beta z$$

where ν = uniformly distributed wind load,

H = total height of frame,

E = Young's modulus of elasticity,

$T_1 = \Sigma A_c.d^2$ (at the lower column level),

A_c = cross-sectional area of column,

d = distance from the column under consideration to the centre of gravity of the columns at roof level.

The storey deflection due to axial shortening is the difference between these two values of δ_{z1} and δ_{z2}.

When axial shortening is significant, then computer-based methods are most appropriate. Majid and Elliott(6) proposed a method for limiting deflection in frames using non-linear programming techniques. Design charts for limiting deflection of single bay fixed-base portal frames were shown. Their general computer method, however, was restrictive because of the excessive computer time and storage space required for the solution.

More recently, Majid and Okdeh(63) proposed a 'deflection profile' technique for the design of multi-storey unbraced frames. To limit deflection, an initial value is specified. The method assumes a 'linear deflection profile' corresponding to the specified sway limit of the frame. This is expressed by a deflection function of the form,

$$x = a_1 + a_2.Y + a_3.Y^i$$

The constants a_1 to a_3 are obtained from the boundary conditions defining the geometry of the frame. The deflection, x, is the horizontal sway corresponding to the position Y and the variable

'i' is the 'economy power'. As the value of 'i' tends to a large value, the deflection profile also tends to be linear. The iterative procedure reduces the frame stiffness to satisfy the deflection limit. It follows that 'i' takes a different value for each frame. Initial design procedures are identical to that proposed by Majid and Anderson(42) described in Section (1.3).

A method of incorporating the effects of compressive axial forces in reducing the overall frame stiffness for direct design to deflection limitation has been suggested by Anderson and Salter(61). The method utilises the matrix displacement method and linear programming techniques for redesign to obtain a feasible solution. Examples were shown and verified by comparing the solution of frames designed by other methods.

1.6 Semi-rigid connections

In many locations, climatic conditions, safety regulations or shortage of skilled labour limit the scope for site welding, and bolted connections are therefore preferred. Bolted connections reduce labour costs because the parts can be prepared in the workshop and transported easily and provide flexibility for on-site erection procedures. All the analysis and design methods described so far, with the exception of that proposed by the SSRC, assume such joints to be either pinned or fully-rigid.

Fully-rigid joints are assumed to provide full rotational continuity between connecting members. Pinned joints are assumed to act as shear pins. This is done despite the fact that experimental

investigations of bolted connections show that 'fully-rigid' connections have some flexibility while 'pinned' connections have some rotational stiffness. Fully-rigid or pinned connections are idealisations which enable engineers to design structures using existing theories and knowledge.

When joint flexibility is taken into account in analysis, redistribution of member forces throughout the structure occurs. Furthermore, in an unbraced frame, sway deflections that were obtained previously by assuming rigid joints, can now become unacceptable. For bolted connections, the most useful characteristic to define is the moment-rotation stiffness behaviour.

A method incorporating semi-rigid end restraint for the analysis and design of beams was proposed by Batho and Rowan(75), which formed the basis of design for 'semi-rigid' frames proposed by the SSRC(5). This was described in Section (1.1). As it is usual in steel structures for the columns to be continuous, the semi-rigid connections were taken to occur at the ends of beams only. End-restraint moments in the beams were determined for certain types of connections and presented as charts in terms of the length and total depth of the beam. The connection type varied from relatively flexible top and seat angle cleats to stiff T-stub connectors. The approach is applicable to simple beams and to low-rise frames that are significantly stiff. The treatment of semi-rigid connections in unbraced frames was examined by Baker(4). The slope-deflection equations were modified by assuming a linear relationship between the relative rotation of the member at a

connection and the bending moment. The method was unsuitable for manual application except for simple frames. For highly redundant structures, therefore, computer methods are necessary.

Monforton and Wu(66) devised a computer program based on the matrix stiffness method for the analysis of frames with semi-rigid end-restraint. A semi-rigid connection could be located at any position in the frame. A linear moment-rotation relationship was assumed and fixed-end coefficients derived. The fixed-end moments were then modified in terms of these coefficients. A number of modified fixed-end moments for different loading cases were given.

Non-linear standardised moment-rotation expressions for several types of connections have been proposed by Frye and Morris(69). These relationships have been incorporated into a matrix stiffness computer program. The standardised moment-rotation expressions were based on experimental and theoretical studies on standard connections. These expressions are applicable to a given type of connection with any variation of the size parameters. The standardised expression was assumed to be represented by a single function for all connections of a given type by,

$$\theta' = \sum_{i=1}^{\infty} C_i . (KM)^i$$

where θ' = rotational deformation of connection,

C = constant,

K = dimensionless factor whose value depends on the size parameters for a particular connection,

M = moment applied to the connection.

The factor 'K' was obtained experimentally and only odd powers in 'i' were considered for the first three terms in the above expression. Generally, the moment-rotation characteristic for each type of connection is of the form,

$$\theta' = a.(KM) + b.(KM)^3 + c.(KM)^5$$

where 'a', 'b' and 'c' are coefficients applicable to a given type of connection.

The effects of semi-rigid connections on sway deflection and redistribution of member forces were shown by a number of examples. As much as 20% additional sway was reported in comparison with the assumed rigid joint analysis.

Full scale experiments to obtain suitable behaviour characteristics are time-consuming and rather expensive. As a result, Krishnamurty et al(66) developed a three-dimensional finite element computer model for the numerical solution of moment-rotation characteristics. A number of types of connections, mainly end-plate connections, have been successfully and accurately modelled.

More recently, the influence of standard semi-rigid connections on the strength and behaviour of steel columns was investigated by Jones et al(67). The strength of no-sway columns including the effects of residual stress, spread of yield, initial curvature, and non-linear end restraints was illustrated. Comparison with a method of column design(50) suggest possible

savings when end restraints are properly taken into account. Experimental evidence was given for three types of end restraints but no recommendations were proposed for rapid assessment of the column strength.

1.7 The scope for the present work

To reduce time spent on calculations, it is helpful to know, at an early stage, whether ultimate strength or the serviceability limit on sway will dominate the choice of sections in the design of multi-storey unbraced steel frames. Batten(34) has reported that strength under combined loading will govern the design only if the deflection limit is relaxed to 1/250th of the total structure height. This contrasts with Design Recommendations(54,55) where sway deflections are restricted to each storey height. However, the critical limit will in fact be influenced by the configuration of the frame and the relative values of vertical to horizontal load and of bay width to storey height.

For multi-storey unbraced frames, combined loading is usually the critical load case in design but little in the way of definite guidance is available to designers. Part of the work described in Chapter (2) attempts to distinguish at an early stage whether the serviceability limit on sway or ultimate strength governs the design under this loading case.

When deflection is found to be the governing criterion, then a check is all that is required for ultimate strength. Rapid methods for the calculation of the elastic critical load are available,

thus avoiding the need for an 'exact' value of the rigid-plastic collapse load. Such an approach makes the Merchant-Rankine formula attractive.

The Merchant-Rankine formula and the modified version due to Wood are subject to criticisms because they are empirical and intuitive. Further, Wood's version is strictly applicable to clad frames. Recent Design Recommendations(54,55) permit the use of the modified Merchant-Rankine formula as an alternative to accurate computer methods for elastic-plastic analysis and design. This is despite the fact that the basis of the validation of the Merchant-Rankine formula rests on model frame tests, or theoretical analyses on frames consisting of a few members only. This apparent weakness was also recognised in an extensive survey(13) and so further comparisons with computer analyses were made. However, these were regarded as a pilot study and were restricted to frames that were only two bays in width and two storeys high.

Recently, Adam(46) demonstrated, by means of an unrealistic slender frame, that the Merchant-Rankine formula is unsafe, but because of the interest now being shown in the Merchant-Rankine formula it is desirable that a study be made of its accuracy when applied to realistic building frames.

One of the restrictions that must be observed when using the modified Merchant-Rankine approach is that frames must show a combined rigid-plastic collapse, and other restrictions are also imposed by the Design Recommendations. The accuracy of the formula and the need for the restrictions are investigated in a parametric

design study of medium-rise unbraced bare frames in the remaining part of Chapter (2). Combinations of realistic horizontal and vertical loads are adopted. The study provides an opportunity to verify the Merchant-Rankine formula as a sound basis for the design of such frames. Examples of designs are shown.

Chapter (3) attempts to seek an alternative form of expression which provides closer agreement with non-linear elasto-plastic computer results. A suitable semi-empirical expression is presented from the study of the 'deterioration' of critical loads of unbraced frames. The accuracy of the expression is also compared with published experimental results and a detailed design example is provided. The estimated results are compared with the accurate elasto-plastic analysis program of Majid and Anderson(41).

Studies reported in Chapter (2) show that frames designed to satisfactory sway limits cannot be guaranteed to satisfy overall ultimate strength. Therefore, the need arises for a method to satisfy adequate strength under combined loading. This should provide information to the designer concerning the required changes of member sections to strengthen a trial design.

An optimum design method is proposed in Chapter (4) which makes use of the new expression developed in Chapter (3). It has been mentioned that there is difficulty in determining an 'exact' value of the rigid-plastic collapse load, but studies in Chapter (2) have revealed a number of likely mechanisms under combined loading. As a result, use is made of a finite number of rigid-plastic collapse mechanisms as a basis for an approximate

optimization design procedure. This contrasts with accurate elasto-plastic analysis, where plastic hinges are traced until collapse occurs, which tends to be lengthy with high consumption of computing time.

The proposed procedure relates the change in the approximate failure load to increase in the overall weight in a particular cycle of iteration. Examples of approximate and accurate rigid-plastic analyses are compared for several rectangular and non-rectangular frames.

The elastic-plastic design method due to Anderson and Islam discussed in Section (1.3) is not appropriate as a manual method, but was found to be convenient on desk-top computers. The method assumes an incomplete pattern of plastic hinges for the design of multi-storey unbraced frames in recognition of the drastic effects of frame instability. Comparison with the design studies reported in Chapter (2) shows that the restriction of plastic hinges to the leeward ends of beams is unnecessarily restrictive. Plastic hinges tend to occur at mid-span as well before collapse occurs.

For single storey buildings, it is recognised that the use of valley beams results in some frames being subjected at the eaves to high concentrated forces due to vertical and wind loading. The design of such frames by rigid-plastic theory may be unsafe due to overall instability.

An approximate semi-analytical method to trace the development of plastic hinges is described in Chapter (5). The proposal adopts

an incremental step-by-step method of analysis. Suitable expressions are derived using the slope-deflection equations to evaluate the load level at which these hinges form. An appropriate failure criterion based on a limited number of plastic hinges occurring on two consecutive floor beams is proposed for multi-storey frames. It is shown that a multi-bay frame can be treated as an equivalent single bay frame, and the procedure is equally applicable to such structures. Initially, the problem is demonstrated for a simple pinned base portal in which the inadequacies of the plastic theory are illustrated for certain types of single storey frames. Several design examples are shown both for simple pinned base portals and multi-storey frames.

Beam-column connections are usually assumed as 'fully-rigid' or 'pinned'. However neither is true of bolted connections. Lateral stiffness of unbraced frames depends on joint rigidity, and excessive sway deflection may occur due to inaccurate assumptions of connection behaviour. Chapter (6) proposes a non-linear elastic computer program for the analysis of frames with any combination of pinned, rigid or semi-rigid connections. Non-linear moment-rotation characteristics for any types of connection may be incorporated. The effects of such connections on the sway deflection of frames are shown. The influence of semi-rigid connections on the strength of no-sway columns is examined and comparisons are made with commonly-assumed values for effective length.

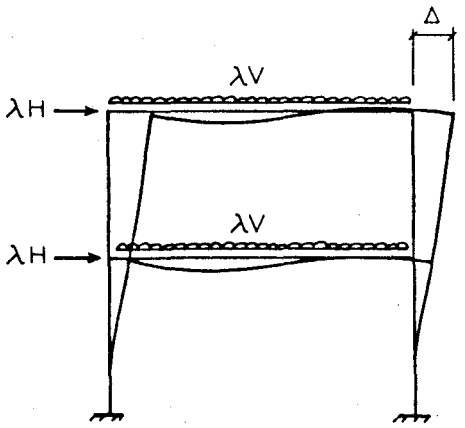

(a) Two storey frame

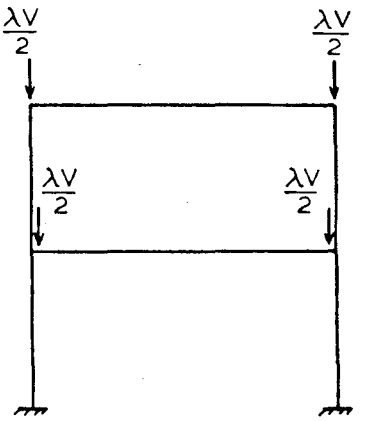

(b) Loading for bifurcation of equilibrium

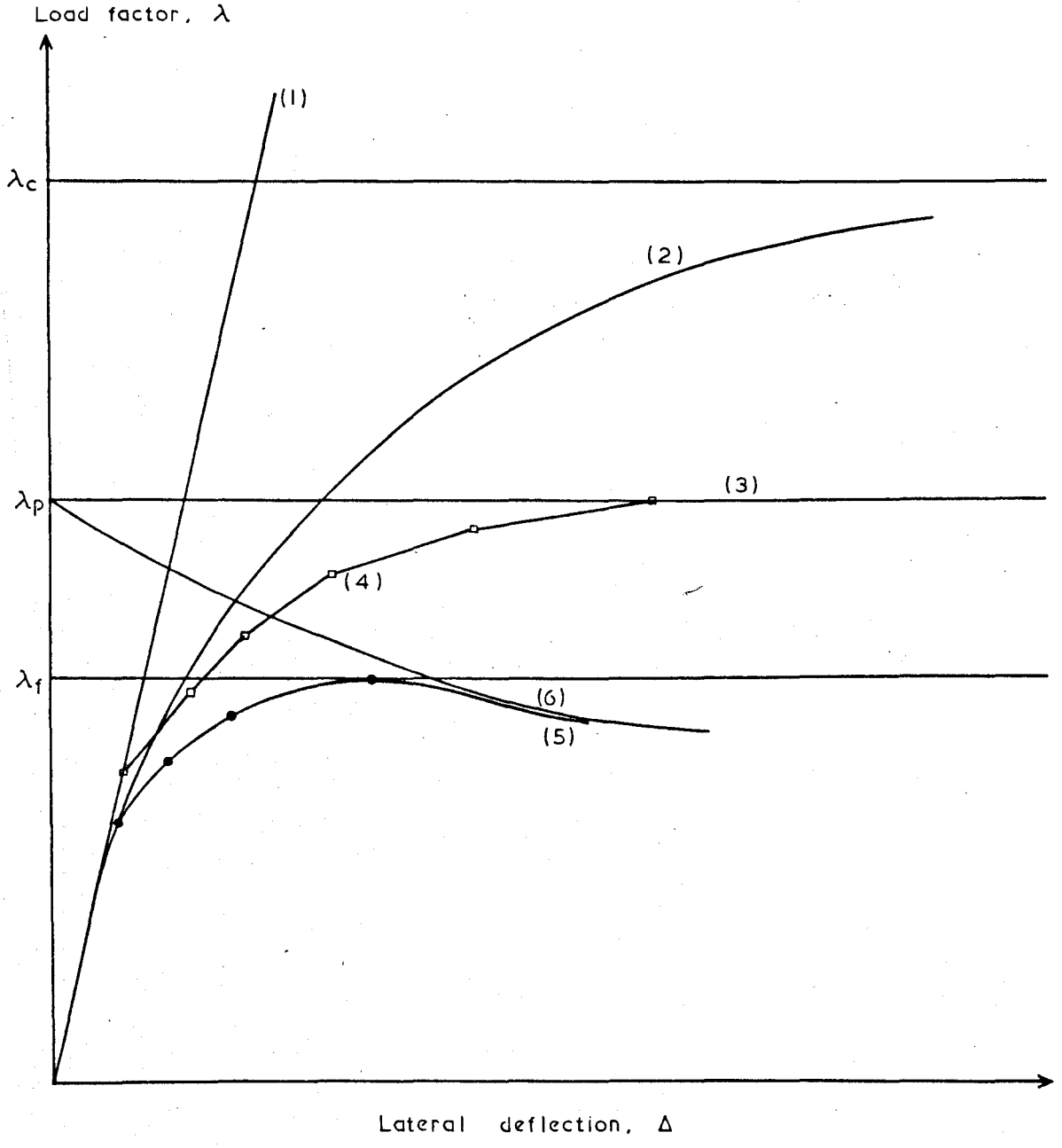

FIG. 1.1 LOAD – DISPLACEMENT BEHAVIOUR

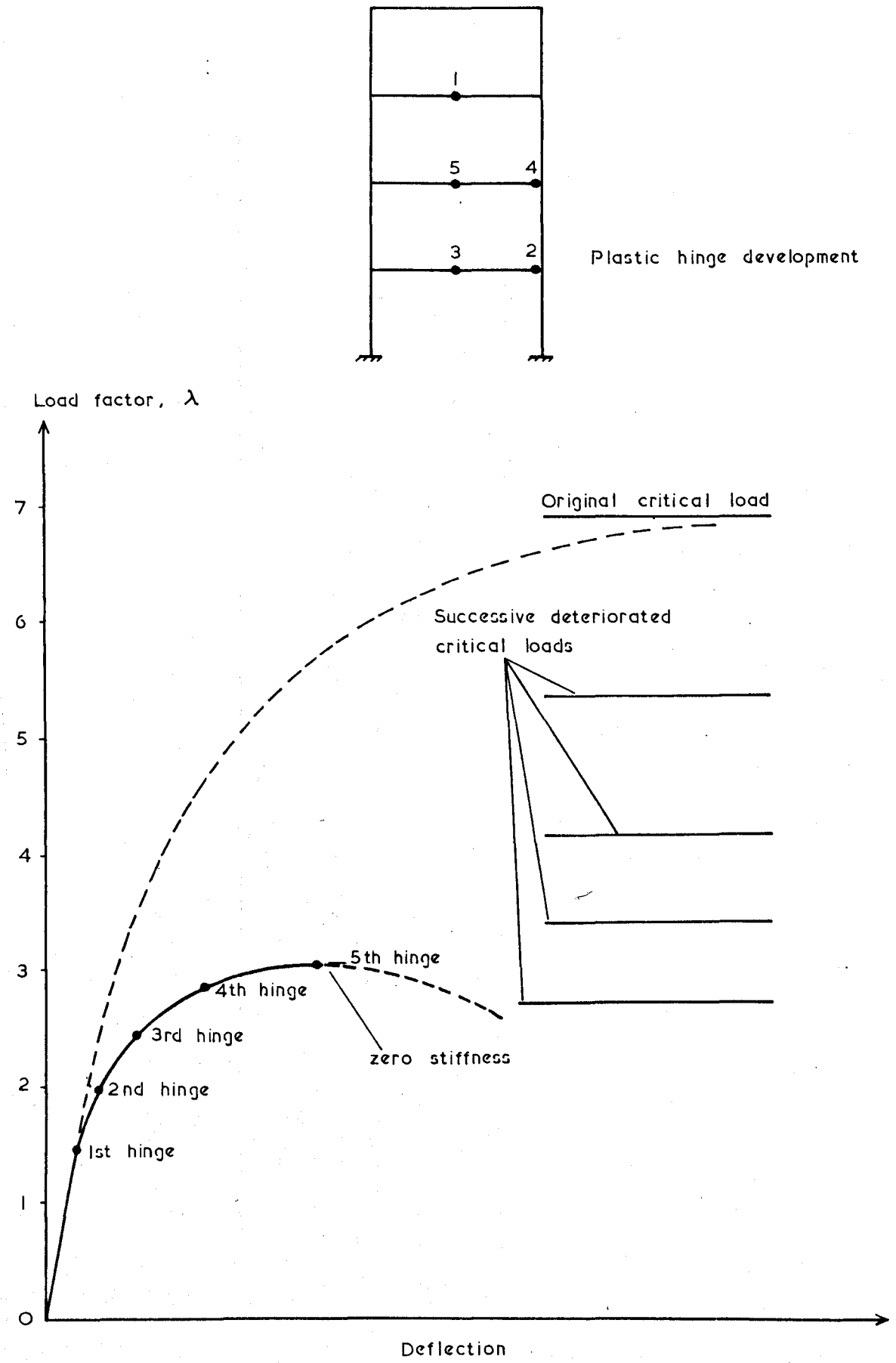

FIG. 1.2 PROGRESSIVE DETERIORATION OF STIFFNESS DUE TO PLASTIC HINGE FORMATION

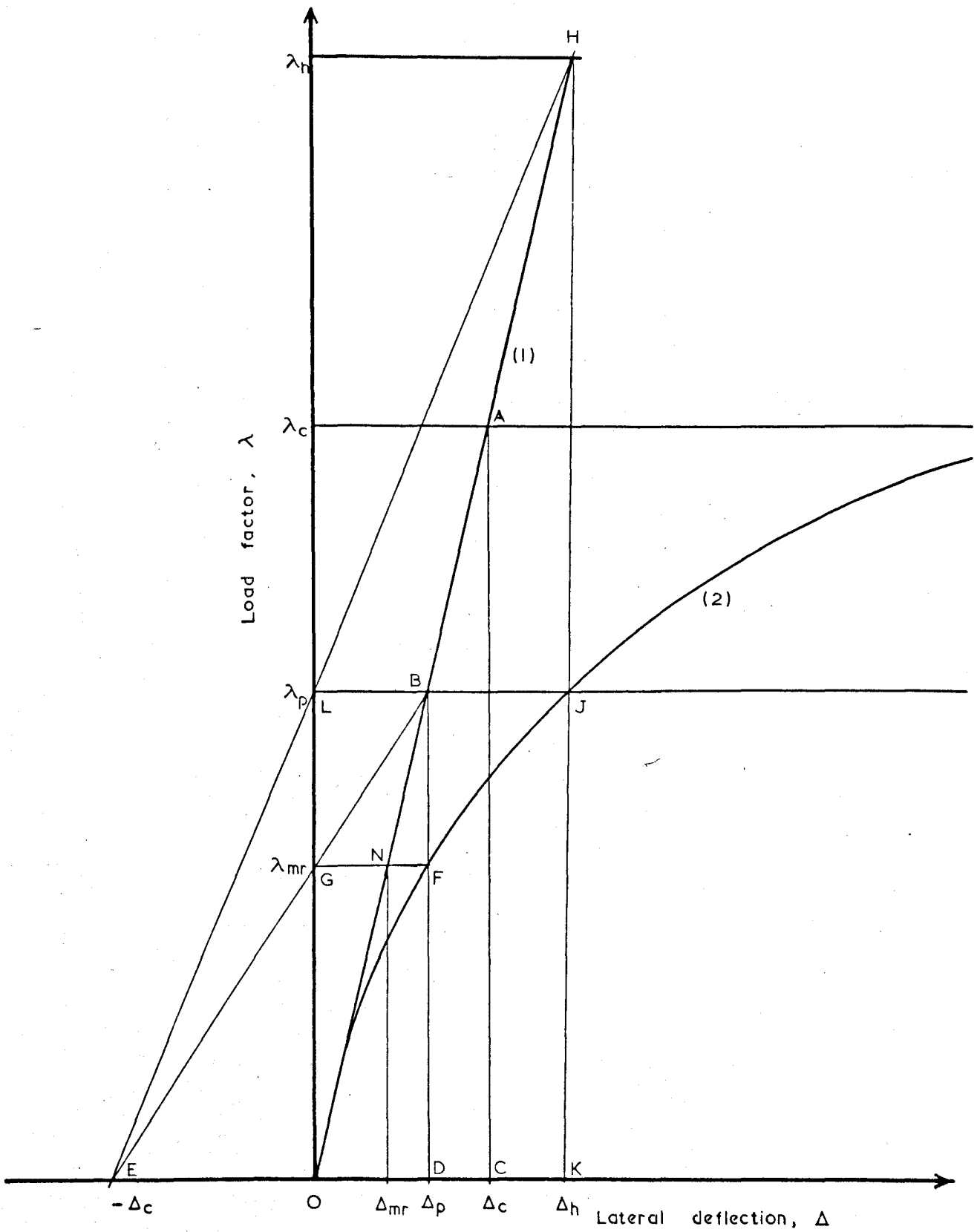

FIG. I.3 TYPICAL LOAD - DISPLACMENT GRAPH

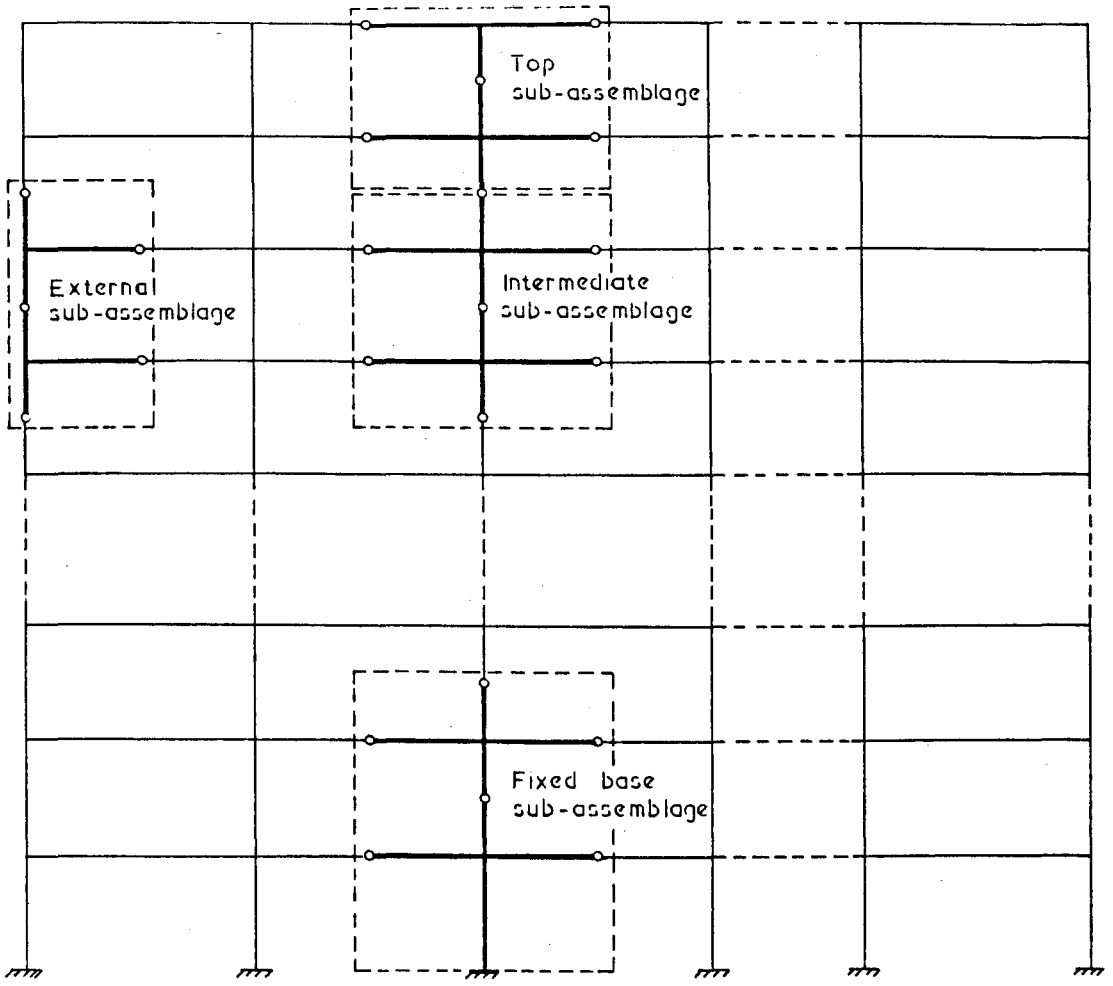

FIG. I.4 STATICALLY DETERMINATE SUB-ASSEMBLAGES

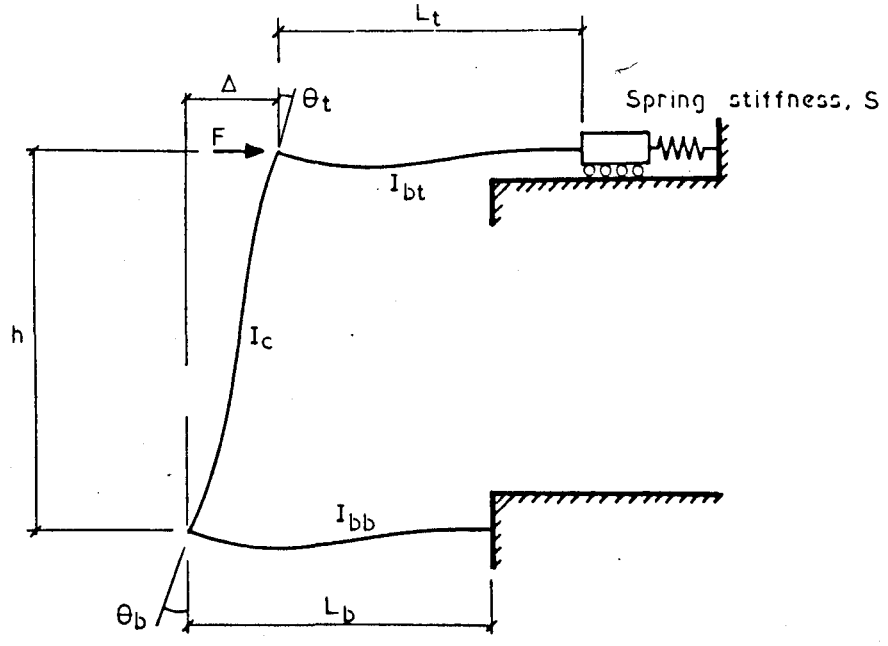

FIG. I.5 SINGLE STOREY SUBSTITUTE FRAME

CHAPTER 2

DESIGN STUDIES OF UNBRACED MULTI-STOREY FRAMES

2.1 Introduction

As shown in Chapter (1), the plastic design of plane unbraced multi-storey steel frames is a relatively complicated task, because of the need to consider instability effects. For this reason, computer-based methods are often the most appropriate. However, if suitable computational facilities and software are not readily available, then the Merchant-Rankine formula(44) provides an attractive alternative for the design of such frames.

This formula has been discussed in Chapter (1), but for convenience its form is repeated here. The load level at failure, λ_{mr} , is given by,

$$\frac{1}{\lambda_{mr}} = \frac{1}{\lambda_c} + \frac{1}{\lambda_p} \qquad (2.1)$$

where λ_p is the load level for rigid-plastic collapse and λ_c denotes the lowest elastic critical load.

To allow for strain-hardening and stray composite action, Wood(50) proposed that the formula be expressed as,

$$\frac{1}{\lambda_{mrw}} = \frac{1}{\lambda_c} + \frac{0.9}{\lambda_p} \qquad (2.2)$$

In this form, the formula has been included in a British draft Code of Practice(55) and in European Recommendations(54).

It has long been recognised that although equation (2.1) is generally conservative, cases can arise in which this is not so. These cases have not caused concern, however, because they arose under unrealistically high ratios of side load to vertical load.

The main aim of this work is to assist the designer in deciding whether ultimate strength or the serviceability limit on sway will be the major influence on choice of sections in an unbraced multi-storey frame. This has been accomplished by a parametric study on a wide range of realistic frames.

Whereas Batten(34) conducted sensitivity studies on medium rise steel frames using 'load factor' design, it is desirable that the parametric studies be based on 'limit state' design philosophy.

The study also provides the opportunity for an evaluation of the accuracy of the Merchant-Rankine formula, in both its forms.

2.2 Design parameters

A total of forty three frames were examined in the studies. The frames were rectangular in elevation, of four, seven and ten storeys in height. The number of bays varied from two to four or five bays. Typical elevations are shown in figure (2.1). The storey height was constant at 3.75 m but two bay widths of 7.50 m and 5.00 m were considered. The frames were taken to be spaced evenly at

4.00 m longitudinally and all bases were fixed. Although unbraced construction provides freedom of layout in a building, it will usually result in a higher weight of steel sections compared with braced alternatives. The study was therefore restricted to ten storeys because it is believed that unbraced construction would be unlikely for structures of greater height. The variation in the number of bays together with changes in wind speed were adopted to enable a wide variation in wind shear per leg to be considered.

Details of the unfactored floor and roof loadings and the basic wind speeds are given in table (2.1). Horizontal forces were calculated from the basic wind speeds by use of CP3: Chapter V: Part 2(70). These forces were based on the total height of the frame and were therefore of equal value at each floor level. The force at roof level was taken as half that at an intermediate floor level. The basic wind speed varied from 38 m/s to 50 m/s with the appropriate S_2 factor corresponding to the height of each frame shown in figure (2.1). S_2 factors were obtained from CP3: Chapter V: Part 2, Table 3 assuming Category 3 and Class B. The values therefore correspond to a fairly exposed small town or the outskirts of a large city. S_1 and S_3 factors were taken as 1.0. Force coefficients are tabulated in Table 10 of CP3: Chapter V: Part 2. The values used in the studies ranged between 1.2 and 1.4.

The wind code permits the designer, if he wishes, to use a reduced wind speed below roof level, based on the actual height of the storey considered. In the interest of simplicity, no advantage was taken of this situation. On the other hand, no allowance was made for eccentricity of vertical loading arising from fabrication

and erection tolerances given in Design Recommendations(54,55). Also, no account was taken of the reduction in live loading permitted in CP3: Chapter V: Part 1(71), for the design of columns.

The partial safety factors, γ_f , were taken from the 1977 British draft steelwork Code(55). For loading at the ultimate limit state, these are,

a)Dead load	1.4
b)Imposed load (in absence of wind)	1.6
c)Imposed load (in combination with wind)	1.2
d)Wind load (in combination with imposed load)	1.2

The design strength of structural steel was taken throughout as 240 N/mm^2, to correspond to the appropriate grade 43 hot-rolled sections. Young's modulus of elasticity was taken as 206 KN/mm^2 . Sway deflections due to unfactored horizontal wind load were to be restricted to 1/300th of each storey height for the bare frame, in accordance with recent Design Recommendations(54,55).

The maximum value of floor loading was combined with minimum values of wind loading and vice-versa. The results are shown in tables (2.2) to (2.4). Several more frames with intermediate values of wind loading were also examined. The results are presented in table (2.5). The procedure followed in the studies is described in Section (2.3) and (2.4) below. Typical calculations are demonstrated by means of an example in Section (2.6).

2.3 Minimum design sections

Design Recommendations(54,55) require a frame to withstand a higher level of vertical loading when full wind load is not included in the loading combinations. Minimum sections were determined, therefore, by designing against failure by beam-type plastic hinge mechanisms or by squashing of the columns, under the higher load factor appropriate to vertical loading only. Thus,

$$\text{Design vertical load} = (1.4\ G_k + 1.6\ Q_k) \qquad (2.3)$$

where G_k and Q_k are the characteristic dead and imposed loads respectively.

Universal beams were chosen for horizontal members, and Universal columns for the vertical members.

2.4 Design under combined loading

To satisfy the limit on sway deflection at working load, the minimum sections were increased as appropriate, using the method of Anderson and Islam(59) described in Chapter (1). Column sections were made continuous over at least two storeys, but the beam sections were changed at each floor level when the need arose. The designs were then subjected to second-order elasto-plastic analysis(41) under the appropriately factored combined vertical and wind loads as follows, i.e.,

$$\text{Combined design load} = (1.4\, G_k + 1.2\, Q_k + 1.2\, W_k) \qquad (2.4)$$

where G_k and Q_k are defined above and W_k is the characteristic wind load.

In the computer analyses, one half of the uniformly distributed load is applied as a concentrated load at mid-span, and one half of the remaining load is applied as a concentrated load at each end of the beam. The verification of the accuracy of this program has been given by Anderson(24), who made extensive comparison with previously established work.

The failure loads, resulting from the elasto-plastic analysis, denoted by λ_f , are shown in tables (2.2) to (2.5). As the factored loads were taken as the reference loads for the analysis, a value of $\lambda_f \geq 1.0$ indicates that the factored load level for the ultimate limit state under combined loading has been achieved. Such a result therefore shows that ultimate strength under combined loading was not the governing factor for the design of that particular frame.

In order to make comparisons with the Merchant-Rankine formula, the rigid-plastic collapse load, λ_p , and the lowest elastic critical load, λ_c , were also determined. For convenience, λ_p was calculated by rerunning the elasto-plastic analysis program(41) with Young's modulus of elasticity given a very high value. λ_p can also be obtained by the same analysis program with all the stability 'ϕ' functions given unit value.

The accuracy of the values for λ_p was checked by the present writer by analysing some frames using a well-established program for rigid-plastic analysis owned by the University of Warwick. This program is based on the work of Livesley(8), described in Chapter (1).

The lowest elastic critical load, λ_c , was determined by using a non-linear elastic analysis program(41) in conjunction with a modified Southwell plot. It should be noted that λ_c was extrapolated from several positions on the plot which were very close to the critical load. These positions were characterised by large horizontal deflections. The dead and imposed vertical loads used as the basis for calculating λ_c , corresponded to the relative values for combined loading, i.e. ,

$$\text{Vertical load for } \lambda_c = (1.4\, G_k + 1.2\, Q_k) \qquad (2.5)$$

These were coupled with a small horizontal disturbing force applied at roof level. The accuracy of the results for λ_c was checked by the present writer by recalculating some values using the charts due to Wood(50).

Finally, the failure loads were calculated from equations (2.1) and (2.2). Values obtained are given in tables (2.2) to (2.5) denoted by λ_{mr} and λ_{mrw} respectively.

2.5 Governing design criterion under combined loading

The failure loads, λ_f are plotted in figures (2.2), (2.3) and (2.4) against the ratio of the sum of the column axial forces, V, to the corresponding total column wind shear, H, in a storey. The ratio of V/H are averaged over all storeys of the frame. The values of V and H were calculated using the factored combined loads,

$$V = \Sigma (1.4 G_k + 1.2 Q_k) \quad (2.6)$$

$$H = \Sigma 1.2 W_k \quad (2.7)$$

The results correspond to the two values of the ratio of bay width to storey height.

For the ten storey frames, figure (2.4), the tendency is clear. With high values of V/H, one should design first for ultimate strength. Two curves have been drawn to show this tendency and they can be used to predict the likely governing criterion for a particular frame. However, some pairs of results, taken in isolation, would indicate a reverse tendency and these need to be examined separately.

Consider the cases indicated by (a) and (b) in figure (2.4). They both correspond to two bay frames, with a bay width of 7.50 m. and were subject to the maximum values of imposed load. The frames are indicated in table (2.5). Intermediate wind speeds were chosen, the wind loading on (a) being 10% lower than that on (b). However, because of the limited number of sections available, the two designs were very similar; λ_c for (a) was only 5% lower than that

for (b). It is not surprising, therefore, that frame (a) showed a slightly higher failure load even though the ratio of V/H was greater than that for (b). The higher failure load of frame (c) compared to frame (d) arises in a similar manner. These frames are indicated in tables (2.5) and (2.4) respectively.

The results for the seven storey frames shown in figure (2.3) are of a form similar to those described above, but those for points (e) and (f) should be examined further. The frames are indicated in table (2.3). Both these cases correspond to maximum imposed load combined with minimum wind speed, frame (e) having four bays while frame (f) had five bays. In both cases, the wind shears per bay were very low, therefore, the minimum sections were identical. The sections chosen to withstand vertical loading were also sufficient to satisfy the limit on sway. Due to the lower column shear in the five bay frame, this showed a slightly higher value of λ_f . As the curves on figure (2.3) are to show the influence of sway deflection on a design under combined loading, the design curves have not been extended to cover such frames whose sections are uninfluenced by this criterion.

If the bay width is 5.0 m (r = 1.33), the four storey frames given in figure (2.2) shows the same general behaviour as the larger structures. However, except for two cases, the frames with the wider bays showed only a small variation in λ_f , despite large variations in the ratio of V/H. This is due to the strong influence of vertical loading on such relatively low frames. Only in case (g) in figure (2.2) which was two bays wide and subjected to minimum vertical loading, was the wind loading sufficiently high

to require an increase above the minimum sections in order to satisfy the limit on sway. The curve showing the influence of sway deflection as a design criterion under combined loading is therefore applicable only to frames with low ratio of V/H and has been drawn accordingly in figure (2.2). However, it is interesting to note that for higher values of V/H, λ_f exceeds unity, showing that the minimum sections provide adequate strength under combined loading. For such cases, strength is the governing criterion in design.

2.6 Design examples

Two examples are shown to demonstrate the earlier results referred to in the design charts. The first example is a seven storey frame and the results have been used to draw the curve in figure (2.3). The second example is a six storey, two bay frame with similar loads and properties to those examined in the parametric studies. This is shown to illustrate the application of the charts given in figures (2.2)-(2.4) to other frames similar to the ones examined here.

2.6.1 Seven storey two bay frame

The frame shown in figure (2.5 (a)) is subjected to the unfactored maximum vertical dead plus imposed floor loads given in table (2.1). The basic wind speed was taken as 38 m/s with a force coefficient, C_f=1.2. The dynamic wind pressure, q, was found to be 0.782 KN/m^2 and therefore the applied characteristic wind load at

each floor level is given by,

$$H = C_f \cdot q \cdot \text{longitudinal spacing} \cdot \text{storey height}$$

$$= (1.2 \times 0.782) \times 4.0 \times 3.75$$

$$= 14.076 \text{ KN.} \qquad (2.8)$$

The sums of the factored combined loads using equations (2.6) and (2.7) for vertical and horizontal loads respectively are shown alongside those of the characteristic dead plus imposed plus wind loads. The average ratio of V/H, calculated in advance was equal to 46.54. With this value, figure (2.3) indicates that the frame will not be governed by strength under combined loading.

The initial procedure is to calculate the minimum beam and column sections required to sustain the factored values applicable to dead plus imposed vertical load only, as given by equation (2.3). These minimum sections have been obtained using simple plastic theory with checks made against squashing and are chosen from the range of British universal sections, with a design strength of 240 N/mm^2 .

a)Roof beam

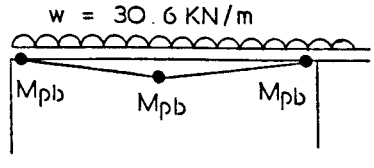

$$Z_{pb} = M_{pb}/f_y$$

$$= \frac{30.6 \times (7.5)^2 \times 1000}{16 \times 240}$$

$$= 448.2 \text{ cm}^3$$

Propose 305 x 102 x 33 UB (M_p = 115.2 KN.m)

b)External roof column

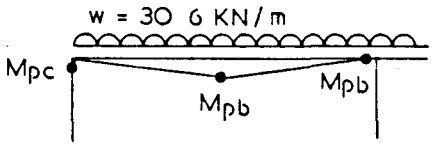

$M_{pc} + 3M_{pb} = wL^2/4$

$M_{pc} = \frac{30.6 \times (7.5)^2}{4} - (3 \times 115.2)$

$= 84.7$ KN.m

$Z_{pc} = 353.0$ cm^3

Propose 203 x 203 x 52 UC (M_p = 136.3 KN.m)

c)Floor beams

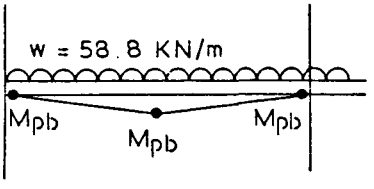

$Z_{pb} = \frac{58.8 \times (7.5)^2 \times 1000}{16 \times 240}$

$= 861.3$ cm^3

Propose 406 x 140 x 46 UB (M_p = 213.2 KN.m)

d)External floor column

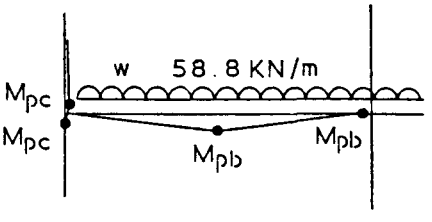

$2M_{pc} + 3M_{pb} = wL^2/4$

$M_{pc} = \frac{1}{2}\left[\frac{58.8 \times (7.5)^2}{4} - (3 \times 213.2)\right]$

$= 93.6$ KN.m

$Z_{pc} = 390.2$ cm^3

Propose 203 x 203 x 52 UC (M_p = 136.3 KN.m)

The columns are taken to be continuous over at least two storeys to reduce fabrication costs. Checks are therefore required for the lower length only to resist squashing in the internal columns and combined bending and axial load in the external columns. As patterned loading has not been considered, it was decided that in the top two storey the internal columns should not have a section less than that of the external columns.

External column

storey	axial load (KN.)	section
6	335.4	203 x 203 x 52 UC
4	776.6	203 x 203 x 60 UC
1	1438.3	254 x 254 x 73 UC

Internal column

storey	axial load (KN.)	section
6	670.7	203 x 203 x 52 UC
4	1553.0	203 x 203 x 60 UC
1	2876.6	254 x 254 x 107 UC

The initial minimum sections are shown in figure (2.5 (b)). The method of Anderson and Islam(59) is then employed to increase the preliminary sections as necessary in order to limit sway at working load. It is recalled that the method of Anderson and Islam provides a minimum cost design. Strictly, this requires iteration for calculation of the cost factor, 'k'. It is assumed that all cost factors take the value of unity.

As column sections are spliced at every two storeys, it is only necessary to consider three different sub-assemblages. These are for the top(n=0), n=2 and n=4 sub-assemblages as indicated in figure (2.5 (a)). Calculation was carried out using the following data,

$$s = H/m = 14.076/2 .$$

$$= 7.038 \text{ KN.}$$

All k's = 1.0 .

r = Bay width / storey height = 2.0 .

Maximum deflection = 1/300th of each storey height.

$\therefore \Delta$ = 12.5 mm.

Young's modulus of elasticity, E = 206 KN/mm^2 .

where H = characteristic wind load at floor level,

m = number of bays,

k = cost factors,

n = integer shown in figure (2.5 (a)).

For the intermediate sub-assemblage, the theoretical inertias are given by,

Internal column

$$I_3 = 600.6 \quad [2n + 3 + 2 \sqrt{(n+1.5)\ (4n+6)}\ ] \qquad (2.9)$$

It is noted that a typographical error exist in one of the equations given by Anderson and Islam(59) for an intermediate storey of a regular frame. Equation (20) in Reference (59) should read,

$$I_3 = \frac{s.h^3}{24E.\Delta} \left[2n + 3 + r \sqrt{\frac{2m(n+1.5).[k_1\ (n+1.0) + k_2(n+2)]}{k_3(m-1) + k_3'}} \right]$$

Equation (2.9) given above is correct.

Lower beam

$$I_2 = \frac{2402.2 \quad (n+2) \quad I_3}{I_3 - [\ 1201.1 \quad (n+1.5)\ ]} \qquad (2.10)$$

Upper beam

$$I_1 = (n+1) \quad I_2 / (n+2) \tag{2.11}$$

For the bottom sub-assemblage, the expressions for the required inertias, with all k's = 1, are,

Internal column

$$I_3 = 1201.1 \quad [n + 1.5 + \quad 1.2 \sqrt{(n+1.5)\ (3n+5)}\ ] \tag{2.12}$$

Lower beam

$$I_2 = \frac{[(15614.5 \quad n) + 30628.4 - I_3] \quad I_3}{6 \quad [I_3 - 1201.1(n+1.5)]} \tag{2.13}$$

Upper beam

$$I_1 = [(n+1) \quad (I_3 + 6I_2)]/[6 \quad (n+2)] \tag{2.14}$$

It can be shown that strength under vertical loading only usually controls the design for the top sub-assemblage and the design for this storey is therefore not required.

Design of the bottom two storeys is governed by the storey next to the bottom to avoid reverse column taper which would otherwise result from the stiffness of a fixed base. Separate expressions for pinned bases are also given in reference (59).

Ideally, the external column inertia should be taken as $I_3/2$, but owing to the discontinuous range of available sections, the selected member is unlikely to observe this criterion. The same kind of difficulty also arises when selecting sections for other members. This apparent weakness in the method is recognised but

should not decrease greatly the specified sway limit. This is because increased column stiffness can be offset to some extent by reduced beam stiffness and vice-versa.

For example, the value of I_3 used to calculate the beam inertias I_1 and I_2 can be based on the column section selected, rather than on the theoretically required value for I_3 . The reverse procedure, in which a beam section is selected and then used as the basis of the column design, can be seen by examining the detailed design of the lower (n=2 and n=4) sub-assemblages.

In the fourth storey (n=2), equation (2.9) gives I_3 =12613 cm^4 This is greater than the minimum section (I=6088 cm^4). Initially, a 254 x 254 x 89UC (I=14307 cm^4) is adopted. Using equation (2.10) for the lower beam gives I_2 =13607 cm^4 which is less than the inertia of the minimum beam section provided (I=15647 cm^4). The minimum beam section (I=15647 cm^4) is retained. Using equation (2.10), a reduced column section can be obtained by solving for I_3. With I_2 =15647 cm^4 , equation (2.10) gives I_3 =10894 cm^4 . Therefore, a 254 x 254 x 73UC (I=11360 cm^4) is adopted for the internal column.

Using equation (2.12) for the bottom sub-assemblage (n=4), the internal column, I_3 =19329 cm^4 , which exceeds the minimum section inertia (I=17510 cm^4). Adopting a 254 x 254 x 132UC (I=22416 cm^4) results in the lower beam, I_2 =16700 cm^4 using equation (2.13). This value exceed the minimum of 15647 cm^4 . Instead of altering two different sections, it was decided to increase the beam section only from a 406 x 140 x 46UB (I=15647 cm^4) to a 457 x 152 x 52UB

(I=21345 cm^4). Using the effective stiffness of I_2 =21345 cm^4 and solving equation (2.13) gives I_3 =16449 cm^4 , which is less than the value (I=17510 cm^4) provided by the initial minimum section. This column section is therefore retained. With I_3 =17510 cm^4 and I_2=21345 cm^4 , the required stiffness for the upper beam is found to be I_1=20219 cm^4 , using equation (2.14). The same section as the lower beam (I=21345 cm^4) was adopted.

The final sections are shown in figure (2.5 (c)). It is noticed that some of the minimum sections have been retained. The minimum sections were sufficient to provide the required stiffness against sway deflection. This is not surprising, because with such relatively heavy vertical load, strength under vertical loading only would be the major influence in design but is not necessarily the most critical. This is shown by the stiffer internal columns in the fourth and fifth storeys and the beam sections for the lower two floors. The sum of the horizontal shears at these levels is significant in and is beginning to affect the choice of sections. Finally, to confirm figure (2.3), the frame is now subject to a non-linear elasto-plastic analysis(41). The failure load was found to be 1.01.

2.6.2 Six storey two bay frame

In order to demonstrate the application of the proposed design charts to other frames, a six storey two bay structure has been designed and shown in figure (2.6 (a)). The frame is spaced longitudinally at 4.50 m and the average ratio of V/H is 31.5. The

following values have been adopted for this design,

G_k (roof) = 3.75 KN/m^2.

Q_k (roof) = 1.50 KN/m^2.

G_k (floor) = 4.80 KN/m^2.

Q_k (floor) = 3.50 KN/m^2.

W_k = 1.005 KN/m^2.

All k's = 1.0 .

r = 6000/375 = 1.6 .

Maximum deflection = 1/300th of each storey height.

$\therefore \Delta$ = 12.5 mm.

Young's modulus of elasticity, E= 205 KN/mm^2 .

Steel design strength = 240 N/mm^2.

It should be noted that as the frame is six storeys high with a value of the ratio of bay width to storey height that is different from the two values plotted in figure (2.2) to (2.4), strictly none of these diagrams apply. However, they can be used as a guide by allowing interpolation.

Figures (2.2) and (2.3) suggests that ultimate strength will not be the governing criterion in the choice of sections under combined loading for this frame. The reason is due to the relatively high horizontal loads in comparison to the simultaneously applied vertical loads. Proceeding in a similar manner as the first example, the final design was obtained and shown in figure (2.6 (b)). It should be noted though that after design using the method of Anderson and Islam(59), the sections were adjusted to achieve greater economy by using the analysis

method of Wood and Roberts(60), with the cladding stiffness parameter, $\bar{s}$, taken as zero.

The latter method can be usefully adopted in this way because it does not rely on fixed relationships, such as equations (2.9) to (2.11), between the inertias of beams and columns. Sway deflections, predicted by the method of Wood and Roberts, at the working load are shown alongside figure (2.6 (b)). Comparison of sway deflection with computer analysis showed good agreement and the design was also found to possess adequate strength under combined loading. The failure load obtained by computer analysis was 1.09. This confirms the initial prediction from the proposed design chart that ultimate strength under combined loading would not be critical for design.

2.7 Verification of the Merchant-Rankine formula

The failure load from equations (2.1) and (2.2) are given in tables (2.2) to (2.5) under the heading λ_{mr} and λ_{mrw} respectively. The ratio of λ_c/λ_p varied from 3.2 to 16.2, thereby covering the range $4 \leq \lambda_c/\lambda_p \leq 10$ proposed(50,54,55) for use of the Merchant-Rankine formula. In all cases, λ_{mr} was below the failure load obtained by second-order elasto-plastic computer analysis.

The tables also indicate the rigid-plastic collapse mechanisms, denoted by,

B Simple beam-type collapse mechanism.

S Column sway mechanism.

C Combined mechanism.

It has been stated(54,55) that the Merchant-Rankine formula should be used only when the rigid-plastic collapse mode is mechanism C, in order to prevent the deliberate choice of a strong-beam, weak-column design with its attendant stability problems(50). A combined mechanism cannot, however, be guaranteed when analysing a trial design and the requirements for such a mechanism will restrict the application of the Merchant-Rankine approach. The results shown in tables (2.2) to (2.5) indicate that λ_{mr} provides a safe result, irrespective of the shape of the rigid-plastic collapse mechanism. This represent a significant departure from the theoretical justification proposed by Horne(25). It is the opinion that the limitations on sway of each storey, already included in Design Recommendations(54,55), together with the need to achieve economy in steel weight and structure height, will be sufficient to cause engineers to avoid strong-beam, weak-column designs.

For several frames, equation (2.1) provides a result that is not unduly conservative. However, the Merchant-Rankine failure load can be as low as 86% of the accurate computer result. From the elasto-plastic computer analyses, one can tabulate the load factor, λ_1 , at which the first plastic hinge formed. Tables (2.2) to (2.5) show that for a number of cases in which column sway formed the rigid-plastic collapse mechanism, λ_{mr} is so conservative that it lies below λ_1 . This occurred particularly in the four storey frames and frames with the maximum number of bays

where strength under vertical load only controlled the design. It was the possibility of unduly conservative results that led Wood(50) to propose the modified formula given by equation (2.2).

The values of λ_{mrw} tabulated in tables (2.2) to (2.5) show that equation (2.2) provides good agreement with the accurate computer result. It tends to overestimate the accurate failure load when collapse is by a local beam-type plastic hinge mechanism, but by no more than 7%. It must also be noted that when the collapse mode took this form, the failure load, λ_f , was always greater than the required value of 1.0. This resulted from the higher partial safety factors specified for vertical dead plus imposed load only which were used in the initial design of individual beams and columns. As this loading case provided a lower bound on section size, an error in λ_{mrw} will not lead the designer to reduce such sections in an unsafe manner.

The same error of about 7% was shown by a ten storey, two bay frame in table (2.4), for which the rigid-plastic mechanism was bottom storey column sway. In all other cases, the agreement obtained from equation (2.2) and the accurate computer analyses was very good, the maximum error being only 4%.

2.8 Slender-bay frames and irregular-bay frames

As described in Chapter (1), early studies by Salem(45) and Low(48) showed that equation (2.1) was particularly conservative when side loads were small compared with the simultaneous applied vertical loads. On the other hand, Ariaratnam(49) demonstrated that

the formula can become unsafe when the side load is substantially higher than those normally encountered in practice.

More recently, Adam(46) found that the Merchant-Rankine load can overestimate the accurate failure load when the side loads are small compared with the vertical loads. The frame examined by Adam(46) was a fixed base, six storey, single bay frame shown in figure (2.7). It was composed of European steel sections and designed using an overall load factor rather than the partial safety factors of limit state design.

It will be noticed that the bay width is only half the height of one storey. Despite the extremely unusual nature of the frame, Adam used it to argue that the Merchant-Rankine formula is unreliable and, by implication, that it should not be included in Design Recommendations. It should be noted that Adam took care to ensure that rigid-plastic collapse occurred by a combined mechanism and that the ratio of λ_c/λ_p were between the limits of 4 and 10 required for use of the formula. No plastic hinges were present in the frame at working load and at this load level the overall sway deflection did not exceed 1/300th of the total height.

To investigate this matter further, the frame shown in figure (2.7) was redesigned using British steel sections in grade 43 steel. The reason for selecting such sections was the absence of the coefficients required for calculation of the reduced plastic moment capacity in European section tables. These coefficients are necessary for the evaluation of collapse loads by the second-order elasto-plastic analysis program(41). Young's modulus of elasticity

was taken as 206 KN/mm^2 and the design strength was 240 N/mm^2 .

At unit load factor, the linear elastic sway deflection was not to exceed 1/300th of each storey height(55). To compare directly with the results obtained by Adam and to obtain a satisfactory design, the following design criteria were adopted,

a)Under combined dead plus live plus wind load, the frame should not collapse until the load factor exceeded 1.40.

b)Under vertical dead plus live load only, collapse should not occur until the load factor exceeded 1.75.

In order to achieve this, the following restrictions were imposed(42),

c)Plastic hinges should not form in beams until the load factor reached 1.00.

d)Under combined loading, plastic hinges should not form in columns until the load factor reached 1.40.

e)Under vertical loading, plastic hinges should not form in columns until the load factor exceeded 1.75.

The preceding criteria were satisfied by successive analysis and redesign(42) using the computer. The final sections are shown in figure (2.8 (a)) along with the resulting sway deflections at unit load factor, given by linear elastic computer analysis under combined loading. For comparison, the values in square brackets were those obtained when the reduction in frame stiffness due to compressive axial forces were considered in a non-linear elastic

analysis(41). It is interesting to note that the difference between the linear and non-linear deflections is significant, even at working load. In fact, some of the non-linear values exceed the limit of 1/300th of storey height. However, the overall non-linear elastic deflection is less than 1/300th of the total height.

The results of the non-linear elasto-plastic computer analysis of the final design are shown in figure (2.8 (b)). The rigid-plastic behaviour with reduction in the plastic moment capacity due to axial forces (but neglecting the effect of such forces on the overall stiffness of the frame) is shown in figure (2.8 (c)).

In order to determine the Merchant-Rankine failure load, the lowest elastic critical load factor was obtained using non-linear elastic analysis under the loading shown in figure (2.8 (d)). The frame was excited at the roof level by a horizontal force of λ KN, and a modified Southwell plot used to calculate λ_c . It was found that λ_{mr} and λ_{mrw} was respectively 8% and 18% higher than the accurate failure load given by second-order elasto-plastic analysis. These values are similar to those obtained by Adam.

The relative dimensions and loadings chosen by Adam, however, are likely to be approached only in the design of sheltered racking systems for use in large storage warehouses. Indeed, bracing would usually be provided across the single-bay depth of the structure. To guard against the possibility of a designer attempting to use the Merchant-Rankine formula on such unusual structures, it is proposed that the formula be used only when the bay width is not

less than the maximum height of one storey.

To examine this proposal, the bay width for the structure shown in figure (2.7) was increased to 5.00 m, to equal the storey height. The frame was then designed to satisfy the sway deflection limit of 1/300th of each storey and also to meet the requirements (a) to (e) described above. The frame was then subjected to the computer analysis procedures in exactly the same manner as for figure (2.8). The results of the final design and values of sway deflection at unit load factor utilising linear elastic analysis are shown in figure (2.9 (a)). The computer analyses for λ_f , λ_p and λ_c are indicated in figures (2.9 (b)), (2.9 (c)) and (2.9 (d)) respectively. It was found that λ_{mr} now underestimated λ_f by 5% while λ_{mrw} overestimated λ_f by 3%.

For multi-bay frames, it is proposed that the formula be allowed, providing the average bay width is not less than the maximum value of any storey height. A frame that just satisfies this requirement is shown in figure (2.10). Once again, it was specified that the sway at each storey due to the unfactored horizontal loads should not exceed 1/300th of each storey height and the conditions listed from (a) to (e) be observed. However, a combined mechanism for rigid-plastic collapse was not insisted on, and the design selected exhibited a sway mode in the bottom storey. The results of their respective analyses are shown in figure (2.10), the ratio of λ_c/λ_p being 4.18. The sway deflections at working load were found to be well within the limit specified. The first column hinge developed at a load factor of $\lambda_{col=1.44}$. Comparisons with accurate elasto-plastic analysis showed that λ_{mr}

underestimated λ_f by 5% and λ_{mrw} overestimated λ_f by 4%.

2.9 Conclusion

Studies carried out on practical multi-storey, unbraced frames have enabled guidance to be given on the relative influences of sway deflection and ultimate strength as design criteria under combined loading. These frames have been subjected to realistic values of vertical and horizontal loads that are normally encountered in practice.

The procedure followed in the studies has been illustrated by the design of a seven storey frame. The design charts which resulted from the study have also been applied to a six storey frame. Interpolation was necessary, but the example showed that the correct guidance had been given to the designer.

The studies have also shown that the Merchant-Rankine formula, given by equation (2.1), provides a safe estimate of the non-linear elasto-plastic failure load, λ_f , for frames of realistic dimensions which satisfy a serviceability limit on sway of 1/300th of storey height, and are designed against premature collapse by simple beam-type plastic mechanisms. The modified formula given by equation (2.2) generally provides better agreement, but in some cases, the predicted load exceeds λ_f . However, the excess load capacity is relatively small with a maximum error not greater than 7%.

The computer program(41) used to calculate the failure load

ignores the beneficial effects of strain hardening and stray composite action. The accuracy of the formula is not significantly affected by the form of the rigid-plastic collapse mechanism, and the present insistence on a combined mode of collapse is restrictive and difficult to observe. It is proposed that this requirement be removed from Design Recommendations, providing it is stated that each storey should satisfy a serviceability limit on sway of 1/300th of storey height. Furthermore, the studies presented are limited to structures not greater than ten storeys as larger buildings are likely to be braced.

It has been confirmed that even the original Merchant-Rankine formula can overestimate the accurate failure load for very tall slender frames. Such unusual frames, in which the bay width is less than the height of one storey and the wind loading is exceptionally low in relation to the simultaneously applied vertical load, would be braced and usually erected in large sheltered or enclosed storage warehouses. In addition, the lower columns are normally reinforced or stiffened to prevent accidental impact by mechanical lifting devices. However, to guard against the possible use of the Merchant-Rankine formula on such exceptionally slender frames, it is proposed that the formula should not be used when the bay width is less than the greatest height of one storey.

For multi-bay frames with unequal bays, the average bay width should be compared with the storey height. Two examples that satisfy this requirement showed that the Merchant-Rankine approach continues to provide close estimates of the failure load obtained by accurate computer analyses.

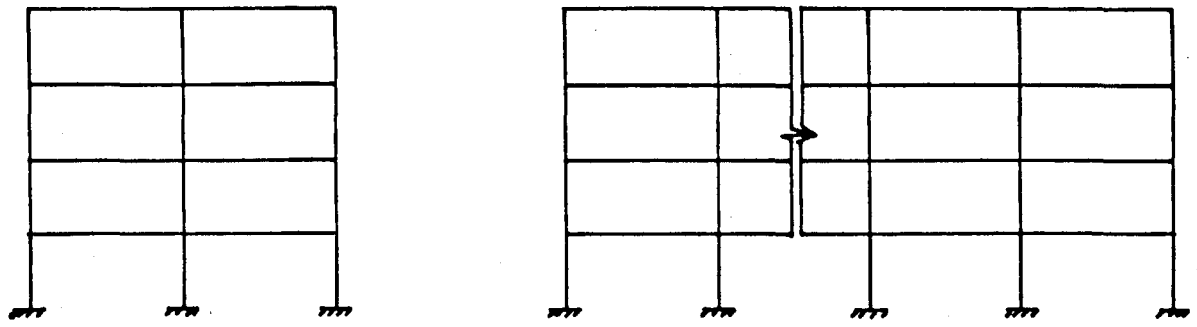

FIG. 2.1(a) FOUR STOREY FRAMES

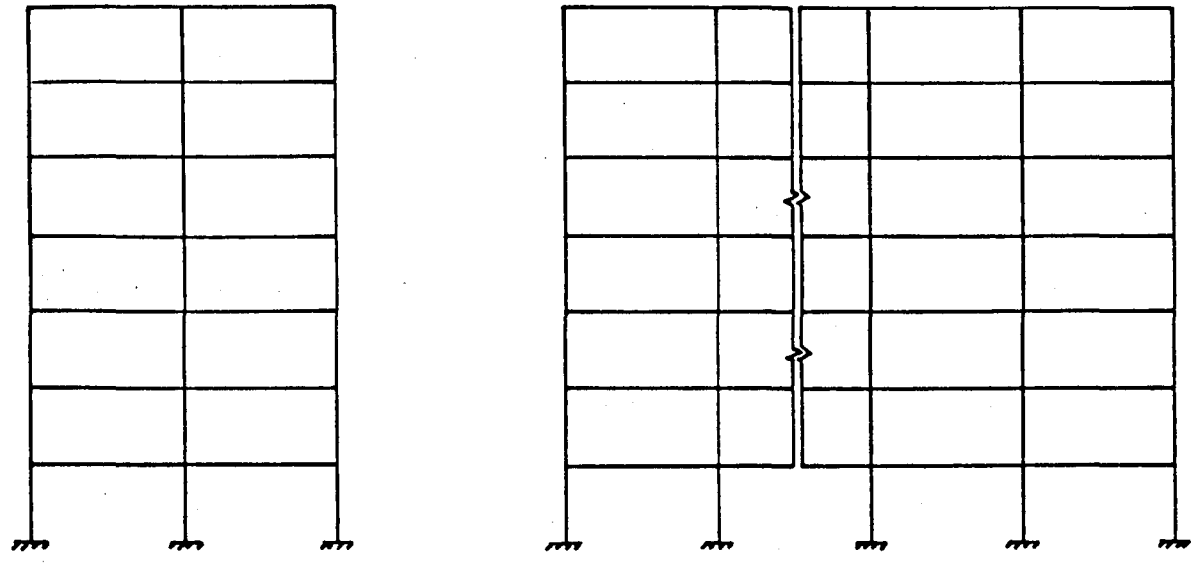

FIG. 2.1(b) SEVEN STOREY FRAMES

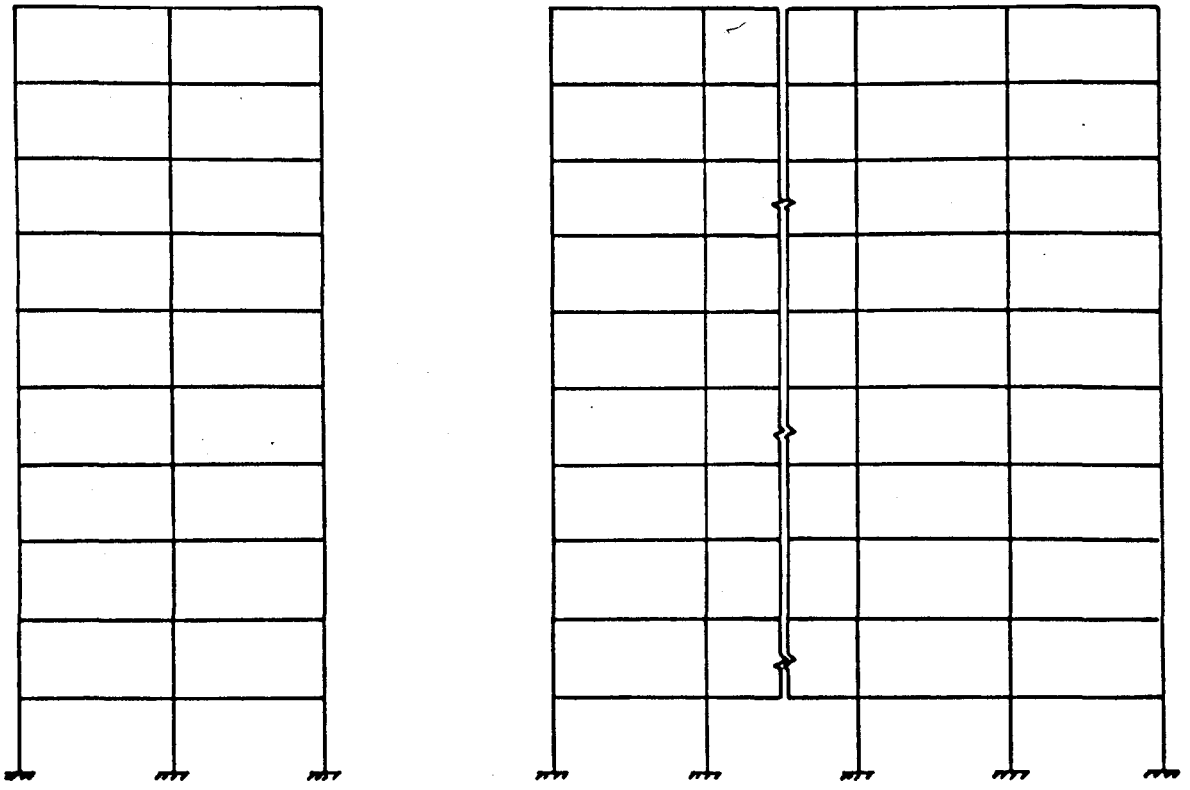

FIG. 2.1(c) TEN STOREY FRAMES

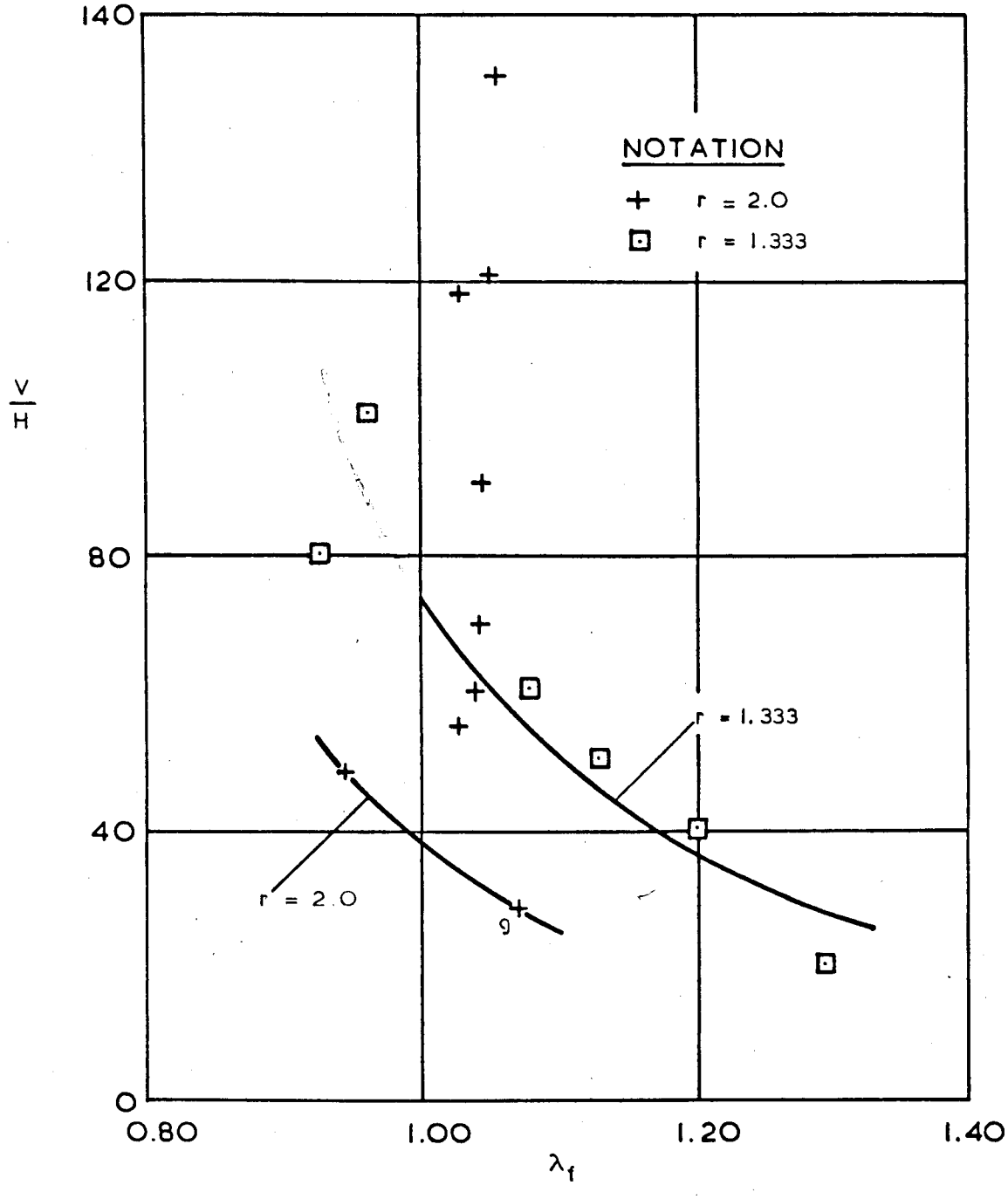

FIG. 2.2 FOUR STOREY FRAMES

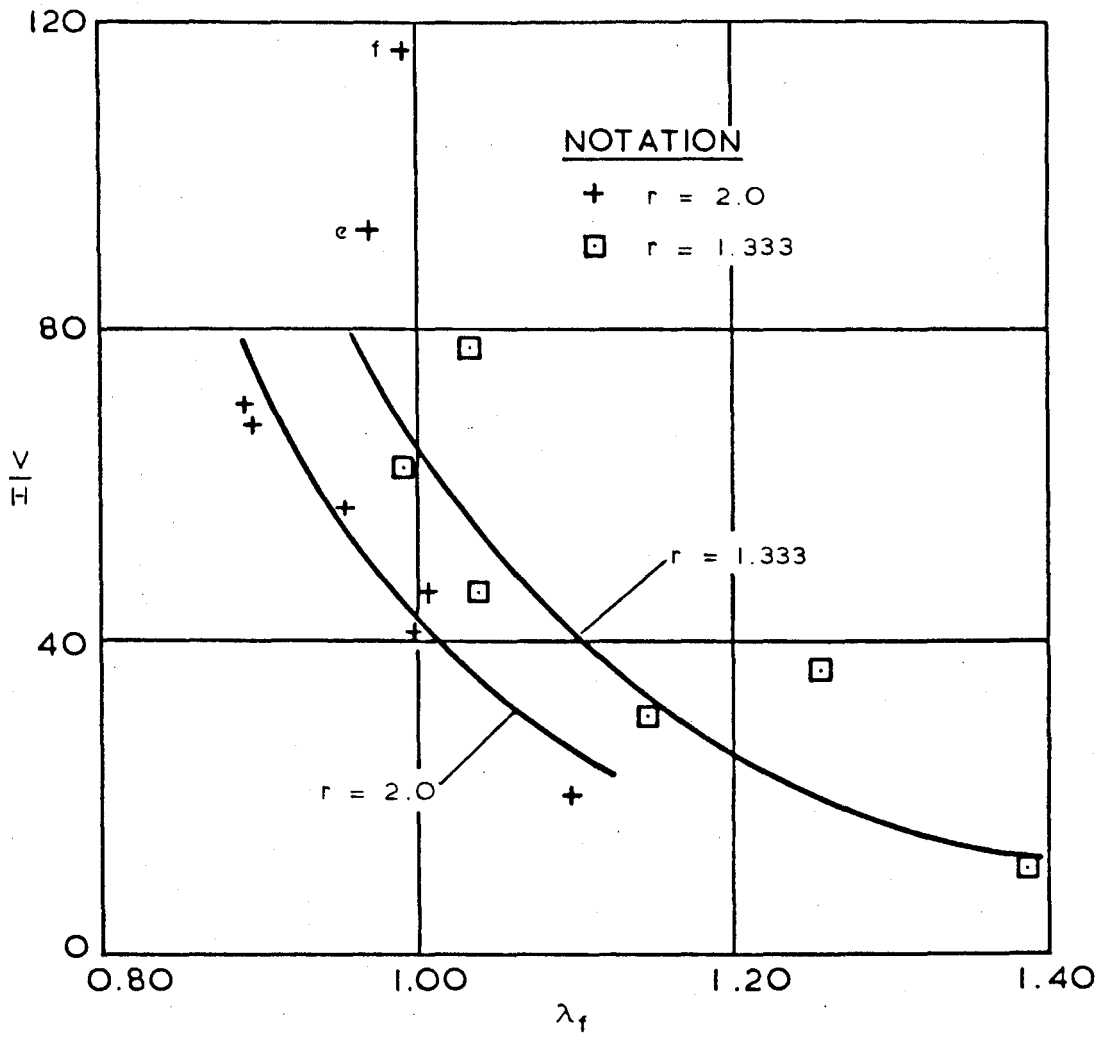

FIG. 2 3 SEVEN STOREY FRAMES

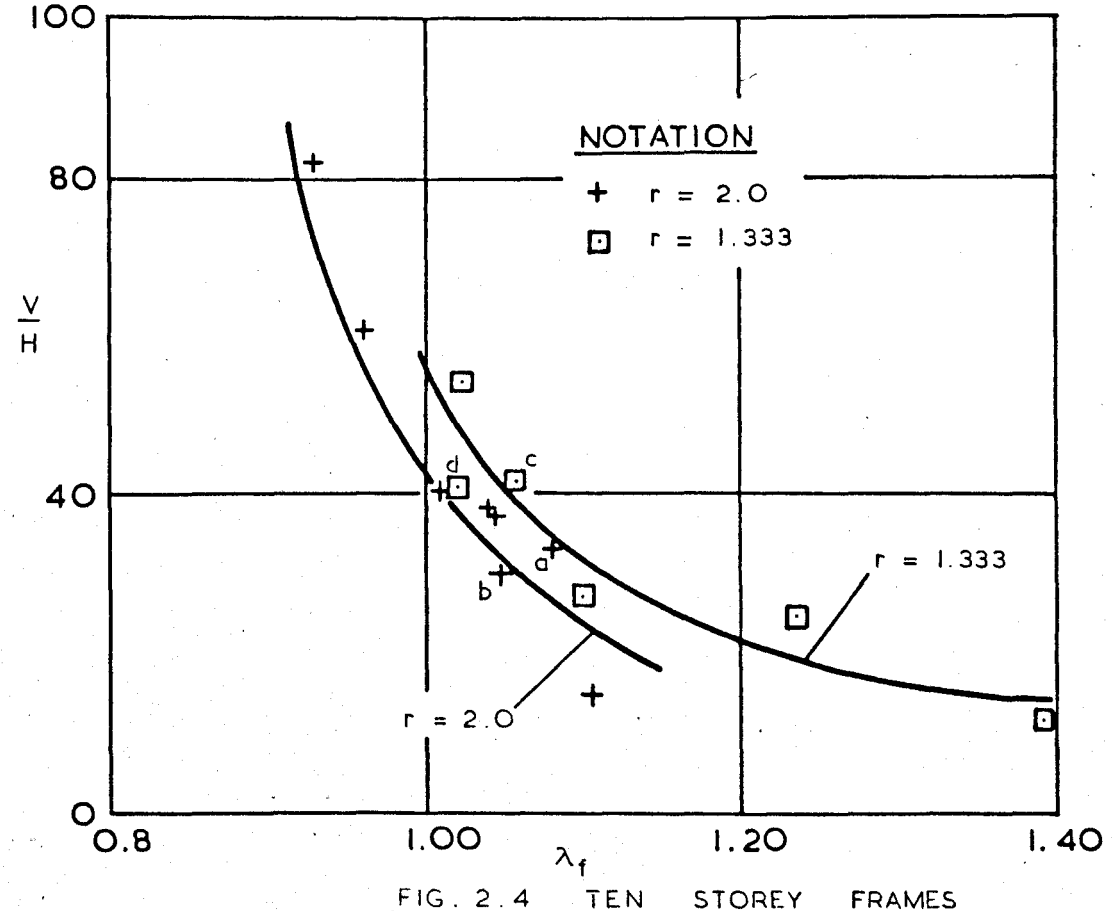

FIG. 2.4 TEN STOREY FRAMES

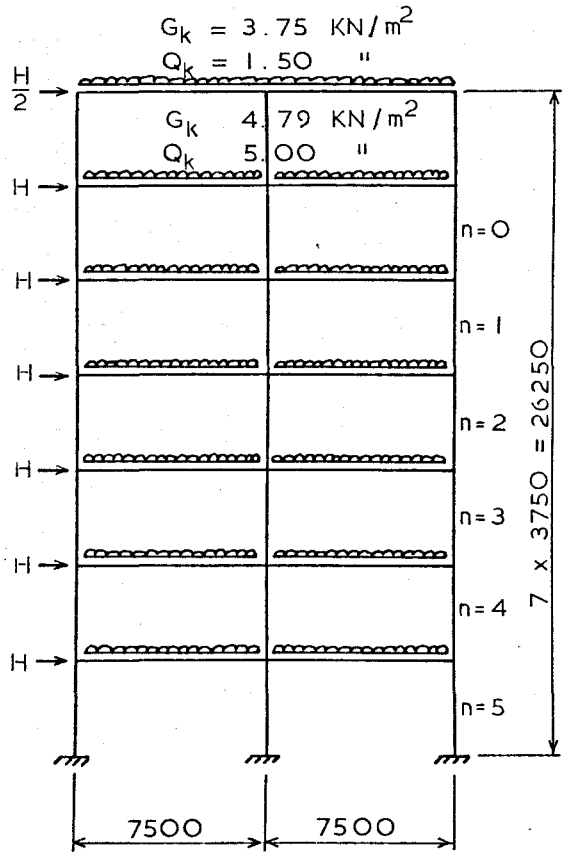

	∑V	∑H	V/H
	425	8.445	50.33
	1185	25.335	46.77
	1947	42.225	46.11
	2709	59.115	45.83
	3471	76.005	45.67
	4233	92.895	45.57
	4995	109.785	45.50

Ave. $\frac{V}{H}$ = 46.54

H = 14.076 KN.

FIG. 2.5 (a) CHARACTERISTIC DEAD PLUS IMPOSED PLUS WIND LOAD (λ = 1.0)

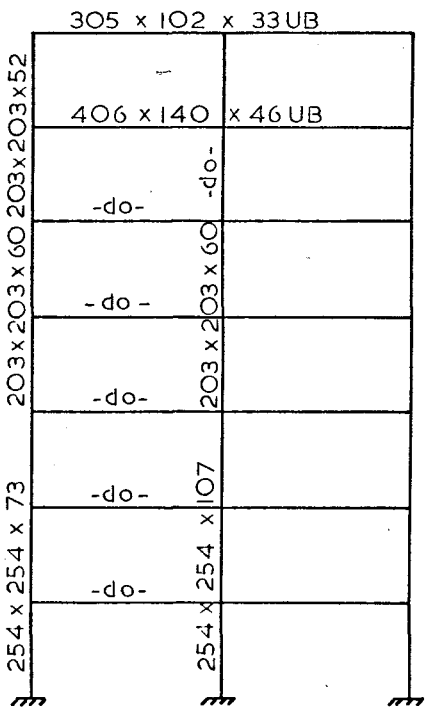

FIG. 2.5 (b) INITIAL MINIMUM SECTIONS

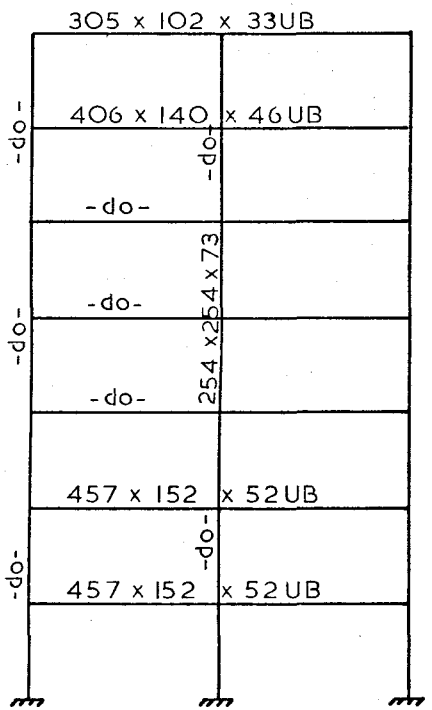

λ_c = 6.25 λ_p = 1.104

λ_{mr} = 0.94 λ_{mrw} = 1.02

FIG. 2.5 (c) FINAL SECTIONS. COLUMNS IDENTICAL TO FIG. 2.5 (b)

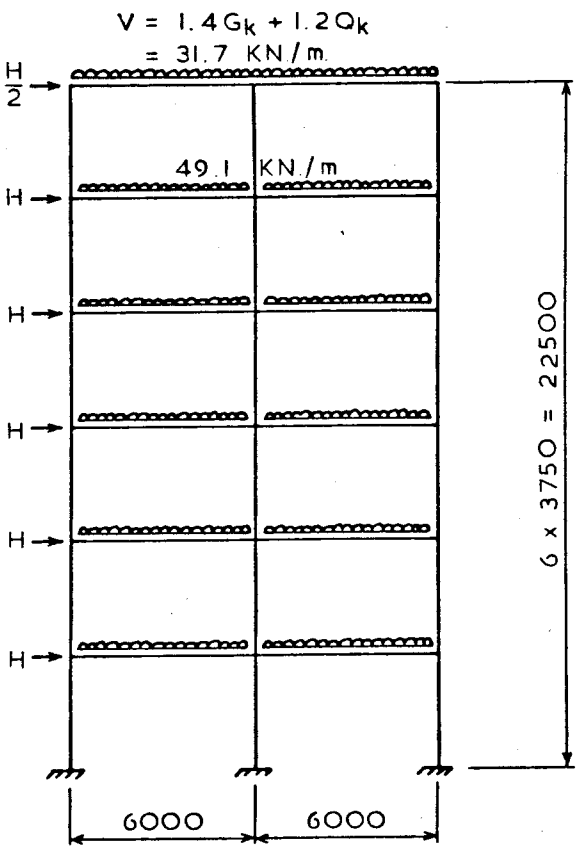

H = 1.2 W_k = 20 4 KN

FIG. 2.6 (a) FACTORED COMBINED LOADING

∑V	∑H	V/H	Working load deflection
380.4	10.2	37.3	h/708
969.6	30.6	31.7	h/350
1558.8	51.0	30.6	h/364
2148.0	71.4	30.1	h/300
2737.2	91.8	29.8	h/354
3326.4	112.2	29.6	h/441

Ave. $\frac{V}{H}$ = 31.5

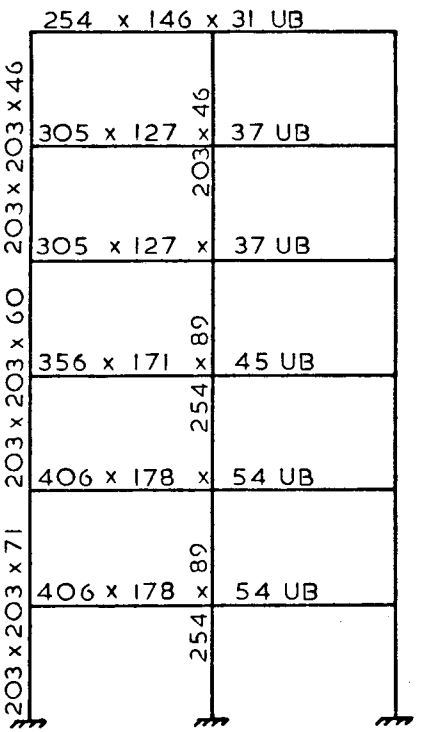

FIG. 2.6 (b) FINAL DESIGN

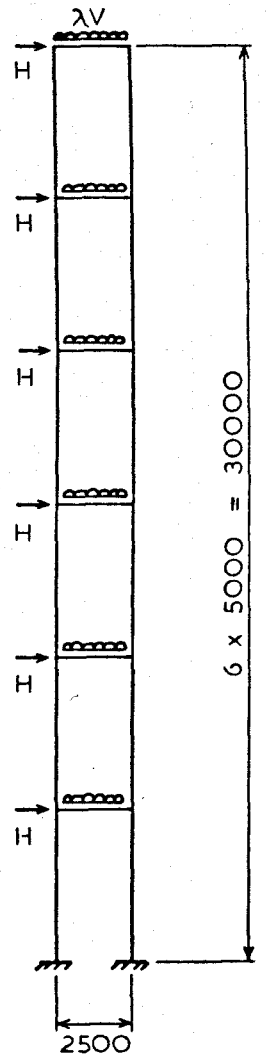

V = 300 KN.
H = 0.02866 λV

FIG. 2.7
SLENDER FRAME

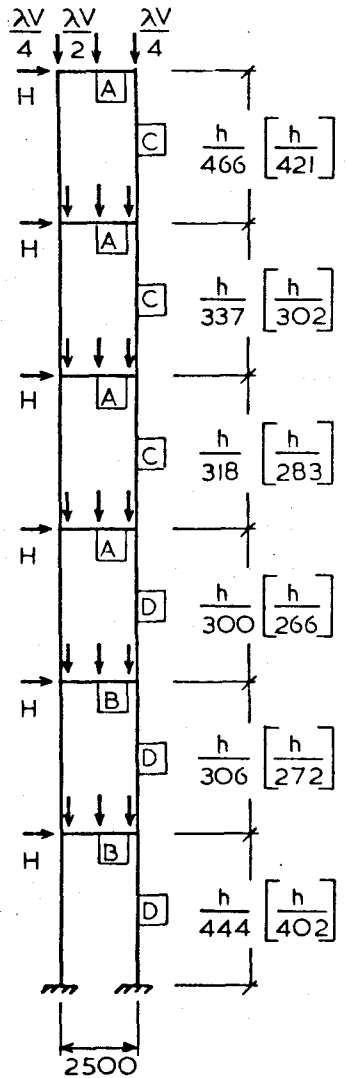

V = 300 KN.
H = 0.02866 λV.

SECTION	BRITISH SECTION
A	305 x 165 x 40UB
B	356 x 171 x 45UB
C	254 x 254 x 73UC
D	305 x 305 x 97UC

NOTE: IDENTICAL LOADING AT EACH FLOOR

FIG. 2.8 (a) FINAL SECTIONS AND SWAY DEFLECTIONS

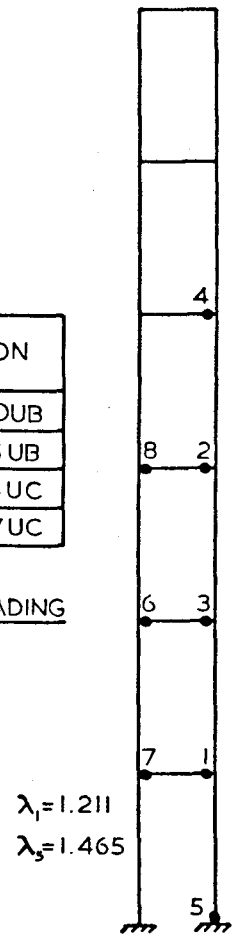

$\lambda_1 = 1.211$
$\lambda_s = 1.465$

FIG. 2.8 (b)
$\lambda_f = 1.52$

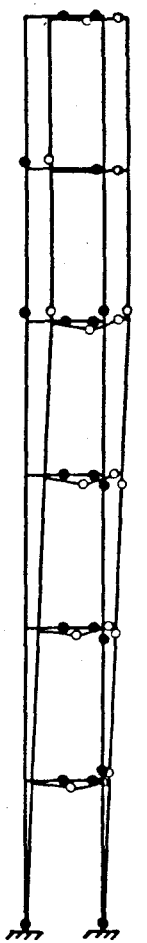

FIG. 2.8 (c)
$\lambda_p = 2.00$

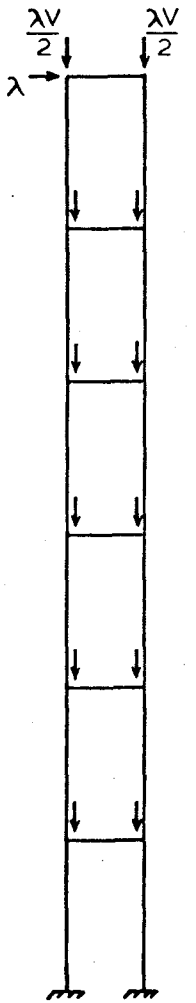

FIG. 2.8 (d)
$\lambda_c = 9.16$

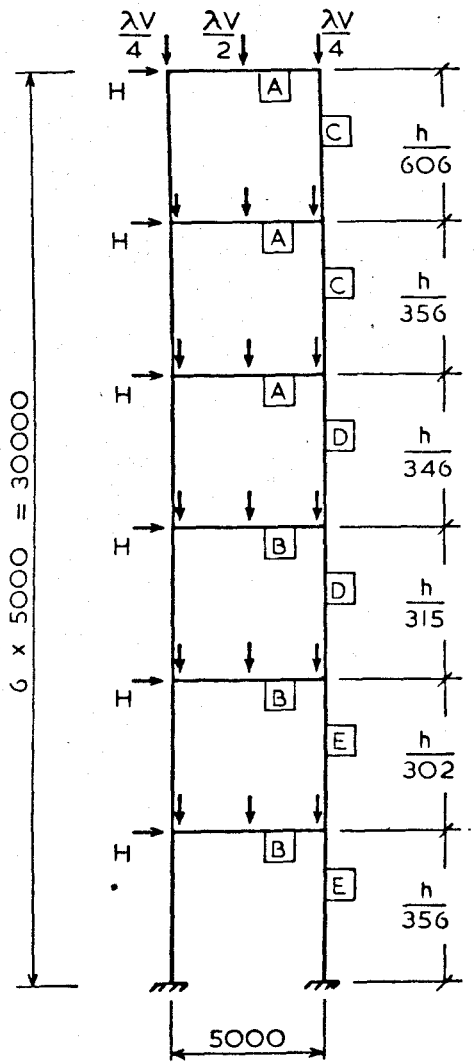

V = 300 KN.

H = 0.02866 λV

FIG. 2.9 (a) FINAL SECTIONS AND SWAY DEFLECTIONS

SECTION	BRITISH SECTION
A	406 x 140 x 39UB
B	457 x 152 x 60UB
C	203 x 203 x 71UC
D	254 x 254 x 73UC
E	254 x 254 x 89UC

NOTE : IDENTICAL LOADING AT EACH FLOOR

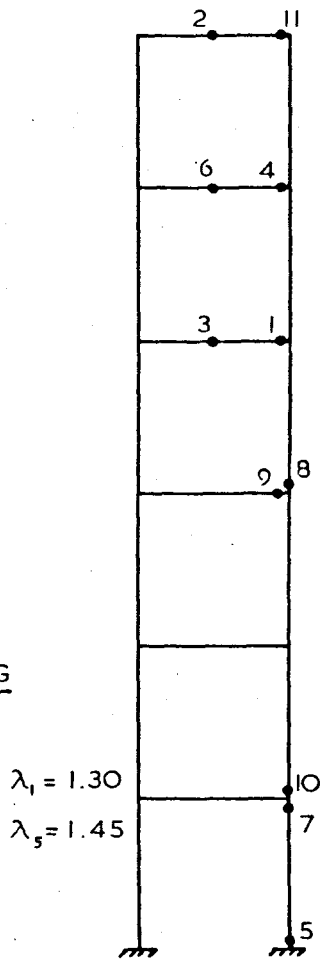

FIG. 2.9 (b)
$\lambda_1 = 1.54$

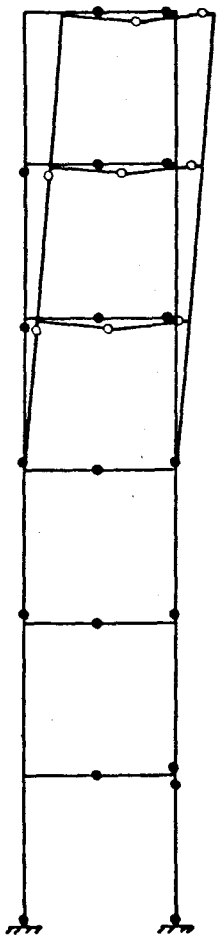

FIG. 2.9 (c)
$\lambda_p = 1.75$

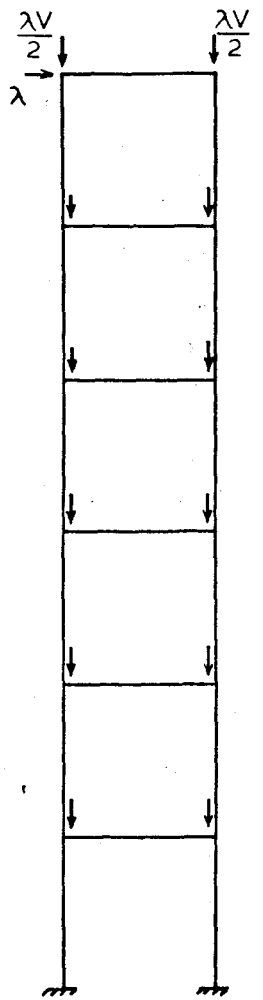

FIG. 2.9 (d)
$\lambda_c = 8.80$

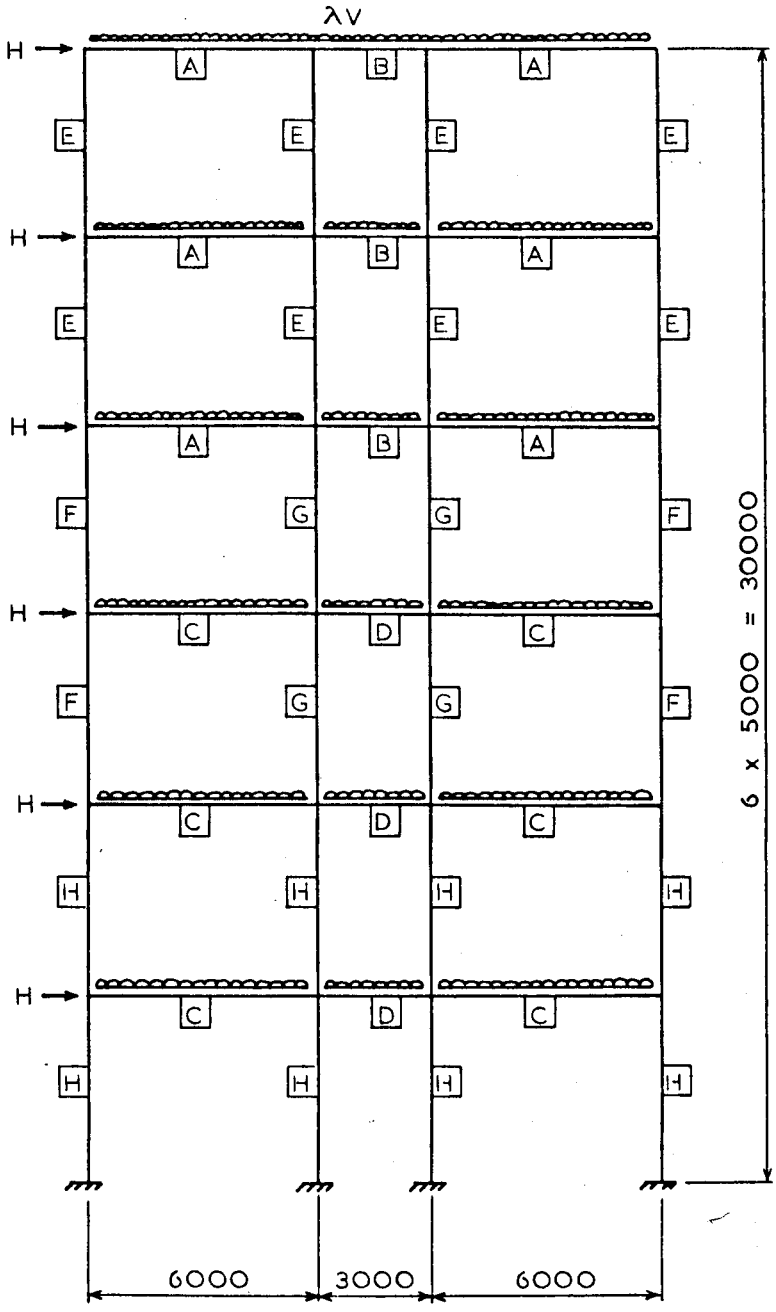

V = 800 KN.

H = 0.02125 λV

λ_f = 1.64

λ_p = 1.93

λ_c = 8.08

λ_1 = 1.25

$\lambda_{col.}$ = 1.44

FIG. 2.10 IRREGULAR BAY FRAME

SECTION	UNIVERSAL SECTION
A	457 x 152 x 52 UB
B	254 x 102 x 22 UB
C	457 x 191 x 67 UB
D	305 x 102 x 33 UB
E	203 x 203 x 71 UC
F	254 x 254 x 73 UC
G	254 x 254 x 89 UC
H	254 x 254 x 107 UC

NOTE : IDENTICAL LOADING AT EACH FLOOR

Loading	Maximum	Minimum
Dead on roof	3.75 kN/m^2	3.75 kN/m^2
Super on roof	1.50	1.50
Dead on floor	4.79	4.79
Super on floor	5.00	2.50
Basic wind speed	50 m/sec	38 m/sec

Table 2.1 Loading Values

4 storey frames		Min. vertical : max. wind						Max. vertical : min. wind					
		λ_1	λ_f	$\frac{\lambda_c}{\lambda_p}$	λ_{mr}	λ_{mrw}	Mech	λ_1	λ_f	$\frac{\lambda_c}{\lambda_p}$	λ_{mr}	λ_{mrw}	Mech
Bay width 7500 mm	2 bay	0.87	1.07	9.15	1.03	1.14	B (9)	0.87	1.04	5.75	0.95	1.04	C
	3 bay							0.93	1.04	5.25	0.95	1.04	S
	4 bay							0.96	1.05	4.93	0.95	1.04	S
	5 bay	0.88	1.04	5.34	0.93	1.01	C	1.00	1.05	4.78	0.95	1.03	S
Bay width 5000 mm	2 bay	1.00	1.30	11.38	1.23	1.34	B	0.94	1.20	6.56	1.07	1.17	B
	3 bay							0.90	1.08	5.37	1.01	1.10	C
	4 bay							0.86	0.92	3.34	0.81	0.88	S
	5 bay	0.91	1.13	5.34	1.07	1.16	C	0.89	0.96	3.19	0.83	0.89	S

Table 2.2 Four Storey Frames

7 storey frames		Min. vertical : max. wind						Max. vertical : min. wind						
		λ_1	λ_f	$\frac{\lambda_c}{\lambda_p}$	λ_{mr}	λ_{mrw}	Mech	λ_1	λ_f	$\frac{\lambda_c}{\lambda_p}$	λ_{mr}	λ_{mrw}	Mech	
Bay width 7500 mm	2 bay	0.87	1.10	12.82	1.07	1.15	B	0.82	1.01	5.66	0.94	1.02	C	
	3 bay							0.78	0.89	4.74	0.82	0.89	C	
	4 bay							0.87	0.97	4.48	0.89	0.96	S	(e)
	5 bay	0.81	0.95	5.06	0.88	0.96	C	0.92	0.99	4.36	0.89	0.96	S	(f)
Bay width 5000 mm	2 bay	1.09	1.39	16.59	1.34	1.42	B	0.88	1.15	7.98	1.09	1.20	B	
	3 bay							0.91	1.04	5.30	0.98	1.07	S	
	4 bay							0.83	0.99	4.11	0.90	0.98	S	
	5 bay	1.04	1.26	5.78	1.14	1.24	B	0.88	1.03	3.98	0.92	1.00	S	

Table 2.3 Seven Storey Frames

10 storey frames		Min. vertical : max. wind						Max. vertical : min. wind					
		λ_1	λ_f	$\frac{\lambda_c}{\lambda_p}$	λ_{mr}	λ_{mrw}	Mech	λ_1	λ_f	$\frac{\lambda_c}{\lambda_p}$	λ_{mr}	λ_{mrw}	Mech
Bay width 7500 mm	2 bay	0.88	1.11	15.33	1.08	1.15	B	0.84	1.01	6.02	0.96	1.05	C
	3 bay							0.81	0.96	4.67	0.88	0.96	C
	4 bay	0.91	1.04	6.57	0.97	1.06	C	0.78	0.91	3.87	0.82	0.89	S
Bay width 5000 mm	2 bay	1.15	1.40	14.90	1.33	1.42	B	0.93	1.10	8.07	1.07	1.18	S
	3 bay							0.93	1.02	6.19	0.95	1.04	S
	4 bay	1.03	1.24	8.23	1.19	1.31	B	0.90	1.02	4.56	0.92	1.00	S

(d)

Table 2.4 Ten Storey Frames

Frame	Bay width (mm)	Vert load	Wind load	λ_1	λ_f	$\frac{\lambda_c}{\lambda_p}$	λ_{mr}	λ_{mrw}	Mech	
4 storey 2 bay	7500	Max.	Intermediate	0.86	1.03	5.82	0.95	1.03	C	
4 storey 3 bay	7500	Max.	Max.	0.81	0.94	5.72	0.89	0.97	S	
4 storey 5 bay	7500	Max.	Max.	0.96	1.03	4.88	0.93	1.02	S	
7 storey 2 bay	7500	Max.	Intermediate	0.79	1.00	6.15	0.94	1.03	C	
7 storey 5 bay	7500	Max.	Max.	0.79	0.89	4.63	0.83	0.91	S	
10 storey 2 bay	7500	Max.	Intermediate	0.87	1.05	8.07	1.02	1.12	B	(b)
10 storey 2 bay	7500	Max.	Intermediate	0.89	1.08	7.64	1.02	1.12	B	(a)
10 storey 3 bay	7500	Max.	Max.	0.89	1.04	6.41	0.99	1.08	B	
10 storey 2 bay	5000	Max.	Intermediate	0.94	1.06	5.78	0.99	1.08	S	(c)

Table 2.5 Various Frames

CHAPTER 3

SEMI-EMPIRICAL METHOD OF DESIGN

3.1 Introduction

The parametric study presented in Chapter (2) confirmed the conservative nature of the Merchant-Rankine formula when realistic combinations of horizontal and vertical load were applied. In some cases, though, the formula is so conservative that the Merchant-Rankine failure load could be below the load level at which the first plastic hinge forms in a computer analysis.

Wood(50) proposed a modified relationship to make some allowance for strain-hardening and stray composite action. This form of the equation will also offset the tendency to underestimate the load level at failure. It has been stated in Design Recommendations(54,55) that the modified formula should be used only when rigid-plastic collapse is by a combined mechanism, and the parametric studies given in Chapter (2) showed that failure using this formula varied between 97% and 104% of computer result when this restriction was observed.

In practice, the designer will frequently wish to analyse a trial set of sections which already satisfy criteria such as adequate stiffness at working load, and a combined mechanism cannot therefore be guaranteed. When the rigid-plastic collapse mode was unrestricted, the study showed that the modified failure load could

now exceed the computer result by as much as 7%. This overestimate was accepted because the modified form strictly applies only to clad buildings, whilst the computer analyses were on bare frames and strain-hardening was neglected.

It is recognised, though, that some engineers will prefer not to rely on strain-hardening and cladding to ensure adequate strength, and also that certain kinds of structure have minimal composite action. Therefore, the need arises for the development of an empirical method for estimating the failure load.

This Chapter attempts to seek an alternative expression for the failure load which will retain the simplicity of the Merchant-Rankine approach, but will provide closer agreement with computer analyses on bare frames, irrespective of the shape of the rigid-plastic collapse mechanism. Whereas Wood(50) used a single factor of 0.9 to allow for the beneficial effects of strain-hardening and composite action (as well as the conservative tendency of the original Merchant-Rankine formula), such effects may best be included as optional items to enhance the basic strength of the frame at the designer's discretion.

3.2 Deteriorated critical loads of frames

Wood(50) demonstrated that the tangential rotational stiffness, of beams bending in symmetrical double curvature, reduces from $3k_b$ to $0.75k_b$ when a pin is inserted at one end of the beam (k_b being defined as the nominal beam stiffness I_b/L_b). A pin inserted at mid-span, coinciding with a point of contraflexure in

the original buckling mode, does not affect the rotational stiffness of the same beam. When a second pin is inserted, the rotational stiffness becomes zero.

An analogy can be made with a full plastic hinge rotating in the same direction at constant moment. The contribution of a beam with two such hinges towards the overall frame stiffness is similarly zero. When such beams are present at consecutive floors of a multi-storey frame, the effect on stiffness can be visualized; the columns are converted to free-standing 'poles' of length greater than the original column length.

Frame instability is not confined to any individual member but concerns the overall behaviour of a frame. Wood(26) proposed the term 'deteriorated' critical load, λ_{det} which controls and defines frame instability, and is the critical load at which the overall stiffness of the remaining elastic parts of the structure becomes zero. It follows that the 'deteriorated' critical load of a structure with a mechanism of hinges is zero. However, it was recognised that because of instability effects, it may not be necessary for there to be a complete mechanism of hinges in the frame for the stiffness to be reduced to zero.

As an example, consider the well-designed four storey rigid-jointed single bay frame of Wood(26) shown in figure (3.1). The frame is subjected to combined horizontal and vertical loading. The sway deflections at working load ranged between h/503 to h/1134, well within the usual limits for a bare frame. 'Deteriorated' critical loads were calculated by Wood(26) for

various possible combinations of plastic hinge locations as shown in figures (3.1 (a)) to (3.1 (f)). They have been recalculated by the present author during a study of the deterioration of frame stiffness. The minimum design load factor for rigid-plastic collapse of the frame was also given by Wood as 2.15. It is noted that the loads used in this example are based on an overall load factor. Therefore, a load factor of unity corresponds to the working load.

To calculate the 'deteriorated' critical load, the plastic hinges were replaced by inserting idealised pins at the corresponding positions in the frame. In each case, the system of loads acting on the frame was identical to that shown by figure (3.1 (a)). The frame was excited at the roof level by a small disturbing force. A non-linear elastic computer program was used under increasing load to obtain the load/displacement curves. At a certain multiple of the load factor, loss of equilibrium occurs when the external disturbing force, however small, will give rise to theoretically infinite displacement. The stiffness of the frame has been reduced to zero and the 'deteriorated' critical load, λ_{det} , has therefore been found.

The original elastic critical load was found to be 12.9. This value indicates that instability effects at the working load were insignificant. When a pin is inserted at mid-span of the third floor beam, the 'deteriorated' critical load, λ_{det} , remains unchanged from the original critical load. This validates the comment made above that a pin occurring at a point of contraflexure will not affect the tangential rotational stiffness of a member.

The elastic buckling mode for unbraced frames inevitably involves sidesway. The corresponding load/displacement curve(a) is shown which tends to infinity at the elastic critical load. A number of curves for different combinations of pin patterns can therefore be obtained.

For example, the pattern of pins shown in figure (3.1 (e)) causes λ_{det} to drop to approximately one-fifth of the original critical load. This is not surprising because the three lower column lengths, with no intermediate restraints from beams, have been converted to a single length of three times the storey height. Finally, the last pattern of pins gave a value of the 'deteriorated' critical load of 2.0. The corresponding load/displacement curve(f) is plotted as shown. Other combinations of pin patterns lead to values of λ_{det} that may be higher or lower than those shown. From the pattern of pins shown in figure (3.1 (f)), it becomes clear that a collapse mechanism is unlikely to occur, thus preventing the rigid-plastic collapse design load of 2.15 being reached.

To verify the concept of 'deterioration' of frame stiffness, a non-linear elasto-plastic analysis was carried out on the frame of Wood. The complete load/displacement behaviour is shown in figure (3.2). Each point on the curve corresponds to the order of plastic hinge formation shown by the frame in the figure. The sequence is shown ringed in the upper diagram and the load levels at which these plastic hinges formed are shown on the curve.

Failure occurred at a load level of 1.91 corresponding to the

pattern of pins shown in figure (3.1 (f)). At this stage, the residual stiffness is represented by its 'deteriorated' critical load of 2.0, which is very close to the current value of the rising load factor, λ , on the applied loads. Above a load level of 1.91, the non-linear elasto-plastic analysis program was unable to locate any further hinges whilst still maintaining equilibrium, and collapse was assumed to have been reached.

At this load level of 1.91, several partially-plastic zones were observed in the computer analysis. The location of these zones correspond to those indicated by Wood(26). Ratios of the appropriate moments at these zones are shown as follows,

Location	M/M(yield)	M/M_p
a)Roof beam - mid span	1.09	0.95
b)Third floor beam - leeward end	1.04	0.91
c)Second floor leeward column		
i)Top end	1.22	0.89
ii)Lower end	1.17	0.86

where M = bending moment,

$M(yield)$ = yield moment = $(1-n).Z_e.f_y$,

M_p = reduced plastic moment of member,

n = ratio of axial force to squash load,

Z_e = Elastic modulus,

f_y = yield stress.

It is noted that the values for $M_p/M(yield)$ for the column are unusually high. This is because both M_p and M(yield) have been

reduced due to axial load. Assuming these zones in turn as idealised pins, in addition to those shown in figure (3.1 (f)), and following the procedure described above, the 'deteriorated' critical loads were determined. It was found that all the values of λ_{det} were less than 1.60. This confirms the above elasto-plastic computer analysis and the non attainment of the rigid-plastic collapse mechanism discussed earlier.

The foregoing study has been adopted as a basis for obtaining a deterioration function to predict the failure load of elastic-plastic plane frames. A close approximation of the failure load can be obtained from λ_{det} if the positions of plastic hinges, such as those indicated in figure (3.2) by elasto-plastic analysis, are reproduced. The opportunity to examine such a proposal is given by the results presented in Chapter (2). The previous Chapter provides the necessary information on the position and load factor at which each plastic hinge forms in a non-linear elasto-plastic analysis. Accurate values of the rigid-plastic collapse load are also available.

In order to calculate the 'deteriorated' critical load corresponding to the sequence of plastic hinge formation, the existing non-linear elastic computer program(41) has been modified. In its unmodified form, the computer program was used in Chapter (2) to calculate the elastic critical load only. This becomes time-consuming because several non-linear analyses are required to determine an initial value close to the critical load. As there were many frames to be examined, a rapid procedure was desirable to estimate close bounds to the elastic critical load and successive

'deteriorated' critical loads.

The procedure adopted takes the form given by the flow-chart shown in figure (3.3). Majid(23) suggested an approximate method for evaluating λ_c by considering the load-displacement behaviour of the linear and non-linear response of a fully-rigid frame. In the following derivation, it can be shown that a close approximation of the elastic critical load and successive 'deteriorated' critical loads can be obtained by one linear and non-linear analysis of the frame.

The well-known displacement amplification factor is given by,

$$\Delta_{\text{non-linear}} = \frac{\Delta_{\text{linear}}}{1 - \lambda/\lambda_c} \qquad (3.1)$$

Let the load factor, $\lambda = 1.0$. Therefore,

$$\Delta_{\text{non-linear}} = \frac{\Delta_{\text{linear}}}{1 - 1/\lambda_c}$$

$$\frac{\Delta_{\text{linear}}}{\Delta_{\text{non-linear}}} = 1 - \frac{1}{\lambda_c}$$

$$\frac{1}{\lambda_c} = 1 - \frac{\Delta_{\text{linear}}}{\Delta_{\text{non-linear}}}$$

Rearranging gives the elastic critical load as,

$$\lambda_c = \frac{\Delta_{\text{non-linear}}}{\Delta_{\text{non-linear}} - \Delta_{\text{linear}}} \qquad (3.2)$$

It is proposed to adopt equation (3.2) to estimate an initial value of λ_c. Equation (3.2) can similarly be used to estimate close bounds of λ_{det}, simply by replacing λ_c by λ_{det} in equation (3.1), and proceeding in the manner described above.

It follows that there are as many critical loads as the number of storeys in a frame because each joint displaces relatively in a storey. In all examples, the frames were excited by a single horizontal force at roof level. The value of λ_c or λ_{det} was taken as the lowest value of all the individual critical loads for each storey and the frame reanalysed to the required degree of accuracy as indicated by the flow-chart in figure (3.3). It is noted that the critical loads were taken as the value characterised by large deflections in Chapter (2). This criterion has been adopted, in addition to calculating the value of the determinant at the corresponding load level in the program. This provide an additional check on the lowest critical load in case it is missed. For convenience, figure (3.3) is shown for the latter criterion only.

As an example on the use of equation (3.2), consider Wood's four storey frame shown in figure (3.1). The 'deteriorated' critical loads for each storey were calculated at working load from the relative linear and non-linear sway displacements. In all cases, the relative linear and non-linear elastic displacements were taken at the windward joint at each floor level. The values of λ_{det} for each storey are shown in figure (3.4) for a range of possible pin combinations. The non-linear elastic computer program was used in each case with the loading given in figure (3.1 (a)). The lowest value of λ_{det} is a good estimate of the accurate

result. The accurate results were obtained iteratively using the proposed computer program. These values were calculated to an accuracy of one decimal place. For comparison, Wood's results are also shown. It can be seen that the values of λ_{det} calculated from the deflections at unit load factor provide good bounds to the accurate results.

3.3 Deterioration of stiffness

As real pins are inserted in a frame at discrete positions corresponding to the sequence of plastic hinge formation in an accurate elasto-plastic analysis, the deterioration of stiffness can be expressed non-dimensionally as an interaction between elastic instability and plasticity as shown by the axes in figure (3.5). Failure is taken to occur when the reducing value of λ_{det} equals the rising load, λ .

To illustrate the interaction of the loss of stiffness under increasing plasticity, two typical results are shown in figure (3.5). The order and load level at which plastic hinges formed are indicated. Values of 'deteriorated' critical loads are shown alongside corresponding to the hinge patterns. The four storey frame of Wood(26) shown in figure (3.1) is also included in the plot. The vertical axis of λ_{det} and λ_c were obtained by the computer program described earlier while the non-dimensional abscissa of λ and λ_p were obtained by the non-linear elasto-plastic analysis program. The 'deteriorated' critical load, λ_{det} only changes when a new plastic hinge forms but these points have been joined by a continuous line to represent a gradual reduction

in frame stiffness. It should be noted though that cases can arise in which λ_{det} remains constant. This is shown by the frame of Wood. The first plastic hinge formed at mid-span, and as explained earlier this does not cause a reduction in the elastic critical load.

It can be seen from figures (3.2) and (3.5) that the three frames failed before the rising load reached the rigid-plastic collapse load. An expression for the failure load has been obtained by seeking a smooth curve to fit these results. It is proposed that the following expression be adopted,

$$\frac{\lambda}{\lambda_p} = \left[1 - 0.4\ \frac{\lambda_p}{\lambda_c}\right]\left[1 - \left(\frac{\lambda_{det}}{\lambda_c}\right)^2\right] \qquad (3.3)$$

When this is plotted for the four storey frame given at the top of figure (3.5), the bold line shown in the diagram is obtained. It can be seen that this is a reasonable representation of the deterioration of stiffness, particularly after the first two hinges have formed. As collapse occurs when the rising load factor, λ equals the 'deteriorated' critical load, λ_{det} , the failure load is found by solving the quadratic for λ ,

$$\frac{\lambda}{\lambda_p} = \left[1 - 0.4\ \frac{\lambda_p}{\lambda_c}\right]\left[1 - \left(\frac{\lambda}{\lambda_c}\right)^2\right] \qquad (3.4)$$

where λ so calculated is the failure load and λ_c and λ_p are the lowest elastic critical load and rigid-plastic collapse load respectively.

The significant difference between the Merchant-Rankine approach

and the proposed expression is that the curve is able to adjust its position to any ratio of λ_c/λ_p , as shown in figure (3.6). Thus, each frame has its own unique failure curve which is related to its ratio of λ_c/λ_p. A high value of λ_c/λ_p implies a stiff design, and the proposed expression permits the curve to move to the right, as appropriate to such design. With a low value of λ_c/λ_p , the frame would be susceptible to early collapse due to the rapid deterioration of frame stiffness. The proposed expression allows for this by shifting the curve to the left. This movement is achieved by the term $(1 - 0.4\ \lambda_p/\lambda_c)$ in the expression.

It can be seen from figure (3.5) that there is a rapid deterioration in the actual behaviour as λ_{det} approaches the rising load factor, λ . Examples of such behaviour are shown for the three frames in figure (3.5). In Wood's example, it was evident that soon after the third plastic hinge was developed, λ_{det} dropped rapidly for a small rise in the load factor as shown in figure (3.5) and figure (3.2) respectively. Figure (3.5) also shows the plunging steep slope for the last few remaining plastic hinges in all the frames. Such behaviour is obtained from the proposed formula by the term $[1 - (\lambda/\lambda_c)^2]$.

Finally, the coefficient of 0.4 has been chosen to give close agreement between λ given by equation (3.4) and failure loads, λ_f , given by computer, but it can be seen from figure (3.5) that the proposal also gives an approximate representation of the deterioration of stiffness once hinges begin to form. Wood's frame is an exception because the first hinge leads to no reduction in the 'deteriorated' critical load. However, as most frames

collapse in the vicinity of the bottom right hand corner of figure (3.5), it is not necessary to consider the initial portion of the curve unless the ratio of λ_c/λ_p is small.

Studies carried out in Chapter (2) have shown that the original Merchant-Rankine formula consistently tends to provide a better estimate of the accurate failure load for frames with high ratios of λ_c/λ_p (> 9) and the modified version tends to overestimate the failure load. In contrast, the original formula was very conservative for frames with low ratios of λ_c/λ_p (< 6) while the modified version provides a better estimate of the failure load. The results showed that the failure loads of approximately 60% of the frames were overestimated by the use of the modified formula. The reason can be seen by examining the area formed by a square at the bottom right hand corner of figure (3.6 (a)) and bounded by the values of λ_c/λ_p equal to 4.0 and 10.0; the failure loads of most of the frames examined in Chapter (2) fall within this region.

Various ratios of λ_c/λ_p have been drawn in figure (3.6 (a)) radiating from the origin (0,0). Several of the proposed curves corresponding to various ratios of λ_c/λ_p are also shown. These curves and the Merchant-Rankine relationships are failure lines obtained by letting λ equalled to λ_{det} . The behaviour of the Merchant-Rankine approach can therefore be described as a continuous linear descending function, for which the loss of elastic stiffness is directly proportional to stages of increasing plasticity. The modified formula deteriorates in a similar manner but the magnitude of plasticity differs from the original formula

because of the introduction by Wood of a factor of 0.9.

Consider the positions (A) and (B) with λ_c/λ_p=4.0 on the original Merchant-Rankine formula and the modified version respectively. To counteract the conservative tendency of the original formula, the failure load should be given by a point such as (C), close to the modified formula. A similar situation arises for high values of λ_c/λ_p and a point such as (F) is required, further away from the modified formula to provide an accurate result. A compromise factor of 0.95 in the modified formula, instead of the present value of 0.9, would be unsatisfactory because this would cause an approximate percentage reduction, no matter what the value of λ_c/λ_p .

The proposed expression for the failure load has been plotted for ratios of λ_c/λ_p equal to 4, 10 and infinity to illustrate its flexibility. The positions of the proposed curves vary with the ratio of λ_c/λ_p, thus offsetting the inclination to overestimate or underestimate the failure load in comparison to the Merchant-Rankine formula. This is exhibited by positions (C) and (F) for low and high ratios of λ_c/λ_p respectively in figure (3.6 (a)).

3.4 Comparison with model experiments

Experiments on model structures have been conducted by Low(48), Salem(45) and Ariaratnam(49). These provide an opportunity to compare the results of the proposed semi-empirical expression to those obtained experimentally. Unfortunately, only the results of

the tests by Low(48) were published and these alone will be considered.

The miniature models were three, five and seven storey, single bay frames of rectangular configuration. All the frames were of equal storey height and the bay width was twice the height of one storey. Most of the frames were subjected to combined horizontal and vertical loads, although some were subjected to vertical loads only. Vertical loads were applied at the quarter points on all the beams for both combined loading and the case of vertical load alone. Horizontal loads were applied as appropriate at each of the floor levels for frames under combined loading.

The results of these frames are shown in tables (3.1 (a)) and (3.1 (b)) for the combined loading and vertical load alone respectively. The failure loads calculated from equation (3.4) are denoted by $\lambda_{prop.}$ and the experimental results by λ_{expt} . A histogram has been constructed for all the frames as shown in figure (3.7). This relates the number of frames to the error in the predicted failure load, expressed as a percentage of the experimental failure loads. Except for a few cases, almost all the results obtained by the three expressions, namely Merchant-Rankine, Merchant-Rankine-Wood and the proposed expression, underestimated the experimental values. The histogram in general displayed similar predictions of the failure load using the proposed expression and the modified Merchant-Rankine formula.

As the experiments were conducted primarily to verify the original Merchant-Rankine formula and to demonstrate the phenomenon

of frame instability, it is instructive to examine the relative comparison of the failure loads given in tables (3.1 (a)) and (3.1 (b)). Low(48) reported that only one, Frame (31), out of a total of thirty-four frames tested was unsafe using the Merchant-Rankine formula but by no more than 1%. This is clearly shown in the figure (3.7). Frame (31) was reported to have a maximum out-of-plumb of 1/160th of the ground storey prior to the loading test.

Frame (24) was also reported to have an initial distortion of 1/120th of a storey height but the predicted failure load using the Merchant-Rankine formula was marginally safe. Such initial distortion is considered excessive but it can be seen that the Merchant-Rankine formula provides safe estimates throughout. However, the figures in table (3.1 (b)) suggest that the Merchant-Rankine formula can be very conservative when no side load is present, irrespective of the ratio of λ_c / λ_p. For such frames, both the proposed expression and the modified formula also underestimated the experimental results in all cases.

With reference to both tables (3.1 (a)) and (3.1 (b)), it is noticed that the ratios of λ_c / λ_p for all the frames, particularly the taller models, are small in an attempt to highlight frame instability. In Design Recommendation(54), the modified Merchant-Rankine formula is not valid for such low ratios of λ_c / λ_p. However, despite this, λ_{mrw} is included for comparison. In all cases where the ratio of λ_c / λ_p exceeds 1.6, the proposed expression provides better agreement than the original formula. At the same time, it also maintains close agreement with the modified

Merchant-Rankine formula, which in general is very successful in predicting the experimental failure loads.

Two frames, numbers (20) and (31), were overestimated using equation (3.4) by 1% and 7% respectively. The unsafe estimate of Frame (31) arises for the reason discussed above. The 1% unsafe estimate exhibited by frame (20) is insignificant. These features are clearly indicated in the histogram given in figure (3.7).

For frames in which $\lambda_c/\lambda_p < 1.6$, the original Merchant-Rankine formula and the proposed expression provide extremely good estimates of the experimental results under combined loading, whilst the modified version tends to exceed the latter results. When the ratio of λ_c/λ_p is less than 1.2, the failure load given by the proposed expression falls below the Merchant-Rankine load irrespective of whether the frames were subjected to combined loading or vertical load alone. The reason is that the proposed expression 'crosses' over the linear Merchant-Rankine line for very low values of λ_c/λ_p as shown in figure (3.6 (b)). These cases have been drawn accordingly. The shaded wedge shows the area bounded by the two relationships. Two wedges are shown to indicate the proposed failure load falling below the Merchant-Rankine failure load. It can be seen that for a small increase in the ratio of λ_c/λ_p such as the curve shown equal to 1.6, estimates of the failure load using equation (3.4) are above the Merchant-Rankine failure line.

3.5 Parametric studies and other comparisons

The parametric study presented in Chapter (2) and used to examine the Merchant-Rankine formula will also demonstrate the accuracy of the proposed equation (3.4). It is worth reiterating that the frames all satisfied a limit of 1/300th of each storey due to unfactored wind load. Loading generally consisted of extreme values of the ratio of vertical to horizontal load, although some intermediate values were also considered.

The results are summarised in tables (3.2) and (3.3). The failure loads given by the proposal are denoted by $\lambda_{prop.}$ and the computer results by λ_f . The rigid-plastic collapse mode is designated by B, S and C indicating simple beam mechanism, column sway and combined mechanism respectively. As two bay widths were considered in the parametric studies, the symbol W and N refers to wide (7500 mm) and narrow (5000 mm) bay widths.

Comparisons show that the proposed expression exceeds the computer results by a maximum of only 3% compared to 7% by the modified Merchant-Rankine approach. Both values are indicated by a ten-storey frame in table (3.2) by an asterisk. A similar situation arises for a four-storey frame where λ_{mrw} and $\lambda_{prop.}$ overestimated λ_f by 7% and 1% respectively. In contrast, both λ_{mrw} and $\lambda_{prop.}$ underestimated λ_f by a maximum of 7% but this was a frame for which λ_c/λ_p was just 3.19, indicated by a square symbol. It has been proposed in Design Recommendations(54,55) that λ_{mrw} should not be used when λ_c/λ_p is less than 4.0. Observing this restriction, λ_{mrw} and $\lambda_{prop.}$ give a maximum underestimate of 3%

and 5% respectively. These cases are indicated by a triangle in table (3.2).

Although extreme errors have been compared, a closer examination of the total of 43 results indicates that the proposal is able consistently to estimate more accurately the computer results than λ_{mrw} . Take for example, the frames indicated by a spot in tables (3.2) and (3.3). They all collapse by simple beam mechanism with λ_c/λ_p between 6.4 and 15.3. Equation (3.4) provides better and more uniform estimates of the computer result. Similarly, for lower ratios of λ_c/λ_p , indicated by a circle, consistently good estimates of the computer results are shown.

A histogram has been constructed to show the variation of the estimates using the three approaches. This is shown in figure (3.8). The histogram displays the conservative tendencies inherent in the original Merchant-Rankine formula. It can be seen that none of the forty-three results examined were overestimated using such an approach. In contrast, the modified version which is strictly applicable to clad buildings showed that the failure load was overestimated for a number of frames.

The results shown by the proposed expression were consistently good throughout with most of the frames falling between 95% and 103% of the accurate failure load. The frequency distribution of the frames appeared to be closer to computer results than the results of the two versions of the Merchant-Rankine approach. It is noted that in all cases examined, $\lambda_{prop} > \lambda_1$, where λ_1 is the load factor at which the first plastic hinge forms in an accurate

elasto-plastic computer analysis.

Other frames from the literature provide further comparison between λ_{mrw} , $\lambda_{prop.}$ and the results of non-linear elasto-plastic computer analysis. The results are shown in table (3.4), the load factors now being multiples of the working loads. Equation (3.4) showed a maximum deviation of +4% from the computer results, while λ_{mrw} overestimated λ_f by 9%.

The cases in which the 9% error occurred are indicated by double asterisk. In defence of the Merchant-Rankine-Wood formula, it should be noted that both frames had sway deflections at working load which exceeded the usual limit of 1/300th of each storey height. Indeed, the roof beam of the second example in table (3.4) was simply supported to enable small column sections to be used. However, it can be seen that equation (3.4) was able to deal with these difficult cases in a significantly more satisfactory manner.

It was found that in the majority of these cases, the error resulting from the use of equation (3.4) was approximately half the error generated by the modified Merchant-Rankine formula.

3.6 Effect of the value of the coefficient on the proposed formula

As the coefficient of 0.4 is increased in equation (3.4), a corresponding reduction in the predicted value of the failure load is observed. It has been mentioned previously that the proposed

value was selected to give close estimates of computer results. A total of 85 frames were compared which showed good agreement with both computer and experimental results.

To investigate the sensitivity of the value of the coefficient, two values of 0.30 and 0.35 were substituted in turn to estimate the failure load given by equation (3.4). These will increase the value of the failure load estimated by the proposed formula. They could be of use if a designer wished to take account of cladding stiffness or strain-hardening by deliberately underdesigning the bare frame.

The results are given in tables (3.5) to (3.8). Two columns representing the coefficient of 0.30 and 0.35 are designated by $\lambda_{0.30}$ and $\lambda_{0.35}$. Each table has the exact format corresponding to tables (3.1) to (3.4).

Tables (3.5 (a)) and (3.5 (b)) shows the comparison of model frames subject to combined loading and vertical load alone to experimental results respectively. It can be seen in table (3.5 (a)) that the proposed expression has now overestimated a number of cases compared to Low's experimental results for frames under combined loading, even when 0.35 was used. It was also observed that the estimate is not very sensitive to changes in the coefficient.

In contrast, the frames subjected to vertical loads alone indicated that the estimated failure loads were still very conservative using a coefficient of 0.3, as shown in table

(3.5 (b)). However, when the coefficient of 0.1 was substituted into equation (3.4), the predicted failure load was in good agreement with experimental results. This is shown by the third column in table (3.5 (b)).

It is proposed that the coefficient of 0.1 be adopted to estimate the failure load of frames subject to vertical loading only. A histogram using such a factor on the 14 model frames is shown in figure (3.9 (a)). The results obtained by both versions of the Merchant-Rankine approach is also shown for comparison. It can be seen that only one frame was overestimated by 1%. The results showed that by using a coefficient of 0.1, the failure loads for three-quarters of the frames were estimated to within 95% of experimental results. It should be noted that the estimated failure loads were in good agreement with experimental results irrespective of the value of λ_c/λ_p .

The parametric studies under combined loading given in tables (3.6) and (3.7) showed that $\lambda_{0.35} < \lambda_{mrw}$ in all cases when frames with $4 < \lambda_c/\lambda_p$ are ignored. However, when $\lambda_{0.30}$ was compared, a number of values exceeded λ_{mrw} . These cases are indicated by a circle in table (3.6) but the difference is insignificant. A histogram showing the two coefficients of 0.30 and 0.35 has been constructed and shown in figure (3.9 (b)). The bottom diagram in figure (3.9 (b)) was redrawn from figure (3.8 (c)) for direct comparison. It can be seen that the estimates are not very sensitive to variations in the coefficient.

Similarly, table (3.8) exhibits the same behaviour when the

frame with the low ratio of λ_c/λ_p was ignored. As a result, the extreme errors quoted previously in section (3.5) remain unaffected.

In conclusion, these studies show that the use of a factor of 0.30 overestimate the failure load of the experimental bare frames subject to combined loading by a maximum of 12.0%. With 0.35, the overestimate falls to 9.0% for the same frame. For realistic frames, the errors were 5.6% and 4.9% corresponding to the above coefficients respectively. For frames subjected to vertical load alone, a factor of 0.1 was proposed, with only one experimental frame overestimated by 1%.

3.7 Application in practice

The comparisons given above have shown the proposed expression being used as an analysis tool with λ determined by solution of equation (3.4), once λ_c and λ_p are known. As accurate comparisons were required to validate the expression, λ_c and λ_p were determined from suitable computer programs. Such programs may not be readily available to the designer and therefore alternative manual methods are needed for the rapid evaluation of λ_c and λ_p . Several methods for calculating both λ_c(50-53) and λ_p(12,17,22) are available. The following procedure is believed to be the most satisfactory for manual design, and is adopted for an example to be shown in the next section.

The most convenient procedure is to take the minimum required design load, λ , as the specified load level for collapse. Using

factored loads as the basis for design, λ will therefore be unity. The elastic critical load, λ_c , for a trial frame can be easily determined to good accuracy from charts given in Design Recommendations(54,55) and by Williams(73). For the required design loads, the rigid-plastic collapse load can then be found by solving equation (3.4) for λ_p. In this manner, an exact calculation of the rigid-plastic collapse load of a trial design can often be avoided. With λ =1.0, equation (3.4) can be rearranged to express λ_p in terms of λ_c,

$$\lambda_p = 1.25 \ \lambda_c(1 - \varepsilon) \qquad (3.5)$$

where $$\varepsilon = \sqrt{1 - \frac{(1.6\ \lambda_c)}{(\lambda_c^2 - 1)}}$$

Equation (3.5) is shown graphically in figure (3.10), safe designs being above the solid line. The Merchant-Rankine formula and its modified version are also plotted. It can be seen that the proposed method gives results which are very similar to λ_{mrw} for low values of λ_c/λ_p , where λ_{mrw} has been found to be particularly successful from the parametric studies described in Chapter (2) and shown in tables (3.2) and (3.3). For higher values of λ_c/λ_p, the modified formula is too optimistic.

Figure (3.10) illustrates that the proposed method successfully caters for this, by requiring higher minimum values of λ_p in order to attain the design load. Two values of λ_c/λ_p have been included to indicate the extent to which λ_{mrw} is applicable. It can be seen that when the value of λ_c/λ_p is greater than 10, λ_{mrw} is taken as λ_p . A cut-off point is shown as a horizontal line

while the proposed expression continues as an asymptote.

3.8 Design example

This design example is presented in detail to demonstrate the manual process using the proposed expression and design criteria outlined in Chapter (2) and in this Chapter.

Consider the six storey two bay frame shown in figure (2.6 (b)) which satisfies the deflection limit of 1/300th of each storey height. Following the preliminary guidance provided by the proposed design charts presented in Chapter (2), the design shown in figure (2.6 (b)) was obtained using the methods of Anderson and Islam(59) and Wood and Roberts(50). This design will now be checked for adequate strength.

Design Recommendations(54,55) permit the calculation of the elastic critical load using a substitute Grinter frame. This is shown in figure (3.11). As discussed in Chapter (1), the basis of the substitute Grinter frame is to assume all joint rotations to be approximately equal at any floor level when the real frame is subject to horizontal loads, and each beam restrains a column at both ends. Beams are therefore bent into approximate double curvature and at any storey, the effective stiffness of the beam in the substitute frame is,

$$k_b = 2 \Sigma 1.5 I_b/L_b \qquad (3.6)$$

where I_b and L_b are respectively the moment of inertia and span of

a beam in the real frame and the summation is over all the bays at that storey level.

The equivalent stiffness of the column in the Grinter frame is the sum of the stiffnesses of the individual columns in the real frame for the storey under consideration,

$$k_c = \Sigma I_c \text{ / storey height} \qquad (3.7)$$

where I_c is the moment of inertia of the column.

These values have been calculated for the six storey frame as follows,

storey	k_b (cm^3)	k_c (cm^3)
6	3x(2x4439)/600 = 44.4	3x4564/375 = 36.5
5	3x(2x7162)/600 = 71.6	" " = 36.5
4	" " = 71.6	(2x6088 + 14307)/375 = 70.6
3	3x(2x12091)/600 = 120.9	" " = 70.6
2	3x(2x18626)/600 = 186.3	(2x7647 + 14307)/375 = 78.9
1	" " = 186.3	" " = 78.9

(3.8)

Values of k_b and k_c are shown in figure (3.11). A first estimate is made of λ_{cr} with allowance for continuity of columns. The following calculations were obtained from the procedure detailed in the European Recommendation(54),

storey	η_u	η_l	$\nu = \Sigma P.h^2 / \Sigma I_c$	l_k/l	λ_{cr}	
6	0.45	0.50	0.39	1.41	26.1	
5	0.50	0.60	1.00	1.56	8.31	
4	0.60	0.54	0.83	1.59	9.64	(3.9)
3	0.54	0.45	1.14	1.46	8.33	
2	0.45	0.46	1.30	1.38	8.17	
1	0.46	0.00	1.58	1.19	9.04	

where

η_u = distribution factor for the upper joint

$= (k_c + k_{cu}) / (k_c + k_{cu} + k_{bu})$,

η_l = distribution factor for the lower joint

$= (k_c + k_{cl}) / (k_c + k_{cl} + k_{bl})$,

ΣP = Total vertical load at any storey in KN.,

h = storey height in metres,

ΣI_c = Total column inertia of storey considered in cm^4 ,

l_k/l =values read off chart with cladding stiffness, $\bar{s} = 0$,

The values of l_k/l are the effective length ratios using the modified degrees of restraint given above by η_u and η_l to allow for continuity in the substitute Grinter frame (or $\sqrt{P_e/P_c}$ where P_e and P_c are the Euler and critical loads respectively),

$\lambda_{cr} = 20.23/[\nu . (l_k/l)]$.

Note that λ_{cr} was calculated based on the value of Young's modulus of elasticity, $E = 20500$ KN/cm^2 for this example only.

The factor of 20.7 used in European Recommendation(54) assumed $E = 21000$ KN/cm^2 .

It can be seen that the second storey is most critical with λ_{cr} =8.17. An improved estimate of λ_{cr} may be obtained by considering the upper and lower storeys adjacent to the critical storey,

$$\eta'_u = \eta_u \left[(k_{cu} + k_c) / (2k_c)\right]$$

$$= \frac{0.45 \times (70.6 + 78.9)}{(2 \times 78.9)} = 0.43 \qquad (3.10)$$

$$\eta'_l = \eta_l \left[(k_{cl} + k_c) / (2k_c)\right]$$

$$= \frac{0.46 \times (78.9 + 78.9)}{(2 \times 78.9)} = 0.46$$

$$\lambda_c = \lambda_{cr}\left[\frac{1 + \eta'_u + \eta'_l}{1 \quad \eta'_u \frac{\lambda_{cr}}{\lambda_{cru}} \quad \eta'_l \frac{\lambda_{cr}}{\lambda_{crl}}}\right]$$

$$\therefore \lambda_c = 8.17 \times \left[\frac{1 + 0.43 + 0.46}{1 + 0.43(8.17/8.33) + 0.46(8.17/9.04)}\right] = \underline{\underline{8.40}}$$

where k_{cu}, k_c and k_{cl} are indicated in figure (3.11) and λ_{cru}, λ_{cr} and λ_{crl} are the critical loads for the upper, middle and lower storeys given by the above calculations.

This improved value is greater than 8.31 given for the fifth storey and therefore the lowest elastic critical load is taken as 8.31.

Alternatively, a rapid calculation for λ_c may be obtained by the method of Williams(53). The procedure was outlined in Chapter (1) but at this stage, it would be useful to illustrate the swiftness of the method and compare the result with the one already

calculated above. The individual 'cells' are divided as shown in figure (3.13). The beam stiffnesses are proportioned randomly and individual joint stiffnesses calculated. Values of ν are taken from equation (3.9). In a similar approach to the procedure above, the effective length ratios (l_k/l) for each 'cell' was read off the appropriate chart(54). The resulting critical loads for each 'cell' was then evaluated. It can be seen from figure (3.13) that the lowest elastic critical load is located on the second storey with a value of 8.17. This compares very well with that shown by equation (3.9) which allowed for continuity of columns.

Irrespective of whichever value of λ_c used (i.e 8.31 or 8.17), equation (3.5) gives,

$$\lambda_p = 1.07$$

A lower bound plastic analysis is required to show that this value of λ_p is not exceeded. Such an approach avoids the need for an 'exact' calculation of λ_p .

Normal practice(3,17) assumes points of contraflexure to exist at mid-height of all columns for the purpose of calculating the windward and leeward column axial forces due to wind loading. Starting at tne roof with factored loads ($1.2W_k$),

storey	column axial load (KN.)
6	(10.2x3.75/2)/12 = 1.6
5	[(10.2x5.625)+(20.4x3.75/2)]/12 = 8.0
4	[(10.2x9.375)+20.4(5.625+1.875)]/12 = 20.7
3	[(10.2x13.125)+20.4(9.375+5.625+1.875)]/12 = 39.8
2	[(10.2x16.875)+20.4(13.125+9.375+5.625+1.875)]/12 = 65.3
1	[(10.2x20.625)+20.4(16.875+13.125+9.375+5.625+1.875)]/12 = 97.2

(3.11)

The results are shown in figure (3.12 (a)). These forces are added onto the combined factored vertical loads ($1.4G_k+1.2Q_k$). The total axial forces in the columns are shown in figure (3.12 (b)). For convenience and to ensure adequate out-of-plane member stability, the moment capacity of a column is taken as the yield moment, calculated as,

$$M(yield) = (1 - n) \cdot f_y \cdot Z_e \qquad (3.12)$$

where n = ratio of axial load to squash load,

f_y = yield stress,

Z_e = elastic section modulus,

It is emphasised that the value of 'n' is calculated for the required value of $\lambda_p = 1.07$

i.e. $n = \lambda_p \cdot$ axial load / squash load

Axial forces shown in figure (3.12 (b)) have to be multiplied by λ_p and moment capacities are then calculated as follows,

storey	n_l	M_l	n_c	M_c	n_r	M_r
6	0.071	100	0.144	92	0.073	100
5	0.178	89	0.368	68	0.190	87
4	0.217	109	0.305	183	0.241	106
3	0.292	99	0.420	153	0.339	92
2	0.303	119	0.535	123	0.367	108
1	0.359	109	0.650	92	0.455	93

(3.13)

where n_l , n_c and n_r refer to the values of n for the left, centre and right hand columns with corresponding moment capacities M_l , M_c and M_r (KN.m. units) respectively.

The moment capacities are shown in figure (3.12 (c)). Axial forces in the beams are small in comparison to the columns, and the full plastic moment capacity of the beam has been assumed. Under combined loading, plastic hinges tend to develop on the leeward end and at mid-span of the beam. Referring to the lower diagram in figure (3.14), the windward end moment for a plastic beam is M_L . By equilibrium,

$$M(\text{free}) = M_p + 0.5(M_p - M_L)$$

$$M_L = 3M_p - 2M(\text{free}) \qquad (3.14)$$

where $M(\text{free}) = \lambda_p wL^2/8$.

For the roof beam,

$$M(\text{free}) = (1.07 \times 31.7 \times 6 \times 6) / 8 = 152.6 \text{ KNm.} \qquad (3.15)$$

For the floor beams,

$$M(\text{free}) = (1.07 \times 49.1 \times 6 \times 6) / 8 = 236.4 \text{ KNm.}$$

For convenience, equivalent point loads are used for calculating bending moments. Using the lower bound approach, the overall bending moment distribution shown in figure (3.14) at a load factor of 1.07 can be obtained. It can be seen that the bending moments nowhere exceed the moment capacities given in figure (3.12 (c)). Therefore $\lambda_p \geq 1.07$ and the design is satisfactory.

For comparison, the lower bound elastic critical load for each storey was calculated from equation (3.2) using the computer program described in Section (3.2). The linear and non-linear displacements under factored (design) loads were taken at the windward joint,

storey	lower bound on λ_c
6	10.33
5	8.98
4	8.54
3	8.35
2	8.30
1	8.30

(3.16)

After performing further iterations, the determinant of the overall stiffness matrix was non-positive at $\lambda_c = 8.60$. The values for λ_c obtained manually were 8.31 and 8.17. These results are in excellent agreement.

Accurate computer analysis showed that failure occurred at a load level of 1.09 and a rigid-plastic analysis exhibited a simple beam collapse of the fourth and fifth floor beams with $\lambda_p = 1.17$.

With the accurate results for λ_c and λ_p , equation (3.4) gave λ_{prop} =1.09 while λ_{mr} =1.03 and λ_{mrw} =1.13. The latter two results are 94% and 104% of the accurate failure load respectively.

The design has so far neglected initial eccentricity. The British Design Recommendation(55) specify that eccentricity shall not exceed 1/1000 of the total vertical height, while European Recommendation(56) require such out-of-plumb to be represented by fictitious horizontal loads,

$$Q = N\tau \tag{3.17}$$

where N = total vertical design load at each floor level,

$\tau = \tau_0 \, r_1 \, r_2$

$\tau_0 = 1/200$,

$r_1 = \sqrt{5/\text{ each storey height in metres}} \quad < 1.0$,

$r_2 = 0.5\,[1 + 1/(\text{number of loaded columns per storey})]$.

As the European specification is more severe, the values of the fictitious horizontal loads are calculated for this example,

$r_1 = \sqrt{5/3.75} = 1.155 > 1.0$

r_1 is therefore taken as 1.0,

$r_2 = 0.5(1 + 1/3) = 0.667$,

$\tau = 1.0 \times 0.667/200 = 1/300$.

At the roof and at all the floor levels, the fictitious horizontal

loads are given by,

$$Q(\text{roof}) = 380.4/300 = 1.27 \text{ KN.} \qquad (3.18)$$

$$Q(\text{floor}) = 589.2/300 = 1.96 \text{ KN.}$$

When these additional loads are added onto the wind forces shown in figure (3.12 (a)), a small increase of column axial forces was observed. However, the fictitious loads are small and have a negligible effect on the moment capacities shown in figure (3.12 (c)). In fact, the moment capacities are almost identical to that shown in figure (3.12 (c)) when these fictitious loads are incorporated. It can be similarly demonstrated that the lower bound plastic analysis is satisfactory when such fictitious loads are included in the horizontal loading.

3.9 Conclusion

A simple expression has been presented for estimating the ultimate load capacity of plane unbraced bare frames under combined loading and vertical load alone. The expression have been compared both with published experimental model tests and accurate computer analysis on realistic frames, and it has provided consistently accurate estimates throughout.

Comparisons with 20 experimental miniature models of three, five and seven storeys under combined loading have shown the calculated values to vary between 90% and 107% of the values given by experimental results. The single unsafe estimate of 7% was not significant because the model was grossly out-of-plumb.

Although the proposed expression is intended for collapse under combined loading, a further 14 model frames subjected to vertical loads only were also compared. The predicted failure loads using a coefficient of 0.4 varied between 71% and 90% of experimental results. A coefficient of 0.1 was proposed for estimating the failure loads of such frames. The studies showed that the use of a factor of 0.1 resulted in the predicted failure loads varying between 84% and 101% of the experimental results. Only a single frame for each of the extreme errors was found. The models used in the studies represent the lower scale for the ratio of λ_c / λ_p with values ranging from as low as 1.1 to 4.0.

Studies on 43 realistic frames under combined loading with ratios of λ_c / λ_p between 3.19 and 16.6 have shown the proposed failure load to lie between 93% and 103% of the figures given by second-order elasto-plastic computer analysis. The lower limit rises to 95% if frames for which λ_c / λ_p is less than 4.0 are neglected. These realistic frames have been designed to practical levels of loading and to deflection limitation at the working load.

Further comparisons of 8 other frames from the literature have also shown the consistency of the proposed method in estimating the failure loads. The maximum error was 4% but this was for a frame that does not satisfy the usual deflection limit and with the presence of real pins on the uppermost columns.

The proposed method will therefore prove acceptable to designers who do not wish to rely on strain-hardening and stray composite action to offset the higher collapse loads that can be

predicted by the modified Merchant-Rankine formula. The proposal should always be used instead of the latter whenever cladding is minimal, especially as the expression is just as easy to apply as the modified approach. This is demonstrated by an example of a rectangular six storey frame. The detailed manual procedure was shown. Several rapid methods for determining the lowest elastic critical load were shown. Comparisons with accurate computer analysis gave excellent agreement.

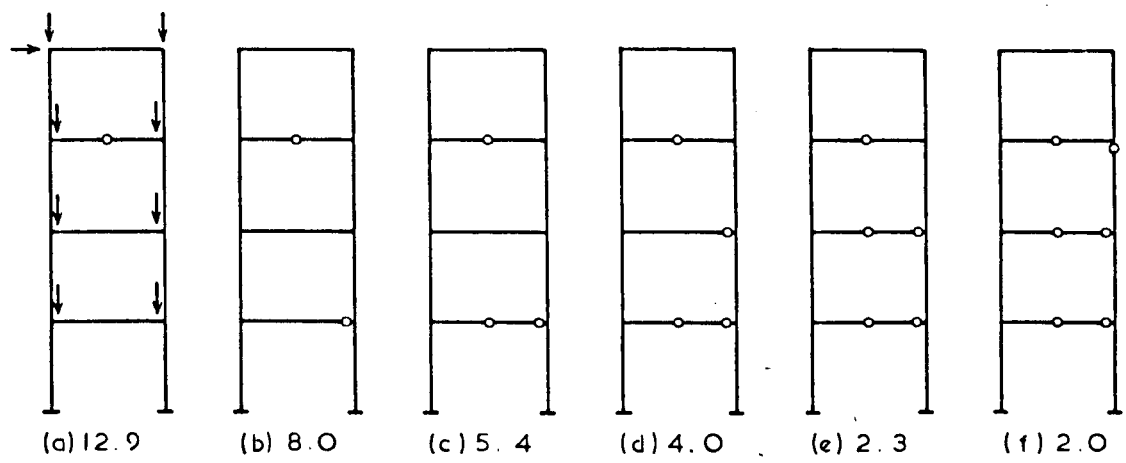

VALUES OF 'DETERIORATED' CRITICAL LOADS, λ_{det}

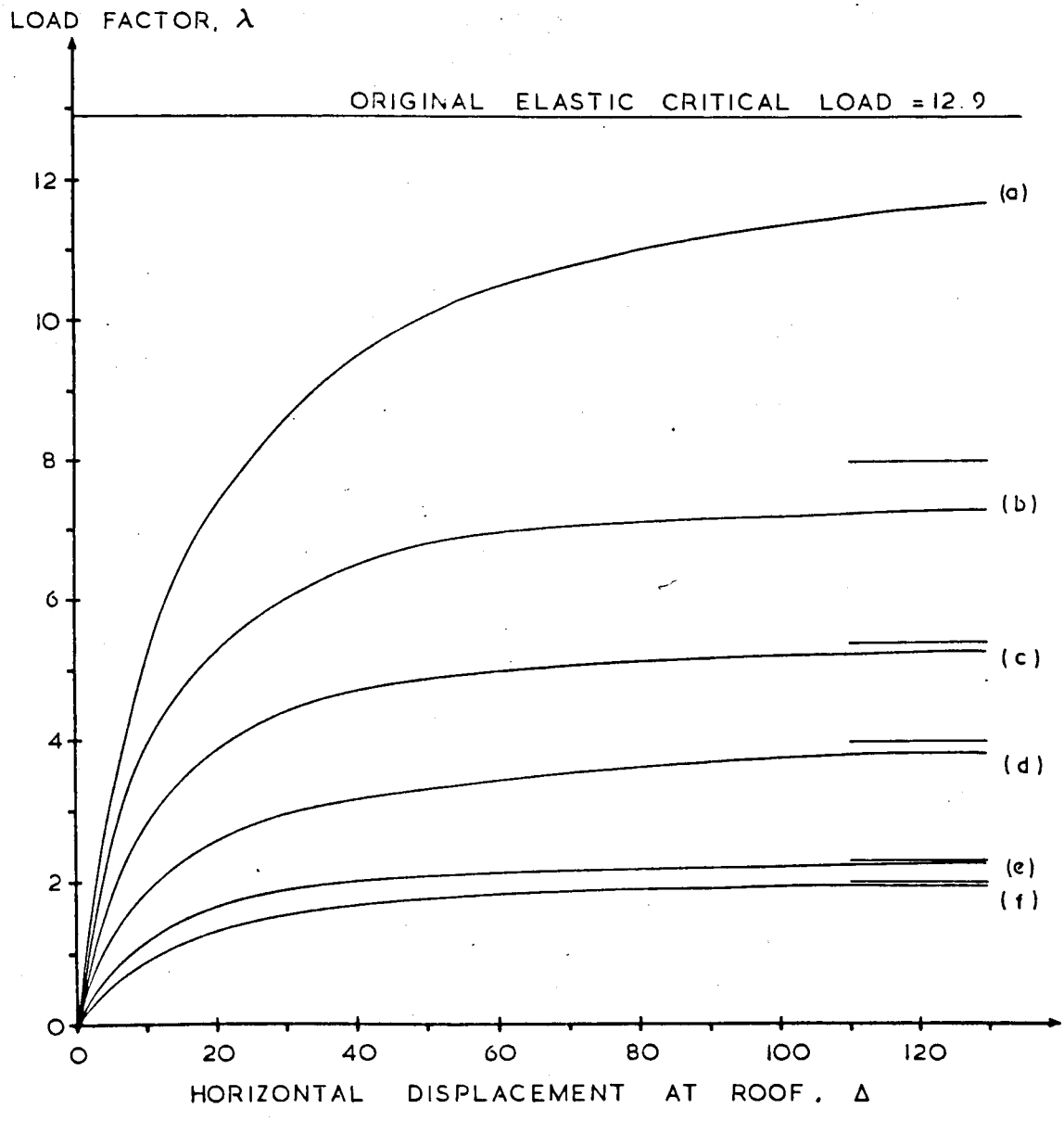

FIG. 3.1 DETERIORATED CRITICAL LOADS OF 4-STOREY FRAME

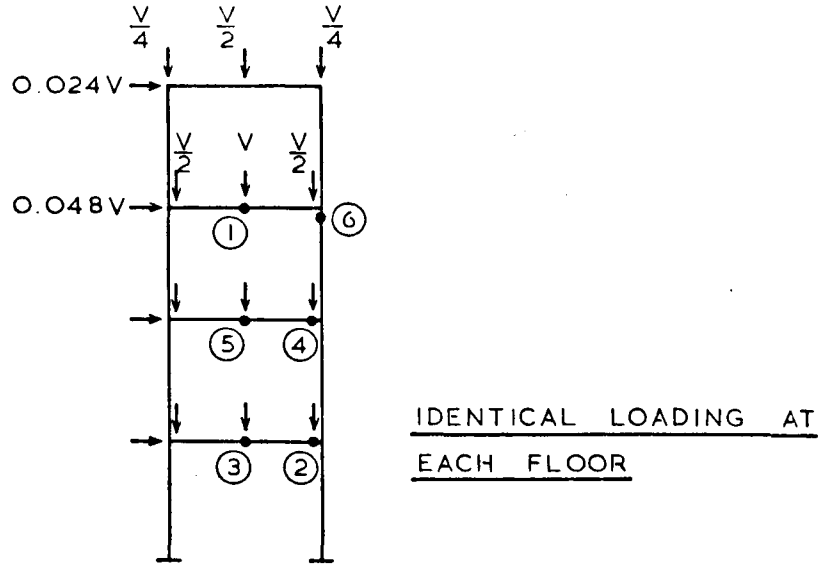

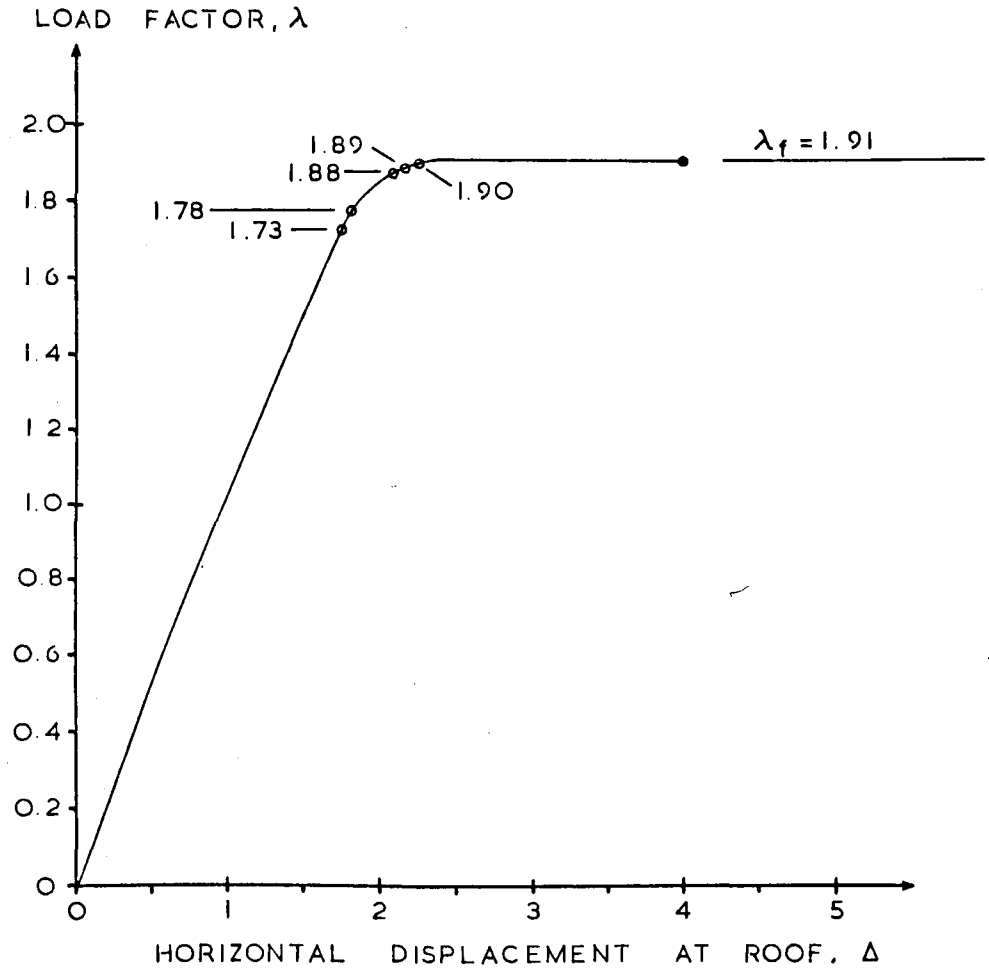

FIG. 3.2 LOAD - DISPLACEMENT BEHAVIOUR OF FOUR-STOREY FRAME

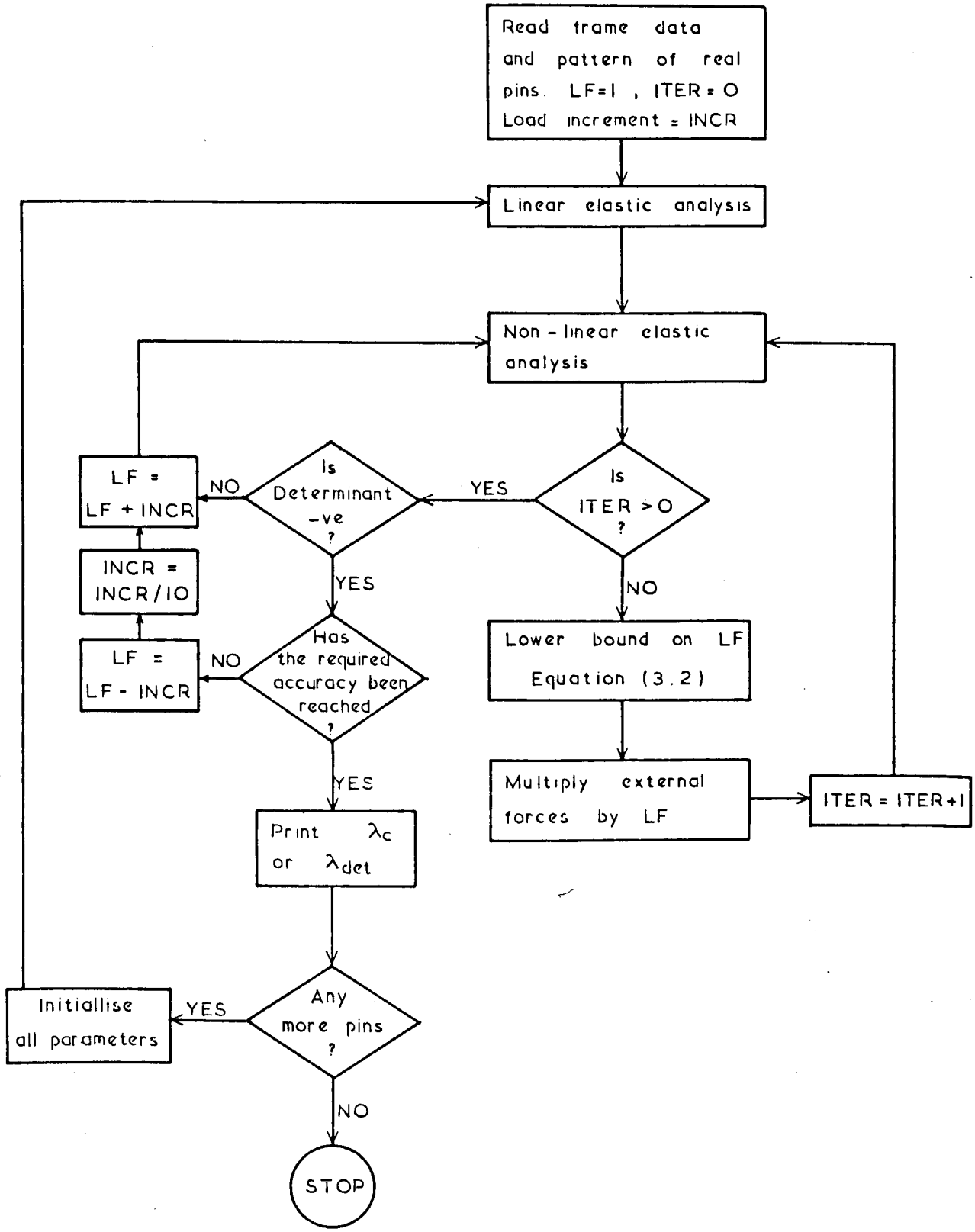

FIG. 3.3 FLOW CHART FOR CALCULATING λ_c & λ_{det}

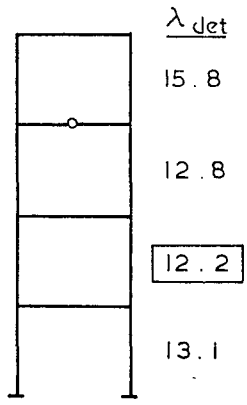

ACCURATE 12.9
WOOD 12.9

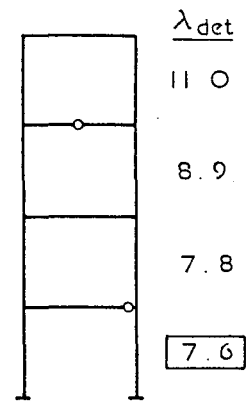

ACCURATE 8.0
WOOD 8.5

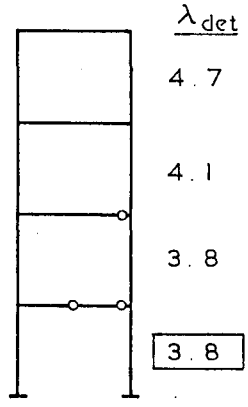

ACCURATE 4.0
WOOD 4.05

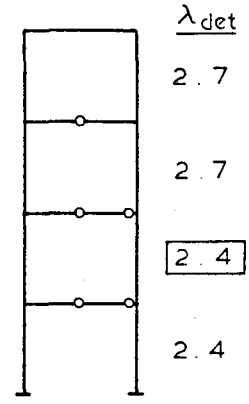

ACCURATE 2.3
WOOD 2.3

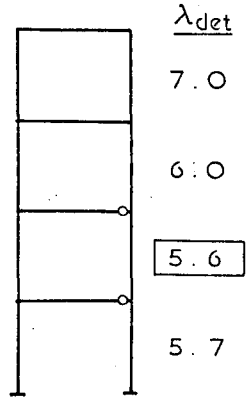

ACCURATE 6.2
WOOD 6.3

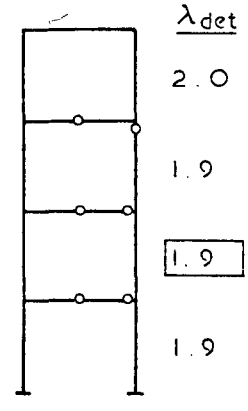

ACCURATE 2.0
WOOD 2.05

FIG. 3.4 COMPARISON OF DETERIORATED CRITICAL LOADS

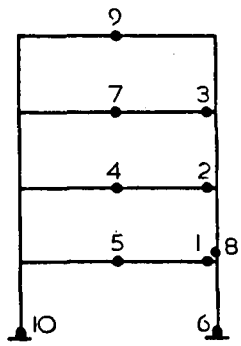

	λ	λ_{det}
1)	1.09	16.1
2)	1.12	11.4
3)	1.29	9.9
4)	1.39	6.3
5)	1.41	5.3
6)	1.46	4.8
7)	1.47	4.2
8)	1.48	3.4
9)	1.49	3.4
10)	1.49	0.7

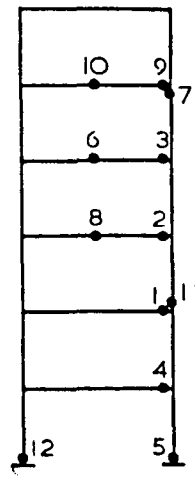

	λ	λ_{det}
1)	1.24	11.1
2)	1.24	8.4
3)	1.24	7.0
4)	1.24	6.3
5)	1.40	6.1
6)	1.41	4.8
7)	1.44	4.0
8)	1.48	2.3
9)	1.48	2.2
10)	1.48	1.8
11)	1.49	1.6
12)	1.49	1.5

ORDER AND LOAD LEVEL OF PLASTIC HINGE FORMATION

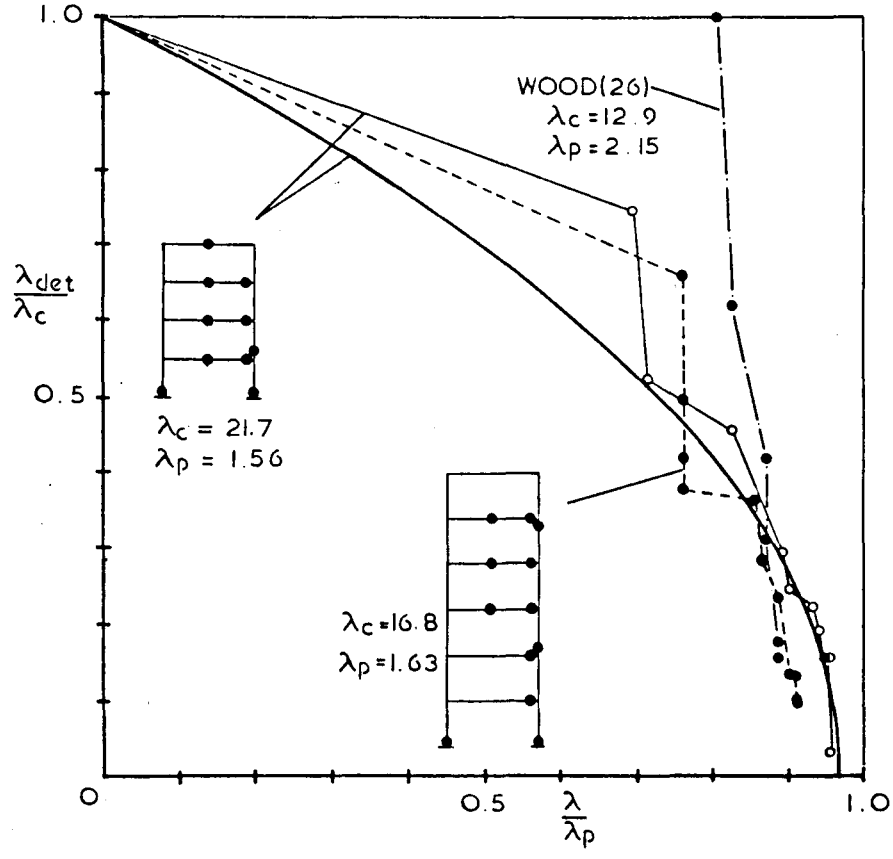

FIG 3.5 DETERIORATION OF FRAME STIFFNESS

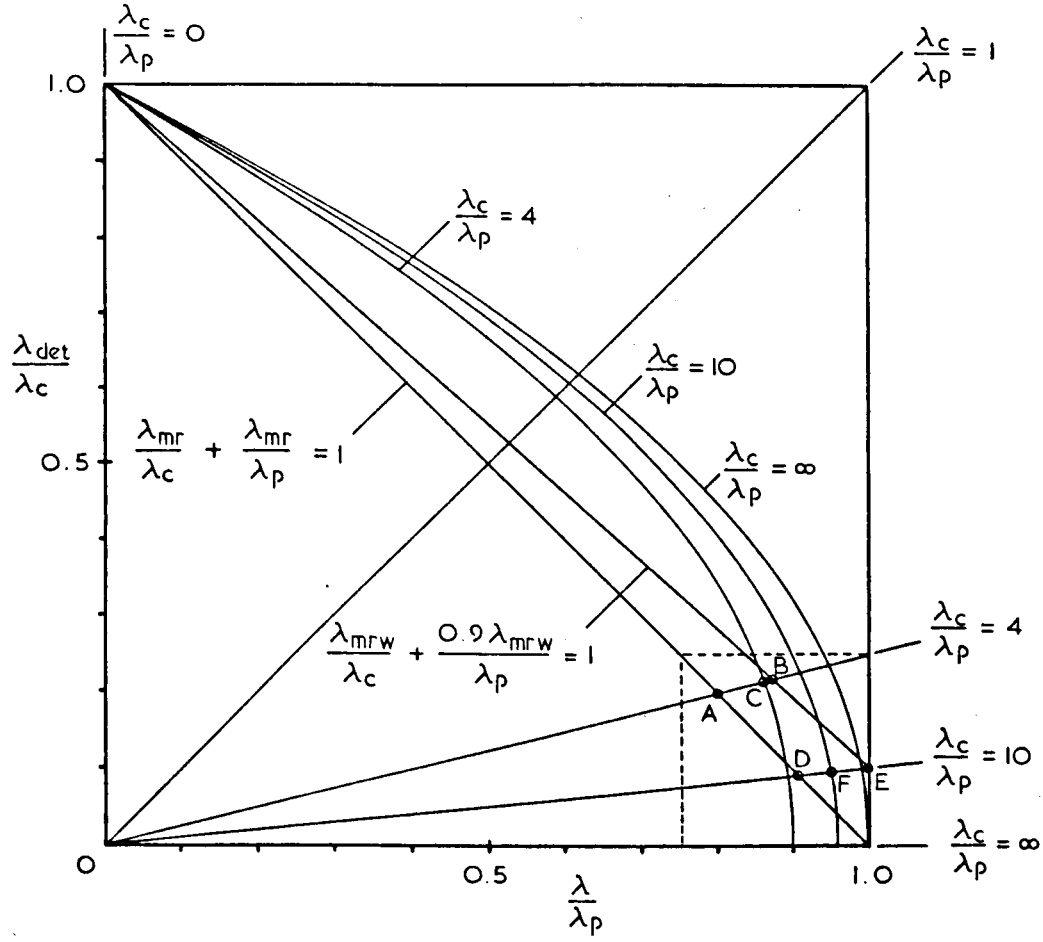

(a) $4 \leq \lambda_c/\lambda_p \leq 10$

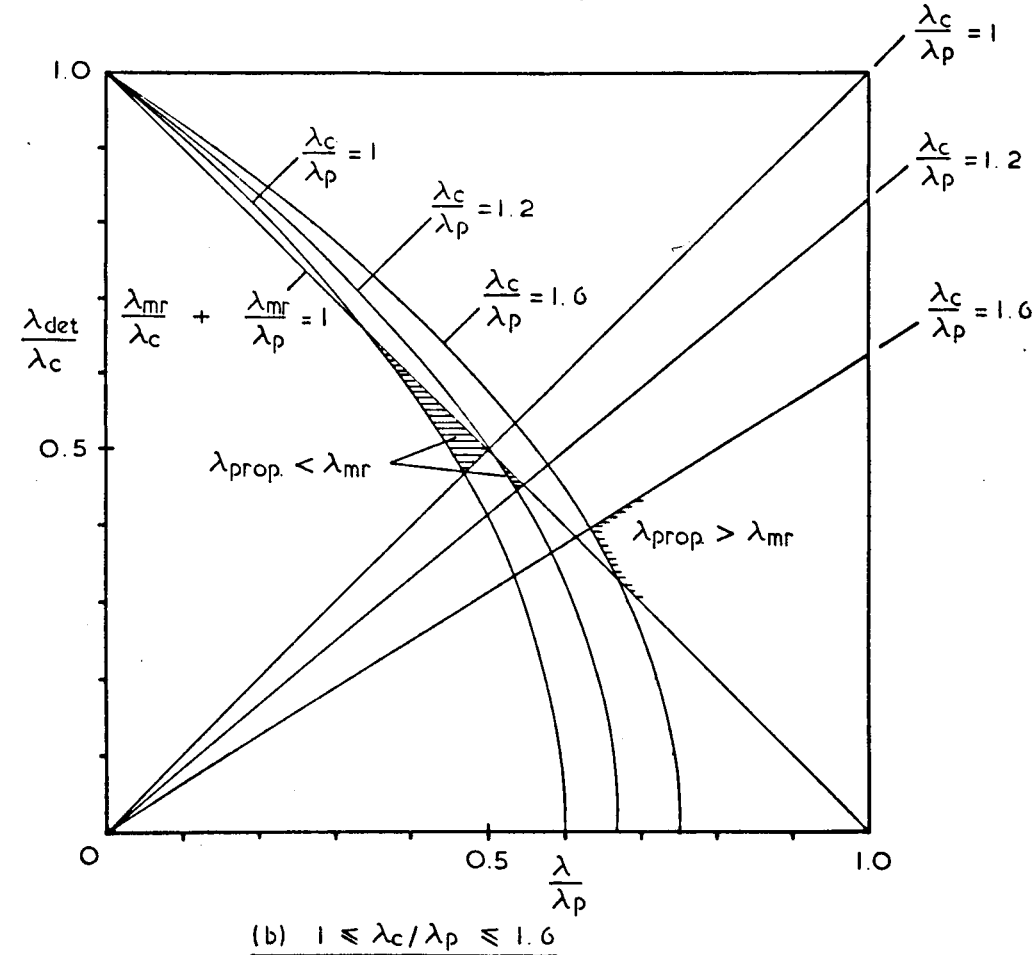

(b) $1 \leq \lambda_c/\lambda_p \leq 1.6$

FIG. 3.6 DETERIORATION FUNCTIONS

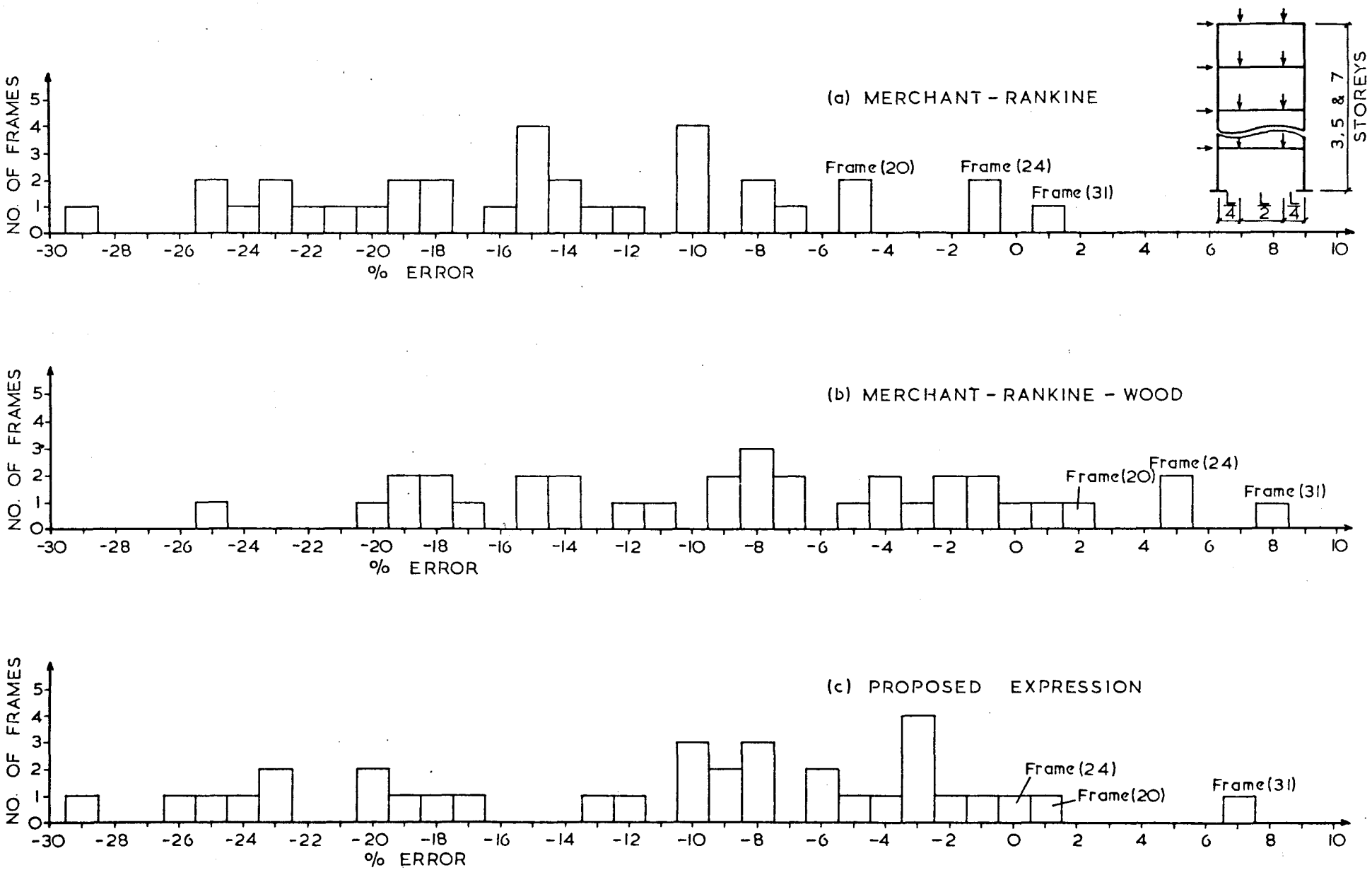

FIG 3.7 COMPARISON OF LOW'S EXPERIMENTAL RESULTS (ALL FRAMES)

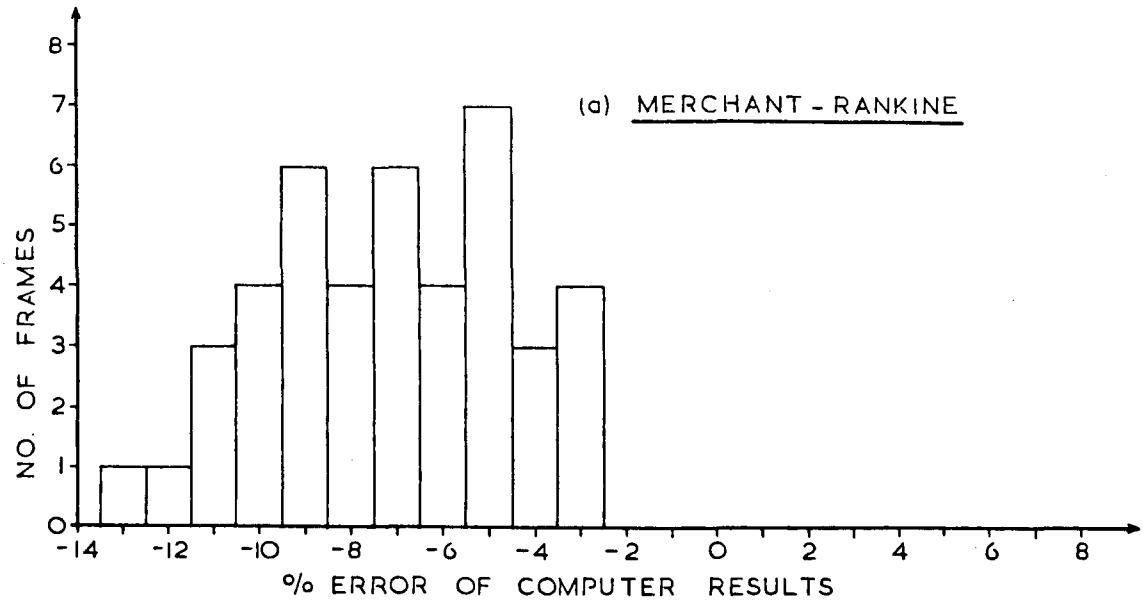

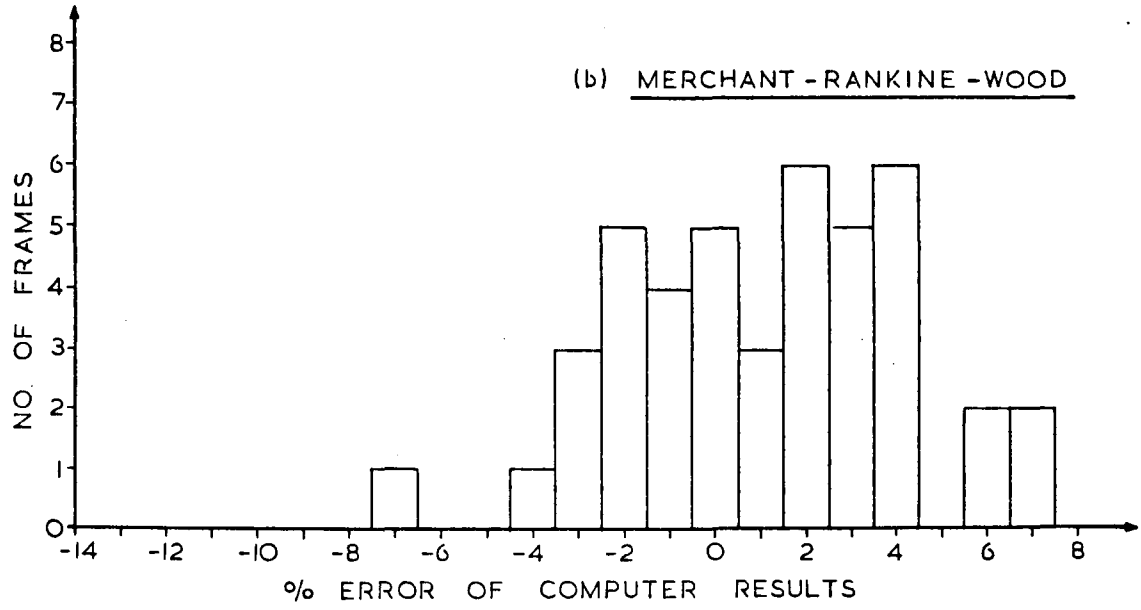

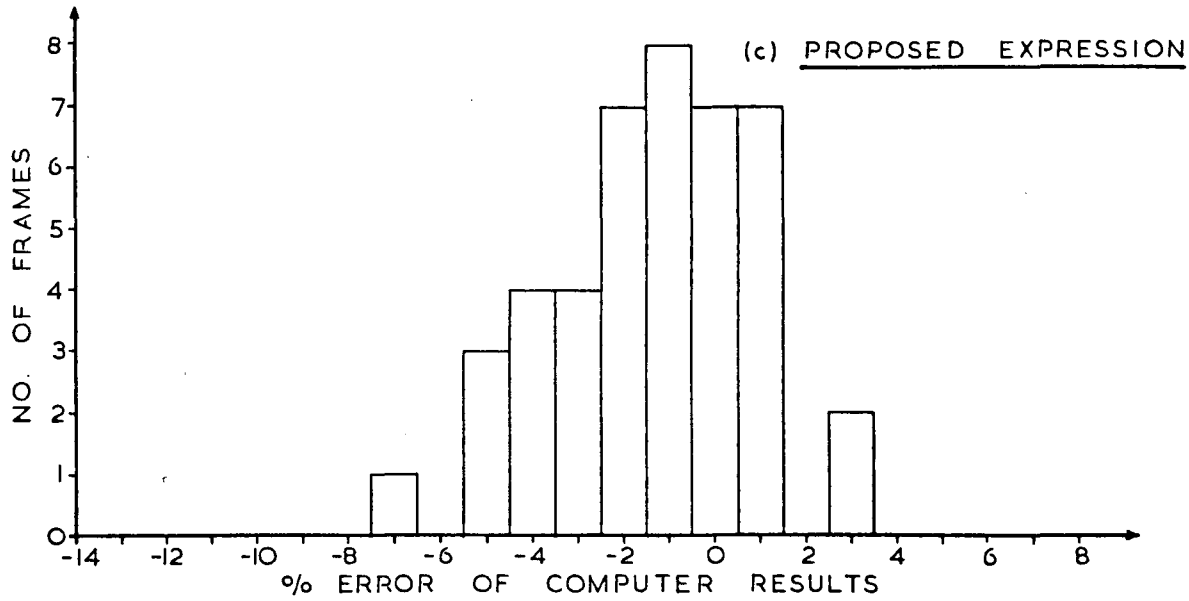

FIG. 3.8 COMPARISON OF RESULTS ON PARAMETRIC STUDIES

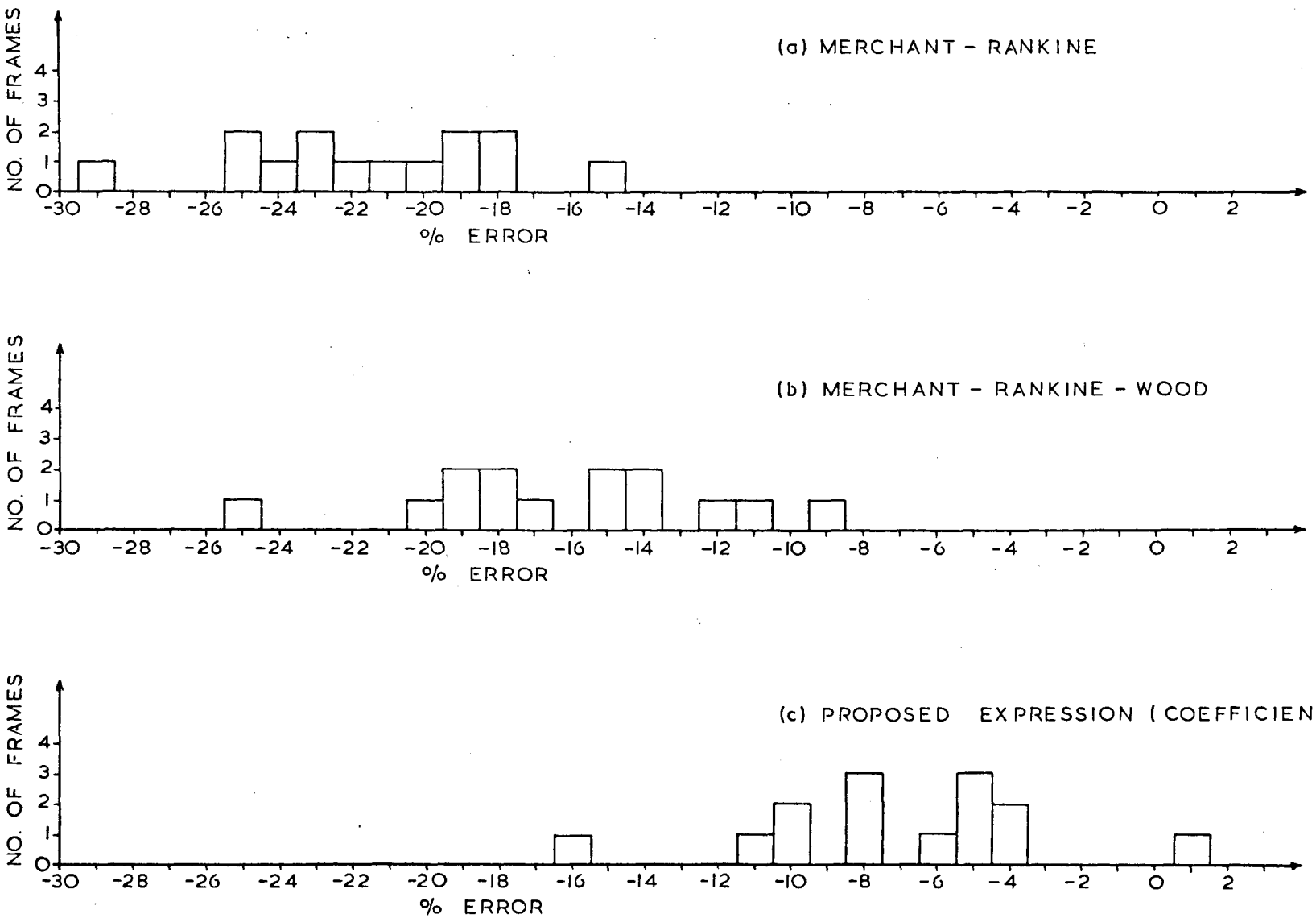

FIG. 3.9 (a) COMPARISON OF LOW'S EXPERIMENTAL RESULTS (VERTICAL LOAD ONLY)

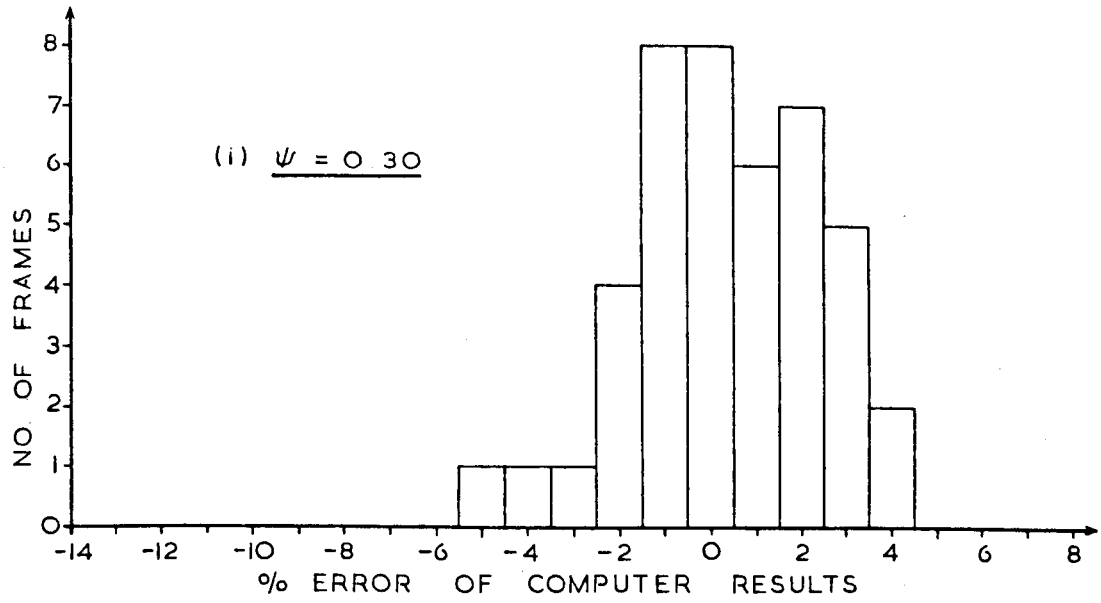

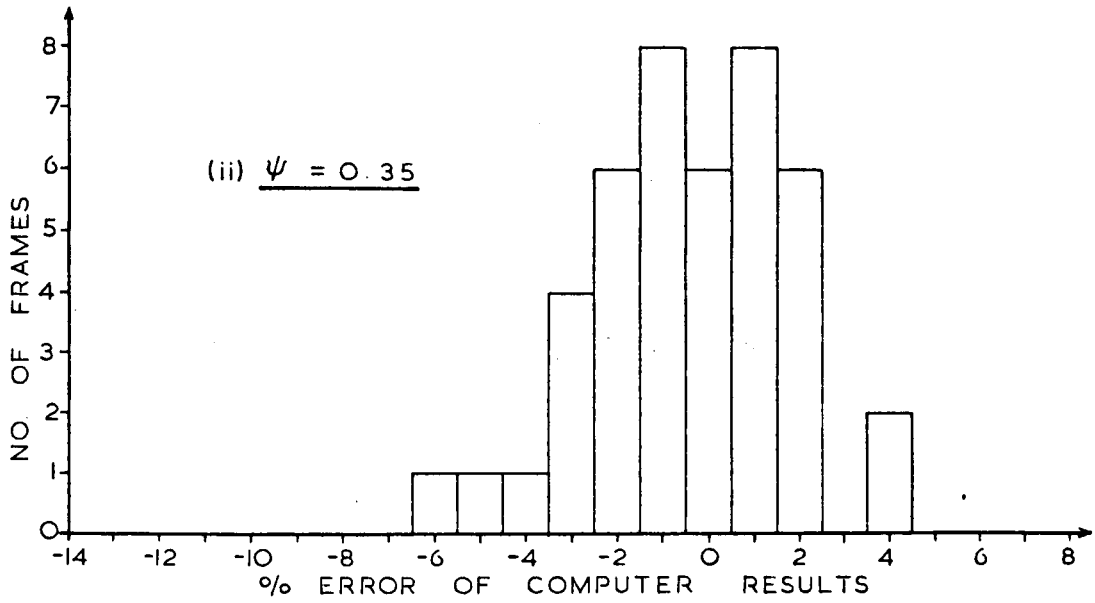

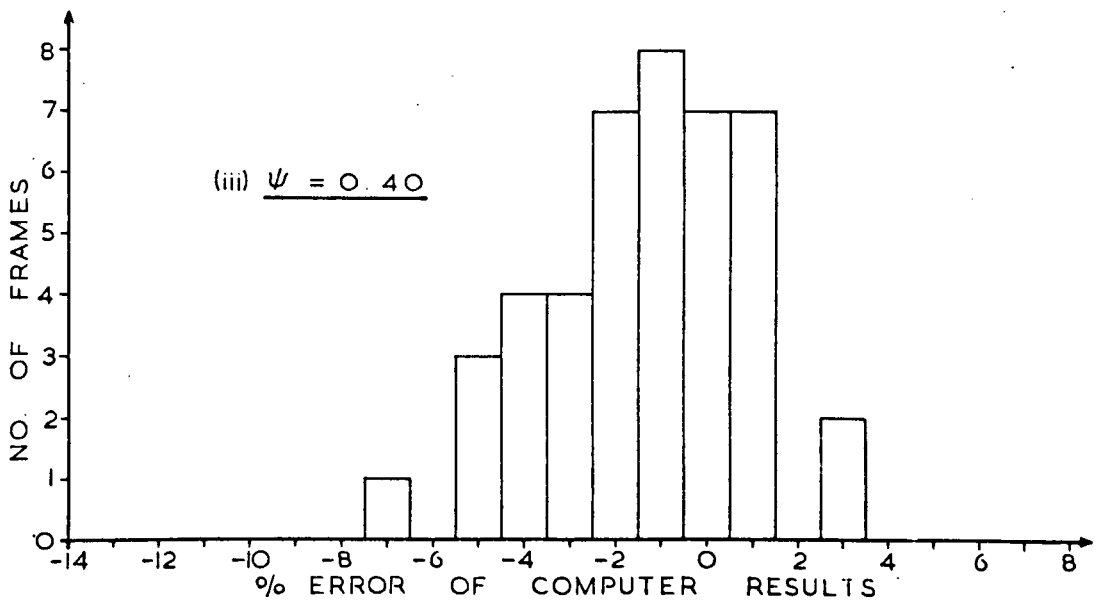

FIG. 3.9(b) VARIATION OF COEFFICIENT, ψ ON PARAMETRIC STUDIES

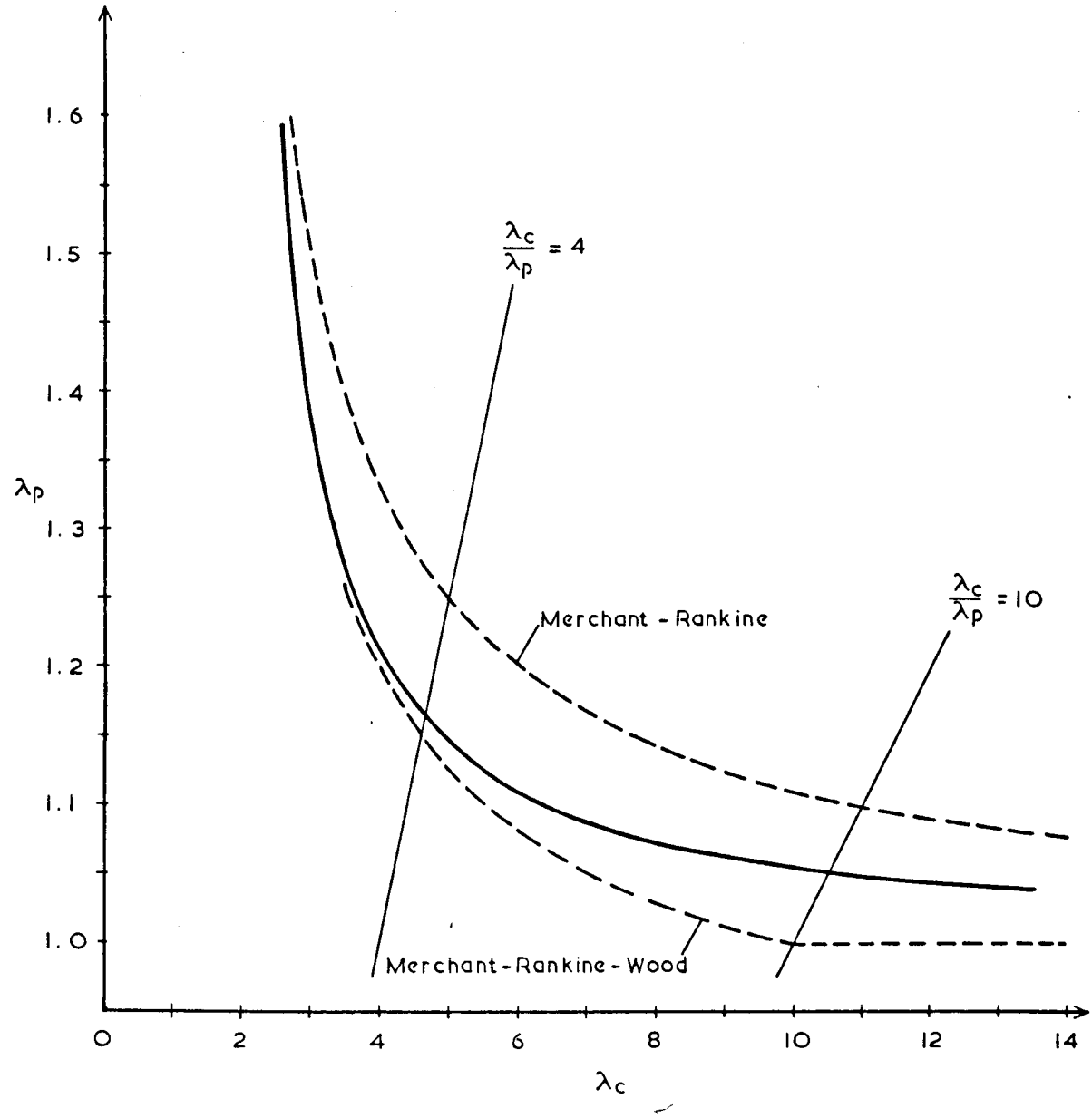

FIG. 3.10 DESIGN CURVE FOR $\lambda = 1.0$

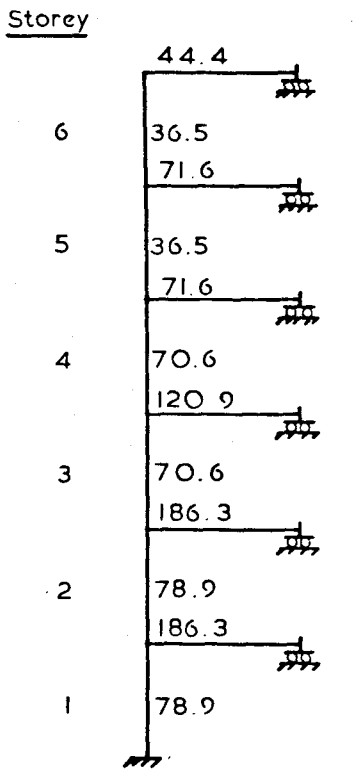

FIG. 3.11 GRINTER FRAME FOR DETERMINING λ_c

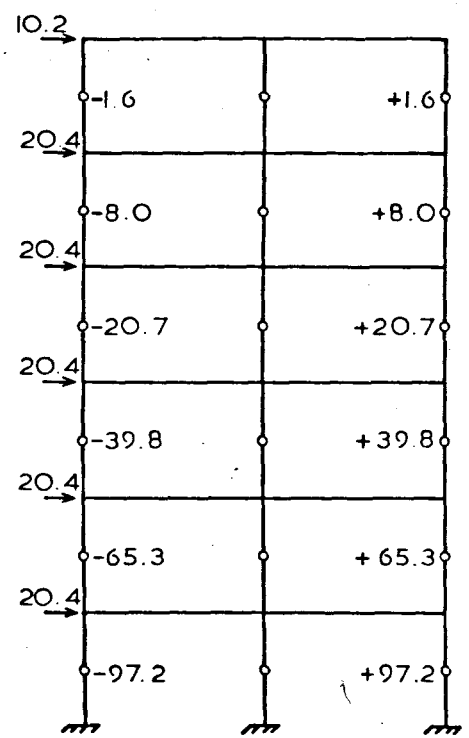

FIG. 3.12(a) AXIAL FORCES DUE TO FACTORED WIND LOADS (KN.)

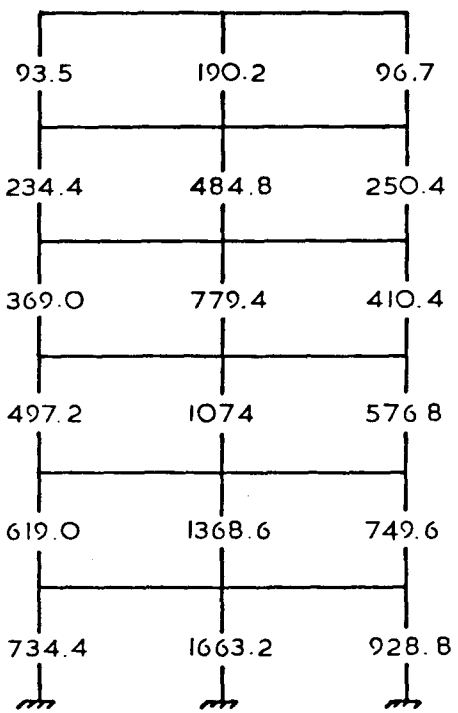

FIG. 3.12(b) COMBINED COLUMN AXIAL FORCES

V (roof) = 380.4 KN.

V (floors) = 589.2 KN.

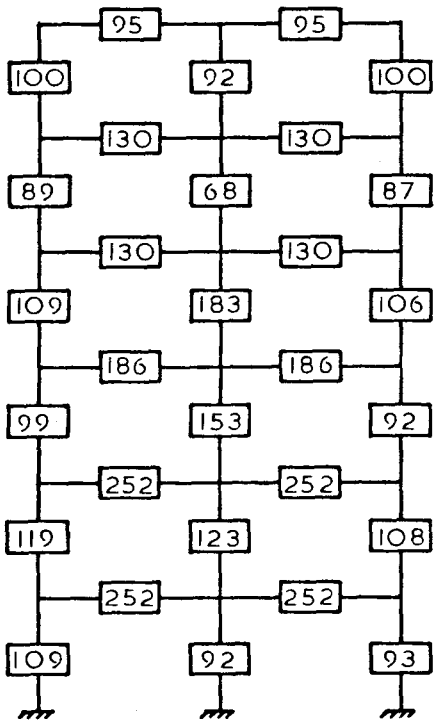

FIG 3.12(c) MOMENT CAPACITIES (KN.m)

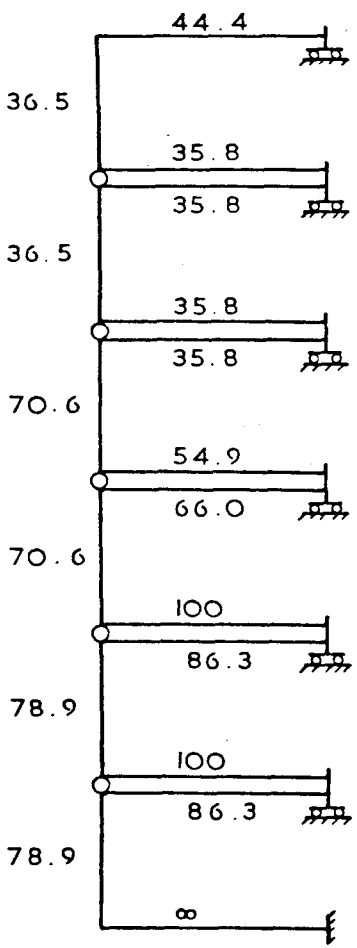

Equivalent member stiffnesses $(cm)^3$	Joint stiffness	$\nu = \frac{\Sigma P.h^2}{\Sigma I_c}$	Effective length ratio ($\bar{s}=0$) l_k/l	$\lambda_c = \frac{20.23}{\nu.(l_k/l)^2}$
	$\eta_t = 0.451$			
36.5		0.39	1.44	25.02
	$\eta_b = 0.505$			
	$\eta_t = 0.505$			
36.5		1.00	1.49	9.11
	$\eta_b = 0.505$			
	$\eta_t = 0.664$			
70.6		0.83	1.68	8.64
	$\eta_b = 0.563$			
	$\eta_t = 0.517$			
70.6		1.14	1.42	8.80
	$\eta_b = 0.414$			
	$\eta_t = 0.478$			
78.9		1.30	1.38	**8.17**
	$\eta_b = 0.441$			
	$\eta_t = 0.478$			
78.9		1.58	1.20	8.89
	$\eta_b = 0$			

FIG. 3.13 CALCULATION OF λ_c BY INDIVIDUAL 'CELLS'

Notation

ΣP = Total vertical load in KN.

h = Storey height in metres.

ΣI_c = Sum of column inertia in cm^4

NOTE

λ_c based on E = 20500 KN/cm^2.

i.e. $\vartheta = \frac{E.\pi^2}{10000} = 20.23$

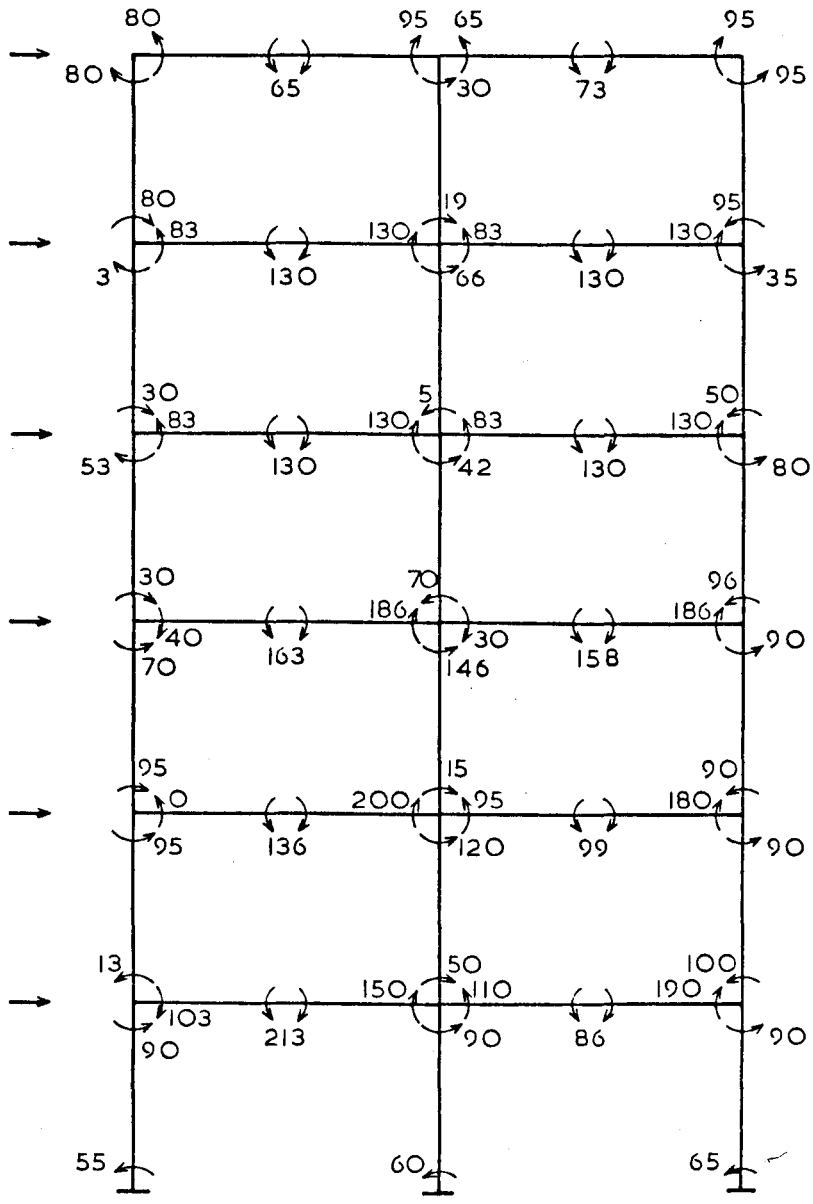

$\sum$ Wind moments
$= \lambda_p \sum H \cdot h$ (KN.m)

41

123

205

286

368

450

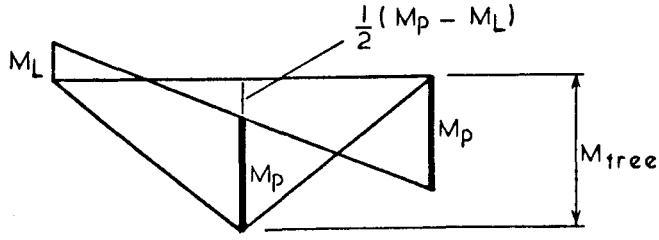

FIG. 3.14 LOWER BOUND (EQUILIBRIUM) PLASTIC ANALYSIS ($\lambda_p = 1.07$)

	Frame No.	$\frac{\lambda_c}{\lambda_p}$	λ_{expt} (lbs)	$\frac{\lambda_{mr}}{\lambda_{expt.}}$	$\frac{\lambda_{prop.}}{\lambda_{expt.}}$	$\frac{\lambda_{mrw}}{\lambda_{expt}}$
3 storeys	5	3.6	448.8	0.90	0.96	0.98
	6	4.0	428.9	0.87	0.94	0.95
	7	4.0	442.5	0.85	0.91	0.92
	8	3.8	645.4	0.85	0.92	0.93
	10	3.5	530.8	0.84	0.90	0.91
	11	3.5	505.7	0.88	0.95	0.96
	12	3.5	492.4	0.90	0.97	0.98
	13	2.7	458.6	0.86	0.92	0.92
	14	2.7	423.8	0.92	0.99	1.00
	15	2.7	434.2	0.92	0.98	0.99
	16	3.0	487.7	0.85	0.91	0.91
	18	2.9	489.8	0.86	0.92	0.93
	19	3.0	458.6	0.90	0.96	0.97
	20	2.9	434.7	0.94	1.01	1.02
5 storeys	23	1.4	577.7	0.93	0.94	0.99
	24	1.4	530.1	0.99	1.00	1.05
	25	1.4	599.7	0.90	0.90	0.95
	29	1.6	609.0	0.95	0.97	1.01
	31	2.3	666.2	1.01	1.07	1.08
7 storeys	37	1.2	680.2	0.99	0.97	1.05

Table 3.1(a) Comparison with Low's results for frames under combined loading.

Frame No.		$\frac{\lambda_c}{\lambda_p}$	λ_{expt} (lbs)	$\frac{\lambda_{mr}}{\lambda_{expt}}$	$\frac{\lambda_{prop}}{\lambda_{expt}}$	$\frac{\lambda_{mrw}}{\lambda_{expt}}$
3 storeys	4	3.6	495.8	0.82	0.88	0.89
	9	3.6	657.1	0.81	0.87	0.88
	17	3.0	534.1	0.77	0.83	0.83
	26	2.7	523.3	0.75	0.80	0.81
	27	3.0	539.8	0.76	0.82	0.82
5 storeys	21	1.3	768.6	0.71	0.71	0.75
	22	1.4	672.2	0.80	0.80	0.84
	28	1.6	756.4	0.75	0.77	0.80
	30	2.3	781.1	0.85	0.90	0.91
7 storeys	32	1.3	799.4	0.81	0.81	0.86
	33	1.1	778.9	0.82	0.78	0.86
	34	1.1	730.5	0.78	0.74	0.82
	35	1.1	707.5	0.80	0.76	0.85
	36	1.1	821.5	0.77	0.74	0.81

Table 3.1(b) Comparison with Low's results for frames with vertical loads only

	Frame storey x bay	Min. vertical : Max. wind					Max. vertical : min. wind.					
		$\frac{\lambda_c}{\lambda_p}$	λ_{mrw}	$\lambda_{prop.}$	λ_f	Mech	$\frac{\lambda_c}{\lambda_p}$	λ_{mrw}	$\lambda_{prop.}$	λ_f	Mech.	
*	4 x 2W	9.15	1.14	1.08	1.07	B	5.75	1.04	1.02	1.04	C	
●	4 x 2N	11.38	1.34	1.28	1.30	B	6.56	1.17	1.14	1.20	B	▲
	4 x 3W						5.25	1.04	1.02	1.04	S	
	4 x 3N						5.37	1.10	1.08	1.08	C	o
	4 x 4W						4.93	1.04	1.02	1.05	S	
	4 x 4N						3.34	0.88	0.87	0.92	S	
▲	4 x 5W	5.34	1.01	0.99	1.04	C	4.78	1.03	1.01	1.05	S	
o	4 x 5N	5.34	1.16	1.14	1.13	C	3.19	0.89	0.89	0.96	S	□
●	7 x 2W	12.83	1.15	1.11	1.10	B	5.66	1.02	1.00	1.01	C	o
	7 x 2N	16.59	1.42	1.38	1.39	B	7.98	1.20	1.15	1.15	B	●
	7 x 3W						4.74	0.89	0.88	0.89	C	o
	7 x 3N						5.30	1.07	1.05	1.04	S	o
	7 x 4W						4.48	0.96	0.95	0.97	S	
	7 x 4N						4.11	0.98	0.97	0.99	S	
o	7 x 5W	5.06	0.96	0.94	0.95	C	4.36	0.96	0.95	0.99	S	▲
	7 x 5N	5.78	1.24	1.21	1.26	B	3.98	1.00	0.99	1.03	S	
●	10 x 2W	15.33	1.15	1.11	1.11	B	6.02	1.05	1.02	1.01	C	o
	10 x 2N	14.90	1.42	1.37	1.40	B	8.07	1.18	1.13	1.10	S	*
	10 x 3W						4.67	0.96	0.94	0.96	C	
	10 x 3N						6.19	1.04	1.01	1.02	S	
o	10 x 4W	6.57	1.06	1.03	1.04	C	3.87	0.89	0.88	0.91	S	
●	10 x 4N	8.23	1.31	1.25	1.24	B	4.56	1.00	0.99	1.02	S	

Notation

W = Bay width 7500

N = Bay width 5000

Table 3.2. Parametric studies under extreme loading

Frame storey x bay	Vertical load	Wind load	$\frac{\lambda_c}{\lambda_p}$	λ_{mrw}	$\lambda_{prop.}$	λ_f	Mech.	
4 x 2W	Max	Inter	5.82	1.03	1.01	1.03	C	
4 x 3W	Max	Max	5.72	0.97	0.94	0.94	S	o
4 x 5W	Max	Max	4.88	1.02	1.00	1.03	S	o
7 x 2W	Max	Inter	6.15	1.03	1.00	1.00	C	
7 x 5W	Max	Max	4.63	0.91	0.89	0.89	S	o
10 x 2W	Max	Inter	8.07	1.12	1.08	1.05	B	•
10 x 3W	Max	Max	6.41	1.08	1.05	1.04	B	•
10 x 2N	Max	Inter	5.78	1.08	1.05	1.06	S	
10 x 2W	Max	Inter	7.64	1.12	1.08	1.08	B	•

W = Bay width 7500 , N = Bay width 5000

Table 3.3 Parametric studies under various loadings

Reference	Frame storey x bay	$\frac{\lambda_c}{\lambda_p}$	λ_{mrw}	$\lambda_{prop.}$	λ_f	
Majid & Anderson (Proc.ICE)	4 x 1	13.88	1.56	1.51	1.49	
Anderson (Ph.D. Thesis)	4 x 1	7.71	1.55	1.49	1.43	**
Anderson (Ph.D. Thesis)	8 x 2	5.06	1.51	1.48	1.48	
Wood (Proc. ICE)	4 x 1	6.01	2.01	1.96	1.91	
Chapter 2 of this thesis	6 x 1	5.02	1.59	1.56	1.54	
Anderson & Islam (Proc. ICE)	6 x 1	10.32	1.63	1.55	1.49	**
Anderson & Islam (Proc. ICE)	15 x 3	3.49	1.37	1.37	1.38	
Chapter 2 of this thesis	6 x 3	4.18	1.70	1.67	1.64	

Table 3.4 Other comparisons

$\frac{\lambda_{0.30}}{\lambda_{expt.}}$	$\frac{\lambda_{0.35}}{\lambda_{expt.}}$
0.99	0.98
0.96	0.95
0.93	0.92
0.94	0.93
0.92	0.91
0.98	0.96
0.99	0.98
0.95	0.93
1.03	1.01
1.02	1.00
0.94	0.92
0.95	0.94
0.99	0.98
1.05	1.03
1.00	0.97
1.06	1.03
0.97	0.93
1.03	1.00
1.12	1.09
1.05	1.01

Table 3.5(a) Low's experimental results

(combined loading only)

$\frac{\lambda_{0.30}}{\lambda_{expt.}}$	$\frac{\lambda_{0.35}}{\lambda_{expt.}}$	$\frac{\lambda_{0.10}}{\lambda_{expt.}}$
0.90	0.89	0.95
0.90	0.88	0.94
0.85	0.84	0.91
0.83	0.82	0.89
0.85	0.83	0.90
0.76	0.73	0.84
0.85	0.83	0.95
0.81	0.79	0.90
0.94	0.92	1.01
0.86	0.84	0.96
0.85	0.81	0.96
0.81	0.78	0.92
0.83	0.80	0.95
0.80	0.77	0.91

Table 3.5(b) Low's experimental results
(vertical only loading)

λ_{mrw}	$\lambda_{0.30}$	$\lambda_{0.35}$	λ_f	λ_{mrw}	$\lambda_{0.30}$	$\lambda_{0.35}$	λ_f	
1.14	1.10	1.09	1.07	1.04	1.03	1.02	1.04	
1.34	1.29	1.29	1.30	1.17	1.15	1.14	1.20	
				1.04	1.04	1.03	1.04	
				1.10	1.10	1.09	1.08	
				1.04	1.04	1.03	1.05	
				0.88	0.90	0.89	0.92	
1.01	1.01	1.00	1.04	1.03	1.04	1.03	1.05	O
1.16	1.16	1.15	1.13	0.89	0.91	0.90	0.96	
1.15	1.12	1.11	1.10	1.02	1.02	1.01	1.01	
1.42	1.39	1.38	1.39	1.20	1.17	1.16	1.15	
				0.89	0.89	0.89	0.89	
				1.07	1.07	1.06	1.04	
				0.96	0.97	0.96	0.97	O
				0.98	0.99	0.98	0.99	O
0.96	0.96	0.95	0.95	0.96	0.97	0.96	0.99	O
1.24	1.23	1.22	1.26	1.00	1.01	1.00	1.03	
1.15	1.12	1.12	1.11	1.05	1.04	1.03	1.01	
1.42	1.38	1.38	1.40	1.18	1.15	1.14	1.10	
				0.96	0.96	0.95	0.96	
				1.04	1.02	1.02	1.02	
1.06	1.05	1.04	1.04	0.89	0.90	0.89	0.91	
1.31	1.27	1.26	1.24	1.00	1.01	1.00	1.02	O

Table 3.6 Parametric studies (1)

λ_{mrw}	$\lambda_{0.30}$	$\lambda_{0.35}$	λ_{f}
1.03	1.03	1.02	1.03
0.97	0.96	0.95	0.94
1.02	1.02	1.01	1.03
1.03	1.02	1.01	1.00
0.91	0.91	0.90	0.89
1.12	1.09	1.09	1.05
1.08	1.07	1.06	1.04
1.08	1.07	1.06	1.06
1.12	1.09	1.08	1.08

Table 3.7 Parametric studies (2)

λ_{mrw}	$\lambda_{0.30}$	$\lambda_{0.35}$	λ_{f}
1.56	1.52	1.52	1.49
1.55	1.51	1.50	1.43
1.51	1.51	1.50	1.48
2.01	1.99	1.97	1.91
1.59	1.59	1.58	1.54
1.63	1.57	1.56	1.49
1.37	1.41	1.39	1.38
1.70	1.71	1.69	1.64

Table 3.8 Other comparisons

CHAPTER 4

OPTIMUM ELASTO-PLASTIC DESIGN OF FRAMES

4.1 Introduction

Minimum weight design based on rigid-plastic theory is well established, following the work of Livesley(8) described in Chapter (1). In such approaches, compressive axial forces are ignored, and the problem is usually converted into one of mathematical programming and solved using techniques such as the simplex algorithm. For all but the simplest frames, solution has to be obtained by recourse to a computer. While this method may produce economical structures, there is no guarantee that premature collapse due to overall frame instability will be prevented.

For this reason, the methods proposed by Horne and Morris(20) and Ridha and Wright(21) enable instability effects to be incorporated in the design routine. However, as explained in Chapter (1), both methods are not based on an accurate assessment of frame instability effects. While Horne and Morris adopt the 'portal' method to estimate sway deflections, Ridha and Wright neglect the deflection constraint completely.

It has been argued in this thesis that it is advantageous for a trial frame to possess adequate stiffness as this can lead to a lower bound design for strength. However, cases can arise where designs are controlled by strength. For such cases, it is uncertain

as to which members should have their sections increased and by what amount in order to achieve a satisfactory design. Therefore, the need arises for a structural optimization method, which in turn requires the rates of change of the failure load with increase in sections of different members. Accurate non-linear elasto-plastic analysis is unsuitable in such a procedure because of the excessive demand on computer time inherent in such approaches.

This Chapter describes a simple but approximate method for the design of multi-storey frames of rectangular configuration that already satisfy criteria such as adequate stiffness. The procedure determines the most economical changes in sections following a series of trial analyses; the latter are based on the expression proposed in Chapter (3) for estimating the ultimate load. Linear programming techniques are avoided because there is only one constraints in the optimization procedure.

4.2 Optimization procedure

Consider the variation of the load factor, λ , of a plane frame such as that of figure (4.1). For convenience in explanation, it will be assumed that all the beams are grouped together so that they have the same section, denoted by S_b. Similarly, the columns are grouped together, the section being denoted by S_c.

Let an initial trial design which satisfies the usual deflection limits at the working load be analysed for the collapse load. The resulting load factor is λ_f , and the design load level is denoted by unity. It is assumed that $\lambda_f < 1.0$. The design

problem is therefore to determine the most economical changes in section sizes that should be made to increase λ from λ_f to unity.

The total weight, W, can be taken as representative of the cost of a frame. Thus, the objective function can be expressed as,

$$W = \sum_{i=1}^{N} w_i . l_i \qquad (4.1)$$

where w_i is the weight per unit length of member 'i', which has a length, l_i.

In practice, costs are still estimated in this way, although usually a percentage increase is made to the weight of plain metal to account for connections. This may differ from member to member. Such differences are ignored in the work below, but could be easily included if desired.

If $\partial\lambda_f/\partial S$ is the rate of change of the load factor with the section size of a member, then for the frame shown in figure (4.1) the problem can be stated as,

$$\text{Minimize} \quad W = (w_b + \Delta w_b).(4L_1 + 2L_2 + L_3) + (w_c + \Delta w_c).(2h_1 + 2h_2 + 3h_3 + 4h_4) \qquad (4.2)$$

subject to

$$\lambda_f + \Delta\lambda_f = \lambda_f + \frac{\partial\lambda_f}{\partial s_b}\Delta s_b + \frac{\partial\lambda_f}{\partial s_c}\Delta s_c \geq 1$$

$$\therefore \frac{\partial\lambda_f}{\partial s_b}\Delta s_b + \frac{\partial\lambda_f}{\partial s_c}\Delta s_c \geq 1 - \lambda_f \qquad (4.3)$$

where W is the total weight of the beams and columns of the frame,

S_b and S_c are the initial section sizes of the beams and columns respectively,

ΔS_b and ΔS_c are changes in the sections corresponding to S_b and S_c in beams and columns respectively,

w_b and w_c are the weight per unit length of a member corresponding to S_b and S_c respectively,

Δw_b and Δw_c are changes in the weight per unit length corresponding to changes ΔS_b and ΔS_c respectively,

L and h are the bay width and storey height respectively.

As w_b and w_c are constants, the objective function given by equation (4.2) can be expressed as,

$$\text{Minimize } W = \Delta w_b.(4L_1 + 2L_2 + L_3) + \Delta w_c.(2h_1 + 2h_2 + 3h_3 + 4h_4) \qquad (4.4)$$

Furthermore, there is only one constraint in equation (4.3). If it is assumed that λ_f varies linearly with change in S_b and change in S_c, it follows that for W to be a minimum, only one of ΔS_b and ΔS_c will be non-zero. Hence, the optimization procedure is reduced to determining the increase in λ_f relative to increase in total weight given by each group,

$$\Lambda = \frac{\partial \lambda_f}{\partial W}$$

$$\therefore \Lambda = \frac{\text{current value } \lambda_f - \text{ initial design value } \lambda_f}{\text{current total weight - initial total weight}} \qquad (4.5)$$

Values of Λ can be obtained by repeating the analysis with M_{pb} and M_{pc} increased in turn, whilst keeping the other value of M_p constant at its initial value. Thus, specialized linear programming algorithms are not required for the solution of the design problem.

In fact, λ_f does not vary linearly with change in S_b or S_c, because of the following reasons,

a)Once a section has been increased sufficiently to reduce or eliminate plasticity in the corresponding members, further increase in section size only lead to increase of stiffness.

b)The stiffness of the frame, which influences susceptibility to instability, is dependant on the moment of inertia of a section.

To take account of non-linearity, iteration is required to determine the most economic change of member sections. The procedure described above is followed, except that when a change in ΔS in section size is to be made, it is restricted to an increase of just one section from the list of available sections. The resulting design is then treated as a new initial design, and the optimization procedure is repeated.

It is usual in structural optimization to assume a continuous range of sections is available, so that a section can be chosen with any specified properties. It can be seen that in the present

work, real sections are adopted. Within a range of real sections tabulated in BCSA Handbook on Safe Loads, an economic section is defined as one which equals or exceeds other sections of equal weight with respect to the plastic modulus or moment of inertia.

Fortunately, the choice of economic Universal beam and Universal column sections is not affected if the moment of inertia is treated as the governing section property, rather than the plastic moment. Tables (4.1) and (4.2) shows the list of economic beam and column sections in ascending order of preferred sections. A similar list can be tabulated with respect to the total depth of the section where restrictions on floor depth are the criterion for the choice of sections in design.

4.3 Overall analysis and design

The overall procedure will be described first, with the details of the calculation methods for λ_p and λ_c given later. It is assumed that the initial design satisfies adequate stiffness and it is first required to determine the ultimate load of the trial frame. If λ_f , obtained from equation (3.4) in Chapter (3) is less than unity, increases in sections are required. The analysis procedure determines λ_p and λ_c for a chosen change in each member group as shown in figure (4.2). Values of λ_f and the total weight of each cycle are evaluated. The rate of change of λ_f to the increment of total weight in each iteration is then determined using equation (4.5).

In this and subsequent Sections, an iteration is defined as

one complete process whereby a group with the highest coefficient, Λ , is selected and a modified design obtained. A cycle is defined as one group change. Therefore, the number of cycles to be performed depends on the number of member groups in a design. Each iteration involves the completion of this number of cycles. Members may be sub-divided into as many groups as desired. The limit of member grouping is therefore equal to the total number of members in the structure. For instance, the frame shown in figure (4.1) may be arranged to have eighteen groups comprising seven beams and eleven columns. A total of eighteen cycles would be executed in each iteration. It is, however, usual to provide column lengths running through at least two floors and beams of the same section on consecutive floors for economy in fabrication and erection, and this arrangement presents no problem for the proposed procedure.

At the end of each cycle, values of $\partial\lambda_f$ and ∂W are determined and stored for comparison with the next cycle. When the cycle is completed, the group with the highest coefficient $\partial\lambda_f/\partial W$ is selected as that to be changed to provide the initial design for the next iteration. The final test compares the failure load for the new design with the required value, terminating when the design load is attained. Otherwise, the whole procedure is repeated until the minimum design load is achieved.

To assist in the calculations, the expression given in the previous Chapter is solved for λ_f and is given by,

$$\lambda_f = \frac{\sqrt{1 + (2\,\Omega\,\lambda_c)^2} - 1}{2} \qquad (4.6)$$

where $\Omega = \dfrac{\lambda_c \lambda_p - 0.4(\lambda_p)^2}{(\lambda_c)^3}$

In order that equation (4.6) may be used, both λ_p and λ_c must be calculated rapidly.

4.4 Rigid-plastic collapse load factor

In considering the more significant parameter, λ_p , it is proposed that the rigid-plastic collapse load be calculated by the method of combination of mechanisms. Although it appears more advantageous to adopt the static form of rigid-plastic analysis as opposed to the mechanism or kinematic approach, it is argued that for most realistic frames, the mode of collapse is by one of a limited number of mechanisms. These mechanisms have been identified for the frames examined in Chapter (2). Therefore, restricting the possible collapse modes to a relatively small number of similar shape to those shown in the parametric studies in Chapter (2) is justified.

Strictly, the mechanism approach demands that all possible collapse modes be found with the result that the lowest calculated value of λ_p is equal to the true value. As an example, consider the seven-storey frame shown in figure (4.3). This is one of a series of seven-storey frames used in the parametric studies and designed in Chapter (2). Figure (4.3 (a)) shows the rigid-plastic collapse mechanism obtained from an accurate computer analysis while the figure on the right was determined by considering the comprehensive combined-type as shown. The value of the collapse

load obtained from figure (4.3 (b)) is in good agreement with the accurate result. A validation exercise will be shown for all the frames examined in Chapter (2) to demonstrate the accuracy of the proposed method based on a finite number of mechanisms.

By limiting the number of mechanisms, computing time in iterative analysis is reduced. The finite number of rigid-plastic mechanisms are shown in figures (4.4) to (4.14). The diagram on the left represents a form of collapse occurring in the mid-height region of the frame, while the one alongside is an identical mechanism but drawn to indicate collapse occurring at a different location in the frame. The bounds of the mechanism vary from storey to storey, to seek the lowest collapse load for each type of mechanism.

Take for example the comprehensive combined-type mechanism shown in figure (4.9). In the first mechanism of this type, the column hinges are located at the base of the top storey with the corresponding beam hinges for the roof members only. Subsequent 2, 3, 4, 5 and 6 storeys are considered as participating in the mechanism. This is achieved by transferring the column hinges downwards and placing plastic hinges on all the beams above the column hinges. The process terminates when all the storeys have been included in the mechanism.

The mechanism shown in figure (4.11) must not be confused with that of figure (4.12). The former allows the column hinges to move downwards while the latter has 'stationary' plastic hinges at the base. In both cases, sufficient beam hinges are inserted as the

process is repeated at the next storey level. An exception to the procedure described above is the simple beam collapse mechanism, where it is recognised that each beam may have different member properties and magnitude of loading. For such a collapse mechanism, each beam is analysed by writing down the appropriate work equation.

For each of the mechanism shown in figures (4.4) to (4.14), the analysis is executed by setting up the virtual work equation. The lowest rigid-plastic collapse load factor is then obtained and the specific mechanism identified.

These collapse modes are associated with frames subject to combined loading and most, if not all, are familiar to design engineers because they have been applied successfully in practice for the design of relatively low-rise frames(17,32). The value of λ_p obtained in this manner is acceptable for use in the optimization procedure although it is concievable that other mechanisms may exist with a lower value than those proposed.

As an example, consider figures (4.4) and (4.9). The rigid-plastic collapse load of the sway mechanism for each storey from the roof to ground level of figure (4.4) is given by,

$$\lambda_p = \frac{2 \sum_{n=1}^{j} M_{pc\,(reduced)_j}}{\left[\sum_{n=1}^{i} H_n \right] h_i} \qquad (4.7)$$

The collapse load of the comprehensive combined mechanism of figure (4.9) is given by,

$$\lambda_p = \frac{\sum_{n=1}^{j} M_{pc}(\text{reduced})_i + \sum_{m=1}^{i} 4 \sum_{n=1}^{k} (M_{pb})_m}{\sum_{m=1}^{i} \frac{1}{2} \sum_{n=1}^{k} V_n L_n + \left[\sum_{n=1}^{i} H_n h_n + \sum_{n=1}^{i-1} H_n h_{n+1} + \sum_{n=1}^{i-2} H_n h_{n+2} + \cdots\cdots \right]} \qquad (4.8)$$

where i = storey level starting at 1 from the top,

j = number of columns in each storey i,

k = number of bays in each storey,

M_{pc} (reduced) = reduced plastic moment capacity of the column at λ_p ,

H_n = horizontal wind load,

h = storey height,

V_n = mid-span vertical load,

L_n = bay width,

M_{pb} = full plastic moment capacity of the beams.

Other types of collapse modes can similarly be shown as a combination or slight modifications of these two equations.

In order to take into account the effects of axial forces on the plastic moment capacities of column members, the analysis of each mechanism is iterative. The assumptions for evaluating the axial forces in the columns are identical to those described and shown in the example in Chapter (3). The reduced plastic moment of each column is given by one of the following expressions,

$$Mp(\text{reduced}) = (Z_p - C.n) \quad f_y \qquad n < F \qquad (4.9)$$

$$Mp(\text{reduced}) = D\,(1 - n)\,(E + n) \quad f_y \qquad n > F \qquad (4.10)$$

where n = |axial load| /[(cross-sect. area).(yield stress)],

Z_p = plastic section modulus.

The expressions apply equally to both tensile and compressive axial forces in the columns. The constants C, D, E and F differ for each of the sections listed in the BCSA Handbook.

The process of iteration terminates for each mechanism when the assumed load factor (used to reduce the plastic moment capacities of the columns) is within a suitable tolerance of the calculated collapse load factor. It was found that oscillation occurred between collapse mechanisms when all the work equations were set up simultaneously at a given (assumed) load factor. This was due to certain mechanisms giving widely different values for the collapse load. To overcome this problem, the collapse load was calculated by iteration for EACH mechanism in turn.

The lowest calculated value of the collapse load of each mechanism is compared with other mechanisms. Simple beam mechanisms are calculated directly for each member, figure (4.13). In this manner, the lowest rigid-plastic collapse load is obtained very rapidly.

Four examples are shown in figures (4.15) to (4.18) using the proposed procedure to estimate the rigid-plastic collapse load factor. Accurate computer analyses for the same frames are shown alongside for comparison. It can be seen that the proposed collapse mechanisms are almost identical to accurate results. A number of frames have been shown primarily to demonstrate the application to irregular and unusual plane frames.

A maximum error of 2.5% was found for the fifteen storey rectangular frame. The frame is subjected to variable wind loads and has different member yield stresses, and the proposal is programmed to deal with such frames. Figure (4.15) is taken from figure (2.7) Chapter (2), while figure (4.16) is taken from table (3.4), Chapter (3). Although strict accuracy is sacrificed for simplicity, the computing time for the fifteen storey building was a small proportion of that required for accurate computer analysis.

In contrast to rectangular frames, figures (4.17) and (4.18) illustrate the application of the proposed method to irregular frames. This is achieved by introducing 'dummy' members so that the mechanisms shown in figure (4.4) to (4.14) are still valid. 'Dummy' sections are input as members with zero stiffness and moment capacity for the beams and columns. In both examples, the mechanism approach showed very good agreement with accurate computer analysis.

As an illustration of the proposed method, consider figure (4.17). The reduced plastic moment capacities were calculated at a load level of 1.24 and are shown adjacent to the plastic hinges given in figure (4.17). From rigid-plastic theory, the work equation gives,

Hinge moments

Beams	$[(493.4 \times 15) + (262.6 \times 6)]\,\theta$	=	$8976.6\,\theta$
Columns	$[\ 230.3 + 183.6 + (185.8 \times 3) +$		
	$227.9 + 300.9 + 163.1\ ]\,\theta$	=	$1663.2\,\theta$
	Total	=	$10639.8\,\theta$

External moments

Wind load $[(75 \times 13) + (50 \times 9) + (55 \times 5)]\,\theta = 1700\,\theta$

Vertical load $[(320 \times 4 \times 2) + (180 \times 4.5) + (340 \times 8.5) + (150 \times 4)]\,\theta = 6860\,\theta$

Total $= 8560\,\theta$

$$\lambda_p = \frac{10639.8\ \theta}{8560\ \theta} = \underline{\underline{1.24}}$$

It can be shown in a similar manner that other mechanisms have higher collapse loads and this is therefore the lowest value.

4.5 Elastic critical load factor

The determination of the elastic critical load, λ_c, is a relatively simple process but considerable emphasis has been given to the dangers of selecting higher buckling modes(50,73). It is proposed to adopt the approximate method of Williams(73). Although the methods of Wood(50) and Williams(73) are basically similar, the latter is most suitable for programming especially on micro-computers. A feature which makes this method attractive is that it guarantees convergence onto the lowest critical load. A brief account only of the work due to Williams is given here but a fuller explanation can be found in reference (73).

Consider the equivalent single storey frame shown in figure (4.19 (a)). It was shown by Williams that the lowest elastic critical load inevitably involves an antisymmetrical sway mode. Therefore, λ_c is given by an analysis of the antisymmetrical

mode. It was assumed that for such mode, the beam rotations at both ends are equal and the slope-deflection equations give,

$$M_{bi} = k_{bi} . \theta_i \qquad (4.11)$$

where $k_{bi} = \frac{6E.I_{bi}}{L_b}$ $(i = 1,2 \text{ ----- } N)$

Using the 'no-shear' stability functions 'n' and 'o' for the 'i'th column shown in figure (4.19 (a)), the column moments are given by,

$$M_{ci1} = n_{ci} . k_{ci} . \theta_i - o_{ci} . k_{ci} . \theta_{i+1} \qquad (4.12)$$

$$M_{ci2} = -o_{ci} . k_{ci} . \theta_i + n_{ci} . k_{ci} . \theta_{i+1} \qquad (4.13)$$

where $k_{ci} = \frac{E.I_{ci}}{h_i}$ $(i = 1,2 \text{ ----- } N)$

θ_i and θ_{i+1} are the joint rotations for the upper and lower end of the 'i'th column respectively,

M_{ci1} and M_{ci2} are the bending moments for the upper and lower end of the 'i'th column respectively.

As the calculations neglect the externally applied moment, equilibrium of the joints is obtained by summing the appropriate equations given from (4.11) to (4.13), and equating the sum to zero. As an example, consider the top storey (i=1). Equilibrium of the top joint, using equations (4.11) and (4.12) gives,

$$M_{b1} + M_{c1(1)} = 0$$

$$\therefore k_{b1} . \theta_1 + n_{c1} . k_{c1} . \theta_1 - o_{c1} . k_{c1} . \theta_2 = 0$$

and equilibrium of the lower joint of the top storey, using equations (4.11) to (4.13) gives,

$$M_{b2} + M_{c1(2)} + M_{c2(1)} = 0$$

$$k_{b2}.\theta_2 - o_{c1}.k_{c1}.\theta_1 + n_{c1}.k_{c1}.\theta_2 + n_{c2}.k_{c2}.\theta_2 - o_{c2}.k_{c2}.\theta_3 = 0$$

The rotation, θ_1, for the top joint can be expressed in terms of θ_2. Substituting this into the lower joint gives θ_2 in terms of θ_3. The procedure can be repeated for the next storey. It has been verified by Williams that the above equations can be reduced to a general form given by,

$$a_i.\theta_i + b_i.\theta_{i+1} = 0 \quad (i = 1,2 \text{ ----- } N) \tag{4.14}$$

$$a_{N+1}.\theta_{N+1} = 0 \tag{4.15}$$

where $a_{i+1} = c_{i+1} - \frac{b_i^2}{a_i}$ $(i = 1,2 \text{ ----- } N)$

$$a_1 = n_{c1}.k_{c1} + k_{b1}$$

$$b_i = -o_{ci}.k_{ci} \quad (i = 1,2 \text{ ----- } N)$$

$$c_i = n_{c\,i-1}.k_{c(i-1)} + n_{ci}.k_{ci} + k_{bi} \quad (i = 2,3 \text{ ----- } N)$$

$$c_{N+1} = n_{cN}.k_{cN} + k_{b(N+1)}$$

For fixed base frames, $k_{b(N+1)} = \infty$, therefore equation (4.14) gives,

$$a_N.\theta_N = 0 \quad , \quad \text{since } \theta_{N+1} = 0 \tag{4.16}$$

Equation (4.16) is satisfied only by $a_N = 0$ or $\theta_N = 0$. Since $\theta_N \neq 0$ in the first sway mode, figure (4.19 (a)), the condition for buckling to occur in this mode is given by $a_N = 0$.

To avoid repeating all the terms above, the value of 'N' must be replaced by 'N-1' in equations (4.14) and (4.15) because the base is fixed.

The procedure is reduced to determining, at a trial value of an assumed multiple of the loads, λ , the signs of a_i. These are given as,

$$\lambda < \lambda_{c1} \quad \text{if} \quad a_i > 0 \quad (i = 1,2 \text{ ----- } N) \tag{4.17}$$
$$\lambda_{c1} < \lambda < \lambda_{c2} \text{ if ONE } a_i < 0 \quad (i = 1,2 \text{ ----- } N)$$

where λ_{c1} and λ_{c2} are the first and second critical loads respectively.

Equation (4.17) ensures that the lowest elastic critical load is found and avoids confusion with higher critical loads. In addition, Williams suggested checking the value of the determinant at every load level given by,

$$d = \frac{a_2}{c_2} \cdot \frac{a_3}{c_3} \cdot \frac{a_4}{c_4} \text{ ---------- } \frac{a_N}{c_N} \tag{4.18}$$

To illustrate the application of the method, consider the irregular four storey frame shown in figure (4.17). Using the procedure described above, the lowest elastic critical load is calculated as follows,

load,λ	a_1	a_2	a_3	a_4	d
12	170.9	323.3	414.8	49.0	0.468
13	169.3	312.0	389.0	-560.9	1.038
12.13	170.7	321.8	411.6	-1.57	-0.03

At a load factor of 12, all the 'a_i' terms corresponding to the number of storeys and 'd' given by equation (4.18) were positive. When a load factor of 13 was used, one 'a_i' was negative, thus satisfying the second of equation (4.17). Further iterations were performed with a load factor between 12 and 13 since only one 'a_i' has been found. The elastic critical load was found to be 12.13.

A plot of 'd' against the load factor is shown in figure (4.19 (b)). Using an accurate non-linear elastic program of Majid and Anderson(41), in conjunction with a modified Southwell plot, the lowest elastic critical load was found to be 11.91. The approximate analysis of Williams(73) is in excellent agreement with this value.

4.6 Comparison with parametric studies and limitations

The elastic critical loads and the rigid-plastic collapse loads given in Chapter (2) were obtained by accurate non-linear computer analyses. As the proposed method considers only a finite number of rigid-plastic mechanisms based on assumed column axial forces, it is necessary to validate such proposals. At the same time, the lowest elastic critical load is calculated by the approximate method of Williams(73) to confirm its accuracy.

A total of forty-three frames of varying rectangular configuration were examined in the parametric studies described in Chapter (2). The results will be compared with those obtained from the proposed method of calculating the rigid-plastic collapse load and the lowest elastic critical load factors. These results are

shown in tables (4.3) and (4.4). Both accurate and approximate results are tabulated for λ_p and λ_c . The layout of the two tables are the same as that shown in Chapter (3). It is noted that the values are given to two significant figures and therefore the ratio of λ_c/λ_p may differ slightly from the values quoted in previous Chapters.

The majority of values given by Williams' method overestimated the accurate answers by an average of 3%. Two results exceeded the accurate values by 13% and 7%. In both cases, this occurred for a ten storey, narrow bay width frame. This does not influence the predicted failure load significantly because λ_f is not sensitive to λ_c . For instance, in the two examples mentioned above, the resulting increases in λ_f given by equation (4.6), are less than one percent.

The general overestimate of λ_c is due to the assumptions made in the physical approximation of the real structure. The results based on the equivalent single bay frame of figure (4.19 (a)) are 'exact' but the behaviour in real terms differs somewhat from that of the equivalent frame. It was assumed that joint rotations are equal at each floor level and the beams bend in symmetrical double curvature. This is approximately true if the frame is subjected to horizontal loads only. Joint rotations for the real frame vary, particularly at the upper storey levels where vertical beam loading is significant in comparison with the horizontal loads. As a result, the stiffnesses for the equivalent single bay frame has been overestimated.

The majority of results for the rigid-plastic collapse load indicate a maximum error of less than 1%. Only in three cases, was λ_p overestimated by more than 1%, but the error did not exceed 3%. These results are indicated by a spot in table (4.3). The frames are relatively large and subject to maximum vertical loads. In such cases, strength would normally be the governing criterion in design under combined loading, so the proposed method is particularly suitable. However, the predicted failure load is still below λ when these estimated values of λ_c and λ_p given in table (4.3) are substituted into equation (4.6). Not surprisingly, the accurate value of λ_p is given by the proposed method when the correct mode of collapse was identical or very similar in appearance to one of the finite number of selected mechanisms.

It is emphasised that the axial forces used in the proposed method to evaluate the reduced plastic moment capacities of columns are approximate. In addition, when the assumed mode of collapse was not identical to the computer results, the latter revealed partially-plastic zones occurring at positions corresponding to those assumed in the proposed method. It is therefore not surprising that when the approximate values of λ_p were substituted into equation (4.6) to recalculate λ_f , the results were in good agreement with accurate computer results.

Certain limitations to the proposed simplified method of mechanisms are now discussed. It was assumed that local instability such as buckling of flanges does not occur. Therefore, sections that are unsuitable for plastic hinge action are excluded in the list of economic sections. Lateral instability of beams is unlikely

to happen due to restraint from floor slabs, and it is also assumed that individual columns are not susceptable to lateral torsional buckling. These criteria can be satisfied by selecting suitable Universal sections.

The frames examined were rigid-jointed with fixed bases but pinned bases can similarly be incorporated, simply by amending the work equation relating to each of the proposed mechanisms shown in figures (4.4) to (4.14). However, it would be uneconomical for realistic frames of this nature to have pinned bases unless soil conditions are critical in design.

Real pins occurring elsewhere cannot be disregarded, particularly at the top of roof columns to reduce excessively large bending moments caused by heavy loading (for example, due to plant). Indeed, real pins can occur anywhere within the structural framework. The proposed method is unable to deal with such cases.

The concept of the sagging mid-span plastic hinge in unbraced construction is an idealisation that does not occur for uniformly distributed loading. A combination of wind and uniformly distributed loads causes the central hinge to form at some location, away from mid-span depending on the relative magnitude of end moments. However, it was shown by Horne and Morris(17) that iterative analysis to locate the exact position of the central hinge does not alter the load factor significantly if a mid-span hinge was assumed instead, and this assumption was used in the proposed method.

4.7 Design examples

Two examples are described using the proposed optimization procedure. The first example is a seven storey three bay rectangular frame in which the initial design satisfies deflection limits at working load. This is one of the seven-storey frames used in the design studies in Chapter (2). A second example is given to illustrate the application of the method to an irregular frame that does not satisfy the usual deflection limit. In the initial design, column sections were chosen to resist only squashing, while the beam sections were selected without considering the higher design load factor applicable to vertical load alone.

4.7.1 Seven storey three bay frame

The sections are shown in figure (4.20) and grouped accordingly as shown. There are two beam and three column groups. Therefore, five cycles of analysis will be performed in each iteration. Initial design was such that the frame was adequate with respect to lateral stiffness when subjected to unfactored horizontal loads. The frame was required to sustain the applied loads as shown. This form of loading corresponds to the ratio of maximum vertical to minimum horizontal wind loading as shown in table (4.3), and indicated by a triangular symbol.

Using the proposed method, the initial design of the frame was found to have inadequate strength with λ_c=4.82, λ_p=0.99 and λ_f=0.88. This initial design is shown in figure (4.21 (b)) along with the accurate results in figure (4.21 (a)). Collapse

mechanisms of the accurate and proposed methods are in good agreement because the former mode has been identified and duplicated in the proposed procedure. The complete optimization procedure is summarised in table (4.5). The group numbers shown in figure (4.20) also serve as the order in which sections are changed in the optimization procedure.

The roof member was selected from a section not listed in the economic section table (4.1) due to restriction on beam depth. Therefore, by replacing this group with an economic section of similar weight will result in an infinite value of Λ given by equation (4.5). The criterion for selection is however, dependant on the highest value of λ_f. Table (4.5) shows that there is no significant increase in λ_f because the critical collapse mechanism do not involve the roof beam. Similarly sections indicated by group "4" did not affect the rigid-plastic collapse load in the first iteration. This is apparent from the table where the values of λ_c, λ_p and λ_f are unchanged in that cycle of analysis. Comparing groups "2", "3" and "5" in the first iteration showed that the best action to cause a significant rise in the ultimate strength would be to replace group "2". As the resulting value of λ_f was less than the minimum design load, a second iteration was performed.

The 'strengthened' design is converted into an initial design for the second iteration. Proceeding in a similar manner as the first iteration, increasing group "5" gives the highest rate of change of the failure load to the total weight. Furthermore, the predicted failure load is now greater than 1.00 and the procedure

is terminated. This final design similarly gave the highest value of λ_p . This is some 8.5% above the initial design in the second iteration and a 16% increase from the inadequate design in the first iteration. The predicted failure load was found to have risen by the same amount. The total weight of the final design was increased by less than 8% compared with the original unsatisfactory design.

In comparison with accurate non-linear elasto-plastic computer analysis(41), the final design was found to possess adequate strength with $\lambda_f = 1.00$ while the approximate proposal gave $\lambda_f = 1.02$, an overestimate of only 2% of the 'exact' result. However, the rigid-plastic collapse load was identical even though the collapse mode was dissimilar. Both modes of collapse are shown in figures (4.21 (c)) and (4.21 (d)), obtained by an accurate and the proposed method of analysis respectively. Values shown in figure (4.21 (d)) are the reduced plastic moment capacities of the appropriate final sections calculated at a load factor of 1.15.

It is noticed that the accurate collapse mechanism in the final design corresponds to the proposed mechanism shown in figure (4.6) but the latter was not selected as the critical collapse mode. To ensure that a wrong mechanism has not been selected from the finite number shown in figures (4.4) to (4.14), it is proposed to illustrate the reason by calculating the collapse load of the mechanism given by figure (4.6). This is performed as follows,

a)At unit load factor, the approximate axial force in the windward column of the second storey is 1015.9 KN.

b)At the same load level, the approximate axial forces in all the ground floor columns are, from left to right, 1189.6, 2498.8, 2498.8 and 1309.2 KN. respectively.

c)Assume a load factor of 1.15 [corresponding to the collapse load shown in figure (4.21 (d))] to evaluate the reduced plastic moment capacities of the appropriate columns.

d)The moment capacity for the second storey windward column is 4295 KN.cm., while the ground floor columns are shown in figure (4.21 (d)) as 2301, 11170, 11170 and 904 KN.cm. from left to right respectively.
These values are determined from equations (4.9) and (4.10) at a load factor of 1.15.

e)Full plastic moment capacity of the beams were assumed.
The values for each section in the group is 26256 KN.cm.

f)The external work due to the wind and vertical forces is determined as follows,

$$[8.445 + (6 \times 16.89)] \times 375.\theta + (190.6 \times 375).\theta$$
$$= 112644.4\ \theta \text{ KN.cm.}$$

g)Hence,

$$\lambda_p = \frac{\text{sum of plastic hinge moments . hinge rotations}}{112644.4\ \theta}$$

$$= \frac{[(3\text{x}26256) + 4295 + 2301 + (2\text{x}904) + (4\text{x}11170)].\theta}{112644.4\ \theta}$$

$$= \underline{\underline{1.17}}$$

This shows that the proposed method calculates the collapse load for the mechanism in figure (4.21 (c)) as (say an average of) 1.16, and therefore it is not regarded as critical. The error arises from the assumption in the approximate method used to determine axial forces in the columns, but it can be seen that this is insignificant. It can similarly be demonstrated that the roof member collapses by a beam-type mechanism at a load factor of 1.16. Therefore, the collapse mechanism shown in figure (4.21 (d)) is the most critical according to the proposed method.

4.7.2 Irregular four storey three bay frame

An example of the optimization procedure applied to an irregular plane frame will now be described. The initial sections have been selected randomly and tabulated in table (4.6). It is required to sustain the applied vertical and horizontal loads given in figure (4.22 (b)). There are two beam and four column groups, thereby requiring a total of six cycles to be executed in each iteration.

The member groups are denoted by integers shown on each section in figure (4.22 (a)). Note that two plots are shown in this figure to illustrate the variation of the rigid-plastic collapse loads and the predicted failure loads at each cycle of every iteration. The vertical axis denotes the load factor and the abscissa represents the number of iterations.

The vertical axis shown in figure (4.22 (b)) represents the total weight of the frame. It is noted that each circle shown in

the figure correspond to the variation of the load factor given in figure (4.22 (a)). The unknown initial design is indicated in both figures (4.22 (a)) and (4.22 (b)). It is seen that the number of iterations on the horizontal axis is shown in ascending order from 1 onwards to represent that particular iteration.

As in the first example, the numbers shown by the groups also serve as the order of member group changes. Each circle on both figures represents a member group change corresponding to the numbered sequence shown in figure (4.22 (a)). A dark spot indicated in each iteration represents the highest coefficient, Λ , for the particular iteration. It follows that this dark spot forms the initial design in the next iteration if the design load has not been attained.
The critical collapse mechanisms corresponding to these spots are shown in figure (4.22 (b)). The circles have been joined to represent the variation of λ_f and λ_p as member groups are changed and analysed. Their corresponding total weights are similarly joined for each cycle.

Consider the initial iteration. The initial design developed a beam-type collapse of the longer middle span as the critical mechanism. This corresponds to the highest rate of change of the failure load to the total weight of the frame. Consequently, this forms the basis for the first iteration. The critical mechanism is shown at the top of the plot in figure (4.22 (b)).

In the first 2 iterations, group "2" was increased by as many sections because it was most economical. In the first iteration,

the mechanism was a simple beam collapse of the same member as the initial critical design. The critical collapse mechanism in the second iteration is given by figure (4.12).

In successive iterations, group "3" was increased once and group "6" twice. Their respective critical collapse modes are shown in figure (4.22 (b)). Finally, group "2" was increased again in order to satisfy the minimum design load.

It is noticed that λ_f was 1.00 when group "2" was increased in the fifth iteration. The reason for not selecting group "2" as the initial design in the next iteration was due to the criterion placed upon Λ given by equation (4.5). Instead, group "6" was chosen because it gave the highest rate of change of the failure load to the total weight. Had group "2" been selected in preference to group "6", the procedure would have been stopped at the end of the fifth iteration.

Not surprisingly, both the fifth and sixth iteration collapsed by beam-type mechanisms since the column group "6", which was increased previously, is independant of such collapse. A slight increase in λ_c was noted in the final design. Increasing the beam group "2" in the last iteration caused the roof beam to collapse by a beam-type mechanism.

In such circumstances, it is tempting to ignore the sixth design but the total weight was just 1% above the fifth design. The total frame weight for these two designs are indicated in figure (4.22 (b)), and the designer could select either. As the method is

approximate and the weights are so close, the writer would choose the sixth design. Such designs are likely to be close to the optimum. Sections for the sixth design is given in table (4.7).

An accurate computer result showed a simple plastic roof beam collapse at λ_p =1.05. The proposed method similarly gave,

$$\lambda_p = \frac{8 \times 888.4 \times 24}{180 \times 900} = \underline{\underline{1.05}}$$

The non-linear elasto-plastic failure load was 1.04 while the approximate equation gave λ_f =1.01. The lowest elastic critical load factor of this final design was 12.00.

It is interesting to compare the sway deflections due to unfactored horizontal loads only of the initial design and the final design. Unfactored wind loads were calculated by dividing the values in figure (4.22 (b)) by 1.2. Linear elastic analysis showed the lateral sway from roof to ground level of 1/369, 1/184, 1/208 and 1/238 of each storey for the initial design, and 1/587, 1/311, 1/292 and 1/358 for the final design. This suggests that an efficient design can be generated even from an initial design which is totally unacceptable in terms of both strength and stiffness.

4.8 Conclusion

An approximate optimization procedure has been shown which considers, in a series of iterations, the most economical increases in section to achieve a minimum weight design. No specialized mathematical programming techniques were required because there is only one constraint. The procedure makes use of the rate of change of the failure load to the total weight as each member group is increased successively. The problem is to determine the highest rate of change in an iteration, until the design load is satisfied.

Each member in the frame may be specified as an individual group in the proposed method but this is unusual for the type of frames examined. The method is particularly suitable for programming on desk-top computers. Examples of the final design were compared and shown to be in good agreement with accurate computer results. The proposed method can be used on frames that are designed by the Merchant-Rankine approach simply by amending the expression for the failure load.

A simple procedure which determines the rigid-plastic collapse load factor by the method of combination of mechanisms was shown to estimate very accurately the true plastic collapse load of plane rigid-jointed unbraced frameworks. The approximation depends only on a limited number of collapse modes to establish the lowest value. Several examples of rectangular and non-rectangular frames were examined and these showed excellent agreement with accurate computer results for the rigid-plastic collapse load.

A further validation exercise on forty-three rectangular frames also provided generally good agreement in λ_p, with only one frame exceeding 2% but less than 3% of the result from accurate analysis. The error was due to an inaccurate assessment of the axial forces in the proposed method. In all cases, the error for λ_p was negligible as a result of close representations of the true collapse mechanisms shown by the computer analysis.

Particular attention was given to the possible occurrence of high column axial loads, variable wind loads and member yield stresses which are encountered in practice. The proposal has included such features in the analysis procedure and has been shown to estimate satisfactorily λ_p for a fifteen storey rectangular building. In comparison with accurate computer analysis, the computing time and storage was reduced dramatically.

The lowest value of λ_p obtained by the proposed method of finite mechanisms was used in conjunction with the lowest elastic critical load to estimate the failure load. The method of evaluating λ_c was based on an equivalent single bay frame. This is very similar to the method proposed in Design Recommendations(54,55) but has the advantage of guaranteeing convergence onto the lowest critical load. The adopted method for calculating λ_c due to Williams(73) provides a convenient technique for programming, especially on desk-top computers. The method has also been verified in this Chapter but the approximate failure load is not sensitive to relatively large changes in λ_c. For the majority of frames examined, an average overestimate of λ_c by about 3% was found when compared with accurate results. This

does not cause any significant variation of the failure load given in equation (4.6).

Two examples were described. In the first example, a seven storey frame was shown to have inadequate strength initially but satisfied the usual deflection limits. Using the proposed procedure, two increases in member groups were sufficient to attain the desired load level. The rigid-plastic collapse load was shown to provide good agreement with accurate computer results even though the mode of collapse was different. Manual calculations showed the true collapse mechanism to have a collapse load which differed by less than 1% from the mechanism selected by the proposed method. The difference was due to the approximate method used to estimate the axial forces in the columns in the proposed method.

The second example of an irregular frame shows that a completely unacceptable initial design can be used to generate an acceptable minimum weight design. The strength was gradually built up by selecting the most economic group to change in each iteration. Several iterations were required to obtain a satisfactory collapse load. The final design was compared with accurate computer analysis and the results showed good agreement in both the failure load and the rigid-plastic collapse load.

Exact elasto-plastic optimum design of frames has never been attempted due to excessive computing time but the proposed method has shown that an approximate solution can be obtained with little loss in accuracy. However, a final check could be made by one

accurate non-linear elasto-plastic analysis, in case of concern over the accuracy of the proposed method.

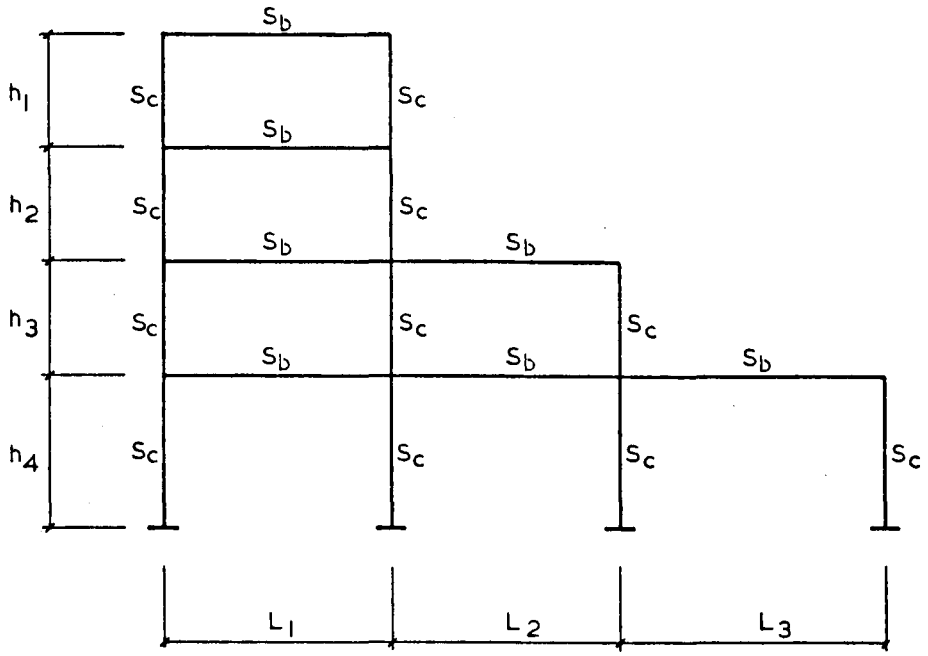

S_b = BEAM SECTION

S_c = COLUMN SECTION

FIG. 4.1 IRREGULAR FOUR STOREY PLANE FRAME

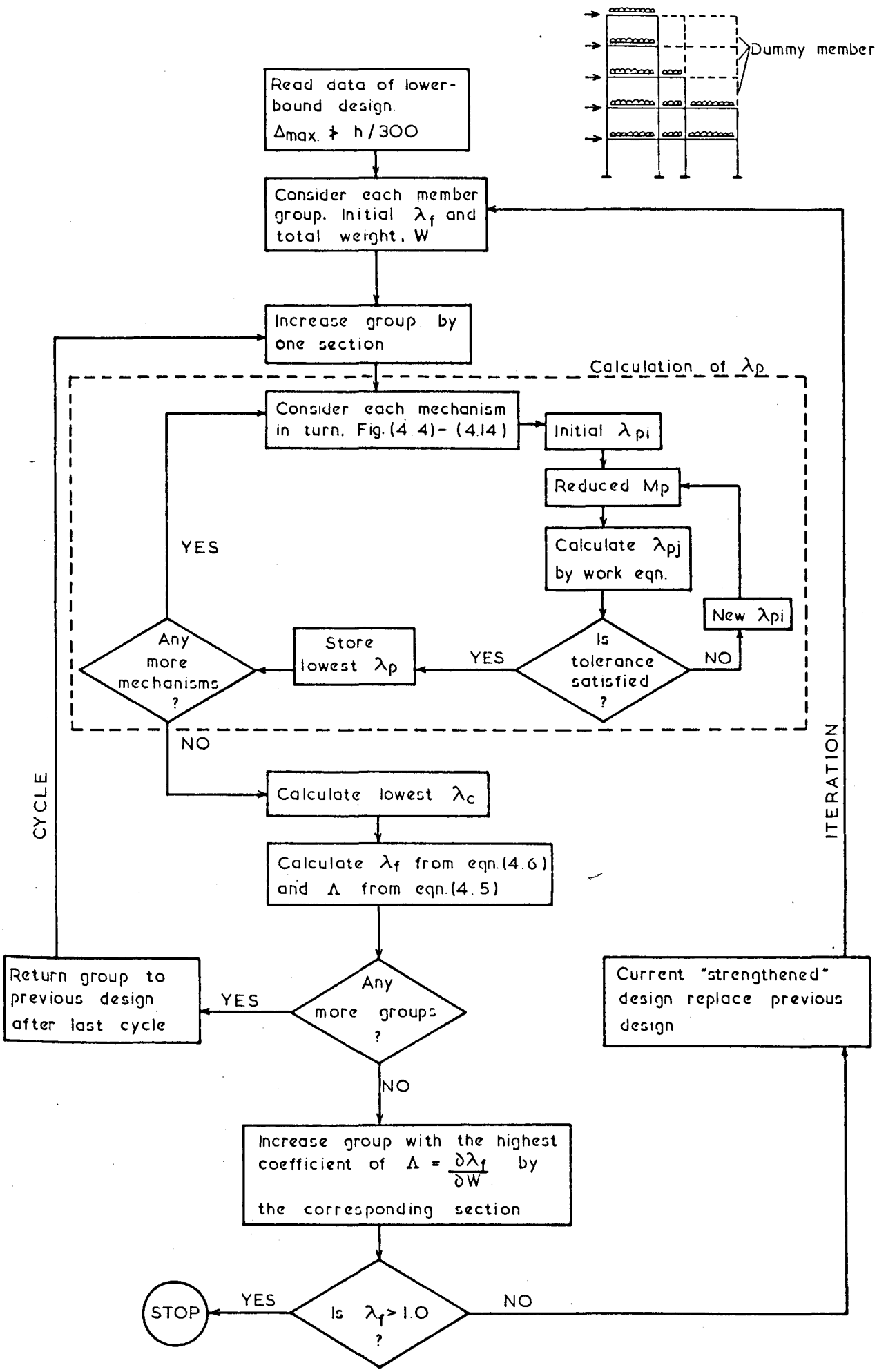

FIG. 4.2 OPTIMIZATION FLOW DIAGRAM

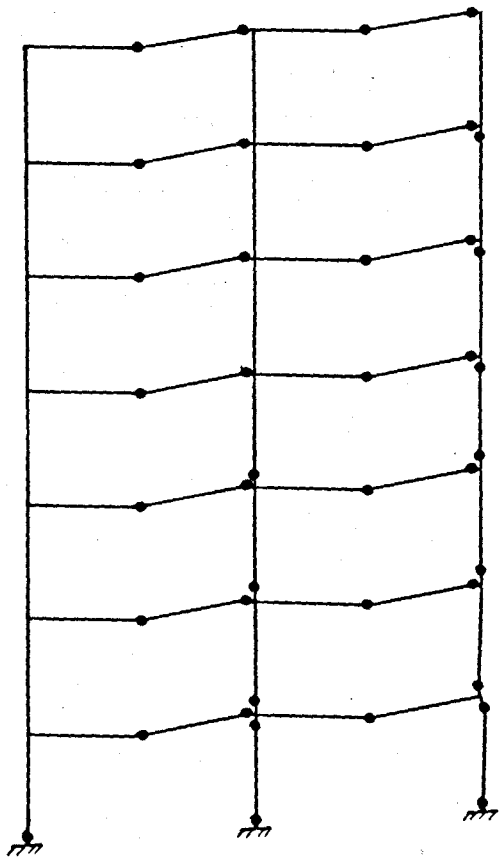

(a) 'Exact' $\lambda_p = 1.104$

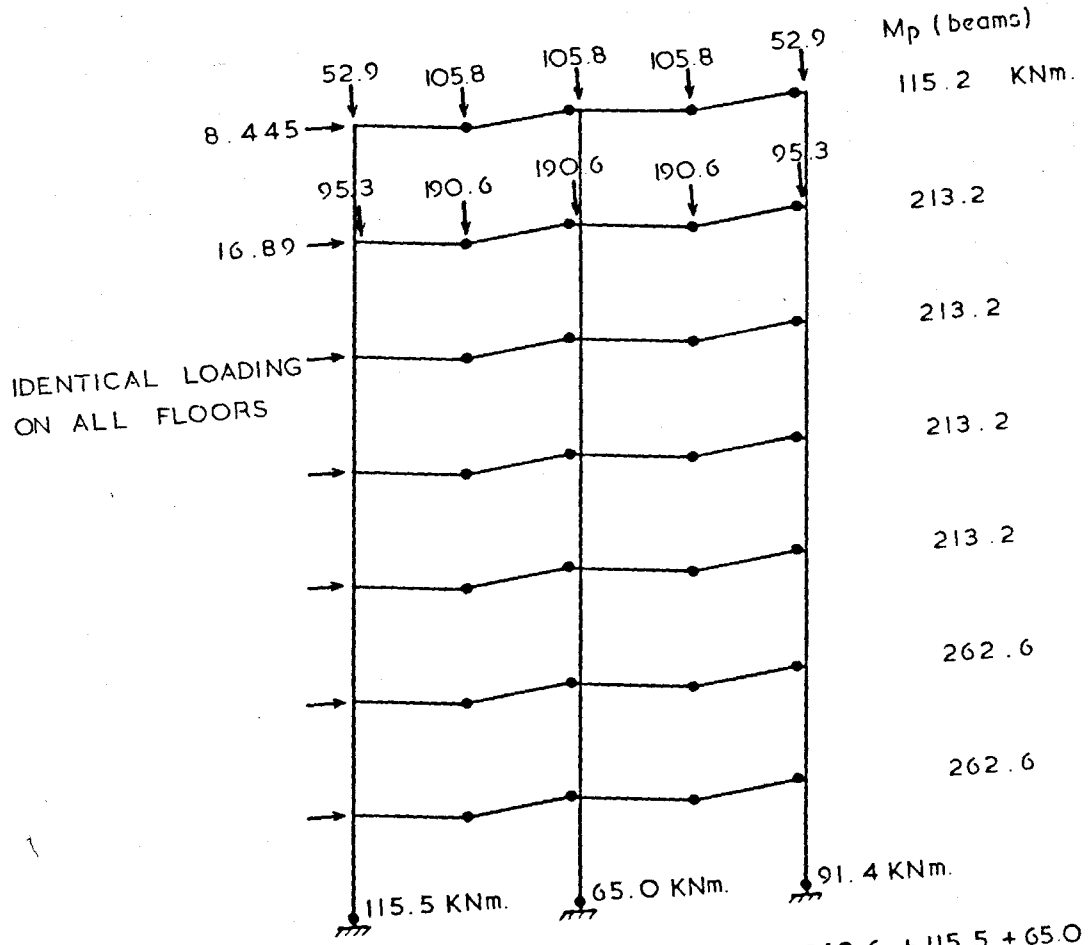

(b) $\lambda_p = \dfrac{8\times115.2 + 32\times213.2 + 16\times262.6 + 115.5 + 65.0 + 91.4}{2\times396.75 + 12\times714.75 + 1615.2}$

$= \dfrac{12217.5}{10987.7} = \underline{1.112}$

NOTE : Reduced plastic moment capacities of columns are calculated at $\lambda = 1.114$

FIG. 4.3 COMPARISON OF λ_p FOR 7-STOREY FRAME

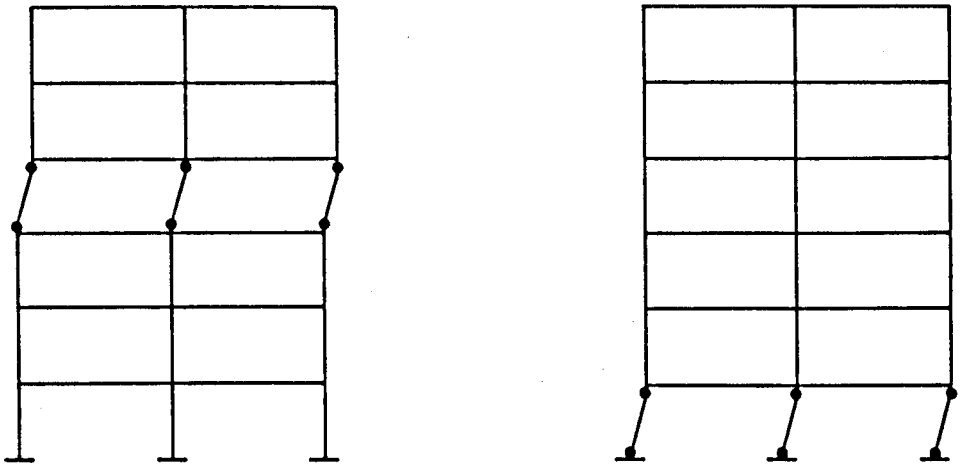

FIG. 4.4 STOREY SWAY MECHANISM

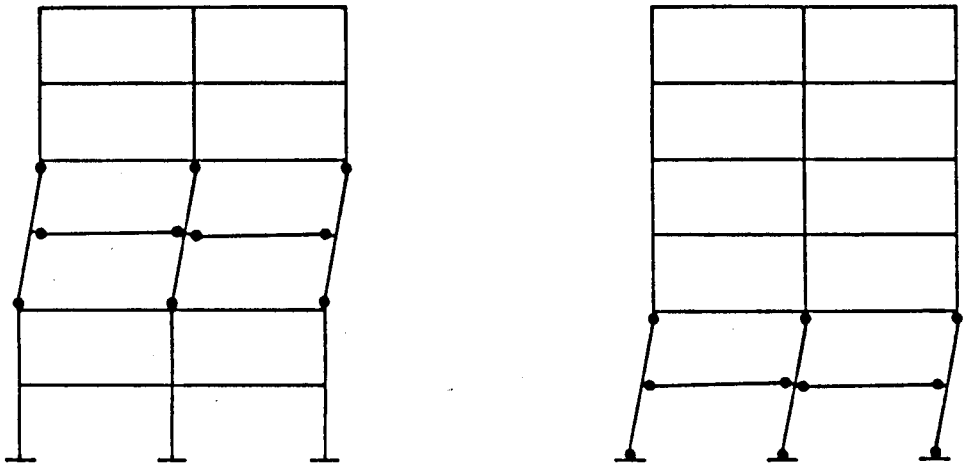

FIG. 4.5 DOUBLE SWAY MECHANISM

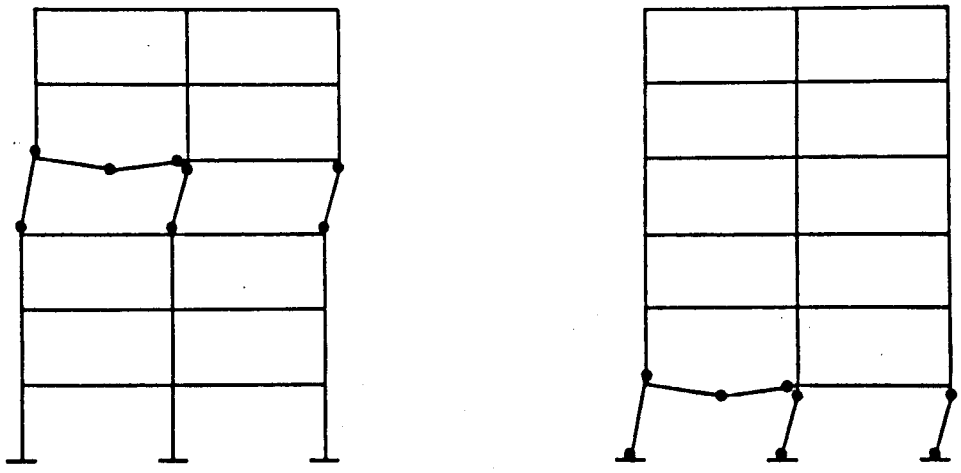

FIG. 4.6 COMBINED SWAY MECHANISM

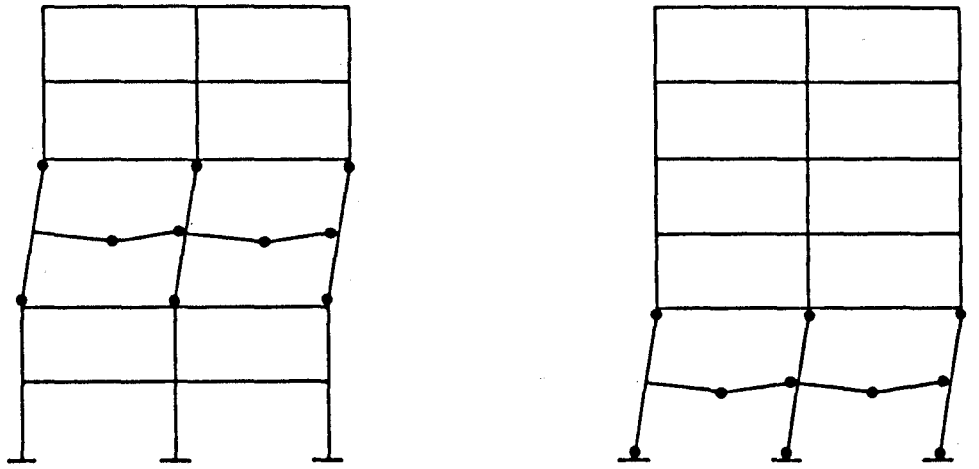

FIG. 4.7 SINGLE COMBINE MECHANISM

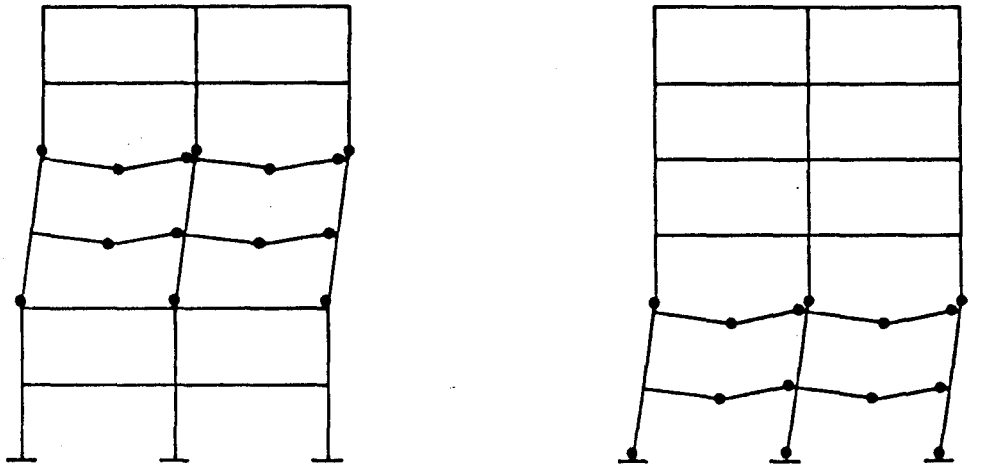

FIG. 4.8 DOUBLE COMBINE MECHANISM

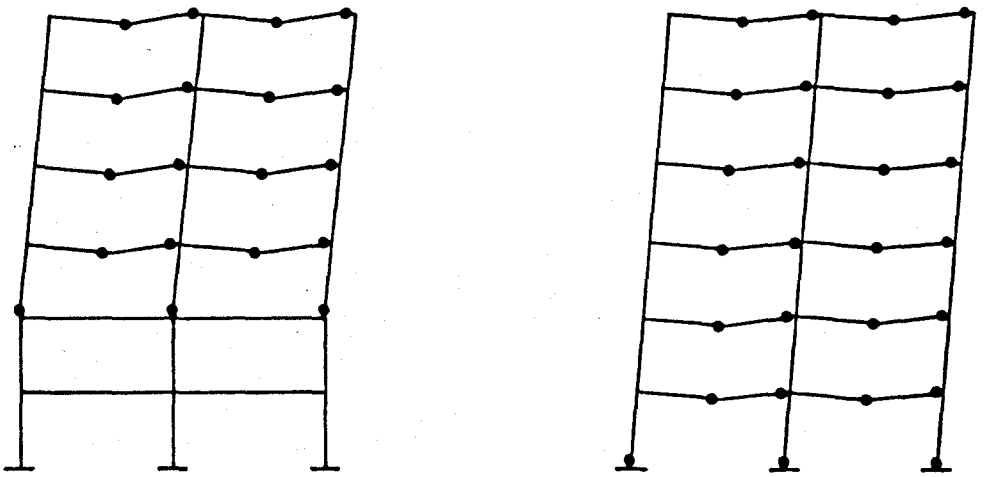

FIG. 4.9 TOP COMBINE MECHANISM

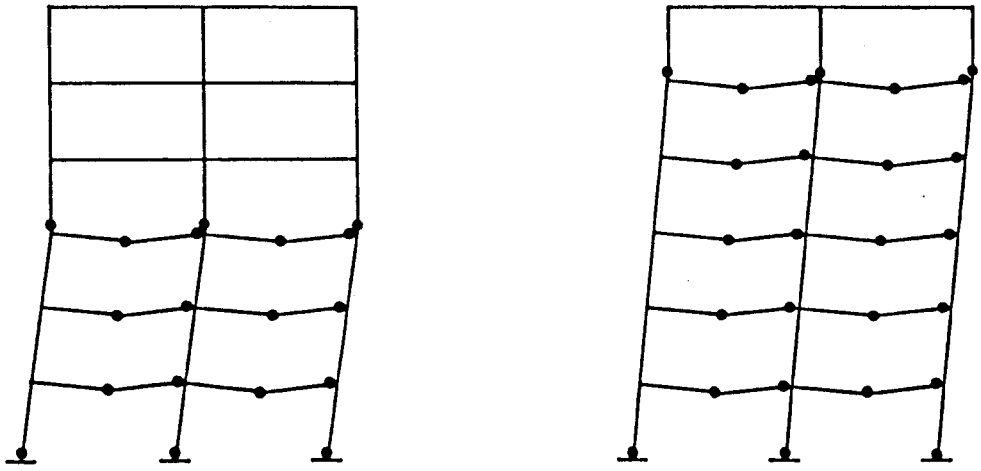

FIG 4.10 BOTTOM COMBINE MECHANISM

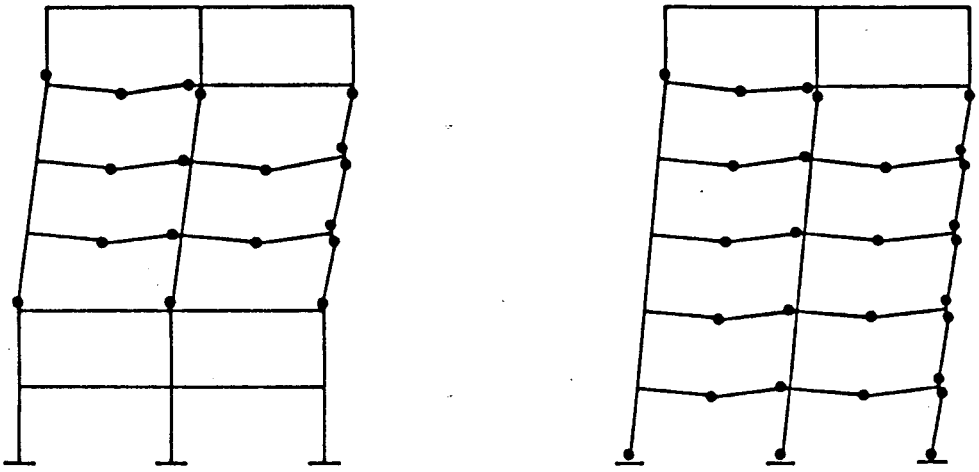

FIG. 4.11 TOP COLUMN COMBINE MECHANISM

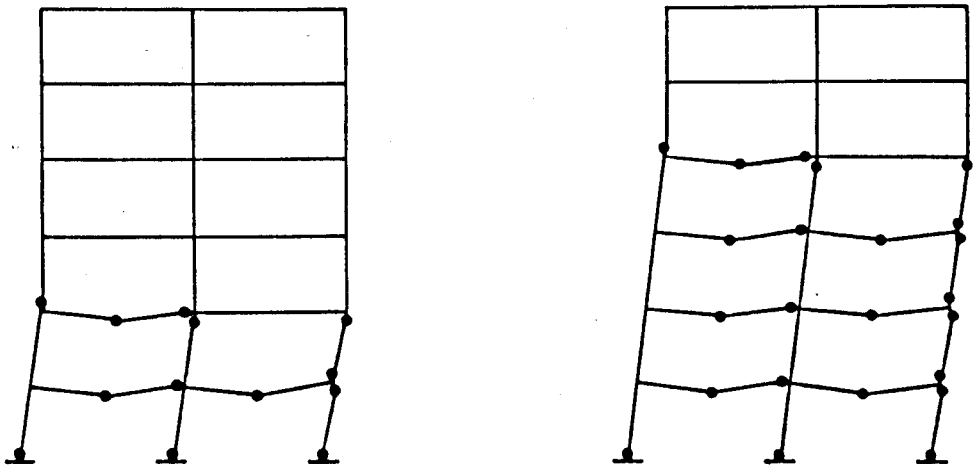

FIG. 4.12 BOTTOM COLUMN COMBINE MECHANISM

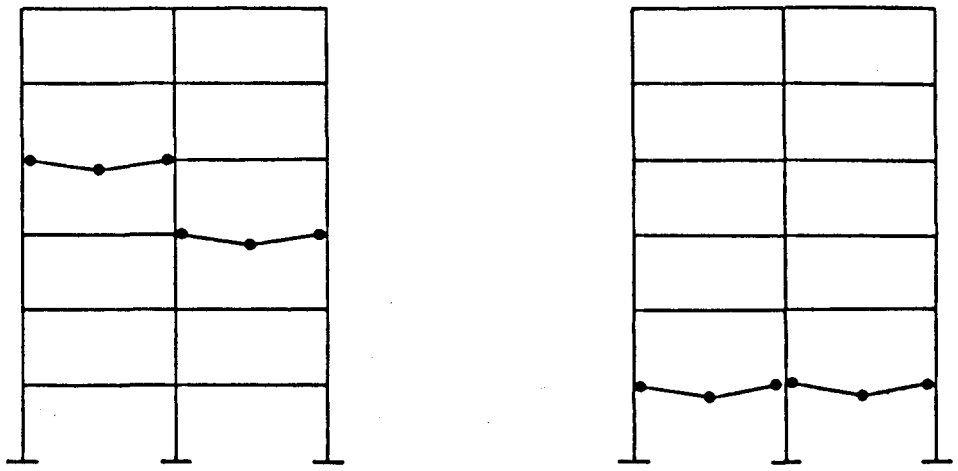

FIG. 4.13 SIMPLE BEAM MECHANISM

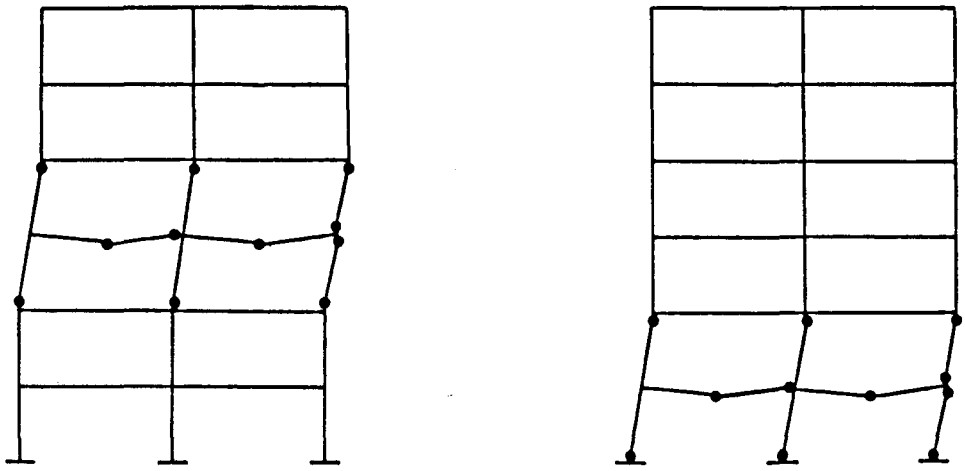

FIG. 4.14 DOUBLE COLUMN MECHANISM

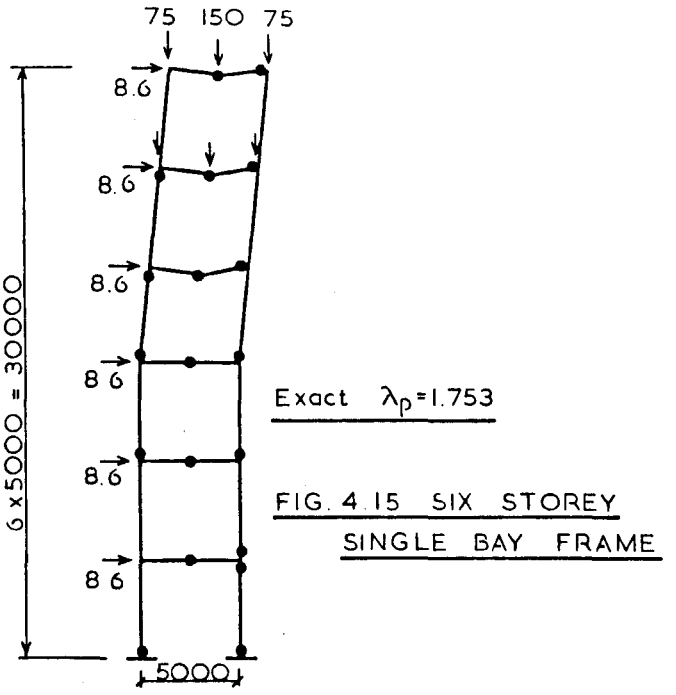

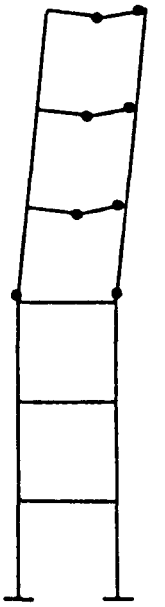

FIG. 4.15 SIX STOREY SINGLE BAY FRAME

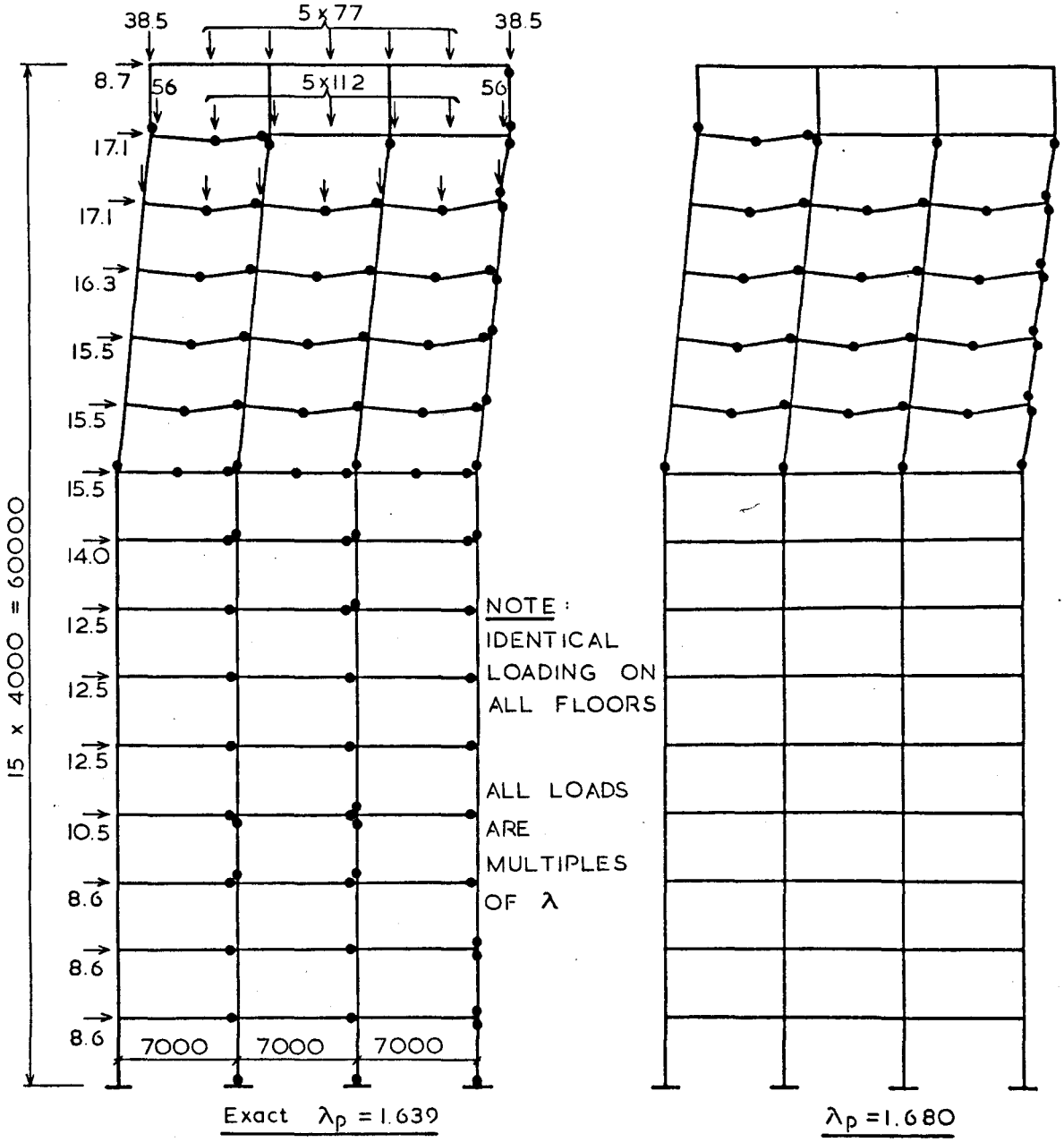

FIG. 4.16 FIFTEEN STOREY THREE BAY FRAME

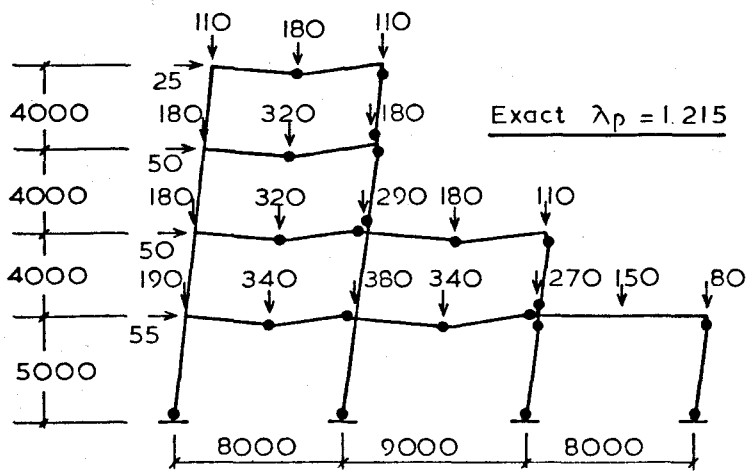

Exact $\lambda_p = 1.215$

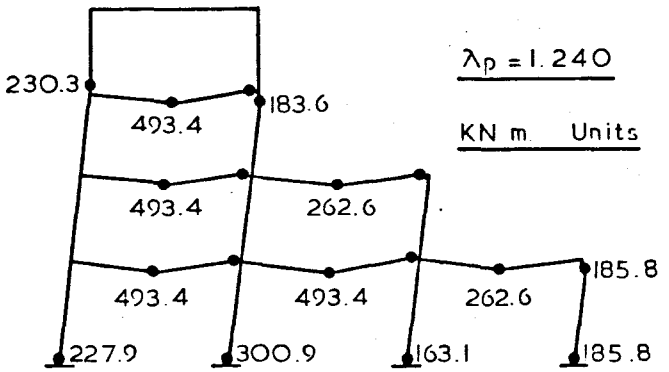

$\lambda_p = 1.240$

KN m Units

FIG 4 17 FOUR STOREY THREE BAY IRREGULAR FRAME

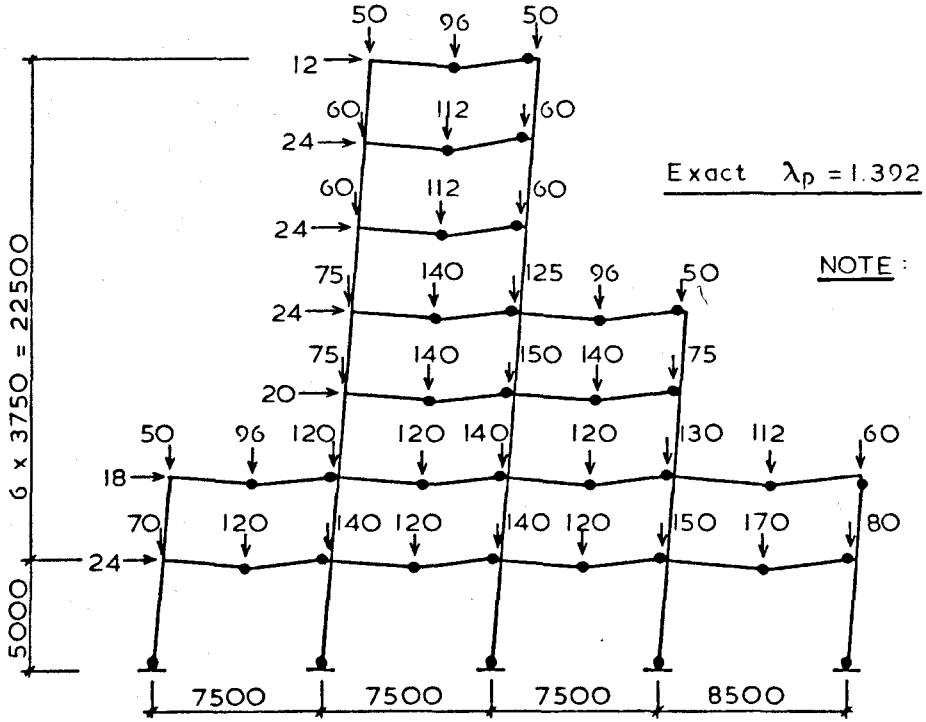

Exact $\lambda_p = 1.392$

NOTE: ALL LOADS ARE MULTIPLES OF λ

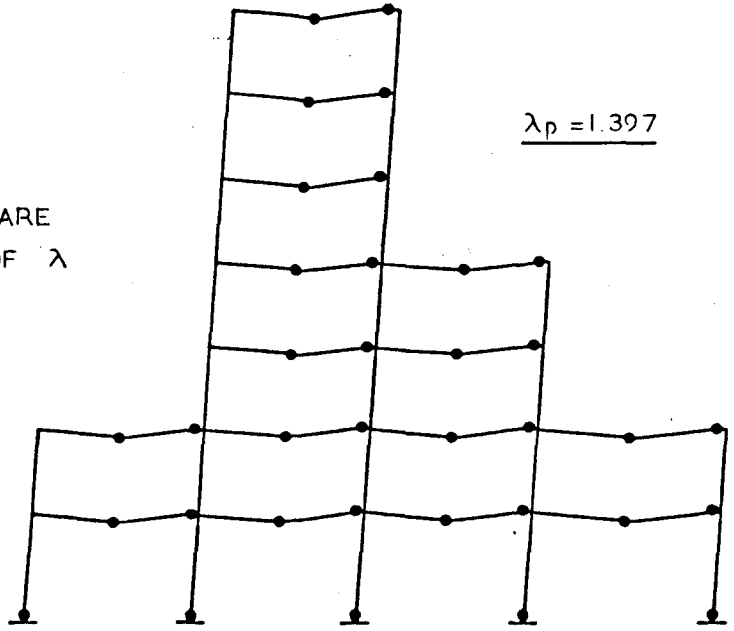

$\lambda_p = 1.397$

FIG 4 18 SEVEN STOREY FOUR BAY IRREGULAR FRAME

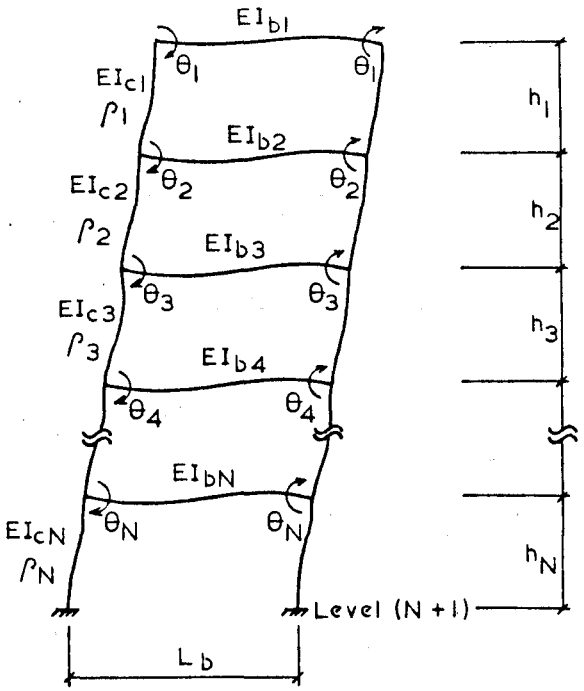

(a) EQUIVALENT SINGLE BAY FRAME

Notation

N = Number of storeys

EI = Flexural rigidity of member

L = Length of beam

h = Length of column

ρ_i = Ratio of compressive axial load to Euler load of i th column

$= \dfrac{P_i (h_i)^2}{\pi^2 EI_{ci}}$

Zero axial load in all beams

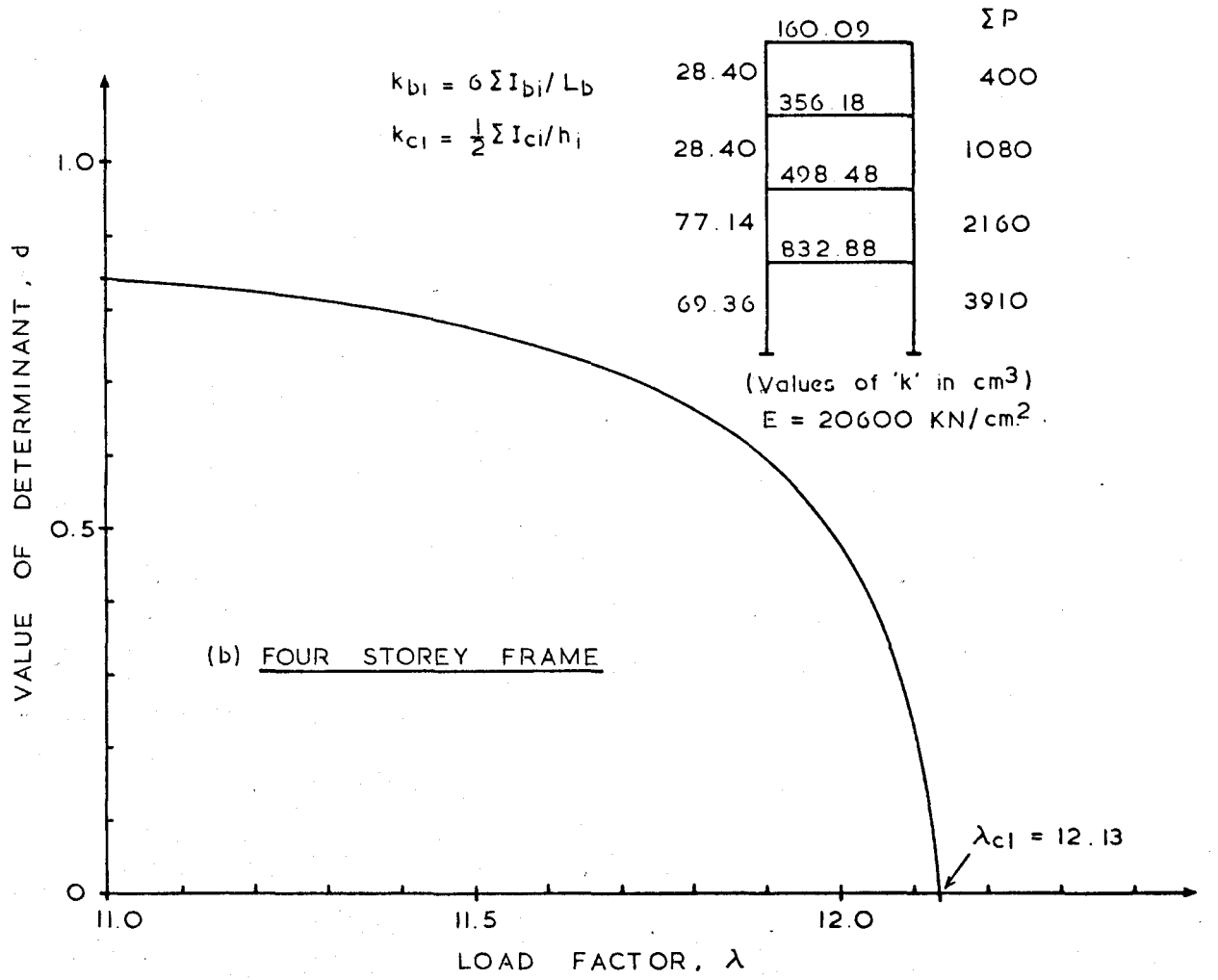

(b) FOUR STOREY FRAME

FIG 4.19 LOWEST ELASTIC CRITICAL LOAD

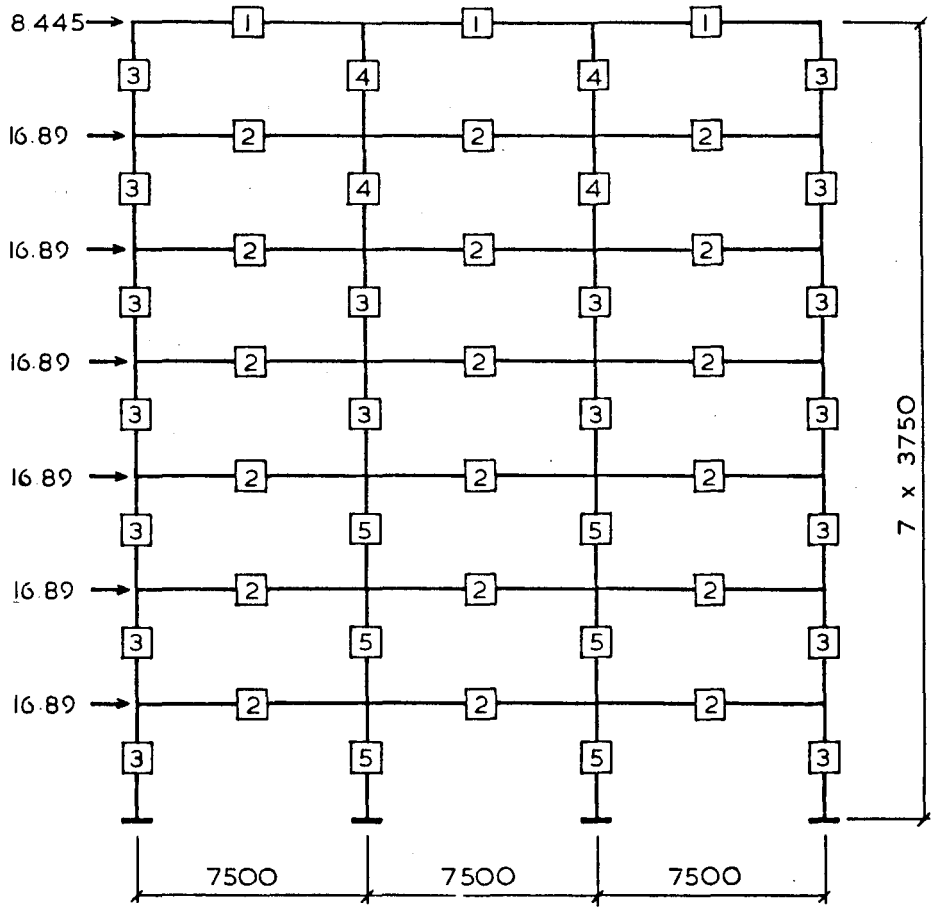

V(roof) = 28.20 KN/m

V(floor) = 50.824 KN/m

E = 206 KN/mm^2

f_y = 240 N/mm^2

GROUP	SECTION	INERTIA cm^4	Z_p cm^3
1	305 x 102 x 33UB	6487	479.9
2	406 x 140 x 46UB	15647	888.4
3	203 x 203 x 52UC	5263	568.1
4	152 x 152 x 30UC	1742	247.1
5	254 x 254 x 107UC	17510	1485.0

INITIAL TOTAL WEIGHT = 13320 Kg.

FIG. 4.20 SEVEN STOREY THREE BAY FRAME

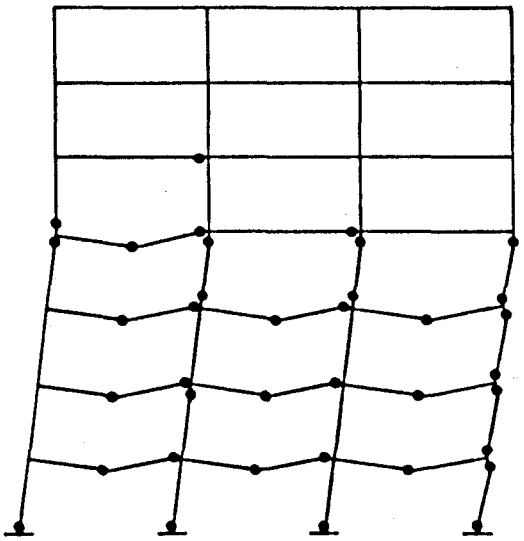

(a) Exact $\lambda_f = 0.89$

" $\lambda_p = 0.99$

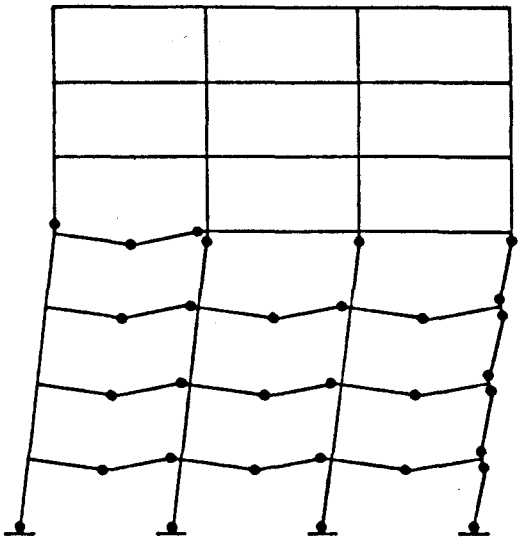

(b) $\lambda_f = 0.88$

$\lambda_p = 0.99$

Mechanism (4.12)

INITIAL DESIGN

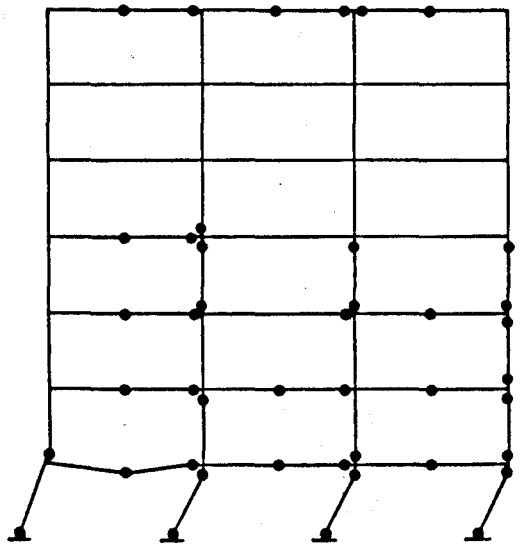

(c) Exact $\lambda_f = 1.00$

" $\lambda_p = 1.15$

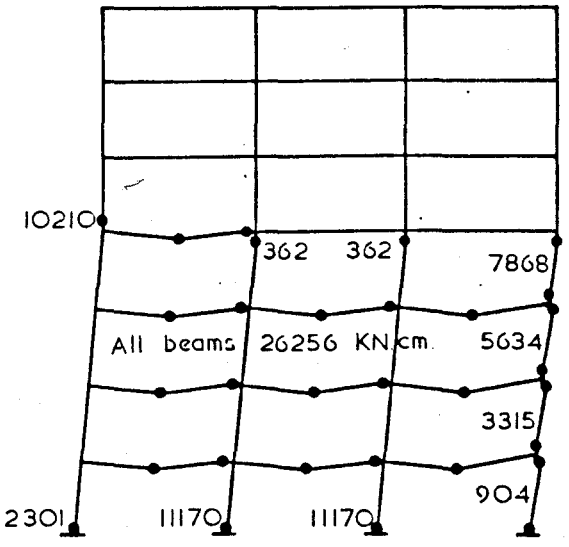

(d) $\lambda_f = 1.02$

$\lambda_p = 1.15$

Mechanism (4.12)

FINAL DESIGN

FIG. 4.21 INITIAL AND FINAL COLLAPSE MECHANISMS

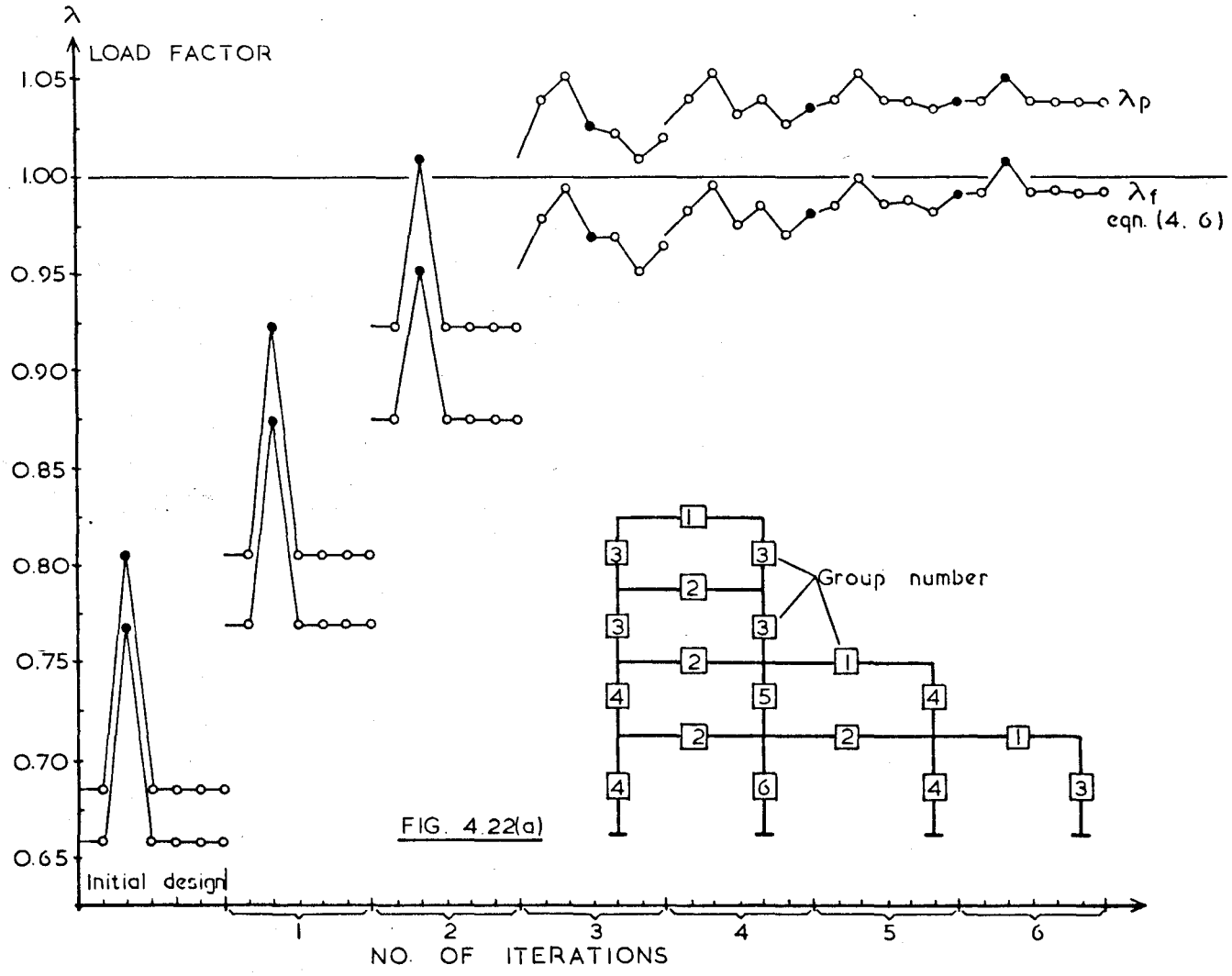

FIG. 4.22(a)

FIG. 4.22 IRREGULAR FRAME

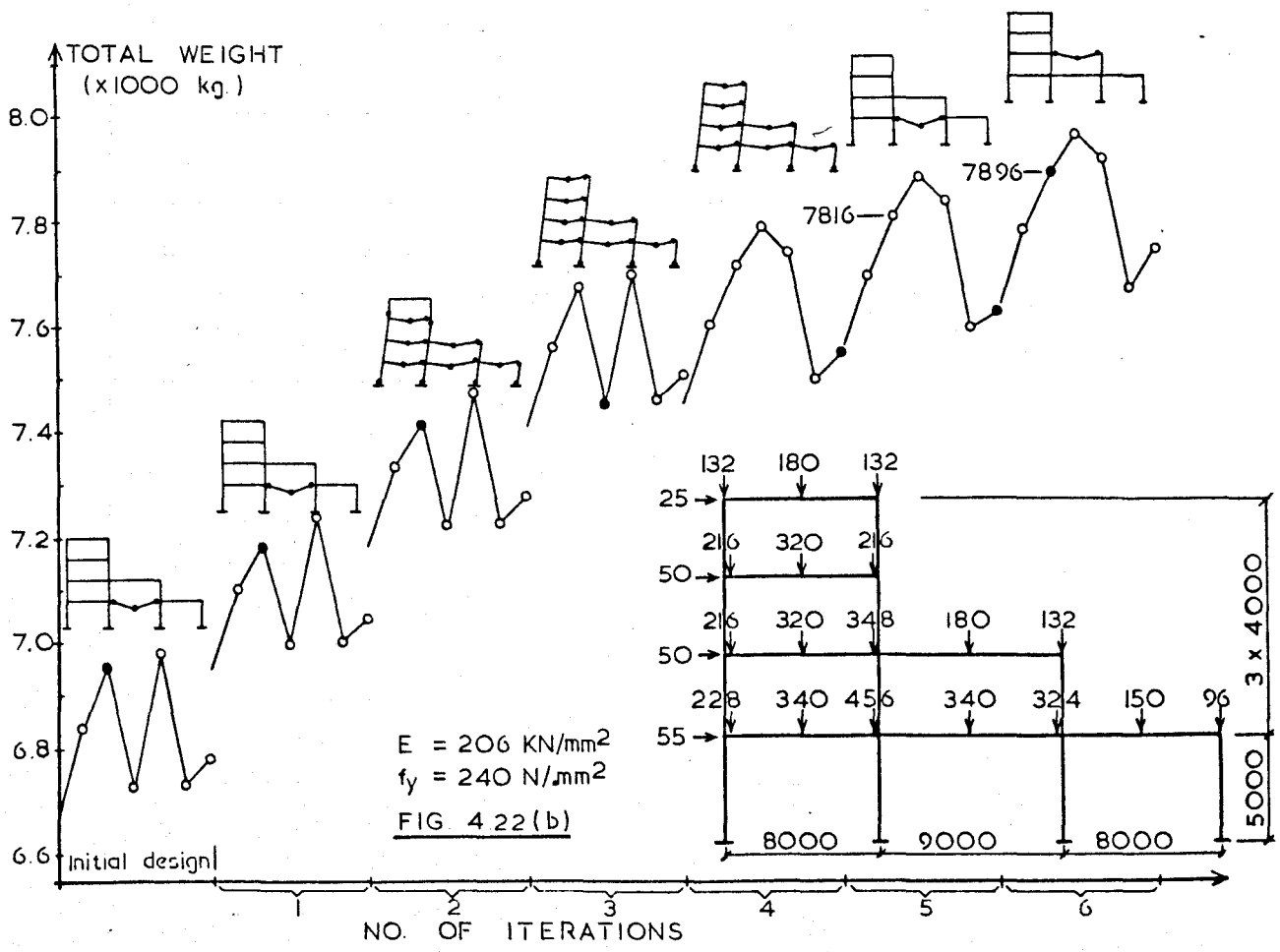

FIG. 4.22(b)

SECTION	Z_p (cm^3)	I_x (cm^4)
205 x 102 x 22	261.9	2867
305 x 102 x 25	337.8	4387
305 x 102 x 28	407.2	5421
356 x 127 x 33	539.8	8200
406 x 140 x 39	720.8	12452
406 x 140 x 46	888.4	15647
457 x 152 x 52	1094	21345
457 x 152 x 60	1284	25464
457 x 191 x 67	1471	29401
457 x 191 x 74	1657	33388
533 x 210 x 82	2056	47491
533 x 210 x 92	2366	55353
610 x 229 x 101	2882	75720
610 x 229 x 113	3288	87431
686 x 254 x 125	3996	118003
686 x 254 x 140	4560	136276

TABLE 4.1 ECONOMIC BEAM SECTIONS

SECTION	Z_p (cm^3)	I_x (cm^4)
152 x 152 x 30	247.1	1742
152 x 152 x 37	310.1	2218
203 x 203 x 52	568.1	5263
203 x 203 x 60	652.0	6088
203 x 203 x 71	802.4	7647
254 x 254 x 73	988.6	11360
254 x 254 x 89	1228	14307
254 x 254 x 107	1485	17510
305 x 305 x 118	1953	27601
305 x 305 x 137	2298	32838
356 x 368 x 153	2964	48525
356 x 368 x 177	3457	57153
356 x 368 x 202	3977	66307

TABLE 4.2 ECONOMIC COLUMN SECTIONS

Frame storey x bay	Min. vertical : Max. wind				Max. vertical : Min. wind				
	Exact		Proposed		Exact		Proposed		
	λ_c	λ_p	λ_c	λ_p	λ_c	λ_p	λ_c	λ_p	
4 x 2W	10.50	1.15	10.54	1.15	6.43	1.12	6.71	1.13	
4 x 2N	15.21	1.34	15.38	1.34	8.08	1.23	8.36	1.23	
4 x 3W					5.95	1.13	6.14	1.14	
4 x 3N					6.43	1.20	6.69	1.21	
4 x 4W					5.63	1.14	5.83	1.14	
4 x 4N					3.53	1.06	3.57	1.06	
4 x 5W	5.89	1.10	6.20	1.11	5.48	1.15	5.64	1.15	
4 x 5N	6.77	1.27	6.95	1.27	3.46	1.09	3.49	1.09	
7 x 2W	14.73	1.15	15.01	1.15	6.25	1.10	6.33	1.11	
7 x 2N	23.52	1.42	24.27	1.43	9.81	1.23	10.08	1.23	
7 x 3W					4.70	0.99	4.82	0.99	Δ
7 x 3N					6.19	1.17	6.23	1.17	
7 x 4W					4.85	1.08	4.97	1.10	●
7 x 4N					4.62	1.12	4.69	1.12	
7 x 5W	5.33	1.05	5.26	1.06	4.75	1.09	4.87	1.12	●
7 x 5N	7.70	1.33	7.73	1.34	4.58	1.15	4.64	1.16	
10 x 2W	17.61	1.15	18.40	1.15	6.75	1.12	6.89	1.13	
10 x 2N	21.13	1.42	24.01	1.43	9.74	1.21	10.08	1.21	
10 x 3W					4.98	1.07	5.03	1.09	●
10 x 3N					6.81	1.10	7.03	1.10	
10 x 4W	7.37	1.12	7.43	1.12	3.99	1.03	4.02	1.03	
10 x 4N	10.98	1.33	11.33	1.34	5.13	1.12	5.21	1.12	

W = Bay width 7500

N = Bay width 5000

Table 4.3 Comparison with parametric studies under extreme loading.

Frame storey x bay	Vertical load	Wind load	Exact		Proposed	
			λ_c	λ_p	λ_c	λ_p
4 x 2W	Max.	Inter.	6.46	1.11	6.72	1.11
4 x 3W	Max.	Max.	5.96	1.04	6.15	1.04
4 x 5W	Max.	Max.	5.47	1.12	5.64	1.12
7 x 2W	Max.	Inter.	6.75	1.10	6.79	1.10
7 x 5W	Max.	Max.	4.69	1.01	4.79	1.01
10 x 2W	Max.	Inter.	9.29	1.15	9.60	1.16
10 x 3W	Max.	Max.	7.33	1.14	7.42	1.15
10 x 2N	Max.	Inter.	6.72	1.16	7.19	1.16
10 x 2W	Max.	Inter.	8.81	1.15	9.10	1.16

W = Bay width 7500

N = Bay width 5000

TABLE 4.4 COMPARISON WITH PARAMETRIC STUDIES UNDER VARIOUS LOADING

	CYCLE	TOTAL WEIGHT (kg.)	λ_c	λ_p	λ eqn. (4.6)	Λ eqn. (4.5) $\times 10^{-3}$	Mech.	SECTION INERTIA	
								PREVIOUS	CURRENT
ITERATION 1	Initial design	13320	4.82	0.99	0.88	—	C	—	FIG. (4.20)
	1	13320	4.82	0.99	0.88	0	C	6487	8200
	2	14130	5.55	1.06	0.95	0.093	S	15647	21345
	3	13860	4.95	1.02	0.91	0.058	C	5263	6088
	4	13425	4.82	0.99	0.88	0	C	1742	2218
	5	13567.5	5.21	1.00	0.90	0.078	C	17510	27601
ITERATION 2	Initial design	14130	5.55	1.06	0.95	—	S	—	Group "2" replaced
	1	14130	5.55	1.06	0.95	0	S	6487	8200
	2	15210	5.92	1.06	0.96	0.007	S	21345	25464
	3	14670	5.76	1.10	0.99	0.069	S	5263	6088
	4	14235	5.55	1.06	0.95	0	S	1742	2218
	5	14377.5	5.82	1.15	1.02	0.290	C	17510	27601

TABLE 4.5 EXAMPLE 1 : OPTIMIZATION PROCEDURE

7 STOREY 3 BAY FRAME

	Storey	Bay 1	Bay 2	Bay 3	
Universal beams	4	406x140x46			
	3	457x152x52			
	2	457x152x52	406x140x46		
	1	457x152x52	457x152x52	406x140x46	
Universal columns	Storey	Column 1	Column 2	Column 3	Column 4
	4	203x203x71	203x203x71		
	3	203x203x71	203x203x71		
	2	254x254x73	254x254x107	254x254x73	
	1	254x254x73	305x305x118	254x254x73	203x203x71

E = 206 KN/mm^2 fy = 240 N/mm^2 Total weight = 6689 Kg.

TABLE 4.6 Initial sections of 4-storey 3-bay irregular frame

	Storey	Bay 1	Bay 2	Bay 3	
Universal beams	4	406x140x46			
	3	533x210x82			
	2	533x210x82	406x140x46		
	1	533x210x82	533x210x82	406x140x46	
Universal columns	Storey	Column 1	Column 2	Column 3	Column 4
	4	254x254x73	254x254x73		
	3	254x254x73	254x254x73		
	2	254x254x73	254x254x107	254x254x73	
	1	254x254x73	356x368x153	254x254x73	254x254x73

E = 206 KN/mm^2 fy = 240 N/mm^2 Total weight = 7896 Kg.

TABLE 4.7 Final sections of a 4-storey 3-bay irregular frame

CHAPTER 5 (PART 1)

AN APPROXIMATE DETERMINATION OF THE FAILURE LOAD OF SINGLE STOREY FRAMES

5.1 Introduction

As the deterioration of stiffness due to plasticity and compressive axial forces is a major concern in the design of unbraced multi-storey steel frames, computer methods are inevitably the most appropriate. Several such methods have been reviewed in Chapter (1). However, manual methods may be preferred for the reasons given in that Chapter.

Both the European Recommendations for Steel Construction and the draft for BS5950 allow the use of the empirical Merchant-Rankine formula as a hand method, but this does not find favour with all engineers because of its intuitive nature. In addition, there is a certain class of single storey portals that are subjected to exceptionally high horizontal wind loads and compressive axial forces which render both the simple plastic method and the Merchant-Rankine approach unsuitable for design.

The method described in this Chapter attempts to trace the development of plastic hinges under proportional increments of loading. The position and load factor at which these plastic hinges form are located using a step-by-step incremental analysis. Expressions are derived by utilising the slope-deflection method of

analysis to obtain the overall bending moment distribution of the frame. The analysis, which is necessarily iterative and more complicated than the Merchant-Rankine formula, is rendered suitable for hand calculation by the use of limited single bay sub-frames. Convergence is rapidly attained by interpolation from successive iterations.

Secondary effects are incorporated by a combination of stability functions and fictitious horizontal loads. Initially, the proposed approach will be explained by reference to a single storey pinned base frame. Derivations of the relevant expressions are shown in the Appendix. In order to embark on the description, some simplified assumptions have to be made.

5.2 Assumptions

The basis of the method rests on a detailed examination of the simple pinned base portal shown in figure (5.1). For convenient comparison with computer analysis, the distributed beam load has been replaced by an equivalent central point load, λV.

Column end loads are represented by $\lambda(RV)$, where R is a positive real value to simulate the applied load. The horizontal load is shown as λH, taken as a point load concentrated at the eaves level. The frame is proportionally loaded, identified by the common load factor, λ , but it must be emphasised that real structures are subjected to pattern load fluctuations. The following assumptions will be used in obtaining the approximate failure load,

a)the reduction in beam stiffness due to compressive axial forces is negligible;

b)the effect of wind loading on the distribution of axial force in the columns can be ignored when calculating the stiffness of these members. i.e. the frames are treated with equally compressed columns;

c)sway due to axial shortening is neglected;

d)the members are originally unstressed and the effects of lack-of-fit are neglected;

e)out-of-plane displacements are prevented and failure occurs in the plane of the frame only;

f)spread of plasticity and the effect of strain-hardening are neglected.

In the last of this list, a member is assumed to possess its original stiffness rigidity, (EI), except at cross-sections where the plastic moment of resistance, M_p, is developed. Plastic deformation is limited to hinge rotation, under constant M_p, in the same direction once started. Reversal of rotation is assumed not to occur under an increase in load. The moment-curvature and stress-strain relationships are shown in figures (5.2) and (5.3).

5.3 Analysis of pinned base single storey frame

While the frame shown in figure (5.1) remains elástic, the bending moments at the possible plastic hinge positions may be obtained by slope-deflection analysis given by,

$$M_{DC} = MH + MV \tag{5.1}$$

$$M_{BC} = MH - MV \tag{5.2}$$

$$M_{CD} = MF - MV \tag{5.3}$$

where MH = wind moment = $\lambda_1 Hh/2 + \lambda_1(FV)\delta$

MV = vertical moment = $\frac{\lambda_1 VL}{8}\left[1 - \frac{2k'}{2k' + s(1-c^2)k''}\right]$

MF = free moment = $\lambda_1 VL/4$

δ = horizontal eaves sway = $\frac{\lambda_1 Hh\alpha_1}{(12Ek'/h) - [2\ \lambda_1(FV)\alpha_1]}$

(FV) = base reaction = $\lambda_1(RV) + \lambda_1 V/2$

$k' = I_b/L$

$k'' = I_c/h$

$\alpha_1 = 1 + \frac{6k'}{s(1-c^2)k''}$

Equations (5.1) to (5.3) have been obtained by considering two analyses. When the simple portal is subjected to the vertical loads, the moment MV is obtained.

Wind moment, MH, is obtained by considering the portal subjected to λH, along with a fictitious load $\lambda[V+2(RV)]\delta/h$. The latter allows for the 'P- Δ' effect which result from the horizontal translation of the vertical loads when sway occurs. The

analysis assumes the joint rotations at (B) and (D) to be equal. The stability functions 's' and 'c' are calculated from the total value of λ(FV). Bending moments are taken as positive when acting in a clockwise direction on the end of a member between two loaded points.

The first plastic hinge is found when the larger in magnitude of M_{DC} and M_{CD} equals the full plastic moment of resistance, M_{pb} or M_{pc}(reduced) whichever is the lower. Due to the constraint imposed on the minimum design load factor for plastic hinges to form in columns, it is usual to ensure that M_{pc}(reduced) > M_{pb}. The value of the load factor at this juncture is denoted by λ_1. Under a further increment of proportional loading, denoted by $\Delta\lambda$, the plastic hinge is replaced by a real pin. As the first plastic hinge can occur either at (C), directly under the central point load or at the leeward end of the beam at (D), two incremental load cases need to be examined.

5.3.1 First hinge at mid-span of the beam

Let the second hinge form at a total load factor, λ_2 , such that $\lambda_2 = \lambda_1 + \Delta\lambda$. When the first hinge forms, the frame is reduced to a statically determinate structure as shown in figure (5.4). Under the increment in mid-span vertical load, the bending moments are equal in magnitude but opposite in sign at (B) and (D) respectively, and are given by,

$$\Delta M_{DB}(V) = -\Delta M_{BD}(V)$$
$$= \Delta\lambda VL/4 \qquad (5.4)$$

When the frame is subjected to the loads shown by figure (5.4 (b)), the incremental moment at (D) on member B-D is the same as the moment at (B),

$$\Delta M_{DB}(H) = \Delta M_{BD}(H)$$
$$= (\Delta\lambda H + Hl).h/2 + \lambda_2(FV).v_1 \qquad (5.5)$$

where Hl = fictitious horizontal load to allow for the increment of vertical load acting on the sway, δ , existing in the frame at λ_1 . δ is shown in figure (5.4 (b)).

Thus $Hl = \Delta\lambda \Sigma V. (\delta/h)$

ΣV = total vertical load on the frame at $\lambda = 1$.

v_1 = incremental sway as shown in figure (5.4 (b))

$$= \frac{(\Delta\lambda H + Hl).h\alpha_1}{(12Ek'/h) - [2 \lambda_2 (FV) \alpha_1]}$$

$\lambda_2(FV)$ = TOTAL base reaction

α_1 = defined earlier but with the stability functions calculated based on the TOTAL load, λ_2 .

5.3.2 First hinge at leeward end of the beam

Figure (5.5) represents the portal with a leeward hinge on the beam. Under incremental loading the leeward column can take no shear as it is pinned at both ends. It follows that an increment of vertical loading will cause no shear at joint (A). First-order analysis therefore gives the same result as for a simply-supported beam,

$$\Delta M_{CD}(V) = \Delta\lambda VL/4 \qquad (5.6)$$

As the frame is now unsymmetrical, the increment of vertical loading will cause sway. It can be shown that this sway is equal to that due to a horizontal force, H3, applied at the eaves,

$$H3 = \frac{3\Delta\lambda VL}{16h}\left[\frac{1}{1 + (k'/k")}\right] \qquad (5.7)$$

Thus, the incremental sway v_2 can be regarded as due to four components of horizontal load,

a)the increment of true horizontal load, $\Delta\lambda H$,

b)the fictitious force, H1, as defined in (5.3.1),

c)the fictitious force, H3, as given by equation (5.7),

d)a further fictitious horizontal force, H2, which allows for the 'P- Δ' moment due to the total vertical load, ΣV, at λ_2 acting on the incremental sway v_2, as shown in figure (5.6),

$$H2 = \lambda_2 \Sigma V.(v_2/h)$$

This term was not necessary in the calculation of v_1 in (5.3.1) because there, stability functions were included to allow for this effect. Here it is proposed that the deflection be calculated without their use.

The horizontal load, H^*, applied to calculate v_2 is therefore given by,

$$H^* = \Delta\lambda H + (H1 + H2 + H3)$$

The deflection v_2 is then,

$$v_2 = \frac{H^* .h^2 \alpha_2}{3Ek'}$$

where $\alpha_2 = 1 + (k'/k")$

The resulting clockwise bending moment at (B) on member B-D is given by,

$$\Delta M_{BD}(H) = (\Delta\lambda H + H1 + H2).h \qquad (5.8)$$

$$\Delta M_{CD}(H) = \Delta M_{BD}(H)/2 \qquad (5.9)$$

It is noted that a linear elastic analysis has been utilised but the fictitious loads provide sufficient influence on the bending moments to offset the reduced stiffness of the columns. As the frame sways under vertical load alone, H3 is included in the total real plus fictitious load, H^*, used to calculate v_2. It is, however, excluded in equation (5.8) because the bending moment $\Delta M_{CD}(V)$ calculated from equation (5.6) takes account of the freedom to sway that now exists at joint (D).

The total moments at (B) or (C) are found by summing the incremental values to those existing at the first load factor. In this manner, the collapse load is found when the total moment with the larger magnitude equals M_{pb} or M_{pc}(reduced).

The solution procedure for both the first and second load factor are clearly iterative but convergence is rapid as long as the frame is still stable as the load level approaches either λ_1 or λ_2 . However, cases may arise when the frame collapses after only one plastic hinge has formed. This is indicated by an inability to converge onto a value for the incremental sway, no matter how low the value of $\Delta\lambda$.

5.4 Verification of the method

Comparison with a second order elasto-plastic computer analysis showed very good agreement, no matter whether the frame collapsed with one or two plastic hinges present. Four separate examples are shown. The two cases of the first plastic hinge occurring at mid-span and at the leeward end of the beam are illustrated. The third example illustrates the possibility of a simple portal collapsing without having to develop a mechanism. The final example shows a frame that is subjected to high wind loads in comparison with the vertical loads. This is necessary before proceeding to the next stage of application to multi-storey frames.

5.4.1 Example 1

In the following examples, Young's modulus of elasticity is taken as 206 KN/mm^2 and the yield stress as 240 N/mm^2 , unless otherwise stated. Consider the frame given by figure (5.1) with the following values,

Beam (356 x 127 x 39 UB)

$I_b = 10087 \times 10^4$ mm^4 $\qquad M_{pb} = 156.86$ KNm.

Column (203 x 203 x 71 UC)

$I_c = 7647 \times 10^4$ mm^4 $\qquad$ Full $M_{pc} = 192.58$ KNm.

Applied loads and dimensions

V = 156 KN $\qquad$ R = 0.5 $\qquad$ H = 24 KN $\qquad$ (FV) = 156 KN

L = 6.00 metres $\qquad$ h = 4.00 metres

Hence $k' = 16811.7$ mm^3 and $k'' = 19117.5$ mm^3

i) Let $\lambda_1 = 0.977$

The stability functions 's' and 'c' are determined based on equal column forces due to vertical load only. The ratio of axial to Euler load is given by,

$$\rho = \frac{0.977 \times 156 \times (4000)^2}{\pi^2 \times 206 \times 7647 \times 10^4} = 0.01568$$

$$s(1-c^2) = 2.9688$$

Referring to Section (5.3) to evaluate the elastic bending moment distribution,

a) $$MV = \frac{0.977 \times 156 \times 6}{8} \left[1 - \frac{2 \times 16811.7}{2 \times 16811.7 + 2.9688 \times 19117.5} \right]$$

$= 71.78$ KNm.

b) $MF = 0.977 \times 156 \times 6 / 4 = 228.62$ KNm.

To determine the wind and (P- Δ) moments, two parameters must be calculated for use in the term MH. These are,

$$\alpha_1 = 1 + \frac{6 \times 16811.7}{2.9688 \times 19117.5} = 2.777$$

$$\delta = \frac{0.977 \times 24 \times 4000 \times 2.777}{(12 \times 206 \times 16811.7/4000) - (2 \times 0.977 \times 156 \times 2.777)}$$

$$= 27.29 \text{ mm}$$

c) MH = (0.977x24x4/2) + (0.977x156x27.29/1000)

= 51.06 KNm.

It is found that the first plastic hinge occurs at mid-span as shown in figure (5.7 (a)). Equations (5.1) to (5.3) give the total bending moment distribution at λ_1 ,

M_{DC} = 51.06 + 71.78 = 122.84 KNm.

M_{BC} = 51.06 - 71.78 = -20.72 KNm.

M_{CD} = 228.62 - 71.78 = 156.84 KNm. ($= M_{pb}$)

ii) Now let the increment of load, $\Delta\lambda$ = 0.114, resulting in the total load of 1.091. The stability functions are calculated based on the total load,

$$\rho = \frac{1.091 \times 156 \times (4000)^2}{\pi^2 \times 206 \times 7647 \times 10^4} = 0.0175$$

$s(1-c^2) = 2.9652$

Referring to Section (5.3.1) for the first hinge at mid-span,

d) Equation (5.4), $\Delta M_{DB}(V) = 0.114 \times 156 \times 6/4$

$= 26.68$ KNm.

Incremental wind plus ($P-\Delta$) moments are obtained by calculating the necessary parameters,

$$Hl = 0.114 \times (2 \times 156) \times 27.29/4000 = 0.243 \text{ KN}$$

$$\alpha_1 = 1 + \frac{6 \times 16811.7}{2.9652 \times 19117.5} = 2.7794$$

$$v_1 = \frac{(0.114 \times 24 + 0.243) \times 4000 \times 2.7794}{(12 \times 206 \times 16811.7/4000) - (2 \times 1.091 \times 156 \times 2.7794)}$$

$= 3.507$ mm

e) Equation (5.5), $\Delta M_{DB}(H) = (0.114 \times 24 + 0.243) \times 4/2 + (1.091 \times 156 \times 3.507/1000)$

$= 6.55$ KNm.

Total moments at λ_2 are determined by summing the existing moments at λ_1 and $\Delta\lambda$,

$M_{DC}(T) = 122.84 + 26.68 + 6.55 = 156.07$ KNm. ($= M_{pb}$)

$M_{BC}(T) = -20.72 - 26.68 + 6.55 = -40.85$ KNm.

The second hinge is located at (D) and a collapse mechanism is now present at an ultimate load factor of 1.09. The total horizontal eaves sway is 30.80 mm. In comparison, accurate elasto-plastic computer analysis indicated failure occurred at $\lambda_f = 1.09$ with a total average sway of 30.88 mm. The manual method is able to trace

the development of the plastic hinges corresponding to that shown by accurate computer analysis. The final bending moment distribution is shown in figure (5.7 (b)) with the accurate results given in brackets.

5.4.2 Example 2

The following values are used in this example,

Beam (457 x 152 x 52 UB)

$I_b = 21345 \times 10^4$ mm^4 $\qquad M_{pb} = 262.56$ KNm.

Column (305 x 305 x 137 UC)

$I_c = 32838 \times 10^4$ mm^4 $\qquad$ Full $M_{pc} = 551.52$ KNm.

$A_c = 17460$ mm^2

Applied loads and dimensions

V = 156 KN $\qquad$ R = 6.0 $\qquad$ H = 72 KN $\qquad$ (FV) = 1014 KN

L = 6.00 metres $\qquad$ h = 4.00 metres

Hence $k' = 35575$ mm^3 and $k'' = 82095$ mm^3

Proceeding in exactly the same way as for the first example,

i) Let $\lambda_1 = 0.993$

$$\rho = \frac{0.993 \times 1014 \times (4000)^2}{\pi^2 \times 206 \times 32838 \times 10^4} = 0.02413$$

$$s(1-c^2) = 2.9517$$

a) $$MV = \frac{0.993 \times 156 \times 6}{8}\left[1 - \frac{2 \times 35575}{2 \times 35575 + 2.9517 \times 82095}\right]$$

$$= 89.81 \text{ KNm.}$$

b) $$MF = 0.993 \times 156 \times 6 / 4 = 232.36 \text{ KNm.}$$

$$\alpha_1 = 1 + \frac{6 \times 35575}{2.9517 \times 82095} = 1.8809$$

$$\delta = \frac{0.993 \times 72 \times 4000 \times 1.8809}{(12 \times 206 \times 35575/4000) - (2 \times 0.993 \times 1014 \times 1.8809)}$$

$$= 29.56 \text{ mm}$$

c) $$MH = (0.993 \times 72 \times 4/2) + (0.993 \times 1014 \times 29.56/1000)$$

$$= 172.75 \text{ KNm.}$$

It can be demonstrated that the first plastic hinge forms at the leeward end of the beam as shown in figure (5.8 (a)). The total bending moment at λ_1 is given by,

$M_{DC} = 172.75 + 89.91 = 262.56$ KNm. ($= M_{plb}$)

$M_{BC} = 172.75 - 89.91 = 82.94$ KNm.

$M_{CD} = 232.36 - 89.91 = 142.55$ KNm.

The plastic hinge forms on the beam because the reduced plastic moment capacity of the column at unit load factor was 474.98 KNm, far in excess of the end moment M_{DC}.

ii) Let the increment of load $\Delta\lambda = 0.156$. Therefore, the total load is 1.149. The analysis described in Section (5.3.2) does not make use of stability functions to determine any of the parameters.

Instead, fictitious loads are evaluated to solve for v_2. Referring to Section (5.3.2),

Real wind load increment, $\Delta\lambda H = 0.156 \times 72 = 11.23$ KN.

$$\text{Fictitious force, H1} = \Delta\lambda \Sigma V.(\delta/h) = \frac{0.156x(2x1014)x29.56}{4000}$$

$$= 2.34 \text{ KN}$$

$$\text{Fictitious force, H2} = \lambda_2 \Sigma V.(v_2/h) = \frac{1.149x(2x1014)x\ v_2}{4000}$$

$$= 0.5852\ (v_2)$$

$$\text{Fictitious force, H3} = \frac{3x0.156x156x6000}{16x4000} \left[\frac{1}{1 + (35575/82095)} \right]$$

$$= 4.78 \text{ KN}$$

Total horizontal load, $H^* = [0.5852\ (v_2) + 18.35]$ KN

where v_2 is given in millimetre units. Further calculations involve the expression given for v_2,

$$v_2 = \frac{H^*\ h^2 \alpha_2}{3Ek'}$$

where $\alpha_2 = 1 + (35575/82095) = 1.4333$

Substituting H^* into v_2 given above,

$$v_2 = \frac{[0.5852\ (v_2) + 18.35] \times (4000)^2 \times 1.4333}{3 \times 206 \times 35575}$$

Hence, v_2 = 49.13 mm and H2 = 28.75 KN.

d) Equation (5.6), $\Delta M_{CD}(V)$ = 0.156x156x6/4

= 36.50 KNm.

e) Equation (5.8), $\Delta M_{BD}(H)$ = (11.23+2.34+28.75)x4

= 169.28 KNm.

The total moments at λ_2 are obtained thus,

$M_{BD}(T)$ = 82.94 + 169.28 = 252.22 KNm.

$M_{CD}(T)$ = 142.55 + 36.50 + (169.28/2)

= 263.69 KNm. (= M_{pb})

This second hinge at mid-span transforms the portal into a mechanism at λ_2 =1.15 with a total sway deflection of (29.56 + 49.13) = 78.69 mm. Accurate computer analysis indicated failure at a load factor of 1.15 and a total average sway of 78.30 mm. Values of computer bending moments are shown in brackets in figure (5.8 (b)).

5.4.3 Example 3

Let the previous member properties be adopted as a third example. The dimensions are the same as example (2) but the applied loads are given below,

V = 156 KN R = 22.82 H = 90 KN (FV) = 3638 KN

As example (2), k' = 35575 mm^3 and k" = 82095 mm^3

i) Let $\lambda_1 = 0.660$

$$\rho = \frac{0.660 \times 3638 \times (4000)^2}{\pi^2 \times 206 \times 32838 \times 10^4} = 0.0575$$

$$s(1-c^2) = 2.8845$$

a) $$MV = \frac{0.660 \times 156 \times 6}{8} \left[1 - \frac{2 \times 35575}{2 \times 35575 + 2.8845 \times 82095} \right]$$

$$= 59.38 \text{ KNm.}$$

b) $MF = 0.660 \times 156 \times 6 / 4 = 154.44$ KNm.

$$\alpha_1 = 1 + \frac{6 \times 35575}{2.8845 \times 82095} = 1.9014$$

$$\delta = \frac{0.660 \times 90 \times 4000 \times 1.9014}{(12 \times 206 \times 35575/4000) - (2 \times 0.660 \times 3638 \times 1.9014)}$$

$$= 35.14 \text{ mm}$$

c) $MH = (0.660 \times 90 \times 4/2) + (0.660 \times 3638 \times 35.14/1000)$

$$= 203.18 \text{ KNm.}$$

The total bending moment at λ_1 is given by equations (5.1) to (5.3),

$M_{DC} = 203.18 + 59.38 = 262.56$ KNm. ($= M_{pc}$)

$M_{BC} = 203.18 - 59.38 = 143.80$ KNm.

$M_{CD} = 154.44 - 59.38 = 95.06$ KNm.

Due to such high column axial load, the reduced plastic moment of

resistance is determined to ensure that the first plastic hinge does not form in the column at this load level,

$$n = \frac{0.660 \times 3638}{(240 \times 174.6 / 10)} = 0.573 > 0.219$$

$$M_{pc}(\text{reduced}) = 0.240 \times [247.9(1-n) \times (10.29+n)]$$

$$= 275.97 \text{ KNm} > M_{pb}$$

This confirms that the first plastic hinge develops on the beam rather than on the column.

ii) Let $\Delta\lambda = 0.001$ such that $\lambda_2 = 0.661$. Proceeding in exactly the same way as the second example to determine the real and fictitious loads,

Real wind load increment, $\Delta\lambda H = 0.09$ KN

Fictitious force, $H1 = 0.064$ KN

Fictitious force, $H2 = 1.202\ (v_2)$

Fictitious force, $H3 = 0.031$ KN

Total horizontal load, $H^* = [1.202\ (v_2) + 0.185]$ KN

$$\alpha_2 = 1.4333$$

$$v_2 = \frac{[1.202\ (v_2) + 0.185] \times (4000)^2 \times 1.4333}{3 \times 206 \times 35575}$$

i.e. $v_2 = -0.76$ mm

The result has shown that the frame is swaying in the opposite direction and H2 will therefore be negative for equilibrium to be maintained. In fact, for zero increment, v_2 cannot be solved.

Computer analysis showed that failure has indeed occurred with one plastic hinge at a load factor of 0.66. The average sway at this load level was 35.20 mm compared with the manual calculated value of 35.14 mm. The total bending moment is shown in figure (5.9) along with the computer result given in brackets.

5.4.4 Example 4

This example demonstrates the applicability of the proposed method in dealing with portals that are subjected to relatively high ratios of horizontal to vertical loads in which it is likely that all the plastic hinges will form at the beam-column joints. European sections are used in this example with the following parameters,

Beam (IPB 260)

$I_b = 14920 \times 10^4$ mm^4 $\qquad M_{pb} = 308.00$ KNm.

$A_b = 11840$ mm^2

Column (IPB 200)

$I_c = 5700 \times 10^4$ mm^4 $\qquad$ Full $M_{pc} = 154.00$ KNm.

$A_c = 7810$ mm^2 $\qquad$ Squash load, $N_{pl} = 1874.4$ KN

Applied loads and dimensions

V = 102 KN $\qquad$ R = 0.5 $\qquad$ H = 104.3 KN $\qquad$ (FV) = 102 KN

L = 10.00 metres h = 2.70 metres

Hence k' = 14920 mm^3 and k" = 21111.1 mm^3

Young's modulus of elasticity, E = 210 KN/mm^2

Yield stress, f = 240 N/mm^2

i) Let $\lambda_1 = 0.667$

European Recommendation(56) allow the calculations to be performed neglecting the reduction in plastic moment due to axial load when the ratio of applied load to the squash load of a column is less than a numerical value of (1/11). In this case,

$$N/N_{pl} = (0.667 \times 102)/1874.4 < 1/11$$

where N = column axial force. In addition, because N is relatively low, the stability functions will be taken as 's'=4 and 'c'=0.5. Following the steps given in example (1),

a) MV = 57.81 KNm.

b) MF = 170.09 KNm.

$\alpha_1 = 2.4135$

$\delta = 33.34$ mm

c) MH = 96.19 KNm.

The total bending moment at a load factor of 0.667 is given by,

M_{DC} = 96.19 + 57.81 = 154.0 KNm. (= M_{pc})

M_{BC} = 96.19 - 57.81 = 38.38 KNm.

M_{CD} = 170.09 - 57.81 = 112.28 KNm.

The first plastic hinge occurs at the top of the leeward column. With reference to the second example given earlier with an increment of $\Delta\lambda$ = 0.347 (total load = 1.014),

N/N_{pl} = (1.014x102)/1874.4 < 1/11

Hence, the reduction in M_{pc} continues to be ignored.

α_2 = 1.7067

$\therefore$ v_2 = 75.82 mm and H2 = 5.81 KN

$\Delta M_{CD}(V)$ = 88.49 KNm.

$\Delta M_{BD}(H)$ = (36.19 + 0.87 + 5.81) x 2.7 = 115.75 KNm.

The total bending moment is obtained by summation of existing values at λ_1 and this increment of 0.347,

$M_{BD}(T)$ = 38.38 + 115.75 = 154.13 KNm. (= M_{pc})

$M_{CD}(T)$ = 112.28 + 88.49 + (115.75/2) = 258.65 KNm.

It can be seen that both plastic hinges developed in the columns. The bending moment is shown in figures (5.10 (a)) and (5.10 (b)).

The results were confirmed by accurate computer analysis which gave $\lambda_1 = 0.67$ and $\lambda_2 = \lambda_f = 1.01$.

5.5 Design criteria of portals

It is interesting at this stage to compare the failure loads calculated above for all the examples to those obtained by rigid-plastic theory. This permits an assessment of the provisions of Design Recommendations(55) for the plastic analysis of portal frames.

Consider examples (1) and (2). The reduced plastic moment capacities of the columns are such that plastic hinges form in the beams, the critical mechanism being the combined mode. Therefore, the rigid-plastic collapse loads are obtained as follows,

Example 1

$$\lambda_p = \frac{4 \times 156.86}{(24 \times 4) + (156 \times 3)} = 1.11$$

% error = 1.11/1.09 = + 2%

Example 2 (5.10)

$$\lambda_p = \frac{4 \times 262.56}{(72 \times 4) + (156 \times 3)} = 1.39$$

% error = 1.39/1.15 = + 21%

In the third example, the critical rigid-plastic collapse mechanism can be shown to be the sway mode [identical to figure (5.10 (b))]. The reduced plastic moment capacities of the columns

were calculated at a load factor of 0.876 (ignoring the effect of horizontal loading), while the fourth example neglects the effect of axial forces in the columns as permitted by European Recommendation(56). The rigid-plastic collapse loads are therefore given by,

Example 3

M_{pc}(reduced) = 157.45 KNm.

$$\lambda_p = \frac{2 \times 157.45}{(90 \times 4)} = 0.875$$

% error = 0.88/0.66 = + 33%

Example 4 (5.11)

$$\lambda_p = \frac{2 \times 154.00}{104.3 \times 2.70} = 1.09$$

% error = 1.09/1.01 = + 8%

The above comparisons indicate that for some frames the errors are unacceptable, and that simple plastic theory should not be used.

In addition to the comparisons above, it is interesting to examine the eaves deflection at working load. This is easily determined by ignoring the second term in the denominator given by δ in Section (5.3),

$$\delta(\text{linear}) = \frac{\lambda H h \alpha_1}{(12Ek'/h)} \qquad (5.12)$$

In the examples, the linear elastic sway deflection is calculated at working load, by dividing the horizontal applied force at the eaves by a factor of 1.2. For comparison, accurate linear elastic

deflections are also shown below. With $\lambda = 1$, the calculated and accurate eaves deflection are shown as,

Example	H (KN)	equation(5.12) (mm)	δ(computer) (mm)	$\frac{\delta(\text{computer})}{h}$
1	20	21.24	21.31	1/188
2	60	20.38	20.50	1/195
3	75	25.47	25.63	1/156
4	86.92	40.67	40.78	1/66

(5.13)

It can be seen that the calculated values of the eaves deflection is in good agreement with computer results for all the examples. The sway in examples (1) and (2) would often be acceptable in practice although the minimum eaves deflection is not specified in Design Recommendations(55) for single storey frames.

It is also interesting to point out that the criterion given in Design Recommendations(55) for sway stability was derived for a multi-bay single storey pinned base portal. The derivation excludes concentrated loads at the top or near the top of columns such as those due to crane systems or pipework (example, in structures for supporting chemical plant). In such cases, the criterion is inapplicable. The proposed method is able to estimate the ultimate load accurately without recourse to a second-order elasto-plastic computer analysis.

In summary of the work presented above, it can be seen that for the examples considered the design of pinned base portals using the simple plastic theory can be unsafe by as much as 33%. Admittedly, this design is governed by squashing of the columns.

Pinned bases are still favoured because of the uncertainty of soil conditions in 'made-up' industrial sites. Cases can arise when engineers prefer to design intermediate portals at certain intervals to resist all the wind loads (figure 5.10 (c)). Therefore, the last example is a real possibility that can occur for shallow, long span portals. The reason for doing this, is so that adjacent bays may be designed to sustain vertical loads alone. Such designs may lead to greater overall economy. Similarly, the stanchions may be omitted in certain frames, support being by valley beams. In this case, high axial loads are applied to the eaves of certain frames. Extreme cases of this are shown in examples (2) and (3). The proposed method is able to deal with such frames satisfactorily without the need for 'exact' computer analysis.

CHAPTER 5 (PART 2)

AN APPROXIMATE DETERMINATION OF THE FAILURE LOAD OF MULTI-STOREY FRAMES

5.6 Analysis of limited frame

The previous analysis has been extended to single bay multi-storey frames, making use of sub-frames. The method is applicable providing plastic hinges do not form in the columns.

In earlier methods for elastic-plastic design (for example, Majid and Anderson, Anderson and Islam, Merchant-Rankine approach, etc.), it has been specified that columns do not develop hinges until the design load is reached. This is because of the deterioration of stiffness that results from such hinges. This restriction is retained here, and therefore the proposed analysis can be used in design.

When plastic hinges form in the beams, it is assumed that failure occurs when two plastic hinges have formed in each of two consecutive floors. Wood(26) has described such behaviour as a tendency towards 'conversion' to chimneys. Failure occurs due to loss of restraint to the columns. In addition, the frames examined in Chapter (2) confirmed that such an assumption is justified.

Whilst the frame is elastic, the sub-frames are as shown in figure (5.11). Under vertical loading, points of contraflexure are

assumed to occur at the mid-height of each column, except those in the bottom storey. The analysis of the top storey is based on an intermediate sub-frame, but with the upper legs removed.

The horizontal sways, δ_1 and δ_2 at each level are obtained from an analysis of a substitute Grinter frame. A program is available in Basic for use on desk-top computers. This makes allowance for the reduction of column stiffness due to compressive axial forces. The assumptions with regard to the Grinter frame has already been described. Incremental storey shears, which include both real and fictitious horizontal loads, are used to obtain the corresponding incremental sway deflections. The derivation can therefore, be based entirely on linear elastic analysis to obtain simplified expressions. However, it must be noted that the total vertical loads are used to determine the reduction in column stiffness at each increment of load.

For an elastic intermediate sub-frame, the analysis under vertical loading is based on the limited frame shown in figure (5.11 (a)). The bending moments resulting from the central vertical load, λV, are given by slope-deflection,

$$M_{DC}(V) = \frac{\lambda VL}{8}\left[1 - \frac{k}{K}\right] = -M_{BC}(V) \qquad (5.14)$$

$$M_{BA}(V) = \frac{\lambda VL}{8}\left[\frac{3k_2}{K}\right] = -M_{DE}(V) \qquad (5.15)$$

$$M_{BF}(V) = \frac{\lambda VL}{8}\left[\frac{3k_1}{K}\right] = -M_{DG}(V) \qquad (5.16)$$

$$M_{CD}(V) = \lambda VL/4 - M_{DC}(V) \qquad (5.17)$$

where $K = (3k_1 + 3k_2 + k)$,

$k_1 = I_1/h_1$, $k_2 = I_2/h_2$, $k = I_b/L$

and the suffices '1' and '2' refers to the upper and lower column respectively.

Bending moments due to horizontal loads are determined from the limited frame shown in figure (5.11 (b)) with δ_1 and δ_2 evaluated in advance from an analysis of the Grinter frame at the corresponding load level. The wind moments at each level are similarly evaluated independently for the joint concerned,

$$M_{DC}(H) = 6Ek\theta_B = M_{BC}(H) \qquad (5.18)$$

$$M_{BA}(H) = 2Ek_2[2\theta_B + \theta_A - 3\delta_2/h_2] = M_{DE}(H) \qquad (5.19)$$

$$M_{BF}(H) = -[M_{BC}(H) + M_{BA}(H)] = M_{DG}(H) \qquad (5.20)$$

where

$$\theta_B = \frac{2k_1(\delta_1/h_1) + 2k_2(\delta_2/h_2) + [(\lambda H1.h_1 + \lambda H2.h_2)/6E]}{2k_1 + 2k_2 + 6k} ,$$

$$\theta_A = \frac{2\delta_2}{h_2} - \theta_B - \frac{\lambda H2.h_2}{12Ek_2} ,$$

H1 = sum of the real wind shear plus allowance for 'P- Δ' effect of the upper storey

$= \lambda\Sigma H + \lambda\Sigma V\,(\delta_1/h_1)$,

H2 = sum of the real wind shear plus allowance for 'P- Δ' effect of the lower storey

$= \lambda\Sigma H + \lambda\Sigma V\,(\delta_2/h_2)$,

H = total horizontal shear in a storey,

V = sum of the column axial forces in a storey.

As in the single storey frame, the first plastic hinge is found when the largest total moment due to combined vertical and

horizontal loading equals the full plastic moment of resistance of the beam. The value of the load factor is λ_1. Further increments of loading are denoted by $\Delta\lambda$ such that $\lambda_2 = \lambda_1 + \Delta\lambda$. In general,

$$\lambda_{i+1} = \lambda_i + \Delta\lambda \qquad (5.21)$$

Analysis of the frame commences at the top and proceed downwards to the base sub-frame by considering each floor level at a time. The bending moments given by the intermediate sub-frame from equations (5.14) to (5.20) are applicable to the top sub-frame by ignoring the terms corresponding to the upper storey (i.e. k_1 ,h_1 ,Hl etc.).

As the assumption of a point of contraflexure at mid-height for the ground storey is grossly inaccurate, further expressions are derived. This makes use of the same principle as the intermediate sub-frame. With reference to the base sub-frame shown in figure (5.11 (a)), the analysis under vertical loading alone is given by,

$$M_{LK}(V) = \frac{\lambda VL}{8}\left[1 - \frac{k}{K'}\right] = -M_{JK}(V) \qquad (5.22)$$

$$M_{JI}(V) = \frac{\lambda VL}{8}\left[\frac{2k_2}{K'}\right] = -M_{LN}(V) \qquad (5.23)$$

$$M_{IJ}(V) = M_{JI}(V) / 2 = -M_{NL}(V) \qquad (5.24)$$

where $K' = (3k_1 + 2k_2 + k)$.

The moment given by $M_{KL}(V)$ is similar to equation (5.17) while $M_{JP}(V)$ is obtained by considering equilibrium at joint (J).

The wind moments are similarly obtained for the base sub-frame shown in figure (5.11 (b)),

$$M_{LK}(H) = 6Ek\Theta_J = M_{JK}(H) \qquad (5.25)$$

$$M_{JI}(H) = 2Ek_2[2\Theta_J - 3\delta_2/h_2] = M_{LN}(H) \qquad (5.26)$$

$$M_{IJ}(H) = 2Ek_2[\Theta_J - 3\delta_2/h_2] = M_{NL}(H) \qquad (5.27)$$

where $\Theta_J = \dfrac{2k_1(\delta_1/h_1) + 6k_2(\delta_2/h_2) + (\lambda H1.h_1/6E)}{2k_1 + 4k_2 + 6k}$

and $M_{LQ}(H)$ is obtained from equilibrium at joint (L).

Iteration is necessary to determine the load level at which the first plastic hinge forms, but convergence is rapid. Derivations for pinned bases can similarly be obtained by slope-deflection but it was felt unnecessary because fixed bases are more usual for multi-storey frames, as discussed in Chapter (4).

Under an increment of load, equations (5.14) to (5.27) may be used. For an elastic sub-frame, the load factor, λ is replaced by the incremental load, $\Delta\lambda$. An allowance for the previous deflection is included in the calculation of the incremental storey shears, $\Delta\lambda H1$ and $\Delta\lambda H2$. When a plastic hinge forms, several alternative positions need examining to derive expressions for the subsequent incremental analysis.

5.6.1 Hinge at leeward end of the beam

Under an increment of vertical load, $\Delta\lambda V$, the intermediate storey is represented by the limited frame shown in figure

(5.12 (a)). The column length is now assumed to equal the storey height with the far ends pinned. However, if the adjacent top or bottom sub-frames continue to remain elastic, then the earlier analysis given by equations (5.14) to (5.17) is applicable to those sub-frames. A system of distributing column end moments is assumed, to compensate for overlapping of the column legs.

As the unsymmetrical sub-frame is prevented from swaying by the action of the forces R1 and R2, the analysis procedure is similar to a propped cantilever given by equation (5.7). The fixed end moment at joint (B) on member B-C is ($\Delta\lambda VL/8$) and the bending moments are given by slope-deflection as,

$$\Delta M_{BC}(V) = \frac{3\Delta\lambda VL}{16}\left[\frac{k}{K''} - 1\right] \qquad (5.28)$$

$$\Delta M_{BA}(V) = \frac{3\Delta\lambda VL}{16}\left[\frac{k_2}{K''}\right] \qquad (5.29)$$

$$\Delta M_{CD}(V) = \frac{\Delta\lambda VL}{4} + \frac{\Delta M_{BC}(V)}{2} \qquad (5.30)$$

where $K'' = k_1 + k_2 + k$

The fictitious forces, R1 and R2, are obtained by dividing the appropriate column moments at joint (B) by their storey height. The total fictitious shear is assumed to be the sum of R1 and R2. An average value is then used in the substitute frame analysis to allow for the increment of sway due to the unsymmetrical nature of the sub-frame. Thus to determine this sway in the sub-frame shown in figure (5.12), a force (R1+R2)/2 is applied at (F) acting to the right, together with (R1+R2)/2 at (A) acting to the left.

The average value of R has been adopted so that the approximate distribution of shear is confined to the particular sub-frame under consideration. If this is not done, an unbalanced quantity is transmitted to the lower sub-frames, giving rise to overestimates of sway. When consecutive sub-frames have a hinge, then the net value at the common joint is incorporated into the cumulative storey shears. Values of R are given for each of the cases as,

$$R(\text{intermediate}) = \frac{3\Delta\lambda VL}{16K''}\left[\frac{k_1}{h_1} + \frac{k_2}{h_2}\right]$$

$$R(\text{base}) = \frac{3\Delta\lambda VL}{16(3k_1 + 4k_2 + 3k)}\left[\frac{3k_1}{h_1} + \frac{4k_2}{h_2}\right] \qquad (5.31)$$

$$R(\text{double hinges})\text{int.} = \frac{\Delta\lambda VL}{2(k_1 + k_2)}\left[\frac{k_1}{h_1} + \frac{k_2}{h_2}\right]$$

$$R(\text{double hinges})\text{base} = \frac{\Delta\lambda VL}{2(3k_1 + 4k_2)}\left[\frac{3k_1}{h_1} + \frac{4k_2}{h_2}\right]$$

Bending moments due to the incremental wind shears are evaluated by considering the limited frame shown in figure (5.12 (b)). The member end moments are given by the usual slope-deflection equations,

$$\Delta M_{AB}(H) = 2Ek_2[2\theta_A + \theta_B - 3\Delta\delta_2/h_2] \qquad (5.32)$$

$$\Delta M_{BA}(H) = 2Ek_2[\theta_A + 2\theta_B - 3\Delta\delta_2/h_2] \qquad (5.33)$$

$$\Delta M_{FB}(H) = 2Ek_1[2\theta_F + \theta_B - 3\Delta\delta_1/h_1] \qquad (5.34)$$

$$\Delta M_{BD}(H) = 3Ek\theta_B \qquad (5.35)$$

$$\Delta M_{ED}(H) = 2Ek_2[2\theta_E + \theta_D - 3\Delta\delta_2/h_2] \qquad (5.36)$$

$$\Delta M_{DG}(H) = 2Ek_1[2\theta_D + \theta_G - 3\Delta\delta_1/h_1] \qquad (5.37)$$

$$\Delta M_{GD}(H) = 2Ek_1[\theta_G + 2\theta_D - 3\Delta\delta_1/h_1] \qquad (5.38)$$

where $\Delta\delta_1$ and $\Delta\delta_2$ are the sways due to the increment of horizontal loads from an analysis of the Grinter substitute frame.

To determine the joint rotations, it is necessary to estimate the distribution of shear for each column length. Figure (5.12 (c)) and (5.12 (d)) depicts a limited frame, separated at the position of the hinge. The far ends of the columns are assumed fixed against rotation but free to displace horizontally and subjected to the shears S and S . The letter 'W' and 'L' denotes the windward and leeward columns respectively.

Exact computer analyses have shown that the distribution of shear can be approximated by considering such a model to represent the behaviour in a real frame. The two assemblies are analysed separately such that the superimposed sub-frames satisfy equilibrium and compatibility. In the derivation, it will first be assumed that shear is constant over the two storey height of the sub-frame. With reference to figure (5.12 (d)), equilibrium at joint (D) gives,

$$M_{DE} + M_{DG} = 0$$

Substituting the relevant slope-deflection equations and solving for the displacements gives,

$$\theta_D = \frac{S_L}{2E}\left[\frac{h_1 + h_2}{k_1 + k_2}\right]$$

$$vD = \frac{S_L . h_2}{4E}\left[\frac{h_1 + h_2}{k_1 + k_2} + \frac{h_2}{3k_2}\right] \qquad (5.39)$$

$$vG = \frac{S_L . h_1}{4E}\left[\frac{h_1 + h_2}{k_1 + k_2} + \frac{h_1}{3k_1}\right]$$

The total sway over the two storeys is given by,

$$v_L(T) = vD + vG$$

$$= \frac{S_L}{4E}\left[\frac{(h_1 + h_2)^2}{k_1 + k_2} + \frac{h_1^2}{3k_1} + \frac{h_2^2}{3k_2}\right] \qquad (5.40)$$

In a similar analysis of figure (5.12 (c)), the above expressions are obtained but with an extra stiffness term for the beam connected at joint (B). This is given by,

$$\Theta_B = \frac{S_W}{2E}\left[\frac{h_1 + h_2}{k_1 + k_2 + 3k}\right]$$

$$vB = \frac{S_W.h_2}{4E}\left[\frac{h_1 + h_2}{k_1 + k_2 + 3k} + \frac{h_2}{3k_1}\right] \qquad (5.41)$$

$$vF = \frac{S_W.h_1}{4E}\left[\frac{h_1 + h_2}{k_1 + k_2 + 3k} + \frac{h_1}{3k_1}\right]$$

The total sway is the sum of vB and vF,

$$v_W(T) = vB + vF$$

$$= \frac{S_W}{4E}\left[\frac{(h_1 + h_2)^2}{k_1 + k_2 + 3k} + \frac{h_1^2}{3k_1} + \frac{h_2^2}{3k_2}\right] \qquad (5.42)$$

Equating the total sways given by (5.40) and (5.42) gives,

$$S_W/S_L = m$$

where m = ratio of the bracket term given by equation (5.40) and (5.42).

$$\text{Thus, } m = \frac{\left[\frac{(h_1 + h_2)^2}{k_1 + k_2} + \frac{h_1^2}{3k_1} + \frac{h_2^2}{3k_2}\right]}{\left[\frac{(h_1 + h_2)^2}{k_1 + k_2 + 3k} + \frac{h_1^2}{3k_1} + \frac{h_2^2}{3k_2}\right]}$$

For compatibility of shear,

$$S_T = S_W + S_L$$

$$= S_L\ (1 + m)$$

Hence,

$$S_L = \frac{S_T}{(1 + m)} \qquad (5.43)$$

and $$S_W = \frac{S_T}{1 + (1/m)}$$

where S_T is assumed to be the total shear for the upper and lower storeys.

However, in practice it was decided that an alternative form to equation (5.43) be adopted. The reason is due to the fact that the wind shears are generally higher for the lower storey and therefore the values of S_W and S_L at joints (A) and (E) should be proportioned appropriately.

Let S_W and S_L be the shears for the upper storey and S'_W and S'_L represent the shears for the lower storey. Accurate computer analyses showed that the shear distribution can be estimated based on the relative stiffnesses of each assembly shown in figures (5.12 (c)) and (5.12 (d)). It is proposed that the distribution of shear for the upper storey be given by,

$$S_W = \frac{(k_1 + k_2 + 3k)}{(k_1 + k_2 + 3k) + (k_1 + k_2)} \cdot S_T(U) \qquad (5.44)$$

$$S_L = S_T(U) - S_W$$

For the bottom storey, it is assumed that the sway displacements at

joints (B) and (D) are equal rather than considering sway compatibility over the two storeys. Therefore, equating the displacements, vB and vD, and redefining the parameter 'm' above gives,

$$m = \frac{[(h_1 + h_2)/(k_1 + k_2)] + (h_2/3k_2)}{[(h_1 + h_2)/(k_1 + k_2 + 3k) + (h_2/3k_2)} \qquad (5.45)$$

In a similar form as equation (5.43), the shear distribution for the lower storey is given by,

$$S_L' = \frac{S_T(B)}{(1 + m)} \qquad (5.46)$$

$$S_W' = \frac{S_T(B)}{1 + (1/m)}$$

where $S_T(U)$ = Sum of real and fictitious shears for the upper storey,

$S_T(B)$ = Sum of real and fictitious shears for the lower storey.

The values of $S_T(U)$ and $S_T(B)$ are of the same form as the single storey pinned base portals described in Part (1) of this Chapter. The total shear comprises,

a) real horizontal wind shear, $\Delta\lambda H$,

b) H3 = fictitious shear to allow for the increment of vertical loading acting on the sway, δ(previous), existing in the frame at the previous load,

$= \Delta\lambda\Sigma V [\ \delta(\text{prev.})/h]$,

c) H4 = fictitious shear to allow for the 'P- Δ' effect due to

vertical loading acting on the total sway existing in the frame at the current load,

$= \lambda(\text{total})\ \Sigma V\ \ \Delta\delta/h.$

The value of H4 is not included in the calculation of deflections in the Grinter substitute frame analysis because the reduction in column stiffness due to axial forces has been taken into account. These values are determined for all increments of load and substituted into the appropriate wind shear term given in Section (5.6).

In addition, the average value of R is included with the real incremental wind shear to evaluate the incremental sway deflections from the Grinter substitute frame analysis. It will be recalled that this force permits account to be taken of sway due to lack of symmetry under vertical loading. Accurate computer analyses indicated this to be a necessary step in order to obtain close estimates of sway deflections. However, after the incremental sway has been determined, R is excluded when calculating the member forces because the force H4 allows for the 'P- Δ' effect of the total vertical load on the incremental sway.

The analysis for the joint rotations can now be determined from figure (5.12 (b)). It is noted that the expressions for the rotations are similar to those of the elastic sub-frame given in Section (5.6). The incremental joint rotations required for use in equations (5.32) to (5.38) are given by,

$$\Theta_B = \frac{2k_1(\Delta\delta_1/h_1) + 2k_2(\Delta\delta_2/h_2) + [(S_W.h_1 + S_W'.h_2)/3E]}{2k_1 + 2k_2 + 3k} \qquad (5.47)$$

$$\theta_F = \frac{2\Delta\delta_1}{h_1} - \theta_B - \frac{S_W.h_1}{6Ek_1} \tag{5.48}$$

$$\theta_A = \frac{2\Delta\delta_2}{h_2} - \theta_B - \frac{S'_W.h_2}{6Ek_2} \tag{5.49}$$

$$\theta_D = \frac{2k_1(\Delta\delta_1/h_1) + 2k_2(\Delta\delta_2/h_2) + [(S_L.h_1 + S'_L.h_2)/3E]}{2k_1 + 2k_2} \tag{5.50}$$

$$\theta_G = \frac{2\Delta\delta_1}{h_1} - \theta_D - \frac{S_L.h_1}{6Ek_1} \tag{5.51}$$

$$\theta_E = \frac{2\Delta\delta_2}{h_2} - \theta_D - \frac{S'_L.h_2}{6Ek_2} \tag{5.52}$$

where the incremental sways, $\Delta\delta_1$ and $\Delta\delta_2$ are obtained from the Grinter substitute frame analysis; the appropriate beam stiffness being reduced from $3k_b$ to $0.75k_b$.

The base sub-frame is similar to the above calculations. Under an increment of vertical loading, the bending moment is obtained, with due account of the base fixity, in a form similar to equations (5.28) to (5.30),

$$\Delta M_{JK}(V) = \frac{3\Delta\lambda VL}{16}\left[\frac{3k}{3k_1 + 4k_2 + 3k} - 1\right] \tag{5.53}$$

$$\Delta M_{JI}(V) = \frac{3\Delta\lambda VL}{16}\left[\frac{4k_2}{3k_1 + 4k_2 + 3k}\right] \tag{5.54}$$

$$\Delta M_{KL}(V) = \frac{\Delta\lambda VL}{4} + \frac{\Delta M_{JK}(V)}{2} \tag{5.55}$$

The incremental moments due to horizontal loads for the base sub-frame are given for the windward assembly as,

$$\Delta M_{JK}(H) = 3Ek\theta_J \tag{5.56}$$

$$\Delta M_{JI}(H) = 2Ek_2[2\theta_J - 3\Delta\delta_2/h_2] \tag{5.57}$$

$$\Delta M_{JP}(H) = 2Ek_1[2\theta_J + \theta_P - 3\Delta\delta_1/h_1] \quad (5.58)$$

where $\theta_J = \dfrac{2k_1(\Delta\delta_1/h_1) + 6k_2(\Delta\delta_2/h_2) + (S_W.h_1/3E)}{2k_1 + 4k_2 + 3k}$,

$$\theta_P = \frac{2\Delta\delta_1}{h_1} - \theta_J - \frac{S_W.h_1}{6Ek_1}$$

For the leeward column, the bending moments are given by,

$$\Delta M_{LQ}(H) = 2Ek_1[2\theta_L + \theta_Q - 3\Delta\delta_1/h_1] \quad (5.59)$$

$$\Delta M_{LN}(H) = 2Ek_2[2\theta_L - 3\Delta\delta_2/h_2] \quad (5.60)$$

$$\Delta M_{NL}(H) = 2Ek_2[\theta_L - 3\Delta\delta_2/h_2] \quad (5.61)$$

where $\theta_L = \dfrac{2k_1(\Delta\delta_1/h_1) + 6k_2(\Delta\delta_2/h_2) + (S_L.h_1/3E)}{2k_1 + 4k_2}$,

$$\theta_Q = \frac{2\Delta\delta_1}{h_1} - \theta_L - \frac{S_L.h_1}{6Ek_1} .$$

When the above calculations were performed, it was found that the bending moments at the ends of adjacent beams, such as member F-G and A-E in figure (5.12 (b)), were lower than computer results. Members F-G and A-E have been omitted in figure (5.12 (b)) for clarity. It is recognised that the members F-G and A-E may or may not have an existing pin. Therefore, it is proposed that the incremental moments at the column ends for the sub-frame under consideration be distributed to adjacent members in relation to their stiffnesses.

The distribution of moment is performed for horizontal loading only. This is because the far ends of the columns (A), (E), (F),

(G) were assumed pinned under vertical loading, but capable of resisting moment under horizontal loading. Incremental end moments given by equations (5.32), (5.34), (5.36) and (5.38) are transferred to the beam and column members at joints (A), (F), (E) and (G) respectively. An identical distribution process applies to the base sub-frame when a leeward hinge is present.

Consider a sub-frame such as that shown in figure (5.12 (b)). If the adjacent upper sub-frame has a leeward hinge, i.e. a hinge at (G) on member F-G, then the windward moment distributed to beam F-G at (F) will be,

$$\Delta M_{FG} = \Delta M_{FB} \cdot \left[\frac{0.75\ k}{k_1 + 0.75\ k} \right] \qquad (5.62)$$

where ΔM_{FB} = the incremental moment at the far end of the windward column given by equation (5.34),

k_1 = adjacent column stiffness (I_c/h) immediately above member F-B,

k = stiffness (I_b/L) of beam F-G.

It follows that the additional mid-span moment of member F-G is half the value of ΔM_{FG} The distributed moment to the leeward column immediately above member G-D at joint (D) is taken to equal in magnitude to ΔM_{GD} given by equation (5.38) but opposite in sign.

The distribution of moments to an adjacent elastic upper sub-frame (i.e. no hinge at (G) on member F-G), is given by,

$$\Delta M_{GF} = \Delta M_{GD} \cdot \left[\frac{k}{k_1 + k} \right] = \Delta M_{FG} \qquad (5.63)$$

The above distribution procedure is repeated for the adjacent lower sub-frame. Consequently, incremental moments are added or subtracted for each adjacent sub-frame as the calculations proceed from the top to the base level.

5.6.2 Double beam hinges

When double hinges are present, the procedure for determining the incremental bending moments are based on figure (5.13). A cantilever is assumed under an increment of vertical load alone. The anti-clockwise moment at joint (B) of member B-C is given by,

$$\Delta M_{BC}(V) = -\Delta\lambda VL/2 \qquad (5.64)$$

The analysis under horizontal loading takes the form shown in figure (5.13 (b)). The principle is the same as that described for figure (5.12 (d)) of a single column length extended over two storeys.

The beam B-D is regarded as a pin-ended strut and therefore the storey shears may be assumed to be shared equally between the windward and leeward columns for both the upper and lower storeys, thus,

$$S_W = S_L = S_T(U)/2 \qquad (5.65)$$

$$S'_W = S'_L = S_T(B)/2$$

Furthermore, the joint rotation at (F), (B) and (A) are assumed to be the same as the rotations at joints (G), (D) and (E). Therefore, equations (5.50), (5.51) and (5.52) are applicable with the condition given by equation (5.65).

When double hinges occur on the beam for the base sub-frame, the procedure is identical to the above. Equation (5.60) and (5.61) may be used in this case to determine the incremental wind moments.

It is unnecessary to evaluate the windward column moments for all the sub-frames because the combined bending moments are not critical for design.

5.6.3 Hinge at mid-span of the beam

When a central hinge forms, the rotational stiffness of the beam subjected to horizontal loading is unchanged. The analysis under an increment of vertical load alone is similar to the pinned base portal given in Section (5.3) in Part (1) of this Chapter. The expression, however, include the contribution of the upper column to the total stiffness at the joint. From slope-deflection, the beam moment is given by equation (5.4) while the column moments are,

$$\Delta M_{DE}(V) = -\frac{\Delta\lambda VL}{4}\left[\frac{k_2}{k_1 + k_2}\right] = -\Delta M_{BA}(V) \qquad (5.66)$$

If the stiffness of the columns are identical, then the bending moments are shared equally at the joint.

Figure (5.14 (b)) shows the sub-frame subjected to an increment of horizontal load, where S_W and S_L are defined by equation (5.65). It is assumed that the joint rotations at (B) and (D) are equal and may be treated in the same way as an elastic limited frame.

As the magnitude of shear is the same on each column, equations (5.18) and (5.20) derived for figure (5.11 (b)) may be used in this case, the terms H1 and H2 being replaced by $S_T(U)$ and $S_T(B)$ respectively,

$$\Delta M_{AB}(H) = 2Ek_2[2\Theta_A + \Theta_B - 3\Delta\delta_2/h_2\ ] = \Delta M_{ED}(H) \qquad (5.67)$$

$$\Delta M_{BA}(H) = 2Ek_2[\ \Theta_A + 2\Theta_B - 3\Delta\delta_2/h_2\ ] = \Delta M_{DE}(H) \qquad (5.68)$$

$$\Delta M_{FB}(H) = 2Ek_1[2\Theta_F + \Theta_B - 3\Delta\delta_1/h_1\ ] = \Delta M_{GD}(H) \qquad (5.69)$$

$$\Delta M_{BC}(H) = 6Ek\Theta_B = \Delta M_{DC}(H) \qquad (5.70)$$

where

$$\Theta_B = \frac{2k_1(\Delta\delta_1/h_1) + 2k_2(\Delta\delta_2/h_2) + \{[S_T(U).h_1 + S_T(B).h_2\ ]/6E\}}{2k_1 + 2k_2 + 6k},$$

$$= \Theta_D ,$$

$$\Theta_F = \frac{2\Delta\delta_1}{h_1} - \Theta_B - \frac{S_T(U).h_1}{12Ek_1} = \Theta_G ,$$

$$\Theta_A = \frac{2\Delta\delta_2}{h_2} - \Theta_B - \frac{S_T(B).h_2}{12Ek_2} = \Theta_E .$$

Equation (5.66) can similarly be used for the base sub-frame, provided the base fixity is taken into account. Under an increment of vertical load alone, the bending moments for the base sub-frame can be shown as,

$$\Delta M_{JI}(V) = \frac{\Delta\lambda VL}{4}\left[\frac{4k_2}{3k_1 + 4k_2}\right] = -\Delta M_{LN}(V) \qquad (5.71)$$

$$\Delta M_{IJ}(V) = \Delta M_{JI}(V)/2 \qquad (5.72)$$

Similarly, equations (5.25) to (5.27) may be utilised for the base sub-frame under an increment of horizontal load. However, the joint rotations are given by,

$$\theta_J = \frac{2k_1(\Delta\delta_1/h_1) + 6k_2(\Delta\delta_2/h_2) + [S_T(U).h_1/6E]}{2k_1 + 4k_2 + 6k}$$

$$= \theta_L$$

$$\theta_P = \frac{2\Delta\delta_1}{h_1} - \theta_J - \frac{S_T(U).h_1}{12Ek_1} = \theta_Q$$

The member end moments are given by equations (5.59) to (5.61).

5.7 Six storey single bay frame

The frame shown in figure (5.15) has been designed by Anderson and Islam(72) to satisfy permissible sways of 1/200th of each storey. The loads shown on the frame are at unit load factor ($\lambda = 1$).

It was specified that plastic hinges should not form in the columns below the minimum design load factor of 1.36 under combined loading. The load factor was chosen in accordance with present-day practice in plastic design. This criterion is adopted here.

It is required to trace the formation of plastic hinges and the load level at which they occur. Initially, a load factor is assumed for the elastic frame and storey deflections calculated from the Grinter substitute frame analysis. It is proposed that a plastic hinge be inserted when the estimated bending moment is within ±0.5% of the plastic moment of resistance of any member.

i) Let $\lambda = 1.239$

Values shown in the fourth column are calculated from the sway deflections obtained by an analysis of the Grinter substitute frame. The sway deflections are calculated with an allowance for the reduction of column stiffness due to compressive axial forces and therefore the terms in each storey listed in the fourth column are excluded in the Grinter frame analysis. It is however used in the manual calculation for member forces. The total shears are shown in the last column from the top to the base.

level	δ (cm)	ΣV (KN)	(a) $\lambda \Sigma V(\delta/h)$ (KN)	(b) $\lambda \Sigma H$ (KN)	(a) + (b) (KN)
i	0.697	192	0.474	13.010	13.484
ii	1.585	472	2.648	39.029	41.677
iii	1.789	752	4.762	65.048	69.810
iv	2.154	1032	7.869	91.067	98.936
v	1.946	1312	9.038	117.086	126.124
vi	1.302	1592	7.338	143.105	150.443

The bending moments are calculated for the whole frame using the appropriate expressions at the given load of 1.239 from the top to the base sub-frame as follows,

Vertical load, M(V)	Horizontal load, M(H)	M(V) + M(H)
Level (i)		
	$\delta_1 = 0$, $\delta_2 = 0.697$	$M_{CB} = 9644$
(5.14) $M_{CB} = 8196$	$\theta_A = 9.439 \times 10^{-4}$	$M_{BC} = 12620$
(5.17) $M_{BC} = 12160$	(5.18) $M_{CB} = 1448$	$M_{AB} = -6748$
Level (ii)		
	$\delta_1 = 0.697, \delta_2 = 1.585$	
	$\theta_D = 1.798 \times 10^{-3}$	$M_{FE} = 17229$
(5.14) $M_{FE} = 12164$	$\theta_G = 3.410 \times 10^{-3}$	$M_{DE} = -7099$
(5.17) $M_{EF} = 18191$	(5.18) $M_{FE} = 5065$	$M_{EF} = 18191$
(5.15) $M_{FJ} = -6082$	(5.19) $M_{FJ} = -4156$	$M_{FJ} = -10238$
$M_{FC} = -6082$	$M_{FC} = -909$	$M_{FC} = -6991$
Level (iii)		
	$\delta_1 = 1.585, \delta_2 = 1.789$	
	$\theta_G = 3.395 \times 10^{-3}$	$M_{JH} = 22682$
(5.14) $M_{JH} = 13120$	$\theta_K = 3.844 \times 10^{-3}$	$M_{GH} = -3558$
(5.17) $M_{HJ} = 17236$	(5.18) $M_{JH} = 9562$	$M_{HJ} = 17236$
(5.15) $M_{JN} = -8966$	(5.19) $M_{JN} = -6414$	$M_{JN} = -15380$
$M_{JF} = -4154$	$M_{JF} = -3148$	$M_{JF} = -7302$

The procedures for levels (iv) and (v) are identical to that shown by levels (ii) and (iii) applicable to an elastic intermediate sub-frame. The calculations as set out above give the overall bending moments for the top and intermediate sub-frames.

The last set of calculations are for the base sub-frame as follows,

Vertical load, M(V)	Horizontal load, M(H)	M(V) + M(H)
	$\delta_1 = 1.946, \delta_2 = 1.302$	$M_{UT} = 32529$
(5.22) $M_{UT} = 13616$	$\theta_S = 4.126 \times 10^{-3}$	$M_{ST} = 5297$
(5.17) $M_{TU} = 16739$	(5.25) $M_{UT} = 18913$	$M_{TU} = 16739$
(5.23) $M_{UX} = -5446$	(5.26) $M_{UX} = -7739$	$M_{UX} = -13185$
$M_{UR} = -8170$	$M_{UR} = -11174$	$M_{UR} = -19344$
(5.24) $M_{XU} = -2723$	(5.27) $M_{XU} = -18733$	$M_{XU} = -21456$

The bending moment distribution at a load factor of 1.239 is shown in figure (5.17 (a)). Three plastic hinges were located on the leeward end of beams G-J, K-N and P-R. As the leeward column moments are more critical for design than the windward columns, the bending moments of the former only are shown.

Values shown in brackets are those from an accurate elasto-plastic computer analysis. It can be seen that both the load factor and position of the plastic hinges are in good agreement with computer results.

To ensure that the moment capacities of the columns are not violated at this load level, the reduced plastic moment capacity of the columns were determined. As the lower of the two column length is subjected to higher combined axial force, only these columns are shown,

column	axial force	M_p(reduced) at $\lambda = 1.239$
F-J	308.666	13317 > 10238
N-R	720.633	19877 > 15490
U-X	1184.639	28900 > 21456

ii) Let $\Delta\lambda = 0.005$

Under an increment of load, it is required to incorporate the fictitious shears due to the increment of the mid-span load. In addition, the 'P-Δ' effect due to the previous sway existing at the load level of 1.239 must also be included. The values of R1 and R2 will be determined first followed by the latter fictitious force.

For each of the limited frames with a leeward hinge, the values of R1 and R2 are given by half the value of R in the first of equation (5.31) applicable to an intermediate sub-frame. These are obtained as follows,

sub-frame	0.5 x R [equation (5.31)]
DFKN	$\frac{0.5\times3\times0.005\times140\times700}{16\times69.847}\left[\frac{15.037}{350}+\frac{32.457}{350}\right] = 0.0892$
GJPR	$\frac{0.5\times3\times0.005\times140\times700}{16\times95.407}\left[\frac{32.457}{350}+\frac{32.457}{350}\right] = 0.0893$
KNSU	$\frac{0.5\times3\times0.005\times140\times700}{16\times132.268}\left[\frac{32.457}{350}+\frac{63.434}{350}\right] = 0.0952$

Values of R1 and R2 are shown in figure (5.16 (a)). The cumulative incremental storey shears have also been calculated and are shown in the figure.

The fictitious forces due to the previous sway existing at the previous load level (i.e. $\lambda_1 = 1.239$) are calculated as follows,

level	δ(previous)	$\Delta\lambda\Sigma V$ [δ(prev)/h]
i	0.697	0.0019
ii	1.585	0.0107
iii	1.789	0.0192
iv	2.154	0.0317
v	1.946	0.0365
vi	1.302	0.0296

Therefore, the total applied shear needed to determine the incremental deflection is the sum of the real wind shear and the values calculated above,

level	Σ Incremental shears
i	0 + 0.0019 + 0.0525 = 0.0544
ii	0.0892 + 0.0107 + 0.1575 = 0.2574
iii	0.1785 + 0.0192 + 0.2625 = 0.4602
iv	0.1845 + 0.0317 + 0.3675 = 0.5837
v	0.0952 + 0.0365 + 0.4725 = 0.6042
vi	0 + 0.0296 + 0.5775 = 0.6071

The resulting incremental deflections obtained from the Grinter substitute frame analysis and the associated values of storey shears can be tabulated as follows,

level	$\Delta\delta$	$\Delta\lambda\Sigma H$	$\Sigma H3$	$\Sigma H4$	S_T(*)
i	0.0049	0.0525	0.0019	0.0033	0.0578
ii	0.0226	0.1575	0.0107	0.0379	0.2061
iii	0.0354	0.2625	0.0192	0.0946	0.3763
iv	0.0343	0.3675	0.0317	0.1258	0.5251
v	0.0204	0.4725	0.0365	0.0951	0.6041
vi	0.0077	0.5775	--	--	--

where $H3 = \Delta\lambda\,\Sigma V\ [\ \delta(\text{previous})/h\ ]$

$H4 = \lambda(\text{total})\ \Sigma V\ [\ \Delta\delta/h\ ]$

It is noted that the fictitious force H4 is not included in the Grinter frame analysis because stability functions have been incorporated to take account of the reduction in column stiffness due to compressive axial forces.

It is noticed that the two uppermost sub-frames and the base sub-frame remain elastic, and therefore the procedure for calculating the incremental moments are identical to the one shown at the previous load factor except that incremental values of deflections and loadings are used instead. The procedure is as follows,

Vertical, $\Delta M(V)$	Horizontal, $\Delta M(H)$	$\Delta M(V) + \Delta M(H)$
Level (i)		
	$\Delta\delta_1 = 0$, $\Delta\delta_2 = 0.0049$	$\Delta M_{CB} = 42$
(5.14) $\Delta M_{CB} = 33$	$\theta_A = 5.637 \times 10^{-6}$	$\Delta M_{BC} = 51$
(5.17) $\Delta M_{BC} = 51$	(5.18) $\Delta M_{CB} = 9$	$\Delta M_{AB} = -24$
Level (ii)		
	$\Delta\delta_1 = 0.0049$, $\Delta\delta_2 = 0.0226$	
	$\theta_D = 1.594 \times 10^{-5}$	$\Delta M_{FE} = 94$
(5.14) $\Delta M_{FE} = 49$	$\theta_G = 9.417 \times 10^{-5}$	$\Delta M_{DE} = -4$
(5.17) $\Delta M_{EF} = 73$	(5.18) $\Delta M_{FE} = 45$	$\Delta M_{EF} = 73$
(5.15) $\Delta M_{FJ} = -25$	(5.19) $\Delta M_{FJ} = -43$	$\Delta M_{FJ} = -68$
$\Delta M_{FC} = -24$	$\Delta M_{FC} = -2$	$\Delta M_{FC} = -26$

As the next sub-frame has a leeward hinge, the expressions required for determining the shear distribution and incremental moments are described in Section (5.6.1).

Vertical, $\Delta M(V)$	Horizontal, $\Delta M(H)$	$\Delta M(V) + \Delta M(H)$

Level (iii)

$\Delta\delta_1 = 0.0226, \Delta\delta_2 = 0.0354$

$S_T(U) = 0.2061, S_T(B) = 0.3763$

(5.44) $S_W = 0.1457, \quad S_L = 0.0604$

(5.45) $m = 1.8890$

(5.46) $S'_W = 0.2461, \quad S'_L = 0.1303$

(5.47) $\Theta_G = 6.593 \times 10^{-5}$

(5.48) $\Theta_D = 3.630 \times 10^{-5}$ $\quad \Delta M_{GH} = 31$

(5.49) $\Theta_K = 1.153 \times 10^{-4}$ $\quad \Delta M_{HJ} = 137$

(5.50) $\Theta_J = 1.007 \times 10^{-4}$ $\quad \Delta M_{JF} = 16$

(5.51) $\Theta_F = 1.727 \times 10^{-5}$ $\quad \Delta M_{JN} = -16$

(5.28) $\Delta M_{GH} = -62$ (5.52) $\Theta_N = 9.042 \times 10^{-5}$ DISTRIBUTION

(5.30) $\Delta M_{HJ} = 91$ (5.32) $\Delta M_{KG} = -9$ (5.63) $\Delta M_{DE} = 21$

(5.34) $\Delta M_{DG} = -35$ $\quad \Delta M_{FE} = 22$

(5.35) $\Delta M_{GH} = 93$ $\quad \Delta M_{EF} = 0$

(5.36) $\Delta M_{NJ} = -30$ (5.62) $\Delta M_{KL} = 4$

(5.37) $\Delta M_{JF} = 16$ $\quad \Delta M_{LN} = 2$

(5.38) $\Delta M_{FJ} = -37$ $\quad \Delta M_{NR} = 30$

The distribution of moments to adjacent member ends is as described in Section (5.6.1) shown at the bottom right-hand corner in the above calculations. Equation (5.63) is used for distributing the end moments to the top members, while equation (5.62) is used for the bottom members.

In a similar manner to the above, the calculations for the next two sub-frames are illustrated as,

Vertical, $\Delta M(V)$	Horizontal, $\Delta M(H)$	$\Delta M(V) + \Delta M(H)$

Level (iv)

$\Delta\delta_1 = 0.0354, \Delta\delta_2 = 0.0343$

$S_T(U) = 0.3763, \quad S_T(B) = 0.5251$

(5.44) $S_W = 0.2660, \quad S_L = 0.1104$

(5.45) $m = 1.7816$

(5.46) $S'_W = 0.3363, \quad S'_L = 0.1888$

(5.47) $\Theta_K = 7.353 \times 10^{-5}$

(5.48) $\Theta_G = 1.060 \times 10^{-4}$ $\quad \Delta M_{KL} = 78$

(5.49) $\Theta_P = 9.369 \times 10^{-5}$ $\quad \Delta M_{LN} = 162$

(5.50) $\Theta_N = 1.124 \times 10^{-4}$ $\quad \Delta M_{NJ} = 2$

(5.51) $\Theta_J = 8.046 \times 10^{-5}$ $\quad \Delta M_{NR} = -2$

(5.28) $\Delta M_{KL} = -63$ (5.52) $\Theta_R = 6.747 \times 10^{-5}$ DISTRIBUTION

(5.30) $\Delta M_{LN} = 91$ (5.32) $\Delta M_{PK} = -45$ (5.62) $\Delta M_{GH} = 13$

(5.34) $\Delta M_{GK} = -24$ $\quad \Delta M_{JF} = 41$

(5.35) $\Delta M_{KL} = 141$ $\quad \Delta M_{HJ} = 6$

(5.36) $\Delta M_{RN} = -64$ (5.62) $\Delta M_{PQ} = 14$

(5.37) $\Delta M_{NJ} = 2$ $\quad \Delta M_{QR} = 7$

(5.38) $\Delta M_{JN} = -41$ $\quad \Delta M_{RU} = 64$

It is noted that equation (5.62) alone is used for the distribution of moments to adjacent members. This is due to the top and bottom beam having a leeward hinge each at (J) and (R) respectively.

In a similar manner to the above calculations, the next sub-frame gives,

Vertical, $\Delta M(V)$	Horizontal, $\Delta M(H)$	$\Delta M(V) + \Delta M(H)$
Level (v)		
	$\Delta\delta_1 = 0.0343, \Delta\delta_2 = 0.0204$	
	$S_T(U) = 0.5251,\ S_T(B) = 0.6041$	
	(5.44) $S_W = 0.3577,\quad S_L = 0.1673$	
	(5.45) $m = 1.7396$	
	(5.46) $S'_W = 0.3836,\quad S'_L = 0.2205$	
	(5.47) $\theta_P = 5.940 \times 10^{-5}$	
	(5.48) $\theta_K = 1.060 \times 10^{-4}$	$\Delta M_{PQ} = 69$
	(5.49) $\theta_S = 4.037 \times 10^{-5}$	$\Delta M_{QR} = 157$
	(5.50) $\theta_R = 8.296 \times 10^{-5}$	$\Delta M_{RN} = -40$
	(5.51) $\theta_N = 9.872 \times 10^{-5}$	$\Delta M_{RU} = 40$
(5.28) $\Delta M_{PQ} = -67$	(5.52) $\theta_U = 2.395 \times 10^{-5}$	DISTRIBUTION
(5.30) $\Delta M_{QR} = 89$	(5.32) $\Delta M_{SP} = -92$	(5.62) $\Delta M_{KL} = 13$
	(5.34) $\Delta M_{KP} = -31$	$\Delta M_{NJ} = 19$
	(5.35) $\Delta M_{PQ} = 136$	$\Delta M_{LN} = 6$
	(5.36) $\Delta M_{UR} = -117$	(5.63) $\Delta M_{ST} = 34$
	(5.37) $\Delta M_{RN} = -40$	$\Delta M_{UT} = 43$
	(5.38) $\Delta M_{NR} = -19$	$\Delta M_{TU} = -5$
		$\Delta M_{UX} = 74$

In the distribution process, the top beam has a hinge while the bottom beam is elastic and therefore equations (5.62) and (5.63) are used as appropriate.

The final set of calculations for the incremental load is for the elastic base sub-frame,

Vertical, $\Delta M(V)$	Horizontal, $\Delta M(H)$	$\Delta M(V) + \Delta M(H)$
	$\Delta\delta_1=0.0204, \Delta\delta_2=0.0077$	$\Delta M_{UT}=$ 189
(5.22) $\Delta M_{UT}=$ 55	$\theta_S = 2.913 \times 10^{-5}$	$\Delta M_{ST}=$ 79
(5.17) $\Delta M_{TU}=$ 68	(5.25) $\Delta M_{UT}=$ 134	$\Delta M_{TU}=$ 68
(5.23) $\Delta M_{UX}=$ -22	(5.26) $\Delta M_{UX}=$ -21	$\Delta M_{UX}=$ -43
$\Delta M_{UR}=$ -33	$\Delta M_{UR}=$ -113	$\Delta M_{UR}=$ -146
(5.24) $\Delta M_{XU}=$ -11	(5.27) $\Delta M_{XU}=$ -98	$\Delta M_{XU}=$ -109

The total incremental moments at each joint are obtained by summing the calculated moments at that level and moments distributed to that member if any.

As an illustration, consider joint (F). The total incremental moment at (F) on member E-F is (94+22)=116 KNcm. The value of 94 is the incremental moment calculated at level (ii) while the value of 22 is the moment distributed from level (iii). Similarly, the total incremental moment at joint (U) of member T-U is (189+43)=232.

The overall bending moment is obtained by summing existing moments at 1.239 to the incremental moments just calculated. This is shown in figure (5.17 (b)). The fourth plastic hinge is located at the leeward end of beam S-U. Again, none of the moment capacities of the leeward columns were violated at a total load of (1.239+0.005)=1.244.

iii) Let $\Delta\lambda = 0.166$

The total load is (1.239 + 0.005 + 0.166) = 1.410. Fictitious horizontal shears due to the mid-span vertical load are shown in figure (5.16 (b)).

The shears for the base sub-frame are calculated from the second expression given in equation (5.31). Further, the previous load is taken as 1.244 with the total sways at this stage being the sum of the storey sways at $\lambda_1 = 1.239$ and $\Delta\lambda = 0.005$.

When the above procedures were repeated, it was found that the column moment capacities were exceeded at (F) in column F-J and at the foot of the leeward column at (X). It is noted that the calculations for the base sub-frame in this iteration is dependant on equations (5.53) to (5.56).

The total bending moment distribution is shown in figure (5.17 (c)). The calculated leeward column capacities at this load of 1.410 can be shown as follows,

column	axial load	M_p(reduced) at $\lambda = 1.410$
C-F	139.1	14249
F-J	351.3	12972
J-N	578.3	21495
N-R	820.1	18737
R-U	1076.7	30419
U-X	1348.1	26583

The load level of 1.410 exceeds the minimum design load for which column hinges are permitted. The calculated moment at (F) exceeds the allowable moment capacity by about 8%. A plastic hinge was not detected at this position by the accurate elasto-plastic computer analysis. This error is not critical because it is usual for the choice of sections of the top few storeys to be governed by the higher load factor applicable to vertical loading alone (a factor not considered in the design being analysed).

In figure (5.17 (c)), the values that would be critical for design under combined loading are in good agreement with computer results. The maximum error occurring at joint (F) is +20% of the accurate results which are shown in brackets. A similar error of about +18% was also detected at joints (U) and (J).

To investigate the criterion placed on the minimum load factor permitted for column hinges, an increment of load of 0.116 was used to recalculate the overall bending moment distribution at λ =1.36. The fictitious shears are evaluated and shown in figure (5.16 (c)).

In an identical procedure as described above, the overall bending moment distribution at a load level of 1.36 is shown in figure (5.17 (d)). Accurate values are shown in brackets and are given in (KN.m) units for direct comparison with published results in reference (72). Comparison with computer results for the column moments showed a maximum error of +16%. This error occurred at the top storey as shown in the figure. It was found that none of the column moment capacities were exceeded and the estimated moment at (F) in member F-J was 1.5% below the allowable value.

As an alternative, an approximation of the total moments at 1.36 can be obtained by interpolation. For example, the bending moment at joint (F) in member F-J is,

$$M_{FJ} = -10343 - \left[\frac{0.116}{0.166} \times (14015 - 10343) \right]$$

$$= -12909 \quad \text{KNcm.}$$

The plastic moment of resistance of column F-J at a load factor of 1.360 was 13078 KNcm. Hence, no column hinges were present and the design is adequate

5.8 Four storey single bay frame

A further example is shown in figure (5.18). The frame was taken from reference (42). Calculation procedure is similar to the previous example with the exception of a sub-frame having double hinges as shown in figure (5.18 (d)). Such a sub-frame was analysed in Section (5.6.2).

The example differs from the six storey frame analysed previously by attaining the proposed criterion for collapse. At this stage, the minimum design load was exceeded and column moment capacities were checked.

It was specified that column hinges are not permitted to form below the design load factor of 1.40. The sequences of plastic hinge development and the estimated bending moment distribution are shown in figure (5.18). Accurate computer results are shown in

brackets. The proposed technique has located accurately the position of the plastic hinges with an average deviation of the load factor of +0.5% from the accurate computer solution.

At all incremental stages, the beam moments were found to provide good agreement with computer results. However, the final leeward column moment in the third storey was overestimated by 29%. As in the previous example, it is argued that the design of such columns are governed by the higher load factor applicable to vertical loading alone.

In all the columns, the maximum moments calculated by the proposed method are still below the plastic moments of resistance at a load factor of 1.413. Calculated moment capacities are given from the top to the base as follows,

floor	axial load (Tons)	M (reduced) at λ = 1.413 (Tons inch.)
top	19.4	1128.9 > 989.4
third	40.1	1080.1 > 915.3
second	62.7	990.0 > 883.9
ground	87.1	1556.1 > 1342.3

The assumed criterion for collapse is attained at this load factor and the manual calculations are terminated. In comparison with computer analysis (in which failure occurred at a load factor of 1.494), the proposed method is shown to provide good agreement for the bending moments that would be critical for design.

5.9 Application to multi-storey, multi-bay frames

Multi-bay frames are treated as an equivalent single bay frame for the determination of the failure load. The equivalent section properties of beams and columns at each storey are assumed to be the sum of the real frame properties. These assumptions are applicable only to regular and rectangular frameworks.

The following proposal summarises the equivalent characteristics that are adopted as the basis for both computer analysis and manual calculations of an equivalent single bay frame,

Equivalent loading

i) vertical load is taken as the sum of the total vertical loads.

ii) horizontal loads remain unchanged and are applied as on the real frame.

Equivalent section property

a) beam sections

i) cross-sectional area is taken as the sum of the areas of all the beams,

ii) moment of inertia is taken as the sum of the moment of inertias of all the beams,

iii) plastic modulus is taken as the sum of the plastic moduli of all the beams.

b) column sections

At each storey, the equivalent properties are calculated as for the beam sections above. The values are then halved to obtain

the properties of the two external columns at each storey.

The modulus of elasticity and the yield stress remain unaltered. Furthermore, the storey height is the same as the real frame but the single bay width is assumed to be the average bay width of the multi-bay frame.

Computer results of the failure load for the equivalent single bay frame provide very good agreement in comparison with the real frame. A typical result of a four storey three bay rectangular frame is shown in figure (5.19). The formation of plastic hinges in the columns have been deliberately suppressed in both figures to obtain comparison with beam hinges only.

The overall pattern of plastic hinges at collapse of the equivalent frame has a striking similarity to the real frame. The order of plastic hinge formation, however, differs considerably. The sequences of formation of plastic hinges are shown by the ringed numerical values in the figures. Under combined loading, formation of plastic hinges in the real frame tends to occur at the leeward ends of the beams first. In the equivalent frame, the plastic hinges appear to form initially at mid-span of the beams.

The failure load of the equivalent frame, however, is estimated to within 1% of the real value. Therefore, preliminary designs can be checked for ultimate strength under combined loading without the need for a rigorous computer analysis of the full-size framework. The demand on storage and computing time is reduced to that of the analysis of a single bay frame.

The design would be adequate provided the load level at failure is above the minimum specified. A check on the real frame at the corresponding load level can then be carried out to ensure that the columns are adequate. When analysis as a single bay frame shows a design to be unacceptable, re-analysis with revised beam sections is a rapid process.

5.9.1 Seven storey two bay frame

A frame that satisfies the minimum design collapse load of unity under factored combined loading is shown in figure (5.20 (a)). The equivalent frame is shown alongside with the calculated values of applied loads. Equivalent section properties are tabulated below the figures for each member as shown.

It is anticipated that plastic hinges would not form in the columns and such members were assumed to have very high values of the plastic moment of resistance. The proposed approximate method for evaluating the failure load is illustrated for the equivalent single bay frame.

The procedures for locating the plastic hinges and the corresponding loads at which they form are identical to the previous multi-storey examples. The final result of the proposed approximate method for the equivalent frame is shown in figure (5.21 (c)).

For comparison, the equivalent single bay frame was analysed using an accurate computer program and the result is shown in

figure (5.21 (b)), while figure (5.21 (a)) shows the sequence of plastic hinge formation in the real frame. The results of the equivalent frames showed excellent agreement in terms of the position and load level at which plastic hinges formed. It is noted that the formation of plastic hinges in the columns have been deliberately suppressed in all of figure (5.21).

The two mid-span plastic hinges at the top floor levels as shown in figure (5.21 (c)) indicate the significant influence of vertical loads on the behaviour of the equivalent frame. Further down the frame, the wind loads are beginning to affect the bending moment distribution. The first plastic hinge was located on the leeward end of the third floor beam. After repeated load increments, the proposed criterion for collapse was reached by the development of the eighth plastic hinge. The collapse load was taken as 1.005.

The order of plastic hinge formation is shown ringed. Only the first plastic hinge appears to form in sequence with the real frame while others were unpredictable. As expected, the pattern of plastic hinges in the equivalent frames shown in figures (5.21 (b)) and (5.21 (c)) are closely comparable to the computer result of the real frame.

The proposed method was shown to provide good agreement for the bending moments in the beams. It was found that the bending moments on the fifth floor beam were within an average of -3% of the plastic moment capacity at this load level. The final bending moment distribution is shown in figure (5.22). Accurate computer

results are shown in brackets corresponding to the pattern of hinges in figure (5.21 (c)).

It is convenient at this stage to assume that the next increment of load would have plastic hinges forming on the fifth floor beam marked in figure (5.21 (c)). However, the error in the failure load is insignificant. The designer has now to show that the column capacities of the real frame are not exceeded at the corresponding load.

It is proposed that if no column hinges are found in the equivalent frame, then it may be assumed that the sum of the column moment capacities of the real frame are adequate. To investigate this proposal, the column moment capacities were calculated under (factored) combined loading for the real frame at a load level of 1.005. The results are shown for each column in figure (5.23 (b)).

Values listed to the right of figure (5.23 (b)) summarises the proposed treatment of column moments in the real frame. The values are obtained by summing the moment capacity of the right-hand column(MR) and half the moment capacity of the internal column(MC/2). It can be seen that these values exceeded some of the column moments calculated in the equivalent frame in figure (5.22). In such cases, it is assumed that no column hinges are present in the real frame.

When the equivalent column moments exceed these summed values, then column hinges are assumed to be present in the real frame. Comparison of these values indicates plastic hinges at the

positions marked by an asterisk in figure (5.22). The proposed method has predicted the existence of such hinges in the real frame. Except for the hinge at the sixth storey, the hinge positions are confirmed by the accurate computer result shown in figure (5.23 (a)) with the columns given real yield stresses. The hinge located at the top of the leeward column on the sixth floor can be neglected due to the reason discussed earlier.

When comparisons are also made of computer results shown in figures (5.22) and (5.23 (a)), the plastic hinge positions are in excellent agreement. The bracket values shown in figure (5.22) indicate column hinges at positions corresponding to that shown in figure (5.23 (a)). This validates the proposed criterion for the existence of column hinges in the real frame.

For frames with an even number of columns across the width, such as the three bay frame shown in figure (5.19 (a)), it is proposed that the total real column moment capacities be taken as the sum of the column moments to the right of the line of vertical symmetry.

5.10 Conclusion

An approximate incremental elastic-plastic method has been shown to evaluate accurately the failure loads of plane pinned base steel portals. Expressions have been derived. Only one trial analysis is necessary to obtain a load factor for the critical bending moment to converge onto the plastic moment capacity of the member.

Several examples were illustrated to include the possible occurrence of discrete plastic hinges when the frame is subjected to combined loading. The likelihood of portals collapsing without a complete mechanism was demonstrated by an inability to converge onto the second plastic hinge.

Calculations for the collapse loads of pinned base portals by the rigid-plastic theory were demonstrated to be unsafe. The proposed method, however, is able to deal with such frames in a satisfactory manner. In addition, the eaves deflections are assessed accurately when the portal is elastic and at collapse. The results have been compared with accurate computer analysis.

The proposal has been extended to multi-storey frameworks. Expressions for the bending moments were derived by considering only an intermediate and a base sub-frame. Each sub-frame is independent from adjacent sub-frames while it remains elastic. A system of distributing moments was shown to be necessary to obtain good agreement of the beam moments with computer results.

Two examples were shown. It was found that the column moments were overestimated by between 20% and 29%. This does not cause undue concern because the conservative values tend to occur at the top few storeys of the frame where design is likely to be governed by vertical load alone. The bending moments that would be critical for design were found to be in good agreement with computer results.

Multi-bay frames are treated as an equivalent single bay structure. Failure loads of the equivalent single bay frame were shown to provide excellent agreement with the real structure. The patterns of plastic hinges at collapse were almost identical in the actual and equivalent frame when both were given by accurate computer analysis.

The manual method is able to trace the development of the plastic hinges in the beams with good accuracy. An example was shown to confirm the proposal. The method may be used as a preliminary assessment for strength under combined loading before a rigorous computer analysis is undertaken on the complete multi-storey multi-bay structure.

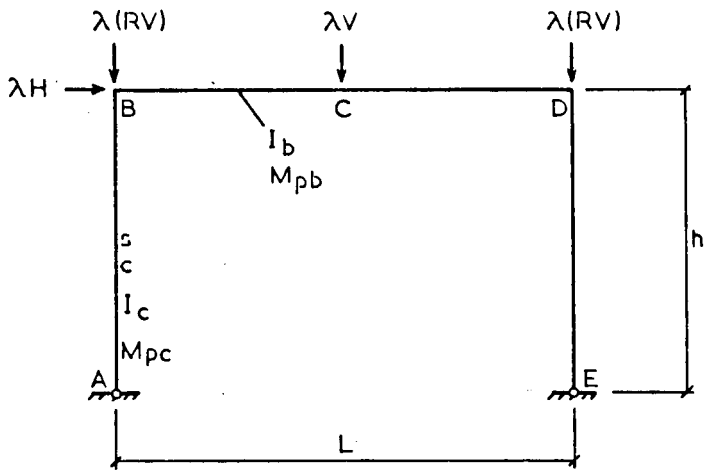

I_c , I_b Second moment of area.

M_{pc} , M_{pb} Plastic moment of resistance.

s , c Stability functions.

FIG. 5.1 PINNED BASE PORTAL

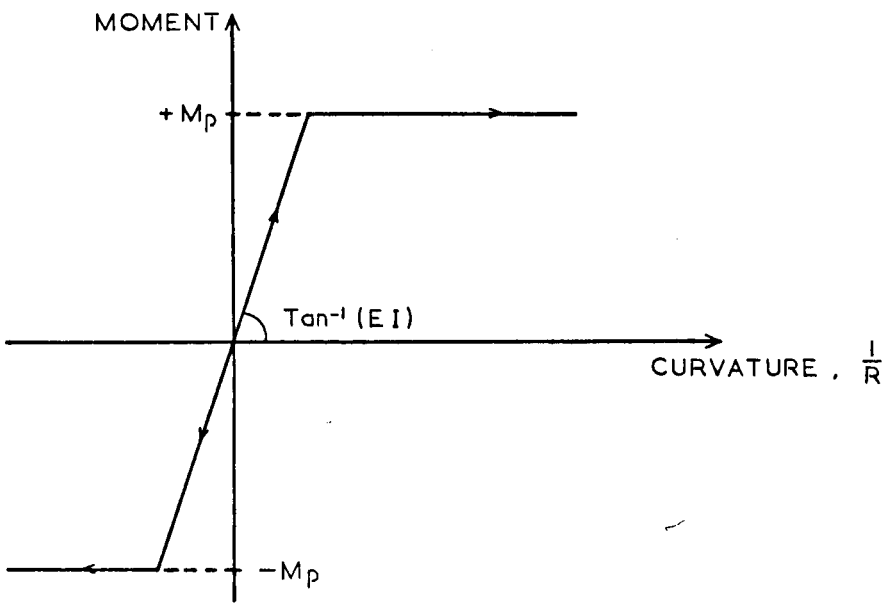

FIG. 5.2 IDEALISED MOMENT – CURVATURE

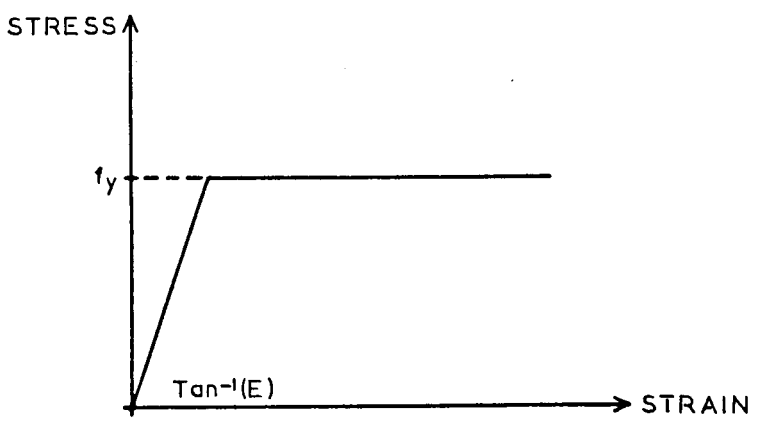

FIG. 5.3 IDEALISED STRESS – STRAIN

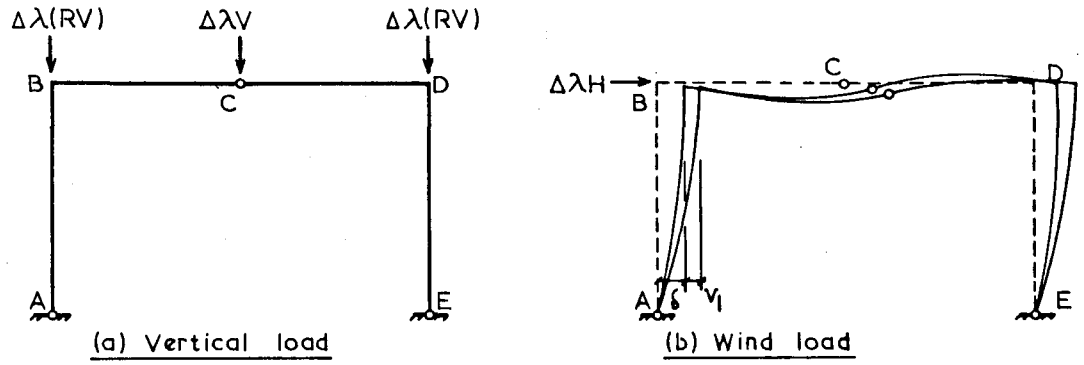

FIG. 5.4 HINGE AT MID-SPAN OF THE BEAM

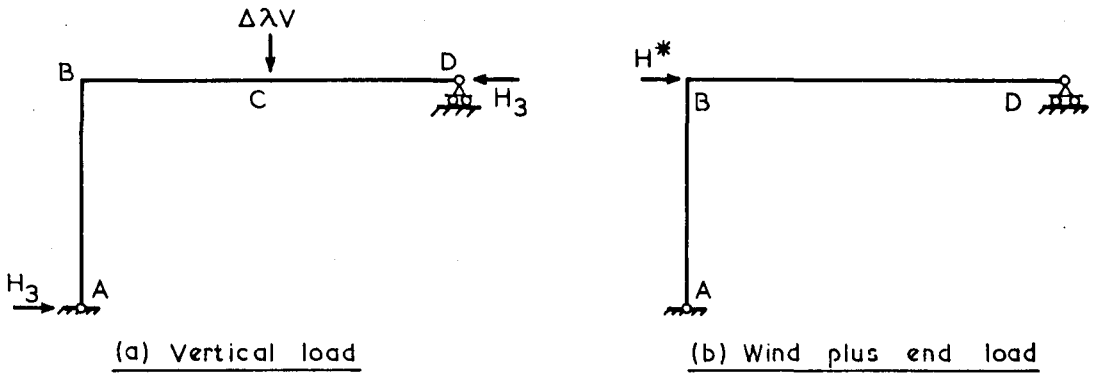

FIG. 5.5 HINGE AT LEEWARD END OF THE BEAM

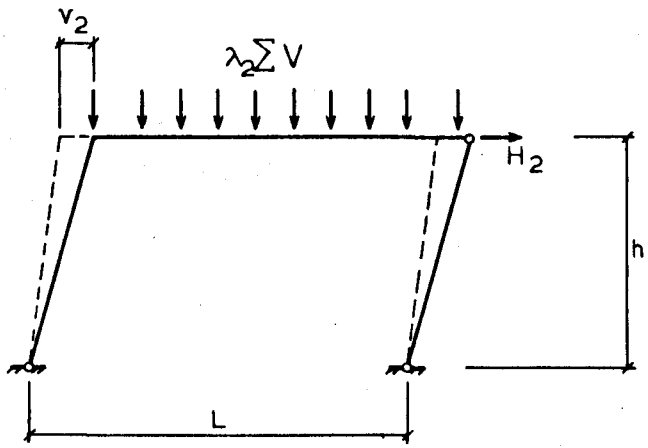

Equilibrium,

$$H_2 = \lambda_2 \sum V \frac{v_2}{h}$$

FIG. 5.6 FICTITIOUS LOAD, H_2

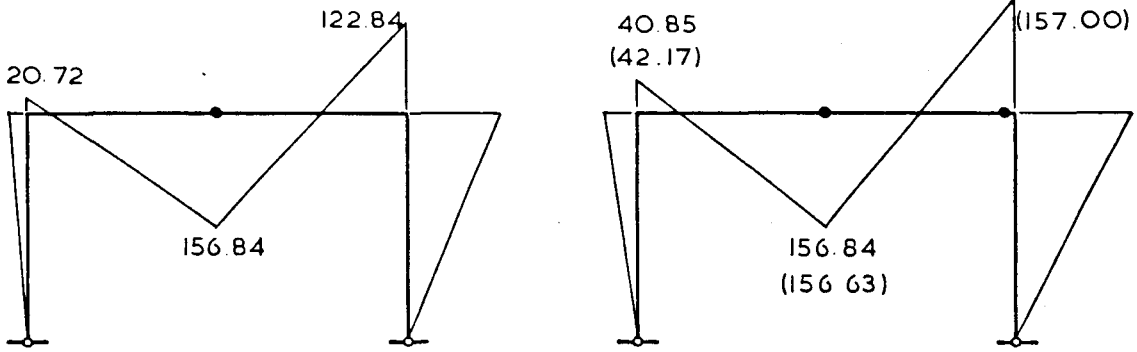

(a) $\lambda_1 = 0.98$ (b) $\lambda_2 = 1.09$

FIG. 5.7 EXAMPLE 1 (KNm. unit)

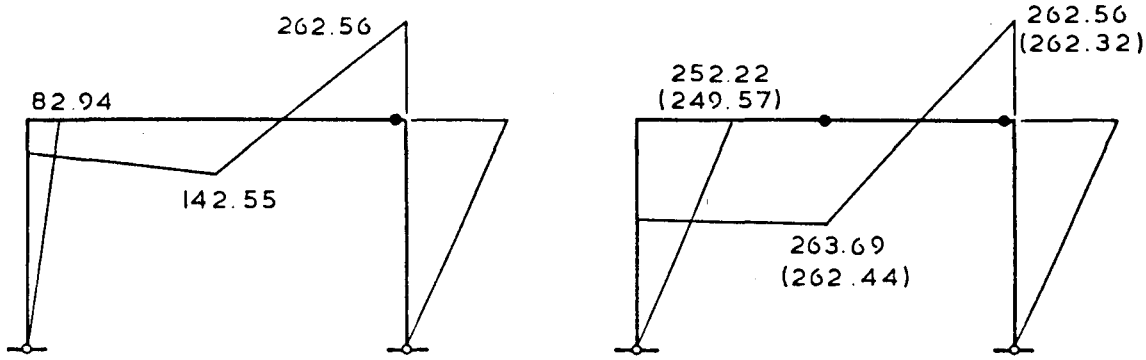

(a) $\lambda_1 = 0.99$ (b) $\lambda_2 = 1.15$

FIG. 5.8 EXAMPLE 2 (KNm unit)

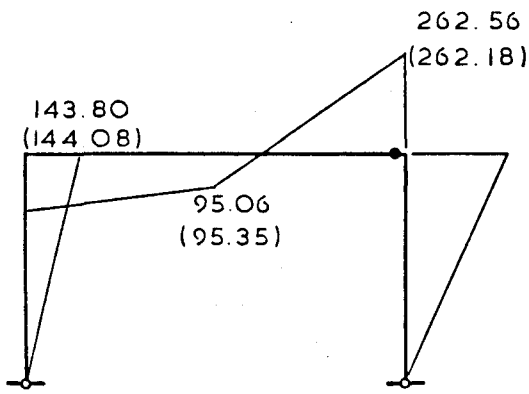

(a) $\lambda_1 = \lambda_f = 0.66$

FIG. 5.9 EXAMPLE 3 (KNm unit)

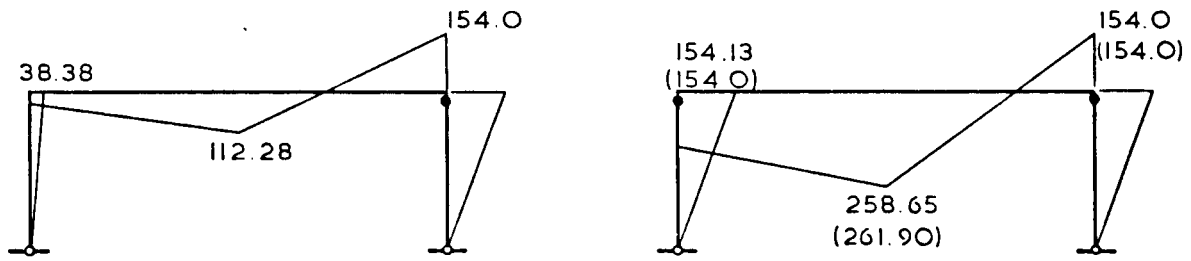

(a) $\lambda_1 = 0.67$ (b) $\lambda_2 = 1.01$

BENDING MOMENT DIAGRAM (KNm units)

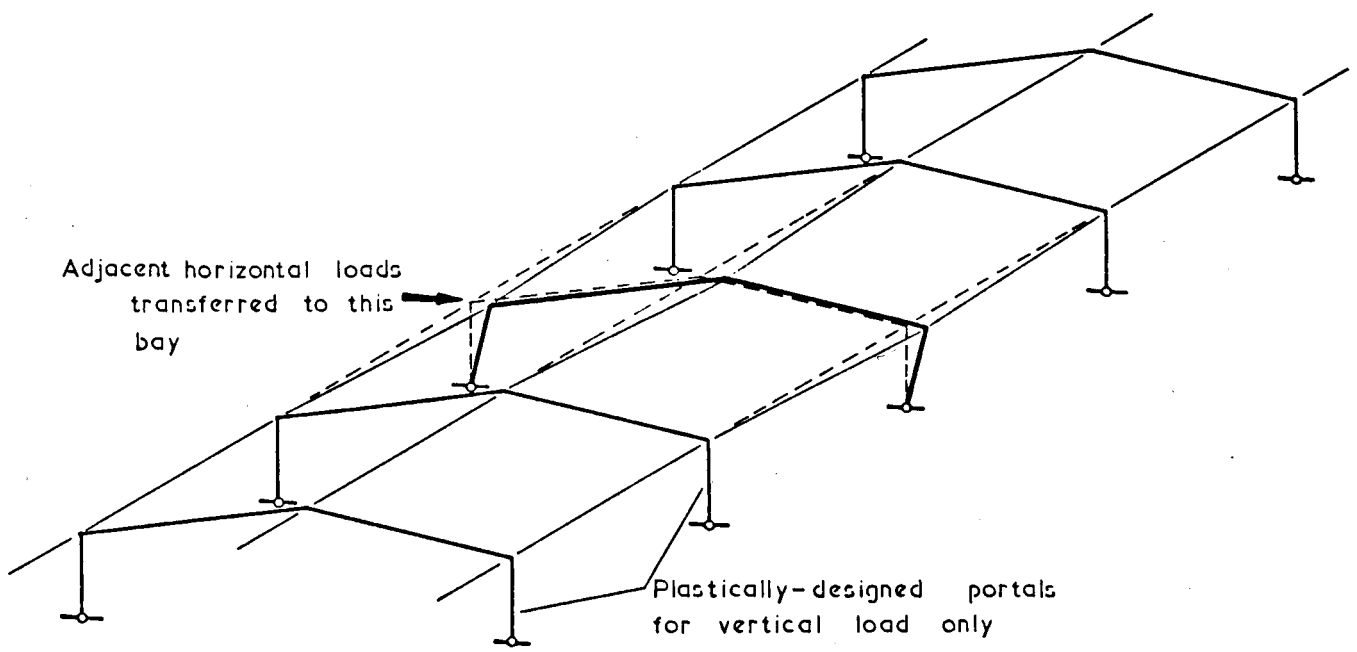

(c) INTERMEDIATE WIND-RESISTING BAY

FIG. 5.10 PORTAL FRAME DESIGN

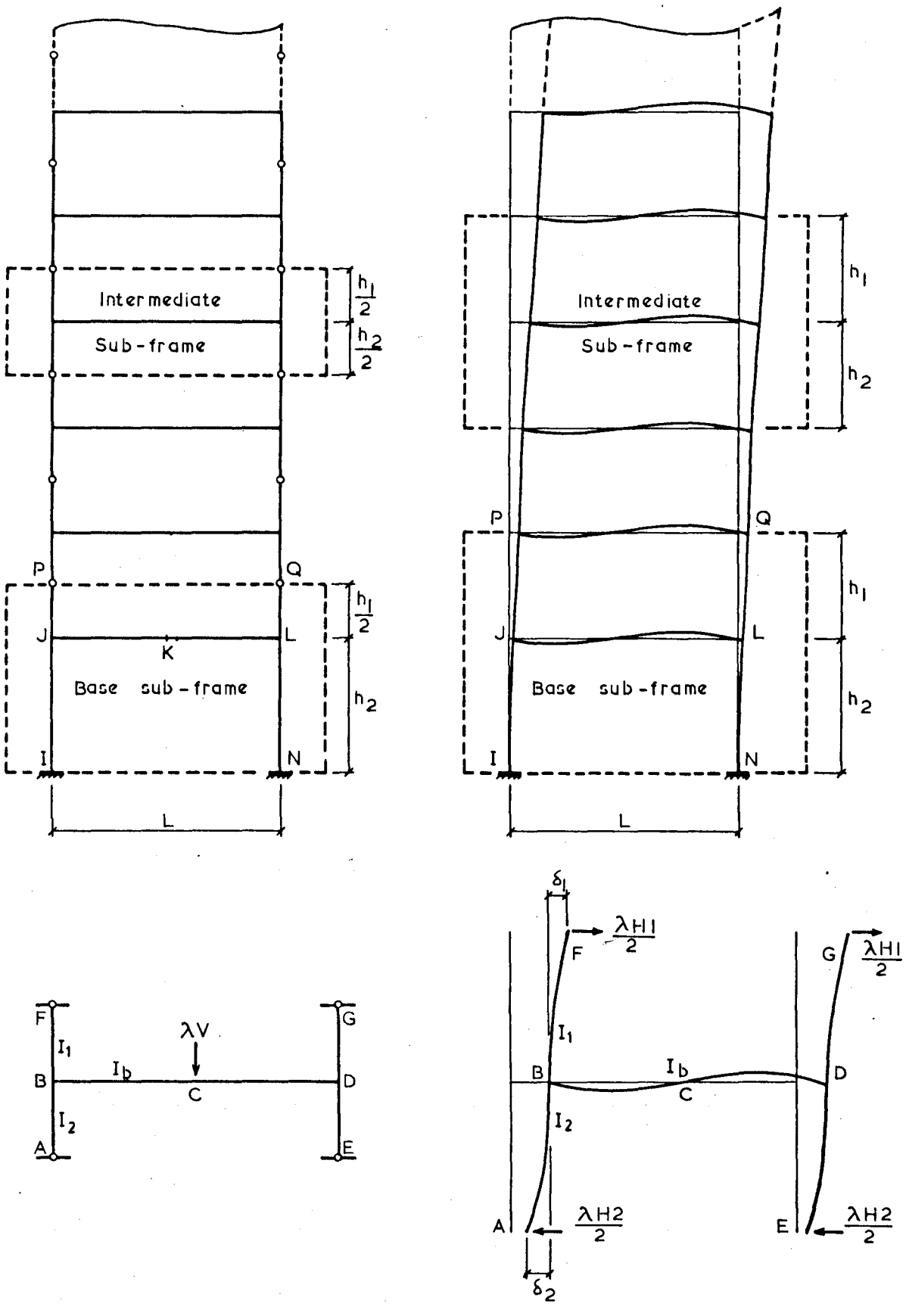

(a) VERTICAL LOADING

(b) HORIZONTAL LOADING

FIG. 5.11 ANALYSIS OF ELASTIC LIMITED FRAME

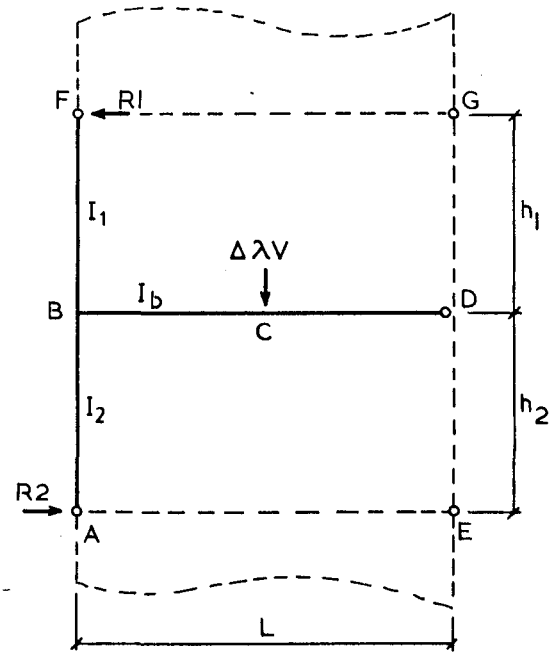

(a) VERTICAL LOADING

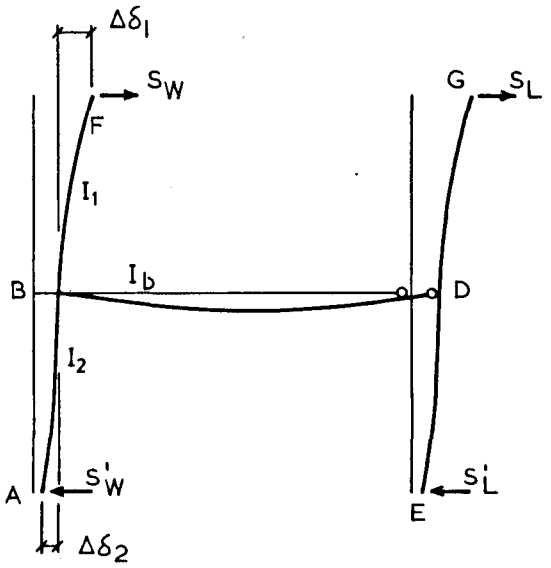

(b) HORIZONTAL LOADING

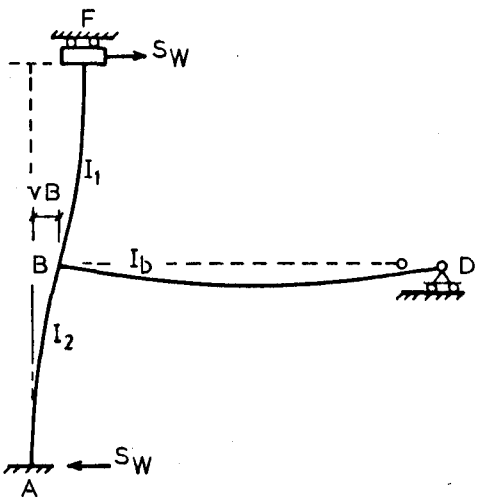

(c) WINDWARD ASSEMBLY

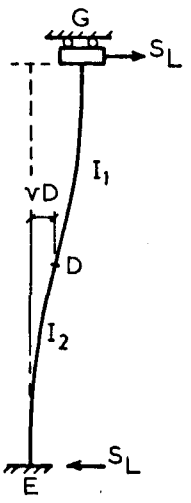

(d) LEEWARD COLUMN

FIG. 5.12 INCREMENTAL ANALYSIS (LEEWARD HINGE)

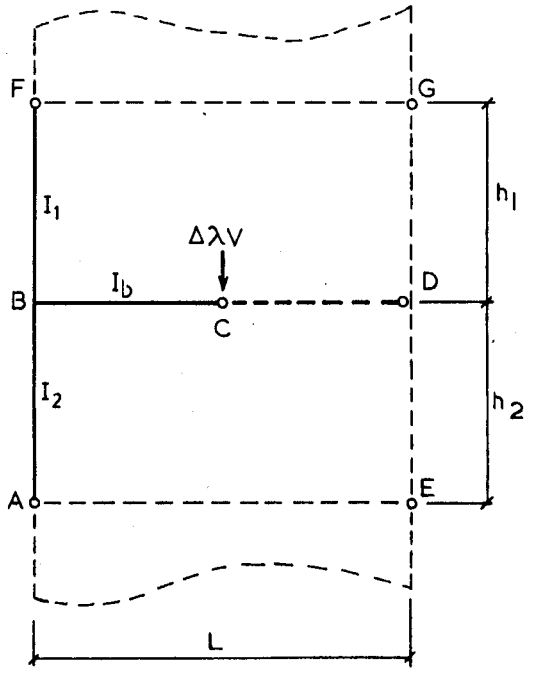

(a) VERTICAL LOADING

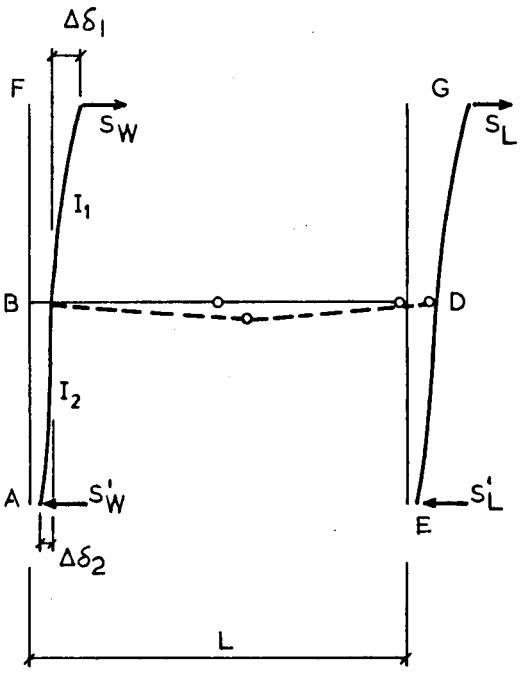

(b) HORIZONTAL LOADING

FIG. 5.13 INCREMENTAL ANALYSIS (DOUBLE HINGES)

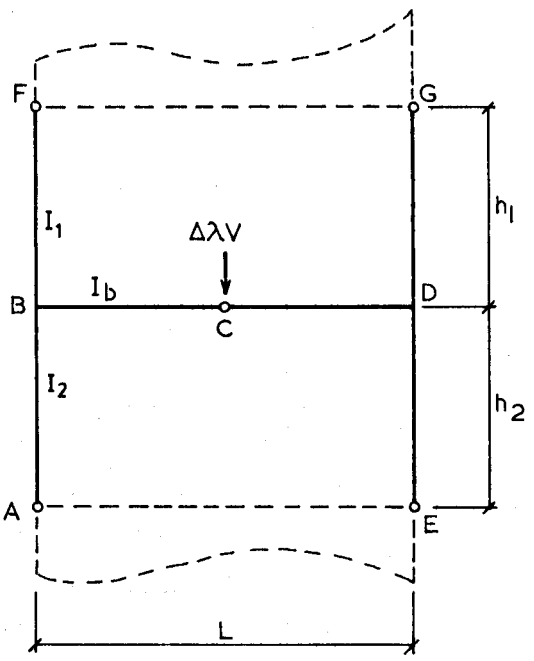

(a) VERTICAL LOADING

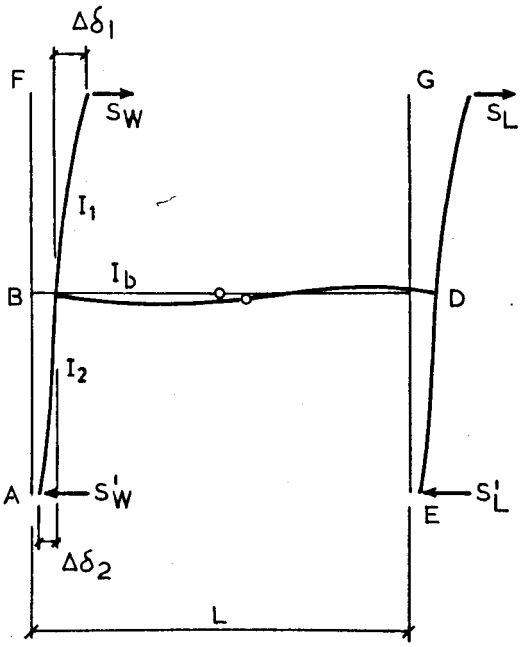

(b) HORIZONTAL LOADING

FIG. 5.14 INCREMENTAL ANALYSIS (MID-SPAN HINGE)

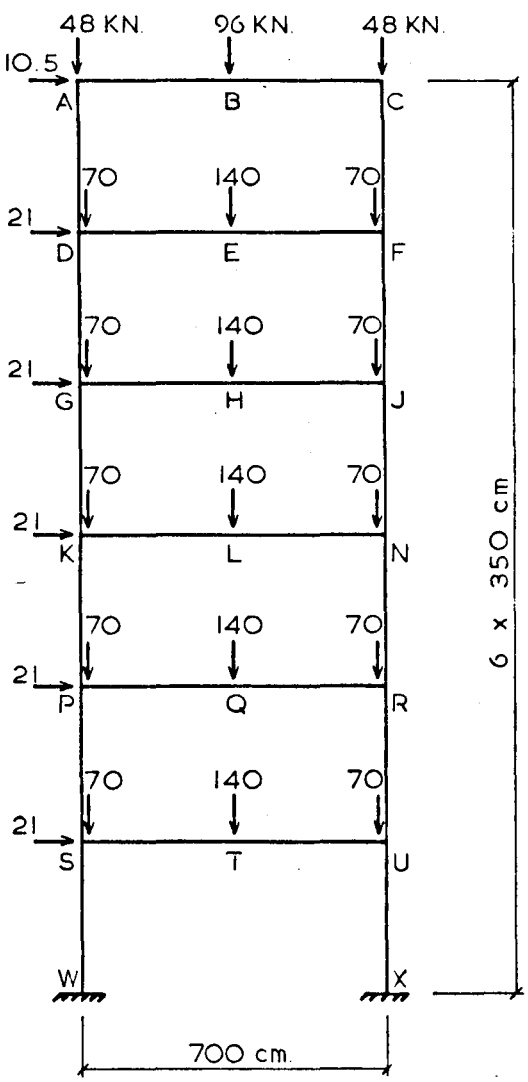

(a) DIMENSIONS & LOADINGS

$\sum H$	
i)	10 5
ii)	31.5
iii)	52 5
iv)	73.5
v)	94.5
vi)	115.5

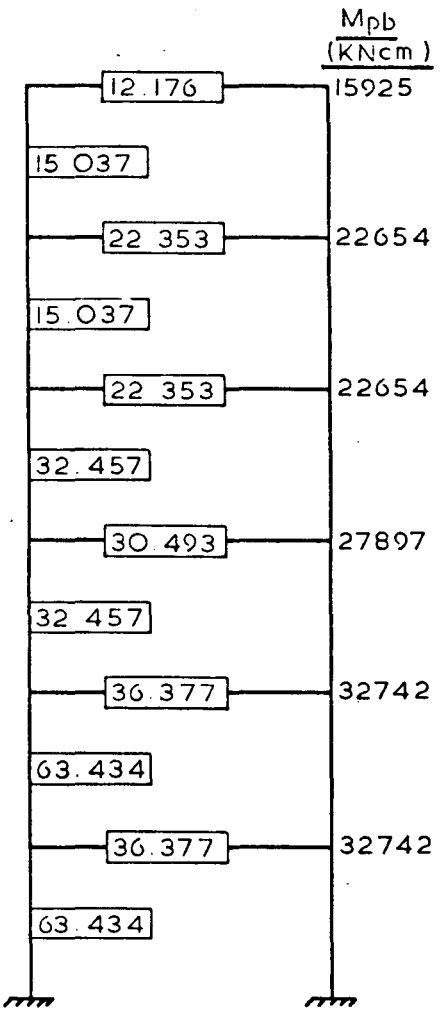

(b) VALUES OF k (cm^3)

MEMBER	SECTION
AC	305 X 165 X 40 UB
DF, GJ	406 X 140 X 46 UB
KN	457 X 152 X 52 UB
PR, SU	457 X 152 X 60 UB
ADG, CFJ	203 X 203 X 52 UC
GKP, JNR	254 X 254 X 73 UC
PSW, RUX	305 X 305 X 97 UC

(c) SECTION TABLE

E = 21000 KN/cm^2

fy = 25.5 KN/cm^2

FIG. 5.15 SIX STOREY SINGLE BAY FRAME

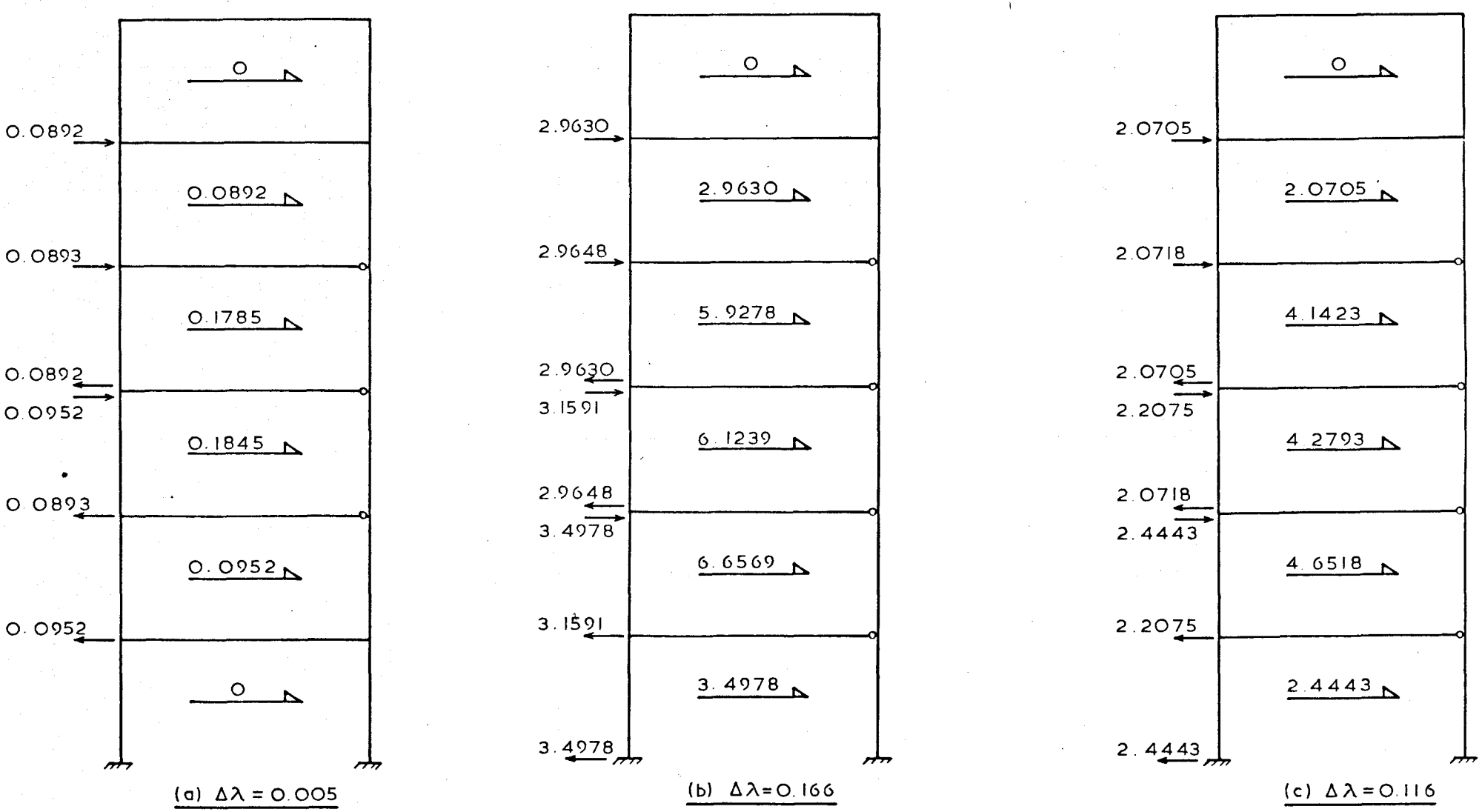

FIG. 5.16 FICTITIOUS SHEARS FOR SUBSTITUTE FRAME ANALYSIS (KN.)

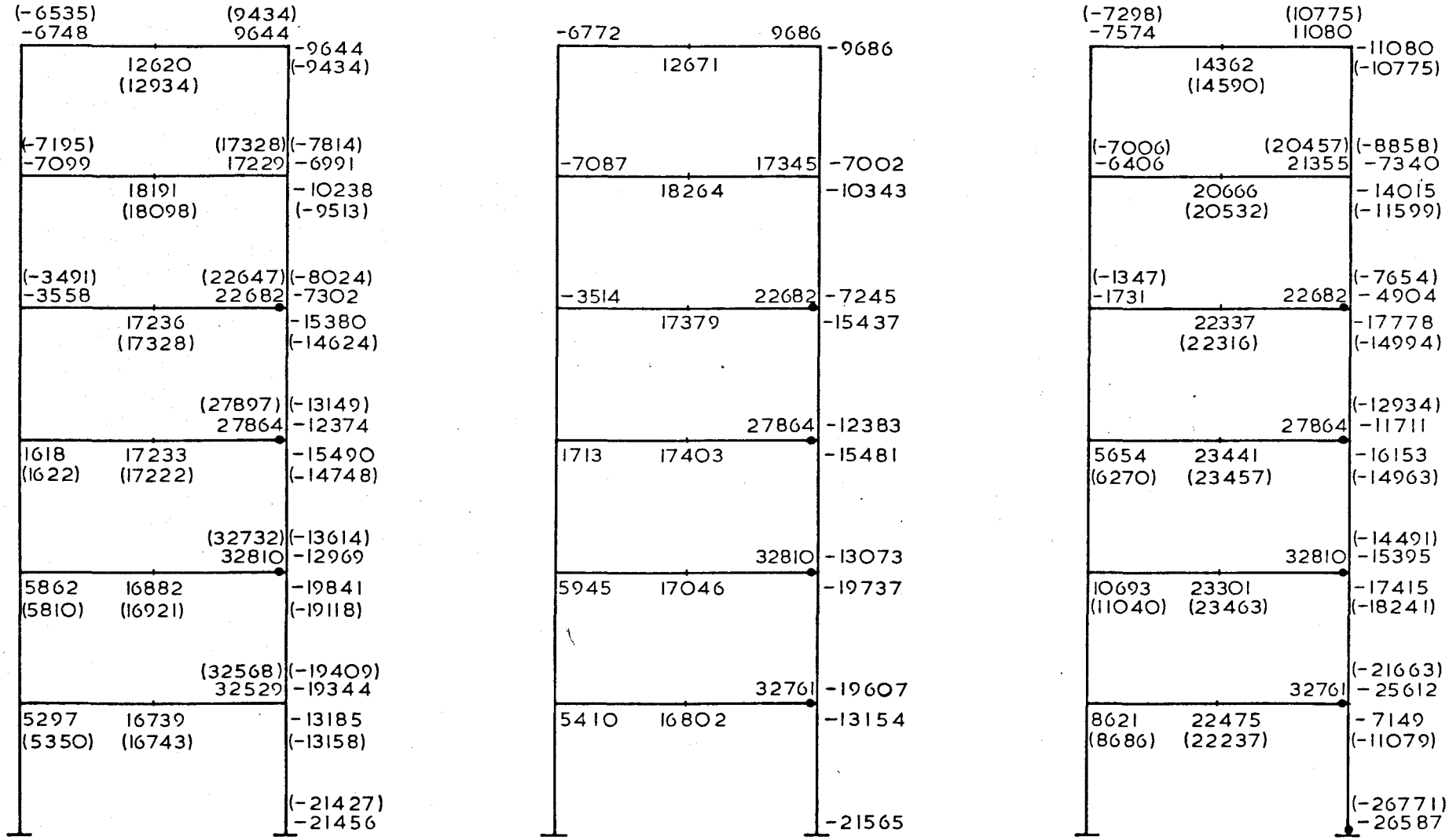

FIG. 5.17 PLASTIC HINGE FORMATION & BENDING MOMENT DISTRIBUTION (KN cm)

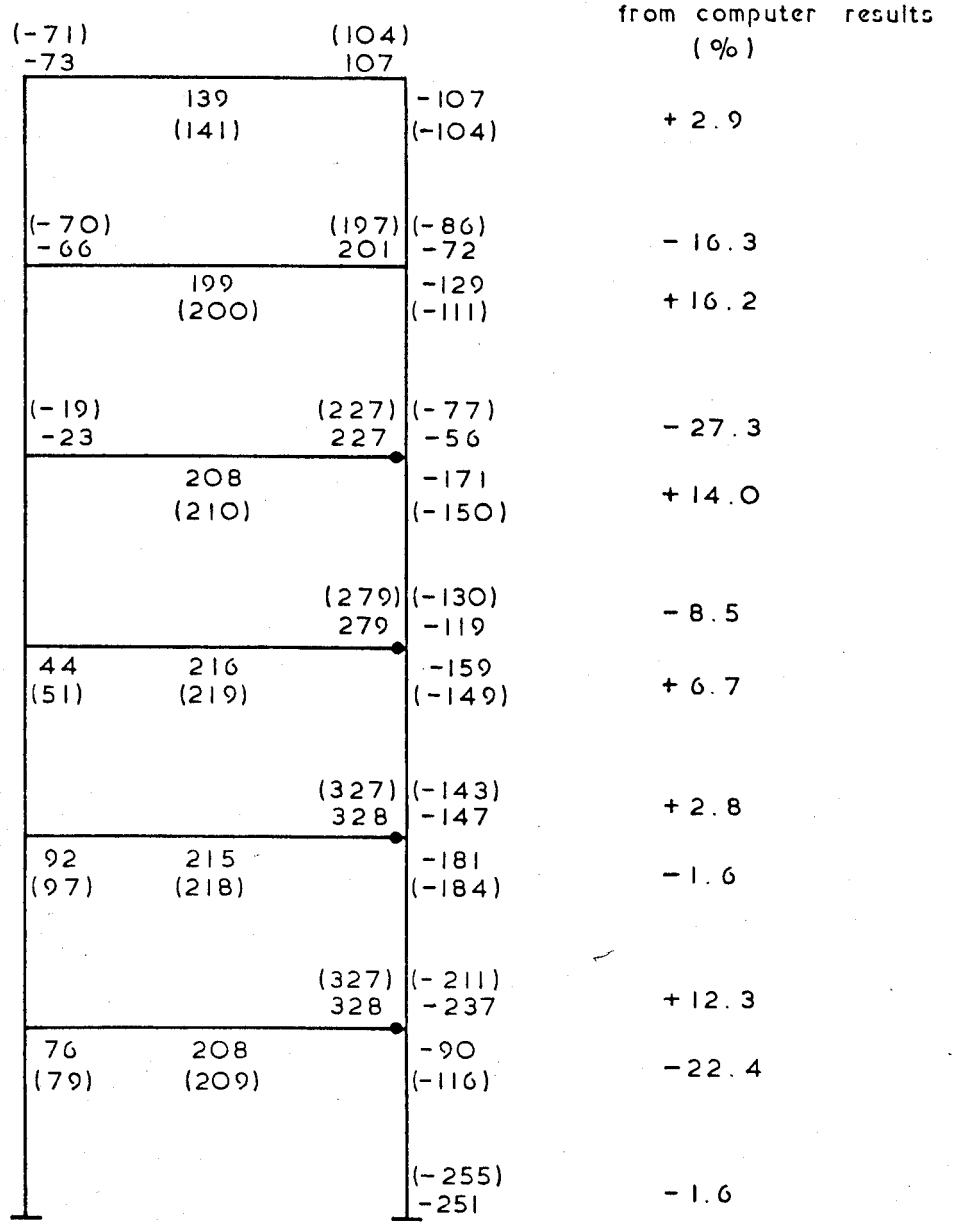

FIG. 5.17 (d) $\lambda = 1.360$

ACCURATE COMPUTER RESULTS IN BRACKETS (VALUES IN KN.m FOR COMPARISON WITH PUBLISHED RESULTS)

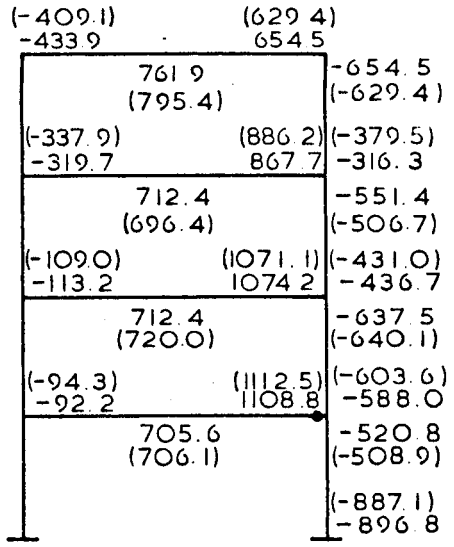

(a) $\lambda_1 = 1.083$ (1.085)

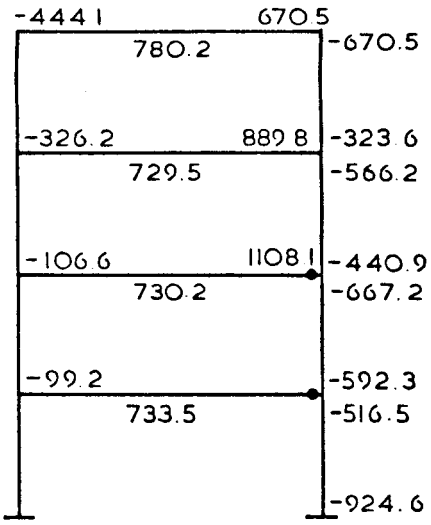

(b) $\lambda_2 = 1.109$ (1.118)

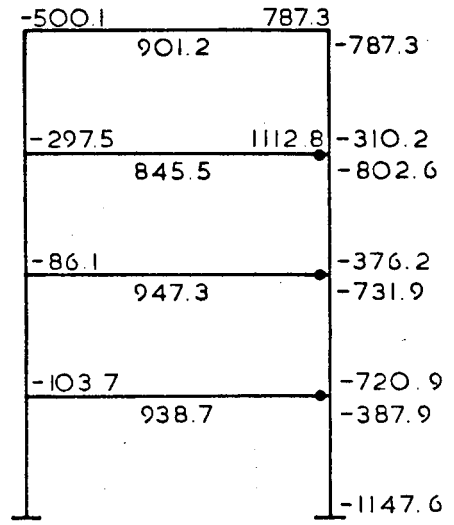

(c) $\lambda_3 = 1.281$ (1.293)

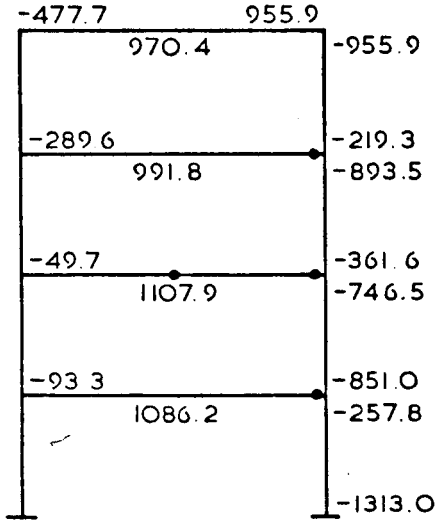

(d) $\lambda_4 = 1.399$ (1.393)

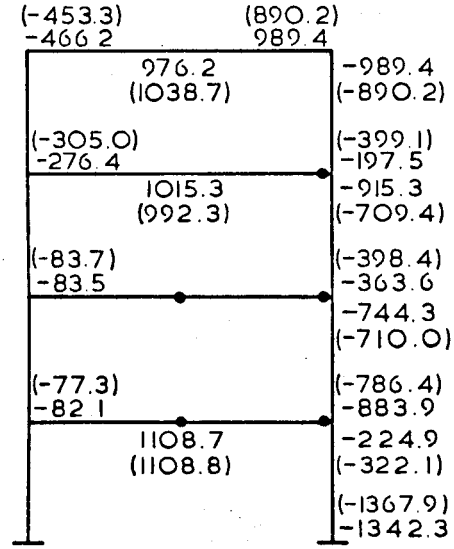

(e) $\lambda_5 = 1.413$ (1.410)

E = 13400 Tons / in^2

fy = 15.25 Tons / in^2

FIG. 5.18 PLASTIC HINGE FORMATION & BENDING MOMENT DISTRIBUTION (Tons. in.)

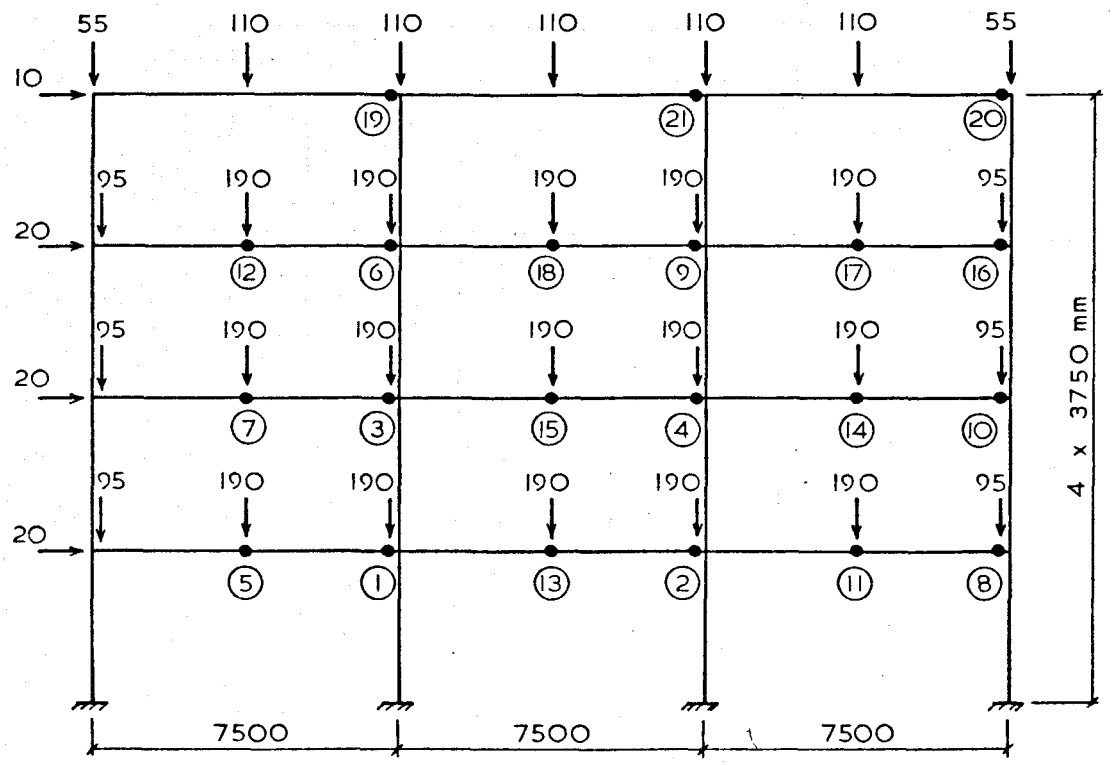

(a) FOUR STOREY THREE BAY FRAME

$\lambda_f = 1.403$

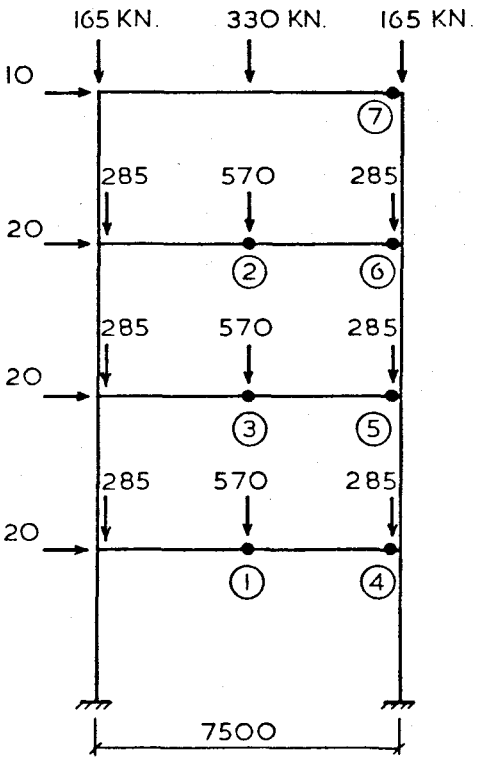

(b) EQUIVALENT SINGLE BAY FRAME $\lambda_f = 1.414$

FIG. 5.19 COMPUTER ANALYSIS OF FRAMES ($E = 206\ KN/mm^2$, $f_y = 240\ N/mm^2$)

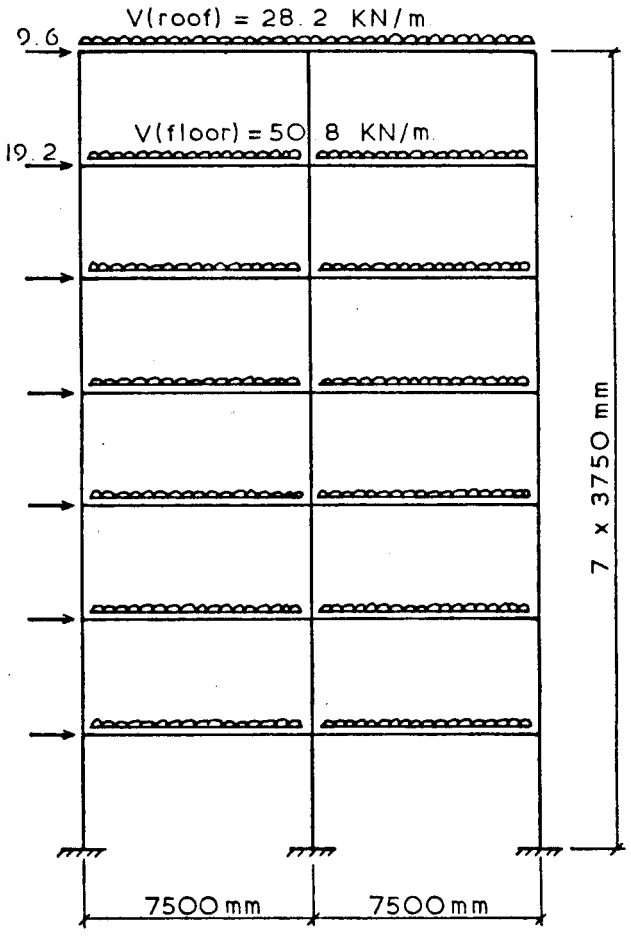

(a) SEVEN STOREY TWO BAY FRAME

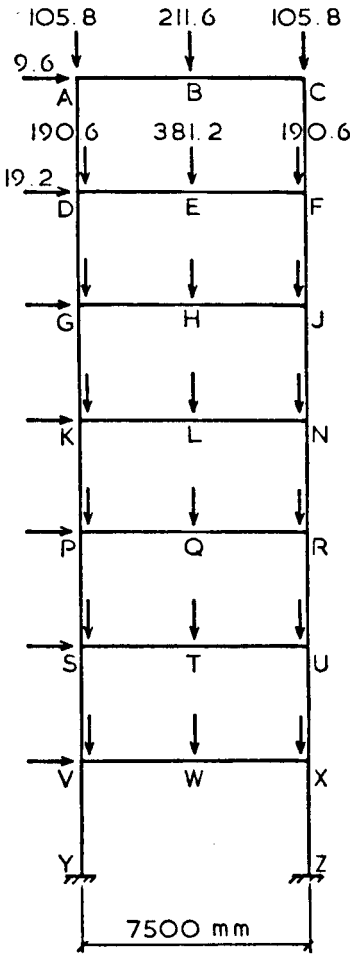

(b) EQUIVALENT FRAME

NOTE : IDENTICAL LOADING ON ALL FLOORS

	SECTION	AREA (cm^2)	INERTIA (cm^4)	FULL Mp (KNcm.)
BEAMS	AC	81.6	12974	23035
	DF, GJ KN, PR	118.0	31294	42643
	SU, VX	133.0	42690	52512
COLUMNS	ADG, CFJ	99.6	7894.5	—
	GKP, JNR	178.4	18217	—
	PSVY, RUXZ	176.8	22568	—

FIG. 5.20 EQUIVALENT SINGLE BAY FRAME

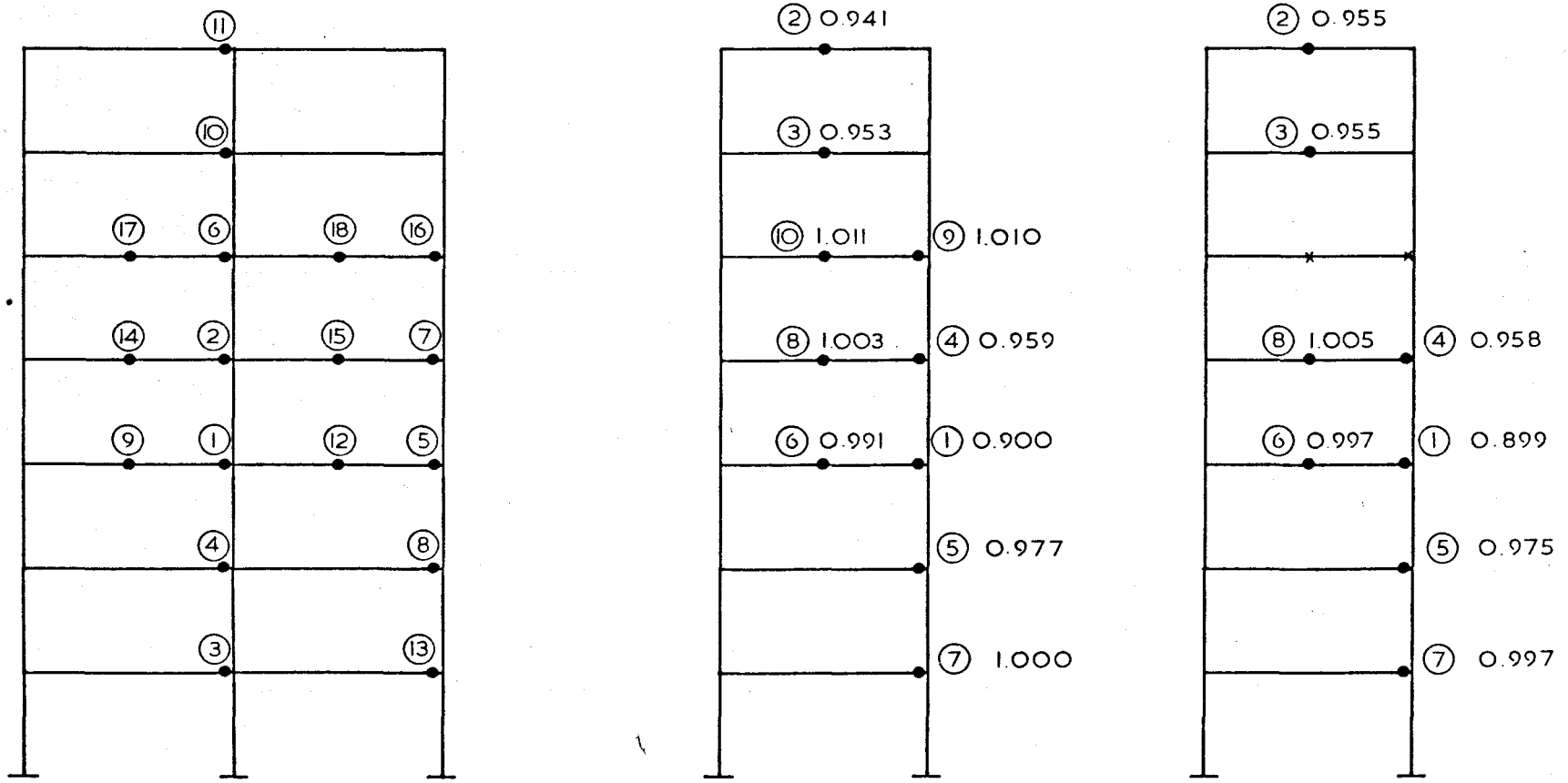

(a) REAL FRAME
COMPUTER METHOD
$\lambda_f = 1.004$

(b) EQUIVALENT FRAME
COMPUTER METHOD
$\lambda_f = 1.011$

(c) EQUIVALENT FRAME
PROPOSED METHOD
$\lambda_{prop} = 1.005$

FIG. 5.21 COMPARISON OF RESULTS

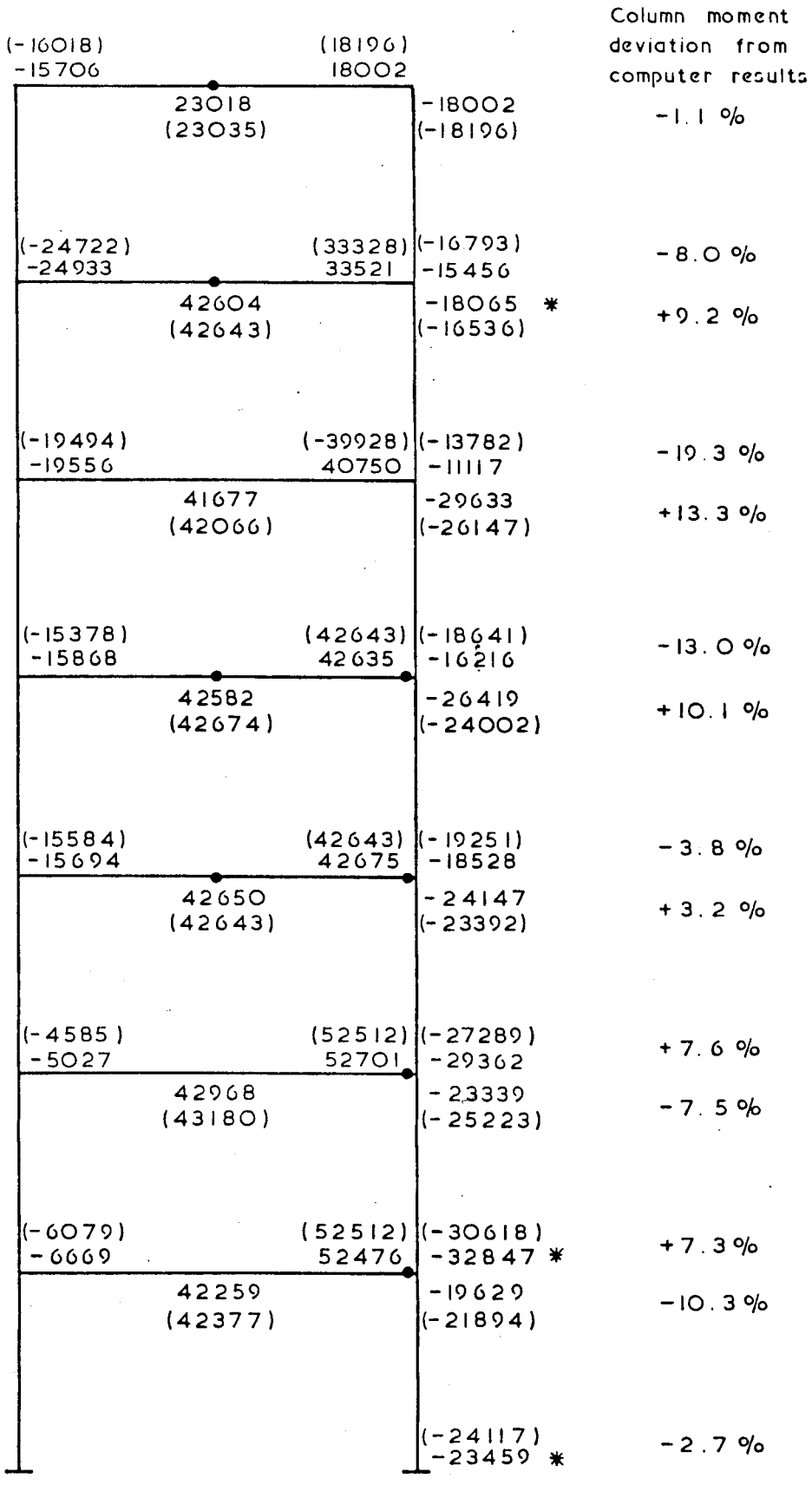

(a) CALCULATED MOMENTS AT $\lambda = 1.005$

(b) COMPUTER RESULTS IN BRACKETS AT $\lambda = 1.003$

FIG. 5.22 COMPARISON OF MOMENTS IN EQUIVALENT SINGLE-BAY FRAME (PROPOSED COLLAPSE CRITERION)

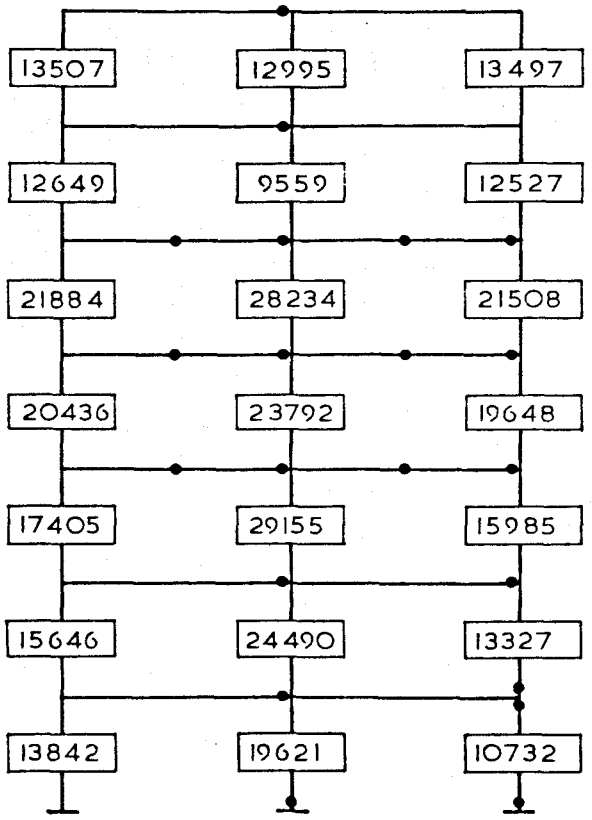

$f_y = 240\ N/mm^2$

(a) ACCURATE COLUMN MOMENT CAPACITIES AT FAILURE $\lambda_f = 1.000$

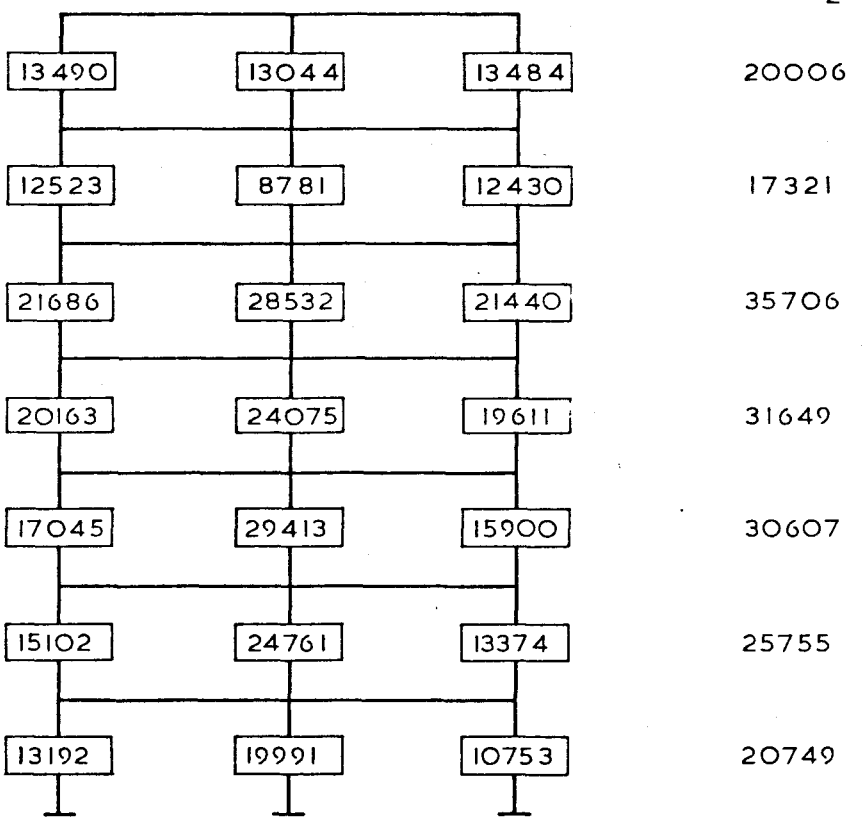

$f_y = 240\ N/mm^2$

(b) CALCULATED COLUMN MOMENT CAPACITIES AT $\lambda = 1.005$

FIG. 5.23 COMPARISON OF COLUMN MOMENT CAPACITIES (KN.cm units)

CHAPTER 6

EFFECTS OF SEMI-RIGID JOINTS ON SWAY DEFLECTION AND EFFECTIVE LENGTH

6.1 Introduction

Traditional methods of analysis and design of structural steel frames depend on the simplified assumption that the end connections of members behave as either fully-rigid or pinned. Despite the fact that neither is true of real bolted connections, engineers continue to adopt such assumed joint behaviour in the analysis and design of structural frameworks.

It is well known that some degree of restraint can provide savings in column sizes which had been assumed 'pinned' previously. Although the British(2,5) and American(14) codes of practice permit semi-rigid construction, it has been rarely adopted, particularly in medium-rise buildings because of the difficulty in establishing an analytical model to predict the complex behaviour of bolted connections. Even the British Draft Standard Specification for the Structural use of Steelwork in Buildings(55) has defined types of construction as 'continuous' or 'simple'.

With the exception of certain types of rigid moment connections, all joints are semi-rigid in practice. Additional sway displacements caused by flexible joints in tall buildings cannot be ignored, even at working load. Furthermore, even if the frame may

be satisfactory with respect to stiffness, a complete redistribution of internal forces can also arise, resulting in overstressed members.

For practical connections, the most useful characteristic is moment resistance to rotational stiffness behaviour. 'Rigid' and 'simple' connections are ideal theoretical assumptions that can never be attained and almost all practical bolted connections exhibit marked non-linear moment-rotation behaviour. Several types of common building connections are shown in figure (6.1). An ideal rigid joint is given by the vertical axis while a perfectly pinned connection is represented by the abscissa. Most connections fall in between these assumed characteristics. The connection rotation is being defined here as the tensile deformation of the bolted assembly under increasing bending after the initial joint rotation has taken place. Compressive deformation of the connection is ignored.

The use of computers enables systematic procedures to be incorporated to simulate actual connection behaviour. Standardised moment-rotation characteristics, applicable to a range of common bolted connections, have been proposed by Frye and Morris(69). A computer program which incorporates the non-linear expressions was suggested but this necessitates the storage of the connection stiffness terms as additional elements in the overall stiffness matrix, thus increasing the size of the latter.

The main purpose of the present Chapter has been to extend a non-linear (i.e. second-order) elastic computer program, based on

the matrix displacement method of analysis, to study the influence of semi-rigid connections on the sway deflection of multi-storey frameworks. The program is capable of analysing any combination of pinned connections, fully-rigid joints and connections with any specified moment-rotation relationship. Indeed, any of those connections shown in figure (6.1) may be used on any part of a member and at any position in the structure. It is therefore suitable for simulating the contribution of cladding to overcome the joint flexibility, otherwise assumed rigid in conventional analysis. In addition, second-order analysis enables column strengths to be evaluated with respect to elastic instability, for any given degree of end restraint. Examples of semi-rigid multi-storey frames are shown for comparison with assumed fully-rigid analysis. It is also intended to demonstrate the effective length of a column by a series of curves representing various end restraints.

A feature of the analysis makes use of the nature of the overall stiffness matrix to modify iteratively the load vector. This is done, instead of incorporating connection details into the stiffness matrix. Unlike previous computer methods, the overall stiffness matrix remained unchanged, thus reducing computer time and storage.

6.2 The stiffness matrix

The development of the analysis program is basically similar to the one described by Majid(23) and Anderson(24). Compact storage of the overall stiffness matrix, $\underline{K}$, is due to the technique of

Jennings(10). The unknown joint displacements of a structure, $\underline{X}$, are solved by an inverse of the stiffness equations,

$$\underline{X} = \underline{K}^{-1} \underline{L} \qquad (6.1)$$

where $\underline{L}$ is the externally applied load vector { H, V, M }
and $\underline{K}$ is the overall stiffness matrix of the structure.

Figure (6.2) represents the contribution of a member with semi-rigid end connections to the overall stiffness matrix. Joints 'i' and 'j' are the first and second end of the member respectively. This is indicated by the direction of the arrow on the member. The member is displaced from its original position with reference to the overall coordinate system of direction as shown. The symbols are defined as,

$$\begin{aligned} a &= EA / L \\ b &= 12\ EI\phi_5 / L^3 \\ d &= -6\ EI\phi_2 / L^2 \\ e &= 4\ EI\phi_3 / L \\ f &= 2\ EI\phi_4 / L \end{aligned} \qquad (6.2)$$

s,c = direction sine and cosine of the angle of inclination of the member measured clockwise positive from the first end 'i' respectively.

and E, I, A and L are Young's modulus of elasticity, second moment of area, cross sectional area and length of the member i-j. The reductions of bending stiffness due to compressive axial forces for second-order analysis are taken into account by the usual stability

' $\emptyset$ ' functions. Extra rows and columns shown hatched represent the connections at both ends of the member. The joint rotations are represented by θ_i and θ_j and the connection deformations are denoted by θ'_i and θ'_j.

The contribution of other members connected to joints 'i' and 'j' are similarly obtained. Each sub-matrix, $\underline{K}_{ii}$, $\underline{K}_{ij}$, $\underline{K}_{ji}$ and $\underline{K}_{jj}$ contain a 4x4 element matrix when both ends of the member have a semi-rigid connection. When the rows and columns corresponding to these connections are deleted in figure (6.2), the stiffness equations are identical to a rigid-jointed member. Consequently, extra rows and columns in the stiffness matrix are not required to be stored. Initially, the assembly of $\underline{K}$ will be described irrespective of whether the joints are semi-rigidly or rigidly connected.

Each numbered joint is considered in ascending order for the construction of the overall stiffness matrix. The total stiffness of the joint is the sum of the individual member stiffnesses connected to that joint. Therefore, non-zero sub-matrices, $\underline{K}_{ii}$ etc., will populate the overall stiffness matrix only at locations corresponding to joint interconnections. Hence, with reference to figure (6.3), the overall stiffness matrix is seen to contain many zero sub-matrices, and the non-zero sub-matrices are directly related to the joint connection list. Further, $\underline{K}$ is symmetric along the leading diagonal.

The method of Jennings makes use of the symmetric feature of the overall stiffness matrix for the storage and rapid solution of

the stiffness equations. This method stores only the first non-zero sub-matrix and the elements on the leading diagonal, inclusive, on one side of the overall stiffness matrix. Null sub-matrices, such as $\underline{K}_{9,7}$, occurring in between these non-zero elements are also stored. Only the irregular half band-width outlined in figure (6.3) is stored and operated on by the compact elimination technique.

Initially, the analysis proceeds by assuming all joints are rigid, except where real pins exist. Once the displacements are known, member end forces are calculated by the slope-deflection equations,

$$M_{ij} = e(\theta_i + \theta'_i) + f(\theta_j + \theta'_j) + d(v_{ij}) \qquad (6.3)$$

$$M_{ji} = f(\theta_i + \theta'_i) + e(\theta_j + \theta'_j) + d(v_{ij}) \qquad (6.4)$$

$$S_{ij} = -(M_{ij} + M_{ji}) / L \qquad (6.5)$$

Here v_{ij} is the vertical joint displacement of the second end 'j' relative to the first end 'i' in the overall coordinate system. Values of e, f and d are defined in equation (6.2).

As the first iteration assumes all connection movements to be zero, values of θ' are obtained only after the member forces have been calculated. Using the current values of end moments from equations (6.3) and (6.4), each connection deformation is determined in the form,

$$\theta' = f(M) \qquad (6.6)$$

where M is the bending moment at a specified joint corresponding to

a semi-rigid connection.

The load vector is then suitably modified for the joint concerned. This is dependant on whether one or both ends of the member are flexibly connected. A new vector of loads, $\underline{L}$, which corresponds to the number of elements of the original load vector is then used to obtain a new set of displacements and member forces. In figure (6.2), the new vector of loads for member i-j is given by,

$$\begin{bmatrix} H_i \\ V_i \\ M_i \\ H_j \\ V_j \\ M_j \end{bmatrix} = \begin{bmatrix} H_i - ds\theta'_i - ds\theta'_j \\ V_i + dc\theta'_i - dc\theta'_j \\ M_i - e\theta'_i - f\theta'_j \\ H_j + ds\theta'_i + ds\theta'_j \\ V_j - dc\theta'_i - dc\theta'_j \\ M_j - f\theta'_i - e\theta'_j \end{bmatrix} \qquad (6.7)$$

Thus, the overall stiffness matrix remains unchanged in subsequent cycles of analysis. Iteration is necessary both for linear (first-order) and non-linear (second-order) elastic analysis. The results tend to converge in a few iterations to a state which satisfies equilibrium, compatibility and connection moment-rotation characteristics. Steps needed for the procedure is summarised by the flow chart shown in figure (6.4).

In a linear elastic analysis (first-order), all 'ϕ' functions are set to unity which indicates no reduction in member stiffnesses due to compressive axial forces. Iteration is continued until all the connection rotations are within a suitable tolerance. A non-linear elastic analysis (second-order) performs the same

process but after each iteration, the calculated member forces are used for an improved solution of the stiffness equations by evaluating new 'ϕ' values. The member forces in the current cycle are then calculated with reduced flexural stiffness, in addition to the connection deformation of the joint.

During each solution, the determinant of $\underline{K}$ is tested. When this is non-positive, the procedure is terminated. The procedure also terminates when very large displacements are encountered to maintain equilibrium in equation (6.1).

In the analysis of large plane frames, considerable economy of storage and computer time is achieved by modifying the load vector alone. Thus, by reference to figure (6.5), the simple fixed base portal requires 45 locations in the compact storage of $\underline{K}$, instead of 61 if terms relating to the connection rotations were retained in $\underline{K}$. In figure (6.5), M_{hk} and M_{hl} are the zero hinge moments corresponding to the hinge rotations θ_{hk} and θ_{hl} respectively. These are included to show a typical structure for $\underline{K}$ when rigid, semi-rigid and pinned connections are present in the same frame.

For the beam i-k, the rotations of the semi-rigid connections at ends 'i' and 'k' may be in the same or opposite directions, depending on the loading condition. This may be visualised for simple frames but a clearer indication of the connection deformation is given by observing the overall bending moment distribution diagram.

6.3 Sign of the bending moment diagram

With reference to figure (6.2), the overall stiffness matrix has been constructed by triple multiplication of $\underline{A}^T\underline{k}\underline{A}$, where $\underline{A}$ and $\underline{k}$ are the displacement transformation and member stiffness matrices respectively. The joint displacements are therefore referred to the overall coordinate system. Member forces given by equations (6.3) to (6.5) are calculated based on these transformed displacements, but their signs are based on the local member coordinate system. Clockwise end moments acting on the members are considered positive. The effect of such actions will be to cause a deformed shape with reverse curvature, as shown in figure (6.2).

It is assumed that all bolted assemblies are symmetrically identical in tension and compression, as shown in figure (6.1) except for the welded top plate. The single member shown in figure (6.2) will tend to 'relax' and straighten out as a result of end connection deformation. Thus, the rotations of the connections will be anti-clockwise. It follows that the sign of the connection rotation is opposite to the sign of the bending moment diagram.

It is assumed in the subsequent examples that all external loads are applied proportionally under static conditions. Loading patterns which may cause incremental or shakedown collapse phenomena are not considered. These assumptions are generally applied in practice for the plastic analysis and design of structures and would be appropriate for the loadings sustained by typical building structures with semi-rigid joints. It is also assumed that connection displacements due to axial and shear forces are negligible.

6.4 Numerical work example

Consider the simplified structure shown in figure (6.6) with a semi-rigid connection at joint (B) on member B-C. In the interest of simplicity, axial deformations of all the members are neglected and it is assumed that the moment-rotation characteristic of the connection is linear and given by the form,

$$\theta' = 2.06 \times 10^{-5} \ (M) \tag{6.8}$$

where M (KNm. unit) is the end moment at the semi-rigid connection.

A linear elastic (first-order) analysis is required to determine the vertical deflection at (C). The overall stiffness matrix is assembled for the structure by assuming joint (B) to be fully-rigid. This is given by a 2x2 matrix,

$$\underline{L} = \underline{K}\,\underline{X}$$

$$\begin{bmatrix} 200 \\ 0 \\ M_{BC} \end{bmatrix} = \begin{bmatrix} 45 & \text{SYMMETRIC} & -45000 \\ -45000 & 90\times10^{6} & 60\times10^{6} \\ -45000 & 60\times10^{6} & 60\times10^{6} \end{bmatrix} \begin{bmatrix} Y_C \\ \theta_B \\ \theta'_B \end{bmatrix} \tag{6.9}$$

The imaginary row and column which represents the semi-rigid connections are shown hatched for illustration and identification. Initial analysis assumes $\theta'_B = 0$. Solving for the displacements gives,

$$\begin{bmatrix} y_C \\ \theta_B \end{bmatrix} = \begin{bmatrix} 8.889 \\ 4.444 \times 10^{-3} \end{bmatrix} \qquad (6.10)$$

where the vertical deflection at joint (C) is given in millimetres and the rigid-joint rotation at (B) in radians.

Next, member forces are calculated using equations (6.3) to (6.5) with all the stability functions equal to 1.0 and all connection rotations equal zero.

With e_1 =60000 KNm., f_1 $=e_1/2$, e_2 $=e_1/2$, f_2 $=e_2/2$ and d_1 =-45000 KN., the bending moment distribution is,

$$\begin{bmatrix} M_{BC} \\ M_{CB} \\ M_{BA} \\ M_{AB} \end{bmatrix} = \begin{bmatrix} -133.3 \\ -266.7 \\ +133.3 \\ +\ 66.7 \end{bmatrix} \qquad (6.11)$$

where the moments are in KNm. units.

As the connection rotation is opposite in sign to the bending moment diagram, the clockwise rotation at joint (B) on member B-C is given by,

$$\theta'_B = 2.06 \times 10^{-5} \times (133.3)$$
$$= 2.746 \times 10^{-3} \text{ radians} \qquad (6.12)$$

A new load vector can be formulated by using equation (6.9) with this value of the connection deformation giving,

$$\underline{L} = \begin{bmatrix} 200 \\ 0 \end{bmatrix} + \begin{bmatrix} 45000\ \theta'_B \\ -60\times10^6\ \theta'_B \end{bmatrix} = \begin{bmatrix} 323.6 \\ -164.8 \end{bmatrix} \qquad (6.13)$$

The previous load vector is replaced by this new load vector to solve for a new set of displacements in equation (6.9),

$$\begin{bmatrix} y_C \\ \theta_B \end{bmatrix} = \begin{bmatrix} 10.720 \\ 3.529 \times 10^{-3} \end{bmatrix} \qquad (6.14)$$

The new displacements (equation (6.14)) are significantly different to those given by equation (6.10) but when the procedure is repeated a few times, all the displacements and member forces converge to satisfy equilibrium, compatibility and connection deformation characteristics. The results are summarised in figure (6.6) for the required number of iterations. The final bending moment distribution indicates a 17% reduction at the semi-rigid joint (B), while the sagging moment at (C) was increased by only half this amount. This suggests that economy in column design may be achieved if realistic representation of the end restraint is properly taken into account rather than the assumed fixed connections currently employed in practice.

The vertical displacement at joint (C) was increased by 17% in comparison with fully-rigid analysis. This is as expected since the connection has contributed deformation, in addition to the rigid-joint rotation.

When compressive axial forces in the columns are significant,

a non-linear (second-order) analysis would be more appropriate. In multi-storey frames the sway deflection can be alarmingly high when secondary effects are included. The proposed method has been shown to analyse such frames conveniently and economically.

6.5 Eleven storey two bay frame

A realistic unbraced office building shown in figure (6.7) has been analysed by Frye and Morris(69) using American wide flange sections. Non-linear standardised moment-rotation expressions applicable to T-stub connections were adopted at all beam-column junctions. Total sway deflections, as a result of incorporating the T-stub connection, was reported to be over 20% higher than the deflections calculated assuming fully-rigid joints. However, no details of the size parameters for each of the connections were given and it was not certain whether these deflections were the result of a linear (first-order) or non-linear (second-order) analysis. More importantly, no information was given of the individual storey sway values. Furthermore, some of the wide flange sections have been discontinued in the current version of the International Structural Steelwork Handbook(1983) published by BCSA.

To investigate the sway behaviour and for comparison with the published results, the frame was analysed using sections chosen from the BCSA publication mentioned above. A section one size larger was adopted to replace those sections that have been discontinued. Their properties necessary for the analysis are shown in table (6.1).

To determine the size parameters required in the non-linear moment-rotation equations, values of 'd' and 'l' for all the beam-column connections were kept constant. The variable 't' was taken as the sum of the flange thickness for the lower column at a splice and the thickness of the stub flange. The bolt diameter 'f' was assumed to increase from 16 to 24 millimetre from the roof to the first floor beam. These values are given in the connection list in table (6.2). A schematic drawing of the connections used is shown alongside the tables for ease of identification. Metric units have been used throughout and Young's modulus was taken as 205 KN/mm^2.

Three curves are shown in figure (6.7) for the sway deflections when the frame is subjected to combined loading. Values of lateral deflection from a linear elastic (first-order) analysis for each storey height indicate unsatisfactory limits according to current Design Recommendations, even when the joints were assumed fully-rigid. The worst storey sway was 1/223 in comparison with the maximum allowable of 1/300. Nevertheless, the total deflection of curve (1) was about 1/290th of the overall height.

Curve (2) represents the same analysis but incorporating the contribution of connection deformation. The total sway deflection is approximately 10% above the rigid-jointed case. The worst storey sway has been increased to 1/210. As the connections are relatively rigid in comparison with those connections shown in figure (6.1), this additional sway is not of particular concern. However, when compressive axial forces are taken into account in a non-linear (second-order) analysis, the deflections were significantly higher

than the ones assuming rigid connections. As a result of the secondary effect, the total sway was over 25% of the value from rigid-jointed analysis. This is shown by curve (3). In fact, a number of storey sways exceeded 1/200th of the column height. These values confirmed the published results.

The effect of incorporating the connection deformation into the analysis is to reduce the bending moments in the beam-column connections near the top of the structure and to increase those near the bottom. The mid-span sagging moment was generally increased by a small amount at all levels of the structure.

6.6 Effects of claddings in semi-rigid construction

It is well known that partitions, infilling the frame and cladding for a multi-storey structure all have a great effect on the lateral stiffness of the frame and the elastic critical load. References (50) and (60) showed that such effects can be incorporated into an analysis by the use of '$\bar{s}$' values. If the infill panels in a given storey have a total stiffness , 'S' (force per unit displacement), the non-dimensional panel stiffness in any storey is given by,

$$\bar{s} = Sh^2/EK \qquad (6.15)$$

where E = Young's modulus of elasticity,

K = sum of column stiffness of that storey,

h = storey height under consideration.

Wood(50,60) has proposed that values of '$\bar{s}$' should be included in calculations for the elastic critical load, and for sway deflections. However, the analysis used in both cases was based on a limited substitute frame with fully-rigid beam-column joints. It is not the intention of this section to criticise such simplified assumptions for use in rapid manual design. The point to remember, though, is that all bolted connections are flexible, apart from a few exceptional cases. Indeed, semi-rigid unbraced frames cannot be modelled in the same way as rigid-jointed frames are by the use of the Grinter frame. The difficulty arises from the uncertainty in determining the degree of connection restraint and its effect on the overall joint behaviour. Further, the principle of superposition is not valid for semi-rigid joints. Connection rotation is unpredictable for an unbraced frame subject to combined loads. A wrong assumption of the direction in which the connection deform would be unsafe.

For deflections at working load, the non-linear (second-order) sway displacements shown in figure (6.7) are unacceptable. It was decided to observe the effects of claddings by incorporating pin-ended struts at the leeward joints. These members may be considered as 'elastic springs' of total axial stiffness 'S', to represent the cladding that would, in practice, contribute certain resistance to the overall sway deflection. The axial stiffness is given by,

$$S_i = EA / L \qquad (6.16)$$

where A and L are the cross sectional area and length of the strut

respectively, and E is Young's modulus of elasticity.

The eleven storey semi-rigid frame shown in figure (6.8) has been analysed with several values of spring stiffness in an attempt to restore the sway deflections to the usual limits. It was assumed that all 'S' values are identical, as would be the case of a fully-clad structure.

As compressive axial forces are significant in this case, all the values shown are based on a non-linear (second-order) analysis. The results showed that a nominal value of 'S' is sufficient to overcome the additional sway deflections of the original framework arising from connection deformation. When 'S'=0.3075 KN/mm was used in the non-linear (second-order) analysis, all the storey sways were found to satisfy the limit of 1/300th of each storey height. Increasing the spring stiffness reduces the overall sway dramatically as shown for the case with 'S'=2.050 KN/mm.

The most severe storey deflections are those of the second and third floors. Two values of storey sway have been calculated for 'S'=0.2050 and 'S'=0.3075 KN/mm, as shown in figure (6.8). These figures of storey deflections suggest that cladding stiffness is unnecessary in the upper storeys.

To investigate this matter, five of the springs were removed from the roof downwards. A non-linear (second-order) analysis was carried out with 'S'=0.820 KN/mm for the remaining springs. The results indicated by 'S(partial)' on the figure showed the storey deflections to be adequate. The laterally unsupported upper parts

of the frame behaved in approximately the same manner as the totally unbraced semi-rigid structure. The result of 'S(partial)' is plotted as dashed lines in figure (6.8).

The example has shown that the proposed procedure is able to deal with any type of partially or fully-clad plane frame with a range of semi-rigid connections either of the same type or a combination of different types of assemblies. It can be used to simulate actual construction when the cladding is being installed progressively, as well as to analyse the completed structure.

6.7 Seven storey two bay frame

The seven storey frame designed to sway deflection limitations in Chapter (2) is illustrated in figure (6.9). Permissible sway limits of 1/300th of each storey height was specified when subject to unfactored horizontal loads. The design, however, was based on fully-rigid joints. An analysis was carried out of the frame by assuming the beam-column joints to be end-plate connections with horizontal column stiffeners. Standardised moment-rotation characteristics have been adopted for the purpose of demonstrating the contribution of connection deformation. The parameters necessary for evaluating the relationships have been calculated by,

$$d = D + 6T \qquad (6.17)$$

where D = total depth of beam section,

T = thickness of beam flange,

d = vertical distance between centres of the furthermost line of bolts.

The end-plate thickness, t, was taken as 20mm throughout. Expressions relating the moment to the connection deformation is also shown in figure (6.9) together with a schematic drawing of the end-plate connection. Member sections and applied loads are given in Chapter (2).

Values of the storey deflection have been calculated for each of the analysis given by the curves. It is apparent that under linear elastic (first-order) rigid-jointed analysis, the design is adequate but not in the case incorporating semi-rigid connections. However, the sway deflections are not as severe as the previous example because the initial specified sway limit was constrained to 1/300th of each storey height. The non-linear (second-order) analysis exhibits a maximum deflection of h/224 when subjected to total working loads.

As in the previous example, the critical sways were located at the bottom few storeys with the exception of the ground floor. In contrast, the value of the TOTAL deflection to the height in all cases was still within the maximum allowed. It was thought that only a nominal value of 'S' would be sufficient at all storey levels to reduce the semi-rigid sways to tolerable limits. It was found that 'S'=0.0742 KN/mm, about one quarter of the axial stiffness of the previous example, was sufficient to reduce the sways to the usual limit. When the effects of axial forces are neglected in the semi-rigid analysis, a value of 'S'=0.0309 KN/mm

was adequate to restore the sway deflections to the usual limits.

The effect of using a stiffer connection such as a T-stub has also been studied. When such a connection was used to replace the end-plate connection in a linear elastic (first-order) analysis, the sway deflections were found to be 1/1078, 1/559, 1/408, 1/304, 1/313, 1/304 and 1/420 from top to bottom storeys. These values are still within tolerable limits. However, when the axial forces were taken into account using the T-stub connection, the limit on storey deflection was violated in the same locations as indicated by curve (3) in figure (6.9), although the maximum value of storey sway was now reduced to 1/262.

6.8 Non-convergence of connection deformation

For the realistic types of connections that were utilised in the examples, connection deformations were found to be small. This is not unusual since the proportionally applied loads were at the serviceability level. Previous examples have indicated that a minimum of four to five iterations is needed to converge satisfactorily onto the desired connection tolerance. The possibility of gross distortion of the connection, however, cannot be ignored in a general analysis program.

Consider the simple fixed base portal shown in figure (6.10). A top and seat angle connection type is assumed. Two load cases have been drawn in figure (6.10), i.e. vertical load alone and combined loading. The analysis for the vertical load alone is denoted by a circle while the combined case is represented by a

triangular symbol. For each load case, two curves are shown. For example, consider the portal subjected to the mid-span vertical load alone. Curve (1) represent the initial total rotation and curve (2) represent the converged total rotations at joint (A). Each point on the curve represents an increasing value of λ . The curves for the vertical load alone starts at λ =5 and terminates at a value of 10 inclusive, while the combined case starts at λ=5 and terminating at λ =8. The vertical axis represents the ratio of the total rotation ($\theta+\theta'$) to the hinge rotation (θ_h) if the joint at (A) and (C) was assumed pinned. Curves (3) and (4) are similarly plotted. Curve (5) is plotted to illustrate the ratio of the connection to joint rotation subject to vertical load alone. A tolerance of 0.001 was used in all cases. Linear elastic (first-order) analysis has been used because the intention was to illustrate the extent of connection deformation on the joint behaviour.

The non-linear moment-rotation expression was calculated from reference (69) as,

$$\theta' = 1.539\text{x}10^{-6}(M) + 6.083\text{x}10^{-13}(M)^3 + 2.472\text{x}10^{-22}(M)^5 \qquad (6.18)$$

where the bending moment is in KNcm. units.

As the end moment increases, the total rotation tend towards a pinned condition. The number of iterations increases dramatically and tends to infinity as indicated by a flat plateau in figure (6.10).

When high rotations are predicted which exceed those of pinned ends, the sign of the bending moment changes. In order to preserve equilibrium of the stiffness equations, the acting moments become restraining moments. At this stage, the solution diverges and the analysis is terminated.

6.9 Effective lengths of end-restrained struts

The effective lengths of no-sway columns specified in traditional elastic design methods are based on the realization that full restraint cannot be achieved in practice. It will be shown that the commonly used values for effective lengths are justified but slight inaccuracies arise when a range of column lengths are examined for the same type of end connections. In the studies, the non-linear (second-order) elastic program has been used to determine the bifurcation load of the column. This is indicated by the singularity of the determinant of the overall stiffness matrix.

The effective length, or sometimes referred to as the equivalent slenderness, is defined here as that length which gives the same strength as for a pin-ended column on the actual column with end restraint. Wood(50) has described this concept by reference to the elastic critical load of columns in sway and no-sway cases given by,

$$l = \sqrt{P_e/P_c} \qquad (6.19)$$

where P_e = Euler load, $\pi^2 EI/L^2$,

P_c = elastic critical load, $\pi^2 EI/l^2$

Values of effective lengths are tabulated in the form of charts but the joints were assumed fully-rigid. In contrast, Jones et. al(67) adopted an accurate step-by-step load-displacement finite element computer technique to calculate the maximum load capacity of a column. Various destabilising effects are also included in their computer program.

The procedure adopted in this section is believed to be more efficient, less time-consuming and provide results which are sufficiently accurate for use in design. Jones assumed beams of infinite stiffness attached to the model column via semi-rigid connection, while the proposed procedure can simulate any given beam stiffness. The results of an analysis on a column length of 4.00 metres is shown in figure (6.11). A top and seat angle connection was assumed using the expressions developed by Frye and Morris. The connection characteristics have been calculated for a range of rigidity by altering values of the size parameters, where the $(M-\theta')$ relationship is given in the form,

$$\theta' = a.(C_i M) + b.(C_i M)^3 + c.(C_i M)^5 \qquad (6.20)$$

where $a = 8.46 \times 10^{-4}$,

$b = 1.01 \times 10^{-4}$,

$c = 1.24 \times 10^{-8}$,

$C(i) = t^{-0.5}\, d^{-1.5}\, f^{-1.1}\, l^{-0.7}$,

and M is given in KNcm. units.

Values of 't', 'd', 'f' and 'l' are defined in the schematic drawing of the connection shown in figure (6.11). The value of C(i) is calculated for each curve, where (i) refers to the integer shown on the curves in figure (6.11). The dimensions for 't', 'd', 'f' and 'l' are selected randomly to provide the appropriate curve and as a demonstration of the effect of end restraint only. These values ranged from 100-380mm, 60-80mm, 12-20mm and 40-60mm respectively. The values of C(i) are as follows,

$$
\begin{aligned}
C(2) &= 1.081\times10^{-4} & C(3) &= 2.453\times10^{-4} \\
C(4) &= 3.581\times10^{-4} & C(5) &= 4.199\times10^{-4} \\
C(6) &= 4.780\times10^{-4} & C(7) &= 5.508\times10^{-4} \\
C(8) &= 6.380\times10^{-4} & C(9) &= 7.367\times10^{-4} \\
C(10) &= 8.641\times10^{-4} & C(11) &= 1.028\times10^{-3} \\
C(12) &= 1.256\times10^{-3} & C(13) &= 1.819\times10^{-3} \\
C(14) &= 3.045\times10^{-3} & C(15) &= 4.003\times10^{-3} \\
C(16) &= 5.983\times10^{-3}
\end{aligned}
\qquad (6.21)
$$

In determining the effective length, the column is assumed to have an initial bow of L/1000 at mid-height in accordance with Design Recommendations(54,55). Axial deformation of all the members are suppressed, as are usual in critical load analysis of columns. The vertical axial load is applied in terms of a commom load multiplier of the Euler load. Therefore, the effective length is determined by,

$$l = \sqrt{1/\lambda_c} \qquad (6.22)$$

In all subsequent analysis, Young's modulus of elasticity was taken

as 210 KN/mm^2 unless indicated and both column and beam members have the same section.

Curves indicated by (1) and (17) represent fully-rigid and pinned end conditions with an effective length of 0.7 and 1.0 respectively. In this simple demonstration, a decrease of end restraint stiffness produces a corresponding increase in column deformation and effective length. It is therefore to be expected that curve (16) gives a value approaching pin-ended conditions. It is emphasised that these values are applicable only to the type of connections used in this exercise.

The effects of different column lengths for a given type of connection have also been examined. Realistic values of 3.0, 4.0 and 5.0 metre columns are subject to the same assumptions and loading criteria mentioned earlier. A 'flexible' header-plate connection, commonly assumed pinned in practice, has been adopted and the results are shown in figure (6.12). A stiffer end-plate connection with column stiffeners is shown in figure (6.13).

Connection characteristics are also given for each of the curves in both figures. It was decided to replace the initial bow of L/1000 by a small disturbing force at mid-height. The reason for adopting such a model is to reduce the number of iterations required to converge. The initial bow of L/1000 was used in the previous example because the connection there was stiffer than either of the two shown in figures (6.12) and (6.13). Due to the comparatively 'flexible' connections large end moments are developed as the compressive axial load is increased. This give

rise to large connection rotations causing the direction of the rotations to change in order to preserve equilibrium. This is illustrated by curve (2) or (3) in figure (6.14).

Figures (6.12) and (6.13) justify the commonly assumed effective lengths for such connections in braced frameworks. However, the values shown suggest the possibility of economy in column design if semi-rigid end restraint is properly taken into account. It is interesting to note that as the column lengths increase, the effective length decreases for any given end restraint. The reason is due to the significant effect of connection deformation being utilised on slender columns in bending. This causes a slight increase in the critical load for such columns.

6.10 Conclusion

A procedure has been presented for incorporating semi-rigid connections into the matrix stiffness method of analysis. A simple technique is proposed by which the load vector is revised iteratively to allow for deformation of the connections. This was shown to provide a convenient and rapid solution, with each iteration taking no longer than an ordinary fully-rigid analysis.

Economy of storage of over 25% has been illustrated for a simple portal by excluding the connection details from the overall stiffness matrix. Substantial savings in total storage of larger frames can be anticipated. The proposal has been programmed to account for any combination of fixed, semi-rigid and pinned

connections. The reduction in member stiffness due to compressive axial forces is also taken into account. This requires an iterative analysis in the same manner as for the connection behaviour. Therefore, no significant computing time is lost in comparison with a fully-rigid non-linear (second-order) analysis. The member forces converge rapidly and the structure satisfies equilibrium, compatibility and connection characteristic behaviour.

Examples on unbraced multi-storey frames have shown that connection deformation contributes substantially to the overall sway displacements in comparison to fully-rigid assumptions. Internal redistribution of member forces is significant with the possibility of overstressing some sections. This may lead directly to the early onset of plasticity at a load factor much lower than that predicted by an analysis assuming rigid joints. This could result in a significant decrease in the ultimate load carrying capacity of the structure.

For the examples studied, it was found that provision of nominal cladding stiffness was sufficient to offset the additional sway resulting from deformation of connections. However, each structure will be unique in the value of cladding stiffness required. It was found that a uniform provision of such cladding at all levels give satisfactory results. Further, the program enables simulation to be made of construction phases. Another benefit of the proposed method is that poor connections are automatically recognised by the analysis not converging due to excessive deformation.

The influence of semi-rigid end restraint on the effective length of no-sway columns suggests possible economy in column design. It has been shown that for several types of connections, the traditional specifications of effective lengths are justified. However, the detailed results apply only to the limited cases examined above. Such results indicate the usefulness of studying the behaviour of each type of commonly-used connection. The tendency for effective lengths to decrease with increasing slenderness has been confirmed. This implies a corresponding increase in the elastic critical load as a result of the semi-rigid connection being fully utilised in flexure.

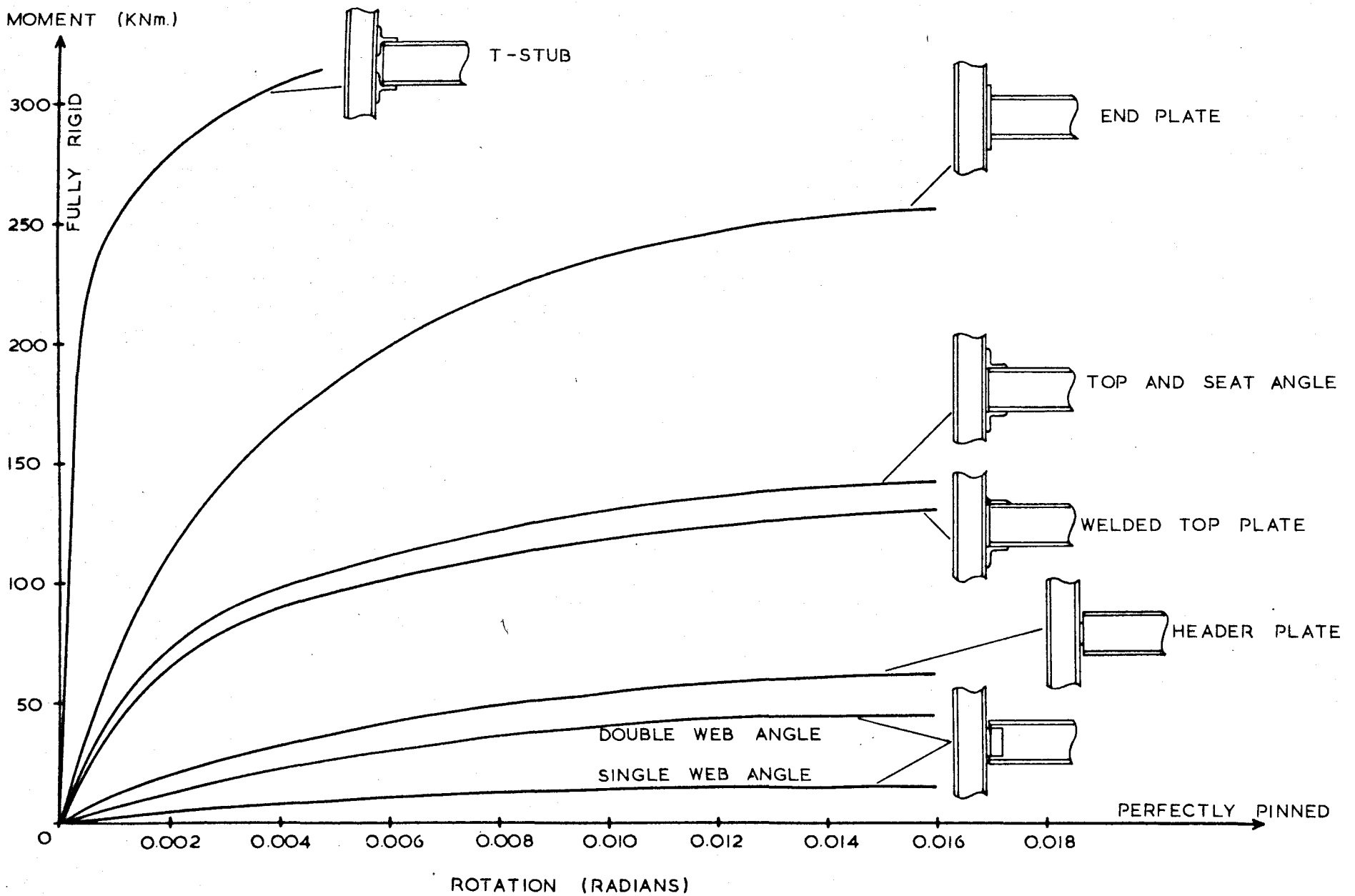

FIG. 6.1 MOMENT - ROTATION CHARACTERISTICS OF SOME COMMON BOLTED CONNECTION

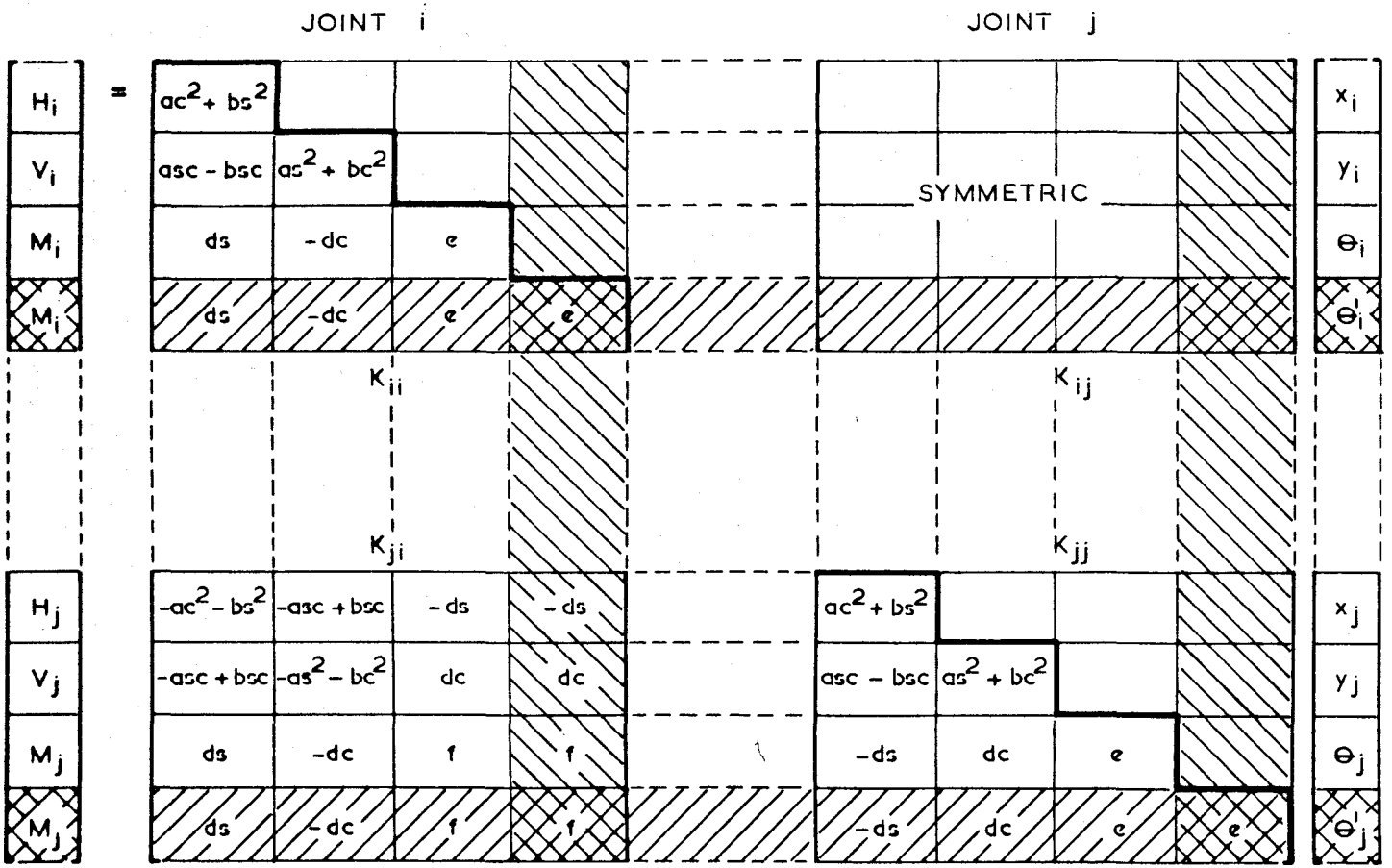

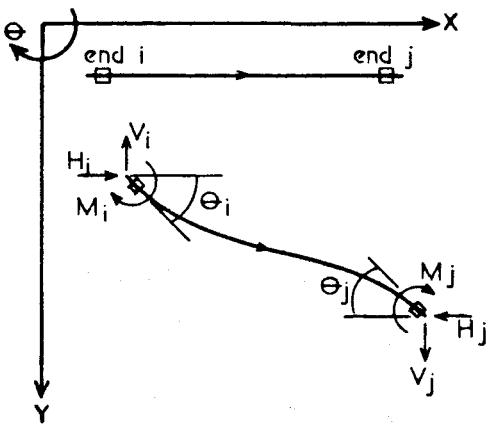

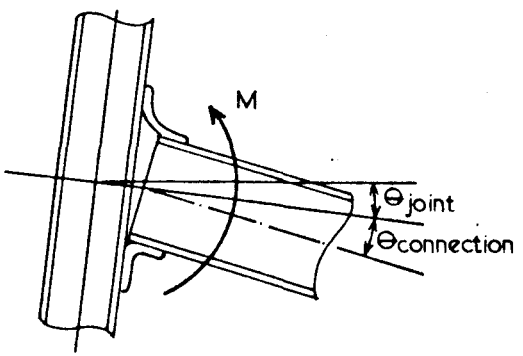

FIG. 6.2 CONTRIBUTION OF SEMI-RIGID JOINTED MEMBER i-j IN THE OVERALL STIFFNESS MATRIX

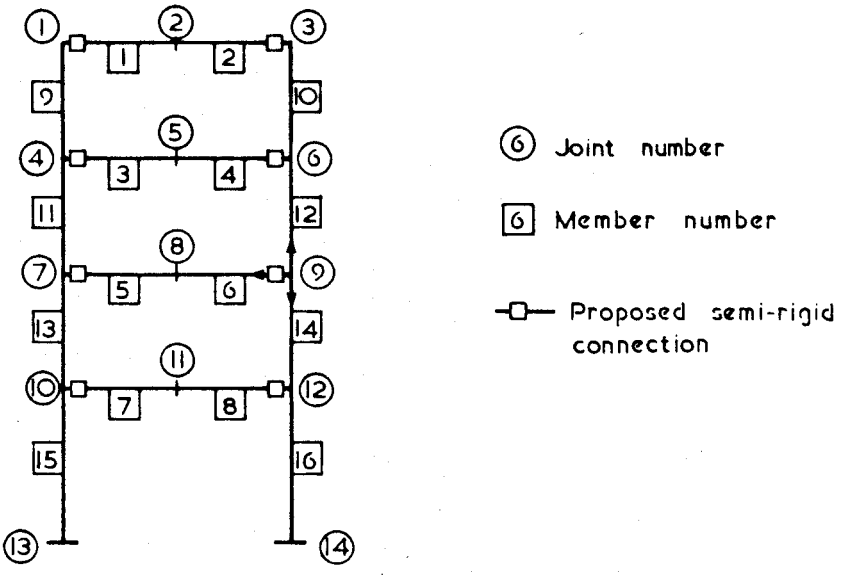

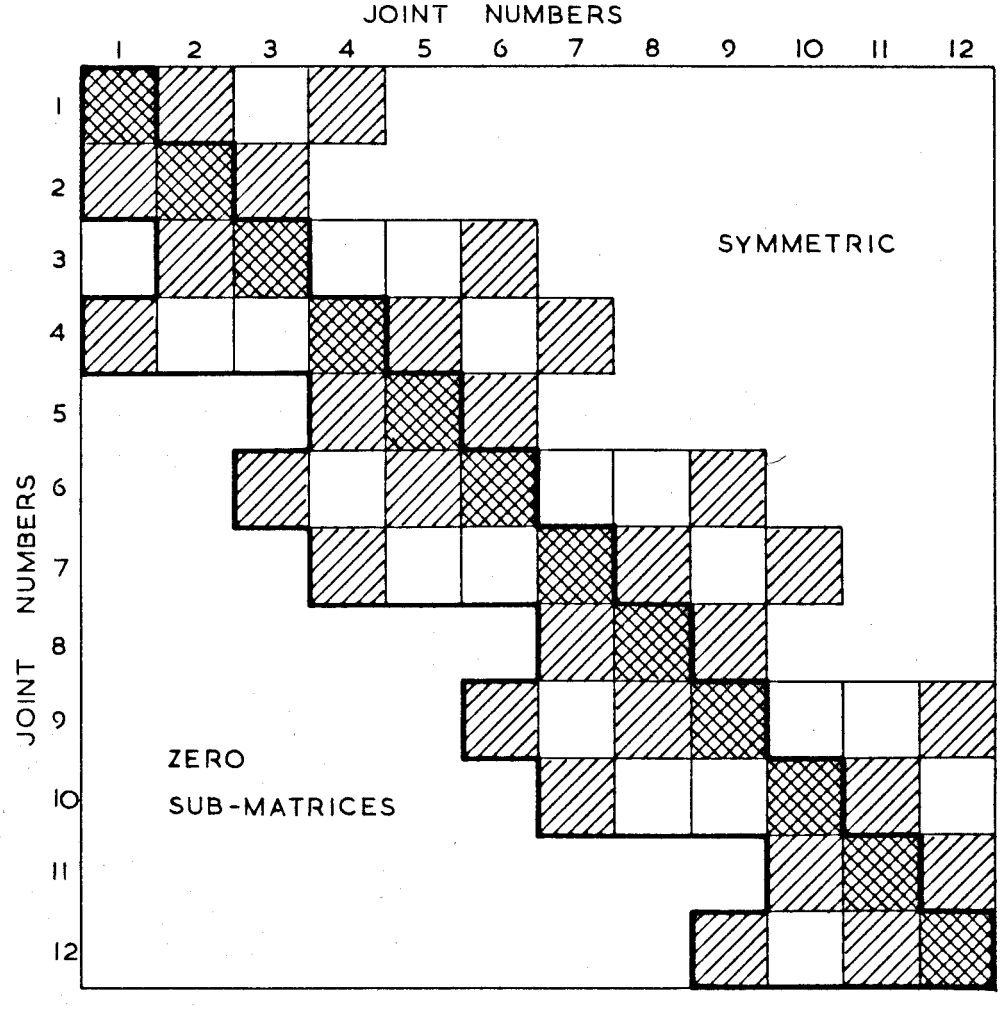

FIG. 6.3 OVERALL STIFFNESS MATRIX OF RIGID JOINTED PLANE FRAME

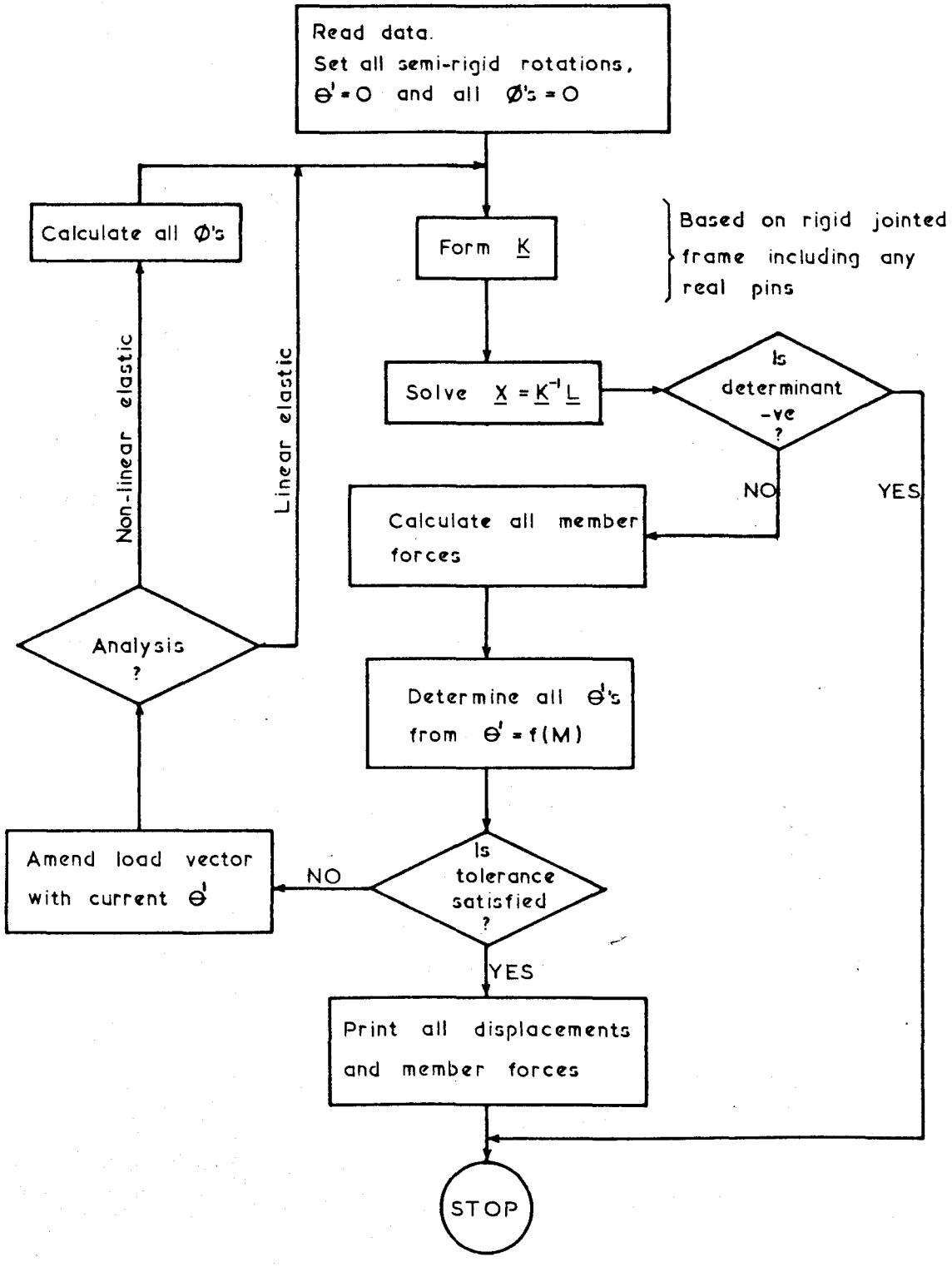

FIG. 6.4 FLOW DIAGRAM FOR THE ANALYSIS OF SEMI-RIGIDLY CONNECTED PLANE FRAMES

$\underline{L} = \underline{K}\,\underline{X}$

H_i =	$a_1 + b_2$			0							0			x_i
V_i	0	$b_1 + a_2$		$-d_1$							0			y_i
M_i	d_2	$-d_1$	$e_1 + e_2$	e_1							0			θ_i
M'_i	0	$-d_1$	e_1	e_1	0	d_1	f_1	0	0	0	0	0	0	θ'_i
H_j	$-a_1$	0	0	0	$2a_1$						0			x_j
V_j	0	$-b_1$	d_1	d_1	0	$2b_1$					$-d_1$			y_j
M_j	0	$-d_1$	f_1	f_1	0	0	$2e_1$				f_1			θ_j
H_k				0	$-a_1$	0	0	$a_1+b_3+a_4$			0			x_k
V_k				0	0	$-b_1$	d_1	0	$b_1+a_3+b_4$		d_1			y_k
M_k				0	0	$-d_1$	f_1	d_3	$d_1 - d_4$	$e_1+e_3+e_4$	e_1			θ_k
M'_k	0	0	0	0	0	$-d_1$	f_1	0	d_1	e_1	e_1	0	0	θ'_k
Mh_k				0				0	$-d_4$	e_4	0	e_4		θh_k
Mh_l				0				0	$-d_4$	f_4	0	f_4	e_4	θh_l

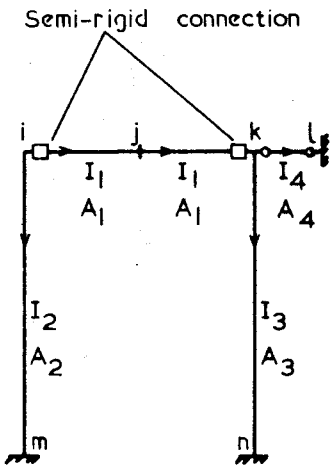

E = Constant

FIG. 6.5 OVERALL STIFFNESS MATRIX OF SIMPLE PORTAL

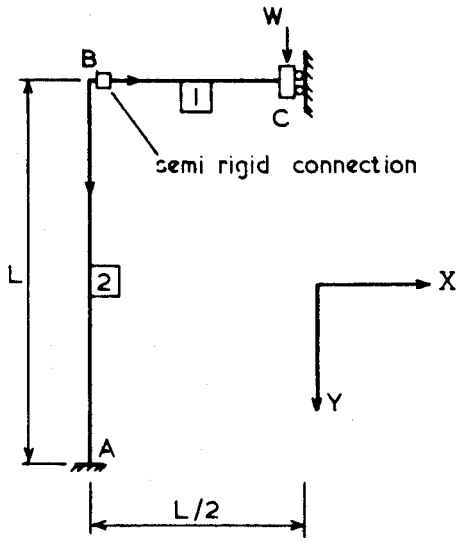

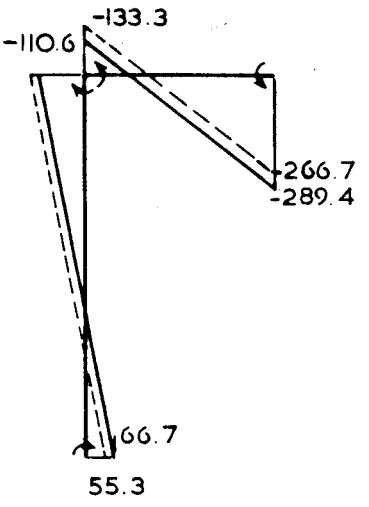

BENDING MOMENT (KNm.)

$E = 200\ KN/mm^2$

$A = 6000\ mm^2$

$I = 15000 \times 10^4\ mm^4$

$L = 4000\ mm$

$W = 200\ KN$

– – – – – rigid

——— semi-rigid

Negative bending moment at B for member B-C. Connection rotation is therefore positive.

Note: axial deformation of all members are neglected

Iteration	θ'_B ($\times 10^{-3}$)	y_c (mm)	θ_B ($\times 10^{-3}$)	M_{BC} (KNm)
1	0	8.889	4.444	-133.3
2	2.746	10.720	3.529	-105.9
3	2.181	10.343	3.717	-111.5
4	2.297	10.420	3.679	-110.4
5	2.273	10.404	3.687	-110.6
6	2.278	10.404	3.687	-110.6

FIG. 6.6 NUMERICAL EXAMPLE

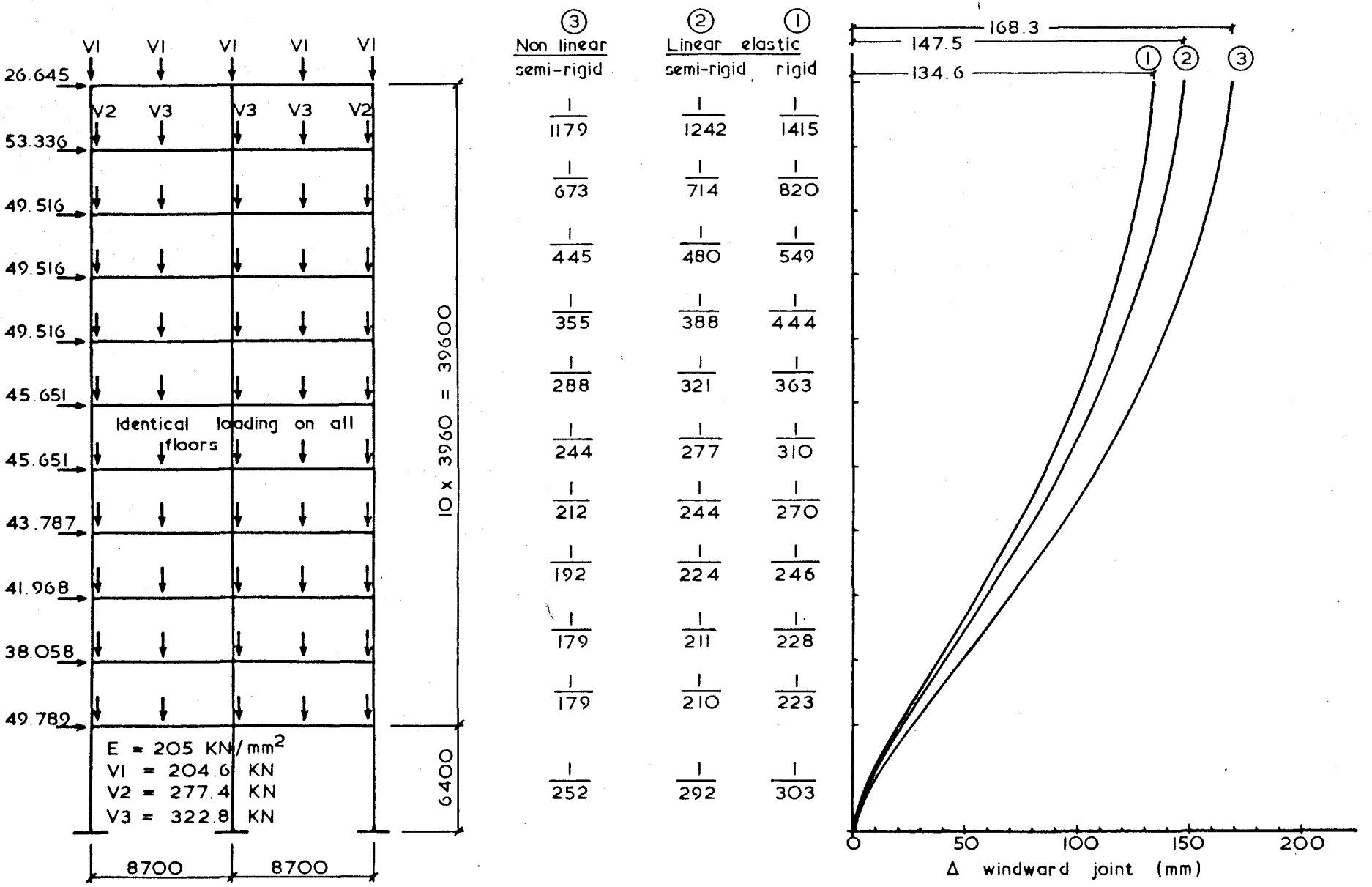

FIG. 6.7 SEMI-RIGID JOINTS IN UNBRACED FRAME

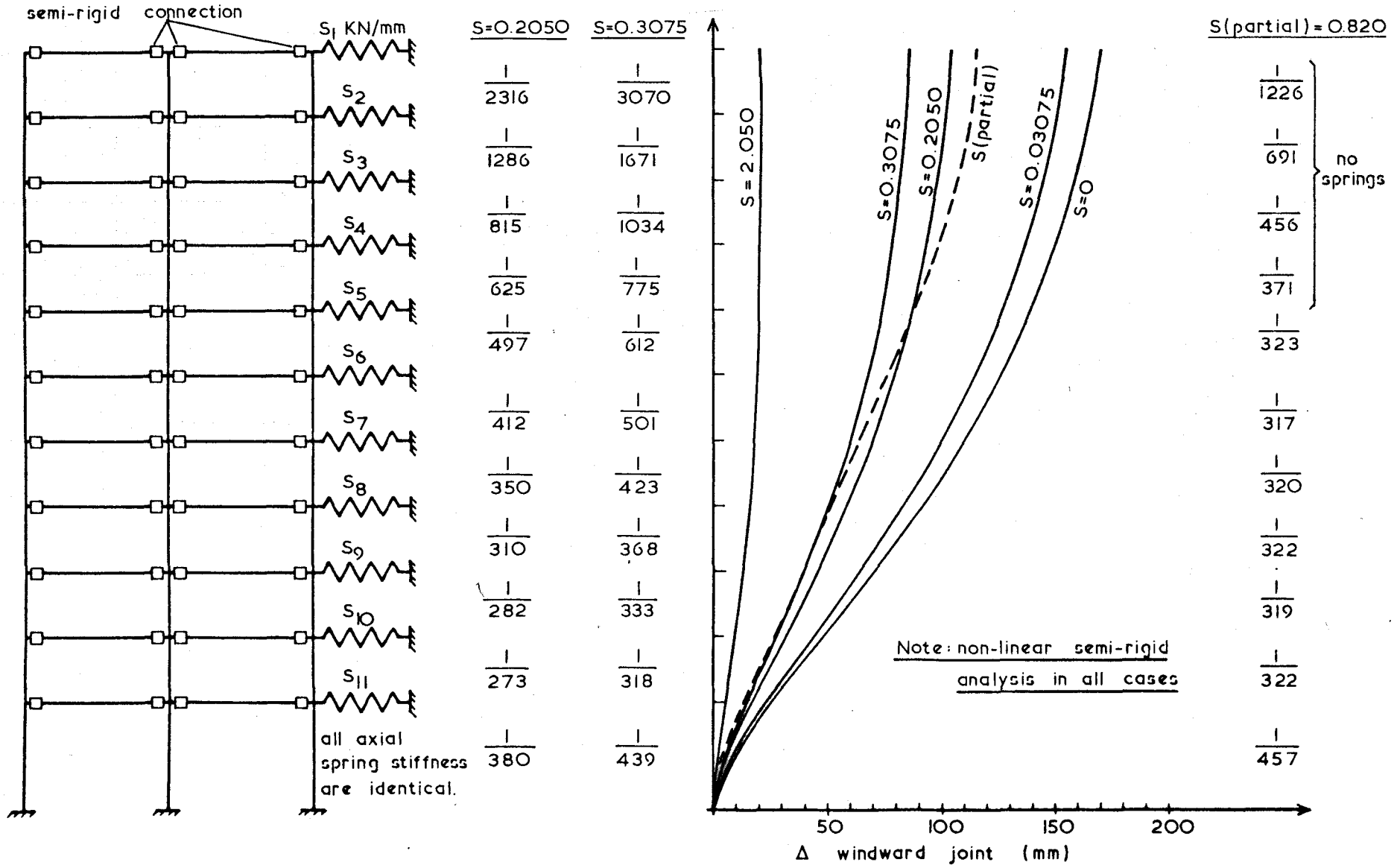

FIG. 6.8 EFFECTS OF CLADDING ON SWAY DEFLECTION

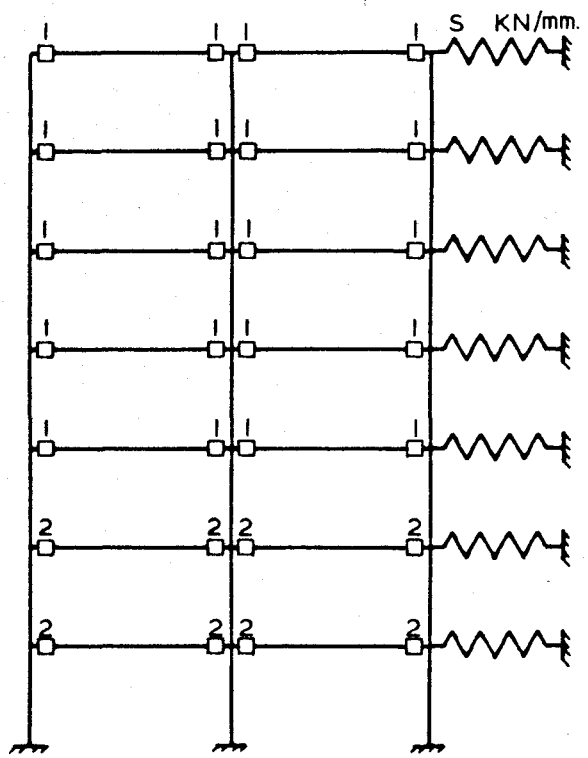

	③ Non-linear elastic S = 0.0742	③ semi-rigid	② Linear elastic semi-rigid	① rigid
	1/1752	1/928	1/992	1/1165
	1/761	1/460	1/510	1/611
	1/488	1/320	1/367	1/454
	1/335	1/229	1/272	1/337
	1/321	1/230	1/273	1/345
	1/302	1/224	1/266	1/326
	1/435	1/333	1/385	1/440
Overall sway	1/447	1/310	1/360	1/440

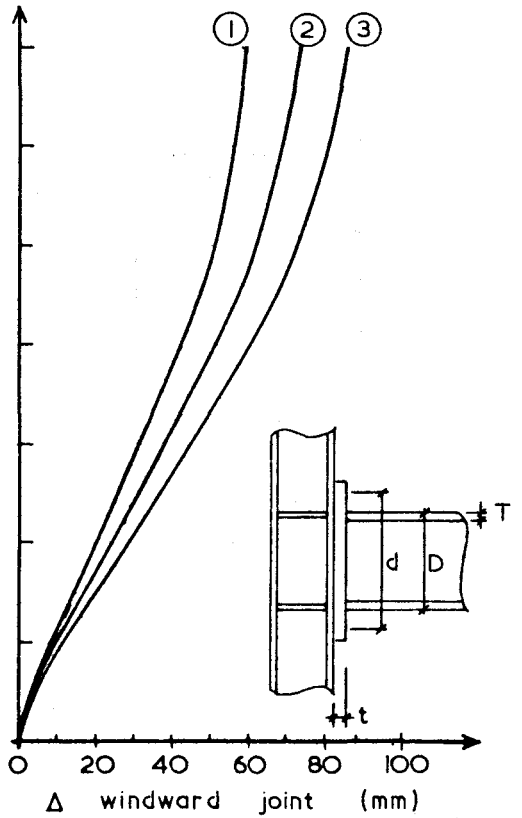

CONNECTION	MOMENT - ROTATION CHARACTERISTIC
1	$1.149 \times 10^{-7} (M) + 4.655 \times 10^{-17} (M)^3 + 2.223 \times 10^{-25} (M)^5$
2	$9.194 \times 10^{-8} (M) + 2.385 \times 10^{-17} (M)^3 + 7.292 \times 10^{-26} (M)^5$

(M) in KNcm.

FIG. 6.9 SEMI-RIGID JOINTED 7 STOREY FRAME

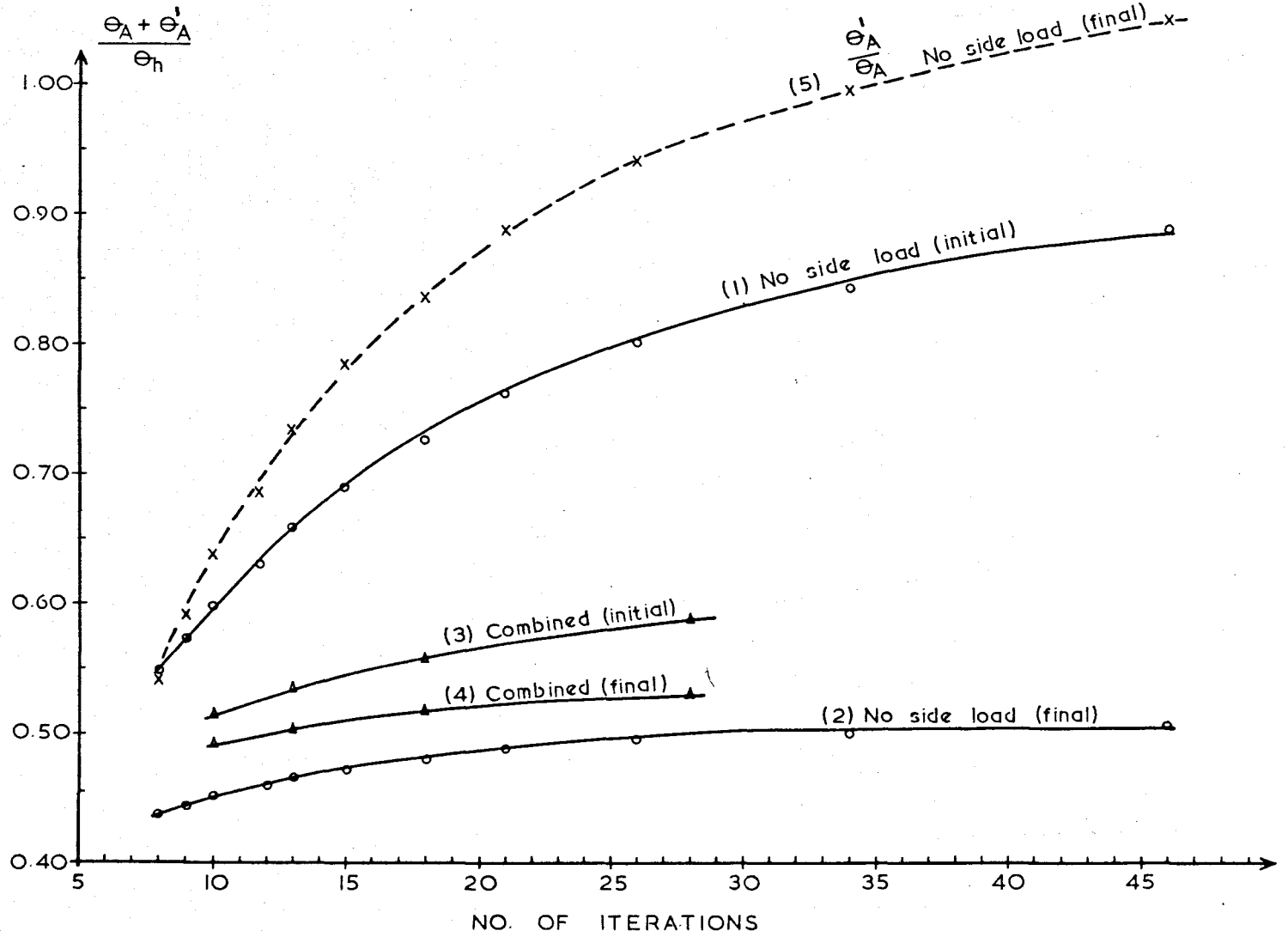

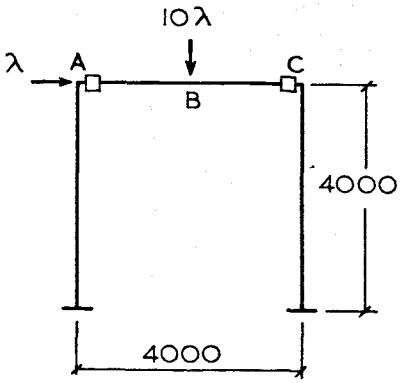

$E = 200 \ KN/mm^2$

$A = 100 \ mm^2$

$I = 10 \times 10^6 \ mm^4$

Note: linear elastic analysis in all cases

FIG. 6.10 CONVERGENCE OF CONNECTION DEFORMATION

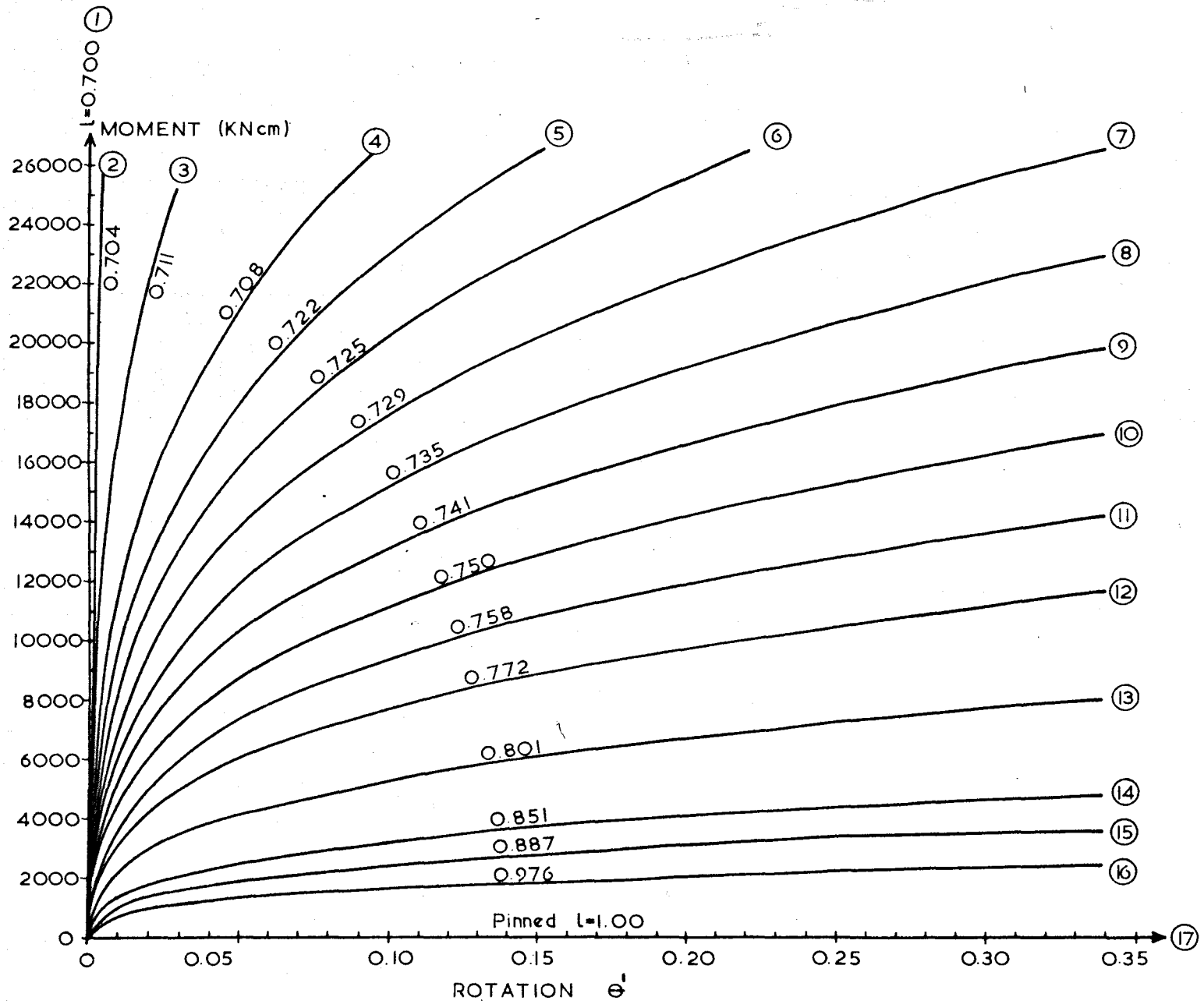

FIG. 6.11 EFFECTIVE LENGTHS (TOP AND SEAT ANGLE END RESTRAINT)

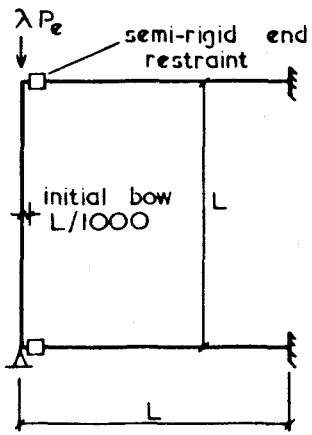

$E = 21000\ KN/cm^2$

$I = 926.4\ cm^4$

$L = 400\ cm$

$l = \sqrt{\frac{I}{\lambda_c}}$

P_e = Euler load

$= \pi^2 E I / L^2$

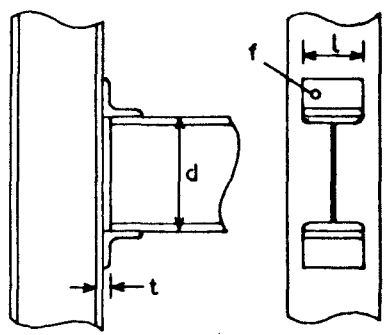

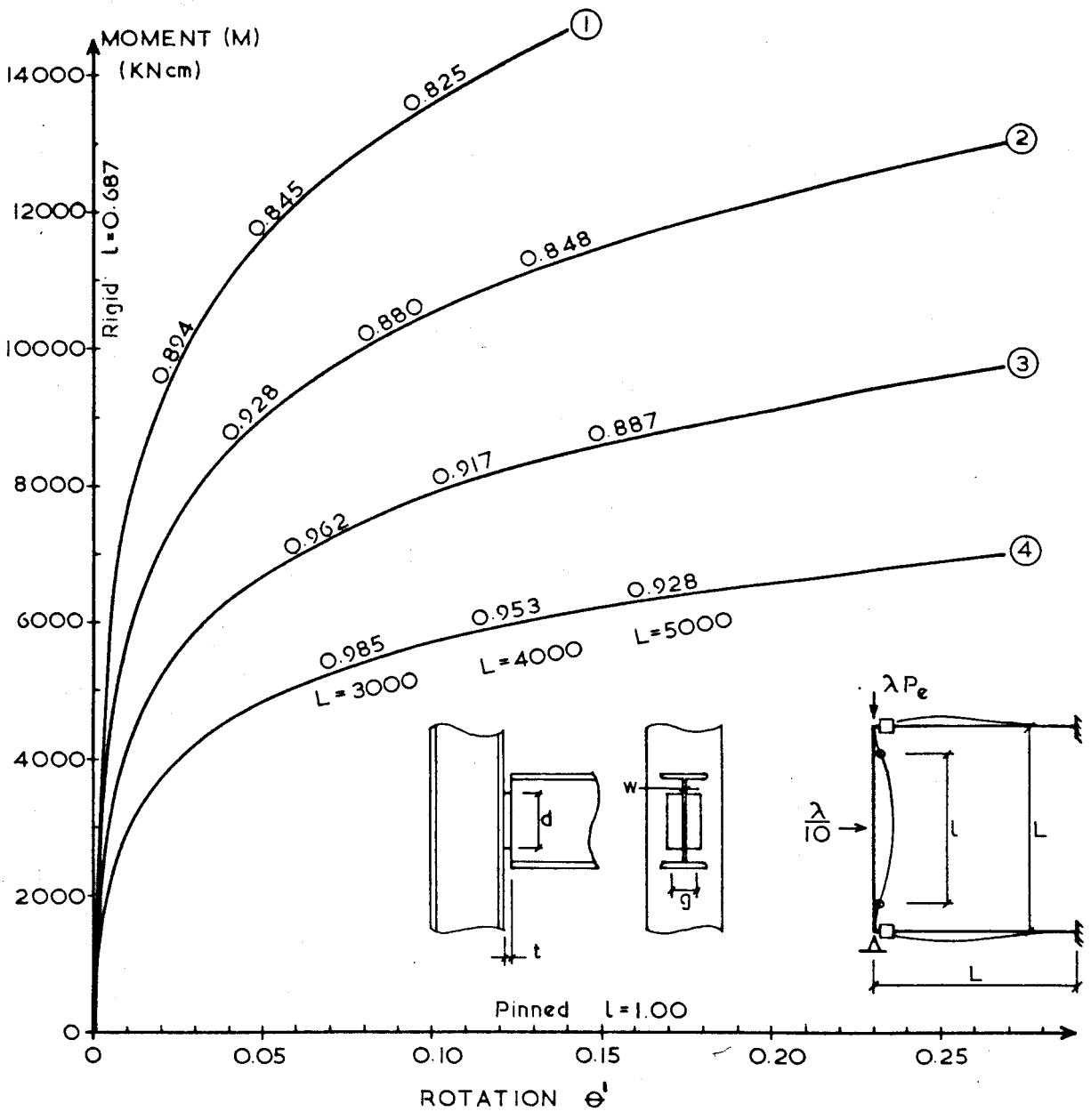

$I = 14307\ cm^4$

CURVE	CONNECTION CHARACTERISTIC
1	$\theta'_1 = 7.654 \times 10^{-7} (M) + 2.096 \times 10^{-15} (M)^3 + 1.827 \times 10^{-22} (M)^5$
2	$\theta'_2 = 9.892 \times 10^{-7} (M) + 4.524 \times 10^{-15} (M)^3 + 6.589 \times 10^{-22} (M)^5$
3	$\theta'_3 = 1.320 \times 10^{-6} (M) + 1.076 \times 10^{-14} (M)^3 + 2.791 \times 10^{-21} (M)^5$
4	$\theta'_4 = 1.837 \times 10^{-6} (M) + 2.898 \times 10^{-14} (M)^3 + 1.455 \times 10^{-20} (M)^5$

FIG. 6.12 EFFECTIVE LENGTHS (HEADER PLATE END RESTRAINT)

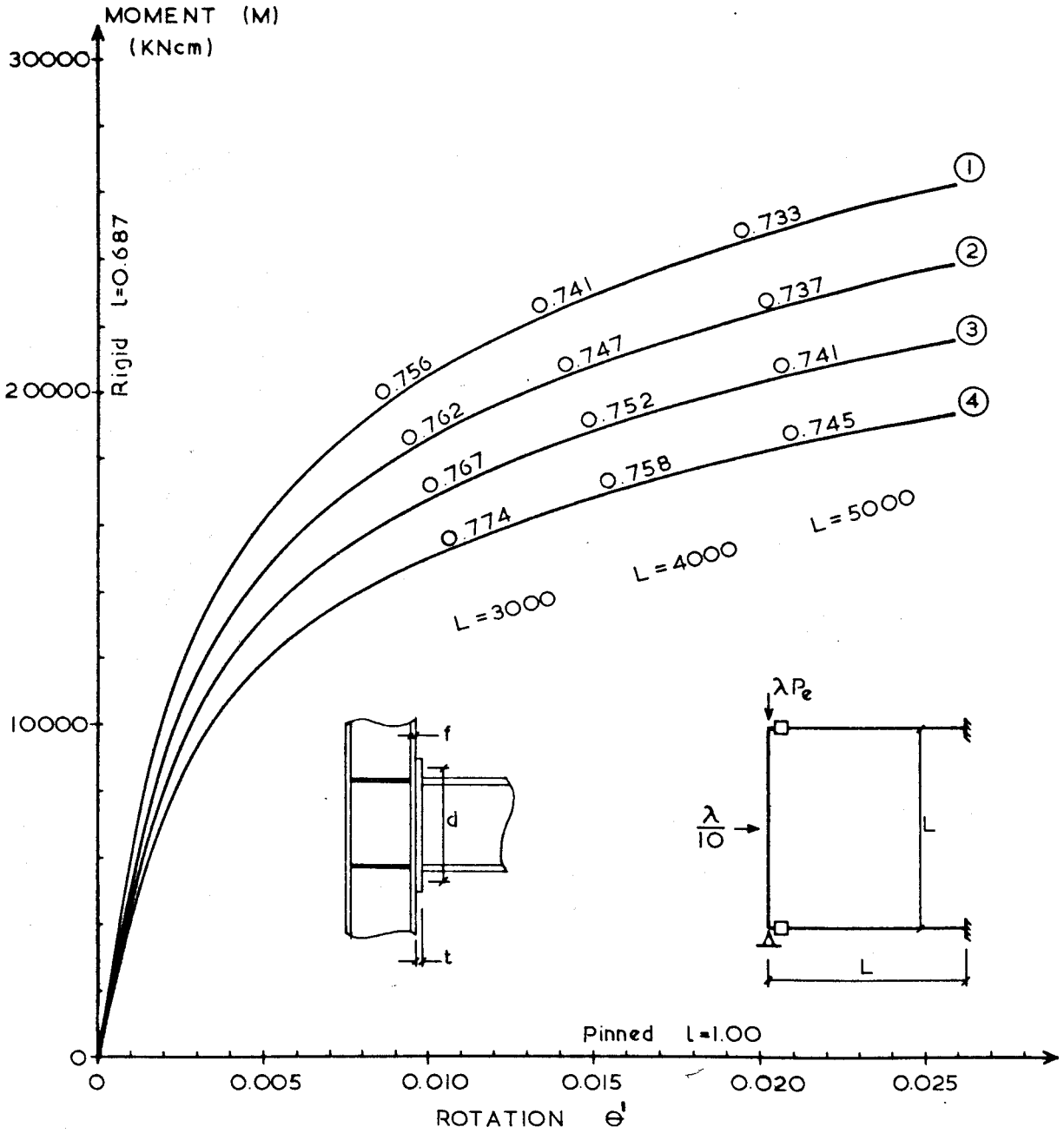

I = 14307 cm^4

CURVE	CONNECTION CHARACTERISTIC
1	$\theta'_1 = 1.679 \times 10^{-7} (M) + 1.452 \times 10^{-16} (M)^3 + 1.480 \times 10^{-24} (M)^5$
2	$\theta'_2 = 1.850 \times 10^{-7} (M) + 1.943 \times 10^{-16} (M)^3 + 2.405 \times 10^{-24} (M)^5$
3	$\theta'_3 = 2.013 \times 10^{-7} (M) + 2.632 \times 10^{-16} (M)^3 + 3.990 \times 10^{-24} (M)^5$
4	$\theta'_4 = 2.275 \times 10^{-7} (M) + 3.615 \times 10^{-16} (M)^3 + 6.770 \times 10^{-24} (M)^5$

FIG. 6.13 EFFECTIVE LENGTHS (END PLATE WITH COLUMN STIFFENERS)

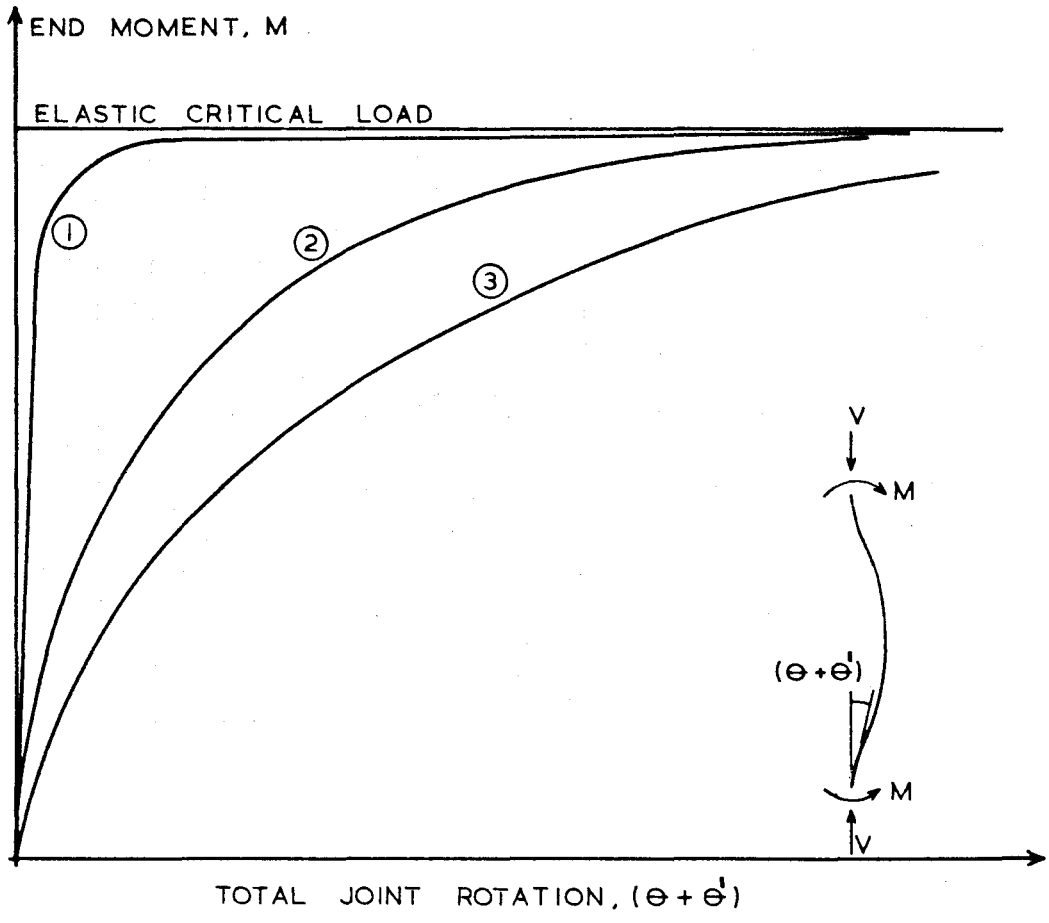

FIG. 6.14 END MOMENT – TOTAL ROTATION BEHAVIOUR

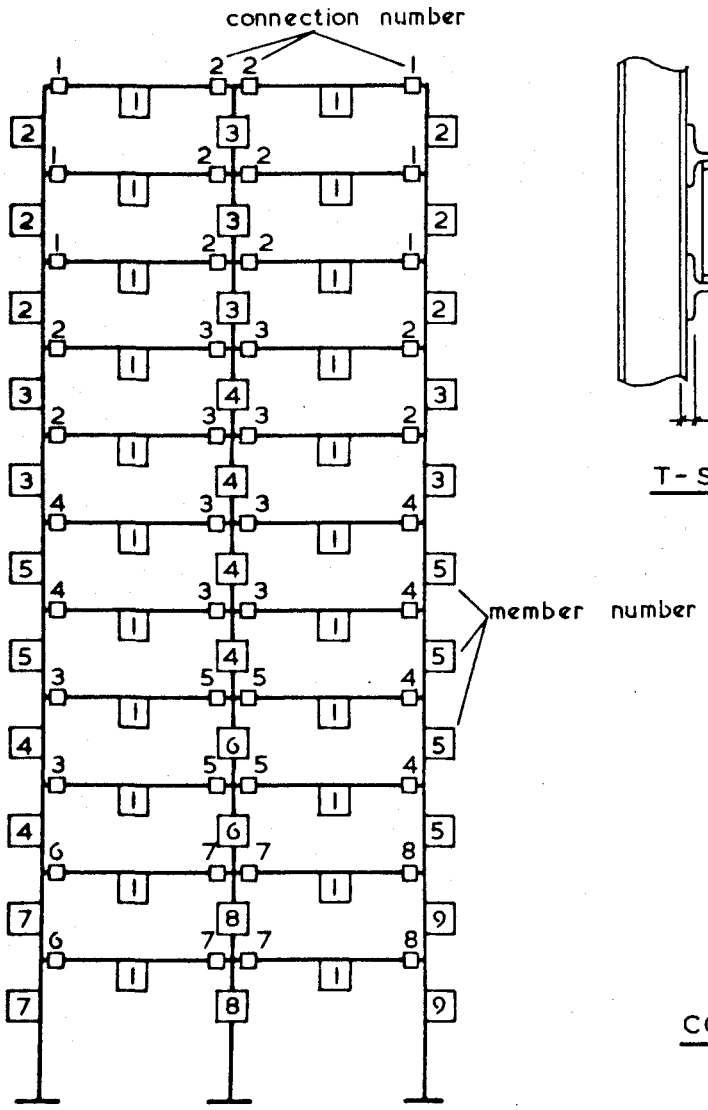

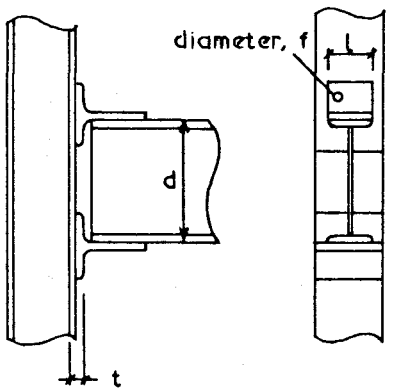

T-STUB CONNECTION

SECTION NO.	AREA cm^2	INERTIA cm^4
1	157.0	76100.0
2	228.0	57500.0
3	335.0	89400.0
4	487.0	141000.0
5	399.0	110000.0
6	590.0	180000.0
7	649.0	205000.0
8	755.0	250000.0
9	537.0	160000.0

TABLE 6.1 MEMBER LIST

TABLE 6.2

CONNECTION LIST

CONNECTION NO.	d cm.	t cm.	f cm.	l cm.
1	54.40	4.78	1.6	21.2
2	54.40	6.66	1.6	21.2
3	54.40	9.60	1.6	21.2
4	54.40	7.92	2.0	21.2
5	54.40	11.48	2.0	21.2
6	54.40	12.54	2.4	21.2
7	54.40	14.46	2.4	21.2
8	54.40	10.52	2.4	21.2

CHAPTER 7

CONCLUSIONS AND SUGGESTIONS FOR FURTHER WORK

The thesis has examined the behaviour and some design problems of rigid-jointed multi-storey unbraced steel frames. The results of the parametric study presented in Chapter (2) enable the designer to predict the likely governing criterion (serviceability limit on sway or ultimate load) for the design of these frames subjected to combined loading. The studies have shown that the original Merchant-Rankine formula is conservative for estimating the failure load and that the modified version due to Wood(50), which is strictly applicable to clad structures, can overestimate the failure load. The studies, however, were based on bare frameworks and ignores the beneficial effects of strain-hardening and stray composite action. A semi-empirical expression has been presented in Chapter (3). Significantly better estimates of the failure load has been achieved in comparison with both forms of the Merchant-Rankine approach. The frames that were examined had equal storey height and equal bay width. However, most building structures have a ground floor which is taller than the storeys above. Furthermore, structures with irregular configurations, particularly with inclined members, and uneven floor loading patterns have not been considered in the design studies. Although limited cases of irregular-bay frames have been examined, further studies should be conducted on frames with the above characteristics. Design guidance charts, similar to those presented in Chapter (2), could be drawn

to include the variable of the average ratio of bay width to storey height. The application of the Merchant-Rankine formula to such frames could then be validated and the accuracy of the improved relationship developed in Chapter (3) examined for irregular frames.

The expression developed in Chapter (3) was based on the study of bare frames. It was suggested that the formulae could be used for frames subjected to vertical load alone by altering the value of the coefficient. It could also be extended to provide an estimate of the failure load of clad frames with certain values of cladding stiffness. This could then be compared with the Merchant-Rankine-Wood approach which is strictly applicable to clad frames.

The optimization procedure described in Chapter (4) is suitable only to regular and rectangular frameworks. Irregular frames with inclined members require sophisticated routines and the use of an accurate elasto-plastic computer program is the only solution to such a problem. However, several improvements can be made to the proposed approximate optimization procedure. In the proposed method, only those sections with the most economical full plastic modulus (or inertia) to weight ratio are included in the list of preferred sections. If it is required to restrict the depth of a member, it may be necessary to select a section that is not one of the 'economical' sections. Furthermore, certain sections that are unsuitable for plastic action may be more 'economical' than the one selected and could be used provided they are not stressed beyond the elastic limit. In addition, use of Universal

beam sections as column members may lead to more 'economical' designs. A routine could be added so that the selection procedure is based on the most 'efficient' section in all cases. A more sophisticated assessment of cost could also be included.

The manual method presented in Chapter (5) is able to estimate accurately the failure load of single storey and multi-storey frames. It was shown in Part (1) that significant overall stability problems can arise for single storey frames subjected to high concentrated loads at or near the eaves level. Part (2) examines multi-storey frames and examples have been shown. The calculations were performed manually but tends to be lengthy. In order to avoid iteration, charts could be produced for use with the method proposed in Chapter (5). This would enable the failure load to be determined swiftly for single storey or multi-storey frames. As suggested above, it would be worthwhile to examine cases with irregular bay width and storey height. Furthermore, a separate study of the top and bottom two storeys would enable more accurate assessment be made to overcome the error in column moments. An investigation should be carried out on the applicability of the method for single storey low-pitch portals. For low pitched frames, it may be possible to treat them as flat-roofed frames. Furthermore, an investigation into fixed base single storey frames should be made. Finally, a computer program suitable for use on micro-computers should be developed, particularly for multi-storey frames.

Finally, a computer program has been proposed which is capable of analysing any combination of pinned, semi-rigid and

rigidly-connected plane frames. This program enables the determination of effective lengths of braced columns with any degree of end restraints. It is possible to extend the technique described in Chapter (6) to determine the ultimate load-carrying capacity of semi-rigidly connected plane steel frames. The program could be used to investigate the behaviour of frames designed to the 'simple' methods of BS449 and BS5950. By including semi-rigid joint behaviour, a better assessment could be made of the real behaviour of such frames, both at the serviceability and ultimate limit states. A more extensive study of effective lengths with semi-rigid joints would enable more detailed recommendations to be made concerning these values, to replace the very crude values given in present day design codes.

REFERENCES

1. Cross, H. 'Analysis of continuous frames by distribution fixed ended moments', Transaction, ASCE, Vol.96, 1932.

2. BS449: Part 2: 1969 'Specification for the use of structural steel in buildings'. BSI. London.

3. Allwood, B.O. et. al., 'Steel Designers Manual', Crossby-Lockwood-Staples, London, 1978.

4. Steel Structures Research Committee. Final Report. HMSO, 1936.

5. Steel Structures Research Committee. Recommendation for design. British Standards Institution, 1959.

6. Majid, K.I. and Elliott, D. 'Optimum design of frames with deflection constraints by non-linear programming', The Structural Engineer, Vol.49, April 1971.

7. Livesley, R.K. 'The application of an electronic digital computer to some problems of structural analysis', The Structural Engineer, Vol. 34, Jan. 1956.

8. Livesley, R.K. 'The automatic design of structural frames', Quart. Jour. mech. and Applied Maths., Vol.9, Pt. 3, 1956.

9. Moses, F. 'Optimum structural design using linear programming', Jour. Struct. Div., ASCE, Vol.93, ST6, Dec. 1964.

10. Jennings, A. 'A compact storage scheme for the solution of symmetric linear simultaneous equations', The Computer Journal, Vol. 9, No. 3, Nov. 1966.

11. Baker, J.F. and Heyman, J. 'Plastic design of frames', Fundamentals, Camb. Univ Press, 1980.

12. Baker, J.F., Heyman, J. and Horne, M.R. 'The Steel Skeleton', Vol. 2, Camb. Univ. Press, 1956.

13. Iffland, J.S.B. and Birnstiel, C. 'Stability design procedures for building frameworks', Chicago, AISC, 1982.

14. A.I.S.C. Code, 'Manual of steel construction', American Institute of Steel Construction, 1963.

15. Neal, B.G. and Symmonds, P.S. 'The rapid calculation of the plastic collapse load for a framed structure', Proc. I.C.E., Vol. 1, April 1952.

16. Horne, M.R. 'A moment distribution method for the analysis and design of structures by the plastic theory', Proc. I.C.E., Vol. 3, Sept. 1954.

17. Horne, M.R. and Morris, L.J. 'Plastic design of low-rise frames', Constrado Monograph, Granada, 1981.

18. Horne, M.R. 'Plastic design of a four storey steel frame', The Engineer, Aug. 1958.

19. Horne, M.R. 'Plastic design of columns', BCSA No. 23, 1964.

20. Horne, M.R. and Morris, L.J. 'Optimum design of multi-storey rigid frames', Optimum Structural Design - Theory and Applications, ed. Gallagher, R.H. and Zienkiewiez, O.C., Wiley, 1973.

21. Ridha, R.A. and Wright, R.N. 'Minimum cost design of frames', Jour. Struct. Div., ASCE, Vol. 93, ST4, Aug., 1967.

22. Neal, B.G. 'The plastic methods of structural analysis', Chapman and Hall, London, 1977.

23. Majid, K.I. 'Non-linear structures', Butterworth, London, 1972.

24. Anderson, D. 'Investigation into the design of plane structural frames', PhD Thesis, Manchester Univ., 1969.

25. Horne, M.R. 'Elastic-plastic failure loads of plane frames', Proc. Roy. Soc., A, Vol. 274, Aug. 1963.

26. Wood, R.H. 'The stability of tall buildings', Proc. I.C.E., Vol. 11, Sept. 1958.

27. Heyman, J. 'An approach to the design of tall buildings', Proc. I.C.E., Vol. 17, Dec. 1960.

28. Stevens, L.K. 'Control of stability by limitation of deformation', Proc. I.C.E., Vol. 28, July 1964.

29. Heyman, J. 'On the estimation of deflexions in elastic plastic framed structures', Proc. I.C.E., Vol. 19, May 1961.

30. Stevens, L.K. 'Elastic stability of practical multi-storey frames', Proc. I.C.E., Vol. 36, Jan. 1967.

31. Holmes, M. and Gandhi, S.N. 'Ultimate load design of tall steel building frames allowing for instability', Proc. I.C.E., Vol. 30, Jan. 1965.

32. Holmes, M. and Sinclair-Jones, H.W. 'Plastic design of multi-storey sway frames', Proc. I.C.E., Vol. 47, Sept. 1970.

33. Lehigh University Summer Conference. 'Plastic design of multi-story frames', Lehigh University, Aug. 1965.

34. Batten, D.F. 'Design studies of medium rise steel buildings', Proc. I.C.E., Vol. 65, Sept. 1978.

35. The Institution of Structural Engineers and The Welding Institute, 'Joint committee's second report on fully-rigid multi-storey welded steel frames', May 1971.

36. Jennings, A. and Majid, K.I. 'An elastic-plastic analysis for framed structures loaded up to collapse', The Structural Engineer, Vol. 43, Dec. 1965.

37. Parikh, B.P. 'Elastic-plastic analysis and design of unbraced multi-story steel frames', Lehigh University, May 1966.

38. Horne, M.R. and Majid, K.I. 'The automatic ultimate load design of rigid-jointed multi-storey sway frames allowing for instability', Conference held at the University of Newcastle, June 1966.

39. Davies, J.M. 'The response of plane frameworks to statical and variable repeated loads in the elastic-plastic range', The Structural Engineer, Vol. 44, Aug. 1966.

40. Davies, J.M. 'Frame intability and strain hardening in plastic theory', Jour. Struct. Div., ASCE, ST3, June 1966.

41. Majid, K.I. and Anderson, A. 'The computer analysis of large multi-storey framed structures', The Structural Engineer, No. 11, Vol. 46, Nov. 1968.

42. Majid, K.I. and Anderson, A. 'Elastic-plastic design of sway frames by computer', Proc. I.C.E., Vol. 41, Dec. 1968.

43. Driscoll Jr., G.C., Armacost, J.O. and Hansell, W.C. 'Plastic design of multistory frames by computer', Jour. Struct. Div., ASCE, ST1, Jan. 1970.

44. Merchant, W. 'The failure load of rigid jointed frameworks as influenced by stability', The Structural Engineer, Vol. 32, July 1954.

45. Salem, A.H. 'Structural frameworks', PhD Thesis, Univ. of Manchester, May 1958.

46. Adam, V. 'Traglastberechnung beliebiger ebener unausgesteifter Rahmentragwerke aus Stahl (The calculation of the bearing capacity of plane unbraced frames)', Dissertation, Technische Hochschule, Darmstadt, 1979.

47. Majid K.I. ' The evaluation of the failure loads of plane frames', Proc. Roy. Soc., A, Vol. 306, Sept. 1968.

48. Low, M.W. 'Some model tests on multi-storey rigid steel frames', Proc. I.C.E., Vol. 13, July 1959.

49. Ariaratnam, S.T. 'The collapse load of elastic plastic structures', PhD Thesis, Univ. of Cambridge, Oct. 1959.

50. Wood, R.H. 'Effective lengths of columns in multi-storey buildings', The Structural Engineer, Vol. 52, July-Sept. 1974.

51. Horne, M.R. 'An approximate method for calculating the elastic critical load of multi-storey plane frames', The Structural Engineer, Vol. 53, June 1975.

52. Bolton, A. 'A simple understanding of elastic critical load', The Structural Engineer, Vol. 54, June 1976.

53. Williams, F.W. 'Simple design procedures for unbraced multi-storey plane frames', Proc. I.C.E., Vol. 63, June 1977.

54. European Convention for Constructional Steelwork: European recommendations for steel construction, London, The Constructional Press, 1981.

55. 'Draft standard specification for the structural use of steelwork in buildings : Part 1 : Simple construction and continuous construction', London, BSI, 1979.

56. 'Ultimate Limit State Calculation of Sway Frames with Rigid Joints ' , ECCS - Technical Committee 8, Structural Stability Technical Working Group 8.2 - Systems, Publication No. 33, First Edition 1984.

57. Lu, L.W. 'Inelastic buckling of steel frames', Jour. Struct. Div., ASCE, ST6, Dec. 1965.

58. Moy, F.C.S. 'Control of deflection in unbraced steel frames', Proc. I.C.E., Vol. 57, Dec. 1974.

59. Anderson, D. and Islam, M.A. 'Design of multistorey frames to sway deflection limitation', The Structural Engineer, Vol. 57B, March 1979.

60. Wood, R.H. and Roberts, E.H. 'A graphical method of predicting sidesway in the design of multistorey buildings', Proc. I.C.E., Vol. 59, June 1975.

61. Anderson, D. and Salter, J.B. 'Design of structural frames to deflection limitation', The Structural Engineer, Vol. 53, August 1975.

62. Moy, F.C.S. 'Consideration of secondary effects in frame design', Jour. Struct. Div., ASCE, ST10, Oct. 1977.

63. Majid, K.I. and Okdeh, S. 'Limit state design of sway frames', The Structural Engineer, Vol.60B, No.4, Dec. 1982.

64. Heyman, J. 'Plastic design of plane frames for minimum weight', The Structural Engineer, p125, May 1953.

65. Monforton, A.R. and Wu, T.S. 'Matrix analysis of semi-rigidly connected frames', Jour. Struct. Div., ASCE, ST6, Dec. 1963.

66. Krishnamurty, N., Huang, H.T., Jefferey, P.K. and Avery, L.K. 'Analytical M-0 curves for end-plate connections', Jour. Struct. Div., ASCE, ST1, Jan. 1979.

67. Jones, S.W., Kirby, P.A. and Nethercot, D.A. 'Column with semi-rigid joints', Jour. Struct. Div., ASCE, ST2, Feb. 1982.

68. Scholz, H. 'A new multi-curve interaction version of the Merchant-Rankine approach', Instability and Plastic Collapse of Steel Structures, Ed. L.J. Morris, Granada, 1983.

69. Frye, M.J. and Morris, G.A. 'Analysis of flexibly connected steel frames', Can. Jour. of Civ. Eng., No. 2, May 1975.

70. 'CP3 : Code of basic data for the design of buildings, Chapter V : Loading, Part 2 : Wind loads', BSI, London, 1972.

71. 'CP3 : Code of basic data for the design of buildings, Chapter V : Loading, Part 1 : Dead and imposed loads', BSI, London, 1967.

72. Anderson, D. and Islam, M.A. 'Design of unbraced multi-storey steel frames under combined loading', Proc. I.C.E., Vol. 69, March 1980.

73. Williams, F.W. 'Hand calculation of critical loads for unbraced multi-storey plane frames', The Structural Engineer, Vol. 54, March 1976.

74. Moy, F.C.S. 'Multistory frame design using story stiffness concept', Jour. Struct. Div., ASCE, ST6, Dec. 1976.

75. Batho, C. and Rowan, H.D. 'Investigation of beam and stanchion connections', second report, Steel Structures Research Committee, DSIR, HMSO, London, England, 1934.

APPENDIX

A1 ANALYSIS OF PINNED BASE SINGLE STOREY FRAME

(VERTICAL LOAD)

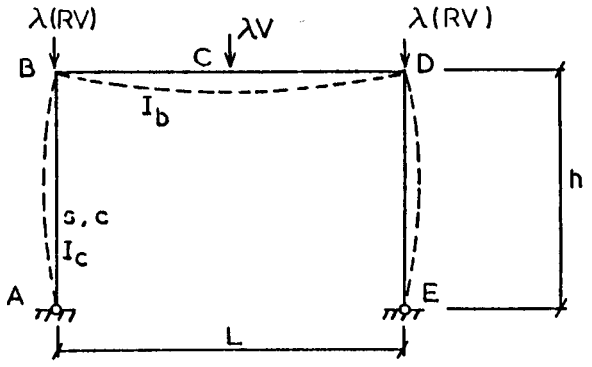

$$M_{AB} = 0$$

$$\therefore \quad \theta_A = -c.\theta_B \qquad \text{(A1.1)}$$

$$M_{BA} = \frac{E.I_c}{h}\,[s.\theta_B + sc.\theta_A]$$

$$= Ek".\theta_B\, s(1 - c^2) \qquad \text{where } k" = I_c/h \qquad \text{(A1.2)}$$

From symmetry of figure above,

$$M_{BD} = -M_{DB} \qquad \text{and} \qquad \theta_B = -\theta_D$$

Hence,

$$M_{BD} = 2Ek'\theta_B - \frac{\lambda V.L}{8} \qquad \text{where } k' = I_b/L \qquad \text{(A1.3)}$$

Equilibrium at joint (B)

$$E.\theta_B = \frac{\lambda V.L}{8}\left[\frac{1}{2k' + s(1 - c^2)k"}\right] \qquad \text{(A1.4)}$$

Substituting (A1.4) into (A1.3) gives,

$$M_{DB} = \frac{\lambda V.L}{8}\left[1 - \frac{2k'}{2k' + s(1 - c^2)k"}\right] \qquad \text{(A1.5)}$$

$$= MV$$

A2 ANALYSIS OF PINNED BASE SINGLE STOREY PORTAL

(WIND PLUS FICTITIOUS HORIZONTAL LOAD)

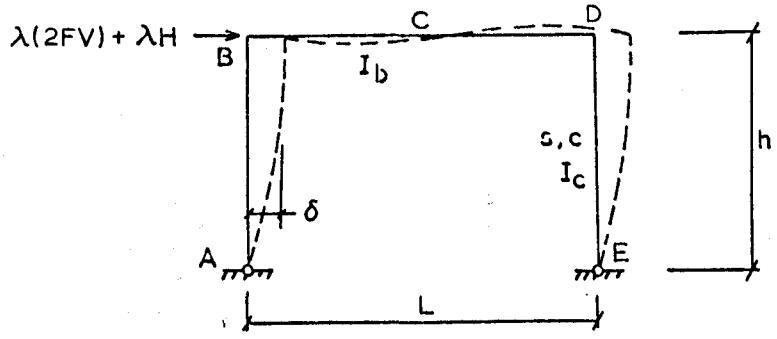

$$M_{AB} = 0$$

$$\therefore \quad s(1 + c).\frac{\delta}{h} = s\theta_A + sc\theta_B \qquad \text{(A2.1)}$$

$$M_{BA} = Ek''[s\theta_B + sc.\theta_A - s(1 + c)\frac{\delta}{h}]$$

$$= Ek'' \; s(1 - c)[\theta_B - \theta_A] \qquad \text{(A2.2)}$$

$$M_{BD} = M_{DB} \qquad \text{and} \qquad \theta_B = \theta_D$$

$$\therefore \quad M_{BD} = 6Ek'\theta_B \qquad \text{(A2.3)}$$

Equilibrium at joint (B)

$$\theta_B = \theta_A \left[\frac{1}{1 + 6k'/s(1 - c)k''} \right] \qquad \text{(A2.4)}$$

Sway equation

$$M_{BA} + \frac{\lambda Hh}{2} + \lambda(FV).\delta = 0$$

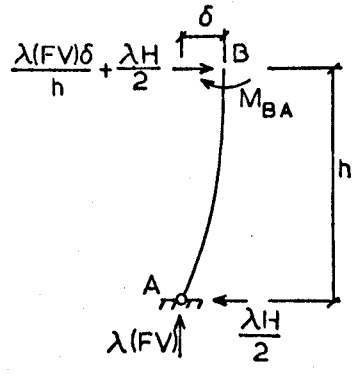

Substituting for M_{BA} from above gives

$$\theta_A = \theta_B + \frac{\lambda H.h}{2Ek"s(1 - c)} + \frac{\lambda(FV)\delta}{Ek"s(1 - c)} \qquad (A2.5)$$

Solving equation (A2.4) and (A2.5) gives the rotations

$$\theta_B = \frac{\lambda H.h}{12Ek'} + \frac{\lambda(FV)\delta}{6Ek'} \qquad (A2.6)$$

$$\theta_A = \frac{\lambda H.h}{2E}\left[\frac{1}{6k'} + \frac{1}{k"s(1 - c)}\right] + \frac{\lambda(FV)\delta}{E}\left[\frac{1}{6k'} + \frac{1}{k"s(1 - c)}\right]$$

Substituting the rotations into equation (A2.1) and rearranging gives,

$$\delta = \left[\frac{\lambda H.h\alpha_1}{12Ek'/h - 2\lambda(FV)\alpha_1}\right] \qquad (A2.7)$$

where $\alpha_1 = \left[1 + \frac{6k'}{s(1 - c^2)k"}\right]$

$k' = I_b/L$ and $k" = I_c/h$

$\lambda(FV) = \lambda(RV) + \lambda V/2$

Finally the bending moments are obtained by substituting the rotations into (A2.2) and (A2.3).

$$M_{BA} = -\left[\frac{\lambda H.h}{2} + \lambda(FV)\delta\right] \qquad (A2.8)$$

$$M_{BD} = \left[\frac{\lambda H.h}{2} + \lambda(FV)\delta\right] \qquad (A2.9)$$

$$= MH$$

A3 FIRST HINGE AT LEEWARD END OF THE BEAM

(MID-SPAN VERTICAL LOAD)

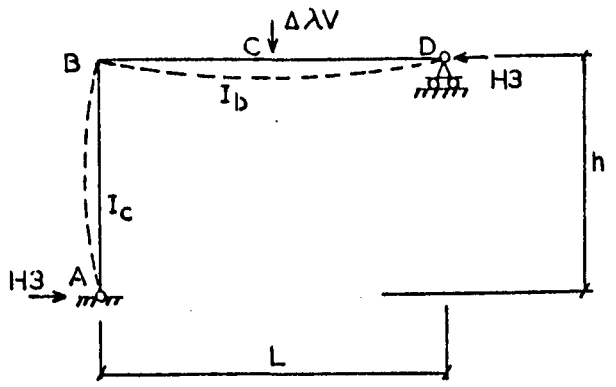

$$M_{AB} = 0$$

$$\therefore \quad \theta_A = \frac{-\theta_B}{2}$$

$$M_{BA} = 2Ek''[2\theta_B + \theta_A]$$

$$= 3Ek''\theta_B \qquad \text{(A3.1)}$$

$$M_{DB} = 2Ek'(2\theta_D + \theta_B) + M^F_{DB} = 0 \qquad \text{where } M^F_{DB} = \frac{\Delta\lambda VL}{8}$$

$$\therefore \quad \theta_D = \frac{-\Delta\lambda VL}{32Ek'} - \frac{\theta_B}{2}$$

$$M_{BD} = 2Ek'(2\theta_B + \theta_D) - \frac{\Delta\lambda VL}{8}$$

Substituting θ_D into above gives,

$$M_{BD} = 3Ek'\theta_B - \frac{3\Delta\lambda VL}{16} \qquad \text{(A3.2)}$$

Equilibrium at joint (B)

$$E\theta_B = \frac{3\Delta\lambda VL}{16}\left[\frac{1}{3k' + 3k''}\right] \qquad \text{(A3.3)}$$

Substituting (A3.3) into (A3.1) and (A3.2) gives,

$$M_{BA} = \frac{3\Delta\lambda VL}{16}\left[\frac{1}{1 + k'/k''}\right] \qquad \text{(A3.4)}$$

$$M_{BD} = \frac{3\Delta\lambda VL}{16}\left[\frac{1}{1 + k''/k'} - 1\right] \qquad \text{(A3.5)}$$

Hence,

$$H3 = M_{BA}/h$$

$$= \frac{3\Delta\lambda VL}{16h} \left[\frac{1}{1 + k'/k''}\right] \qquad \text{(A3.6)}$$

A4 FIRST HINGE AT LEEWARD END OF THE BEAM

(WIND AND FICTITIOUS LOADS)

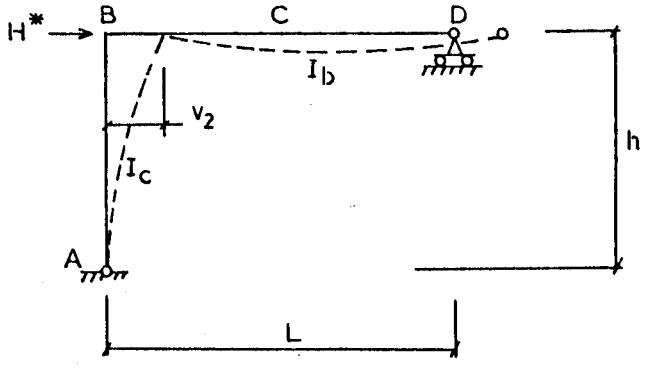

$$M_{AB} = 2Ek''[2\theta_A + \theta_B - \frac{3v_2}{h}] = 0$$

$$\therefore \quad \frac{3v_2}{h} = 2\theta_A + \theta_B \qquad \text{(A4.1)}$$

$$M_{BA} = 2Ek''[\theta_A + 2\theta_B - \frac{3v_2}{h}]$$

$$= 2Ek''[\theta_B - \theta_A] \qquad \text{(A4.2)}$$

Similarly,

$$M_{BD} = 3Ek'\theta_B \qquad \text{since} \quad \theta_D = -\frac{\theta_B}{2} \qquad \text{(A4.3)}$$

Equilibrium at joint (B)

$$\theta_B = \theta_A \left[\frac{1}{1 + 3k'/2k''}\right] \qquad \text{(A4.4)}$$

Sway equation

$$M_{BA} + H^* h = 0$$

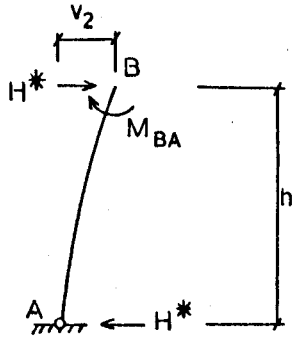

Substituting for M_{BA} from above gives,

$$\theta_A = \theta_B + \frac{H^* h}{2Ek''} \qquad \text{(A4.5)}$$

Put (A4.5) into (A4.4) and rearringing gives,

$$\theta_B = \frac{H^* h}{3Ek'} \qquad \text{(A4.6)}$$

and

$$\theta_A = \frac{H^* h}{3Ek'} + \frac{H^* h}{2Ek''} \qquad \text{(A4.7)}$$

Equation (A4.1) therefore gives,

$$v_2 = \frac{H^* h^2 \alpha_2}{3Ek'} \qquad \text{(A4.8)}$$

where $\alpha_2 = (1 + k'/k'')$

$H^* = \Delta\lambda H + (H1 + H2 + H3)$

A5 ANALYSIS OF INTERMEDIATE LIMITED FRAME

(MID-SPAN VERTICAL LOAD)

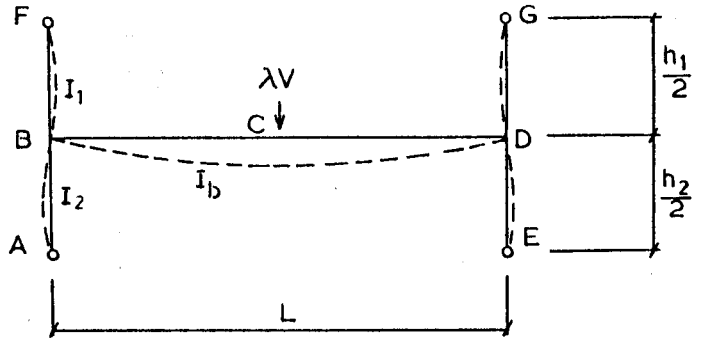

$$M_{AB} = 0$$

$$\therefore \quad \theta_A = \frac{-\theta_B}{2} \qquad \text{(A5.1)}$$

$$M_{BA} = \frac{EI_2}{h_2/2}(4\theta_B + 2\theta_A)$$

Substituting for θ_A gives,

$$M_{BA} = 6Ek_2\theta_B \qquad \text{where } k_2 = I_2/h_2 \qquad \text{(A5.2)}$$

Similarly for the upper leg,

$$M_{BF} = 6Ek_1\theta_B \qquad \text{where } k_1 = I_1/h_1 \qquad \text{(A5.3)}$$

$$M_{BD} = -M_{DB} \qquad \text{and} \qquad \theta_B = -\theta_D$$

$$= 2\frac{EI_b}{L}(2\theta_B + \theta_D) - \frac{\lambda VL}{8}$$

$$= 2Ek\theta_B - \frac{\lambda VL}{8} \qquad \text{where } k = I_b/L \qquad \text{(A5.4)}$$

Equilibrium at joint (B)

$$E\theta_B = \frac{\lambda VL}{8}\left[\frac{1}{6k_1 + 6k_2 + 2k}\right] \qquad \text{(A5.5)}$$

Substituting (A5.5) into slope-deflection equations give,

$$M_{DC} = \frac{\lambda VL}{8}\left[1 - \frac{2k}{6k_1 + 6k_2 + 2k}\right]$$

$$= \frac{\lambda VL}{8}\left[1 - \frac{k}{K}\right] \qquad \text{where } K = 3k_1 + 3k_2 + k \qquad \text{(A5.6)}$$

$$= M_{DC}(V)$$

$$M_{BA} = \frac{\lambda VL}{8}\left[\frac{3k_2}{K}\right] \qquad \text{(A5.7)}$$

$$= -M_{DE}(V)$$

$$M_{BF} = \frac{\lambda VL}{8}\left[\frac{3k_1}{K}\right] \qquad \text{(A5.8)}$$

$$= -M_{DG}(V)$$

and $M_{CD}(V) = \frac{\lambda VL}{4} - M_{DC}(V)$

where $K = [3k_1 + 3k_2 + k]$

$k_1 = I_1/h_1$, $k_2 = I_2/h_2$ and $k = I_b/L$

A6 ANALYSIS OF INTERMEDIATE LIMITED FRAME

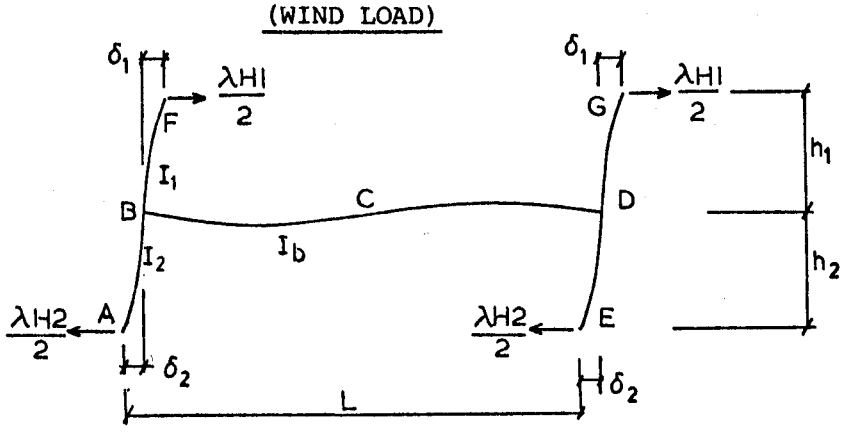

$$M_{BF} = 2\frac{EI_1}{h_1}\left[2\theta_B + \theta_F - \frac{3\delta_1}{h_1}\right] \qquad (A6.1)$$

$$M_{BA} = 2\frac{EI_2}{h_2}\left[2\theta_B + \theta_A - \frac{3\delta_2}{h_2}\right] \qquad (A6.2)$$

$$M_{BD} = 2\frac{EI_b}{L}(2\theta_B + \theta_D) \qquad \text{but} \qquad \theta_D = \theta_B$$

$$\therefore \quad M_{BD} = 6\frac{EI_b}{L}\theta_B \qquad (A6.3)$$

Equilibrium at joint (B)

$$4Ek_1\theta_B + 4Ek_2\theta_B + 2Ek_1\theta_F + 2Ek_2\theta_A - 6Ek_1\delta_1/h_1 - 6Ek_2\delta_2/h_2 + 6Ek\theta_B = 0 \qquad (A6.4)$$

Sway equation of upper leg

$$M_{BF} + M_{FB} + \frac{\lambda H1 h_1}{2} = 0$$

$$6Ek_1\theta_B + 6Ek_1\theta_F - 12Ek_1\delta_1/h_1 + \frac{\lambda H1 h_1}{2} = 0$$

$$\therefore \quad \theta_F = 2\delta_1/h_1 - \theta_B - \frac{\lambda H1 h_1}{12Ek_1} \qquad (A6.5)$$

Sway equation of lower leg gives,

$$\theta_A = 2\delta_2/h_2 - \theta_B - \frac{\lambda H2 h_2}{12Ek_2} \qquad (A6.6)$$

Substituting (A6.5) and (A6.6) into (A6.4) and rearranging gives,

$$\theta_B = \frac{2k_1(\delta_1/h_1) + 2k_2(\delta_2/h_2) + [(\lambda H1.h_1 + \lambda H2h_2)/6E]}{2k_1 + 2k_2 + 6k} \qquad \text{(A6.7)}$$

The bending moments are obtained by backsubstitution of (A6.5) to (A6.7) into the appropriate slope-deflection equations.

A7 ANALYSIS OF BASE LIMITED FRAME

(MID-SPAN VERTICAL LOAD)

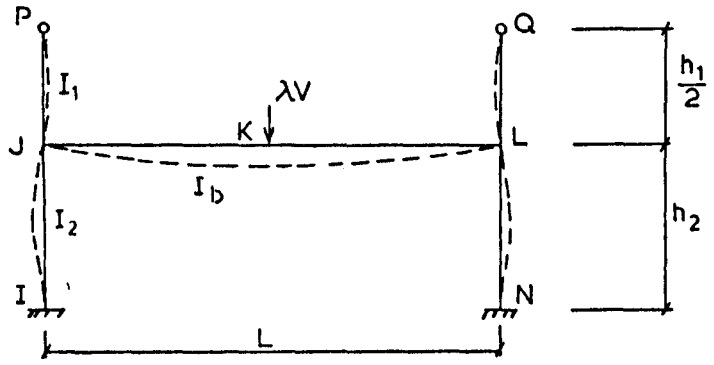

$$M_{PJ} = 0$$

$$\therefore \quad \theta_P = \frac{-\theta_J}{2}$$

$$M_{JP} = 2\,\frac{EI_1}{h_1/2}\,[2\theta_J + \theta_P]$$

$$= 6Ek_1\theta_J \qquad \text{(A7.1)}$$

$$M_{JI} = 2\,\frac{EI_2}{h_2}\,(2\theta_J) = 4Ek_2\theta_J \qquad \text{Also, } M_{JL} = -M_{LJ} \qquad \text{(A7.2)}$$

$$M_{JL} = 2\,\frac{EI_b}{L}\,(2\theta_J + \theta_L) - \frac{\lambda VL}{8} \qquad \text{and } \theta_L = -\theta_J$$

$$= 2Ek\theta_J - \frac{\lambda VL}{8} \qquad \text{(A7.3)}$$

Equilibrium at joint (J)

$$M_{JP} + M_{JI} + M_{JL} = 0$$

$$\therefore \quad E\theta_J = \frac{\lambda VL}{8}\left[\frac{1}{6k_1 + 4k_2 + 2k}\right] \qquad \text{(A7.4)}$$

Substituting (A7.4) into above gives,

$$M_{LJ} = \frac{\lambda VL}{8}\left[1 - \frac{k}{K'}\right] \qquad \text{(A7.5)}$$

$$M_{JI} = \frac{\lambda VL}{8}\left[\frac{2k_2}{K'}\right] \qquad \text{(A7.6)}$$

$$M_{IJ} = M_{JI}/2 \qquad \text{(A7.7)}$$

where $K' = (3k_1 + 2k_2 + k)$

A8 ANALYSIS OF BASE LIMITED FRAME

(WIND LOAD)

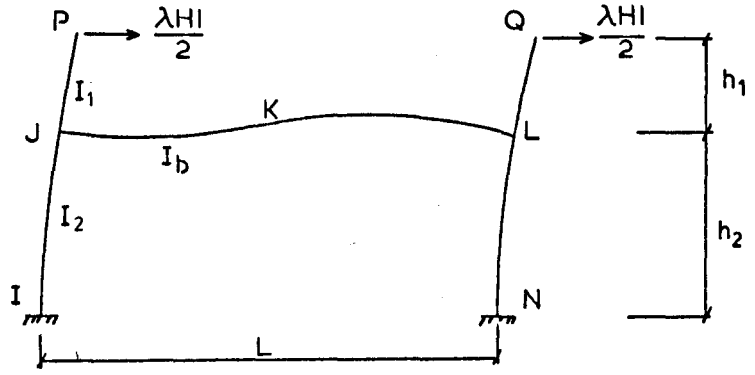

Proceeding in exactly the same way as shown in Appendix (A6) but ignoring the rotation at (I) of the base gives the equilibrium at joint (J) as,

$$4Ek_1\theta_J + 4Ek_2\theta_J + 2Ek_1\theta_P - 6Ek_1\delta_1/h_1 - 6Ek_2\delta_2/h_2 + 6Ek\theta_J = 0 \qquad (A8.1)$$

Substituting (A6.5) for θ_P gives,

$$\theta_J = \frac{2k_1(\delta_1/h_1) + 6k_2(\delta_2/h_2) + (\lambda H1\, h_1/6E)}{2k_1 + 4k_2 + 6k} \qquad (A8.2)$$

Substituting (A8.2) into the relevant slope-deflection equation gives the appropriate bending moments.

A9 HINGE AT LEEWARD END OF THE BEAM

(MID-SPAN VERTICAL LOAD)

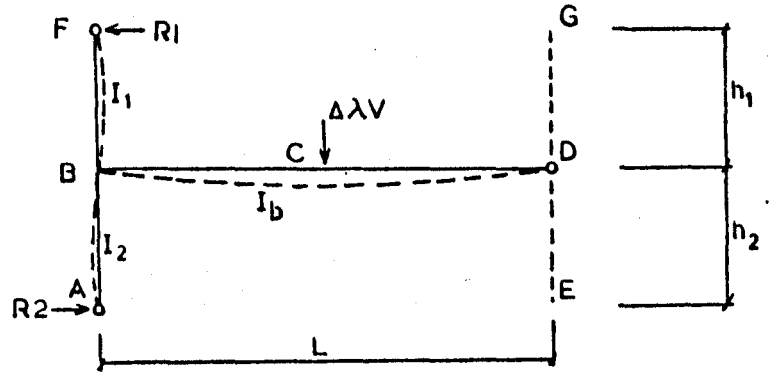

$$\Delta M_{AB} = 0$$

$$\therefore \quad \theta_A = \frac{-\theta_B}{2} \qquad \text{(A9.1)}$$

$$\Delta M_{BA} = 2\,\frac{EI_2}{h_2}\,(2\theta_B + \theta_A)$$

$$= 3Ek_2\theta_B \qquad \text{(A9.2)}$$

Similarly,

$$\Delta M_{BF} = 3Ek_1\theta_B \qquad \text{(A9.3)}$$

In a similar manner to the derivation given in Appendix (A3), the rotation at D is given by,

$$\theta_D = \frac{-\Delta\lambda VL}{32Ek'} - \frac{\theta_B}{2}$$

$$\Delta M_{BD} = 2Ek'(2\theta_B + \theta_D) - \Delta\lambda VL/8$$

Substituting for θ_D gives,

$$\Delta M_{BD} = 3Ek\theta_B - \frac{3\,\Delta\lambda VL}{16} \qquad \text{(A9.4)}$$

Equilibrium at joint (B)

$$E\theta_B = 3\,\frac{\Delta\lambda VL}{16}\left[\frac{1}{3k_1 + 3k_2 + 3k}\right] \qquad \text{(A9.5)}$$

Substituting (A9.5) into (A9.2) and (A9.3) gives,

$$\Delta M_{BA} = 3\,\frac{\Delta\lambda VL}{16}\left[\frac{k_2}{K''}\right] \qquad \text{where } K'' = k_1 + k_2 + k \qquad \text{(A9.6)}$$

$$\Delta M_{BF} = 3\,\frac{\Delta\lambda VL}{16}\left[\frac{k_1}{K''}\right] \qquad \text{(A9.7)}$$

The forces R1 and R2 are given by

$$R2 = \Delta M_{BA}/h_2 \qquad \text{and} \qquad R1 = \Delta M_{BF}/h_1$$

$$\therefore \quad R = R1 + R2$$

$$= 3\,\frac{\Delta\lambda VL}{16K''}\left[\frac{k_1}{h_1} + \frac{k_2}{h_2}\right] \qquad \text{(A9.8)}$$

$$= R \quad \text{(Intermediate)}$$

The average value of R is taken as half its values given by equation (A9.8).

For a fixed base limited frame ($\theta_A = 0$) and equilibrium of joint B gives,

$$E\theta_B = 3\,\frac{\Delta\lambda VL}{16}\left[\frac{1}{3k_1 + 4k_2 + 3k}\right] \qquad \text{(A9.9)}$$

similarly,

$$\Delta M_{BA} = 3\,\frac{\lambda VL}{16}\left[\frac{4k_2}{3k_1 + 4k_2 + 3k}\right] \qquad \text{(A9.10)}$$

$$\Delta M_{BF} = 3\,\frac{\Delta\lambda VL}{16}\left[\frac{3k_1}{3k_1 + 4k_2 + 3k}\right] \qquad \text{(A9.11)}$$

and the average value of R is in the same way obtained as,

$$R = \frac{3\,\Delta\lambda VL}{16[3k_1 + 4k_2 + 3k]}\left[\frac{3k_1}{h_1} + \frac{4k_2}{h_2}\right] \qquad \text{(A9.12)}$$

$$= R \text{ (base)}$$

For double beam hinges the force, R, is similarly obtained.

A10 DISTRIBUTION OF SHEAR

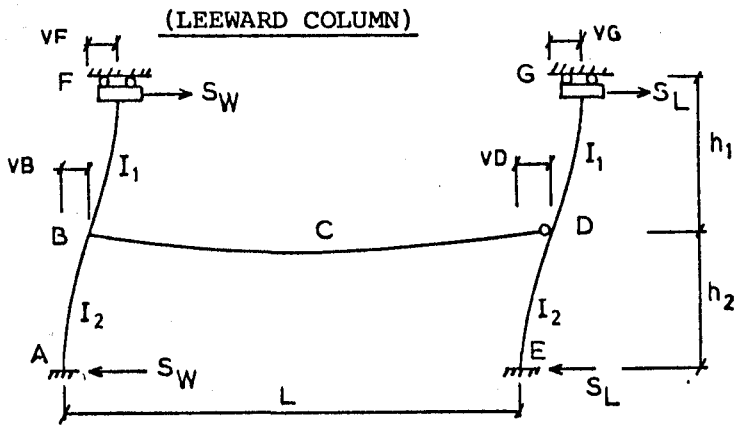

Equilibrium of joint (D)

$$\Delta M_{DE} + \Delta M_{DG} = 0$$

$$4k_1\theta_D + 4k_2\theta_D = 6k_1(vG/h_1) + 6k_2(vD/h_2) \qquad \text{(A10.1)}$$

Sway equation (upper leg)

$$\Delta M_{DG} + \Delta M_{GD} + S_L.h_1 = 0$$

$$6Ek_1\theta_D - 12Ek_1(vG/h_1) + S_L.h_1 = 0$$

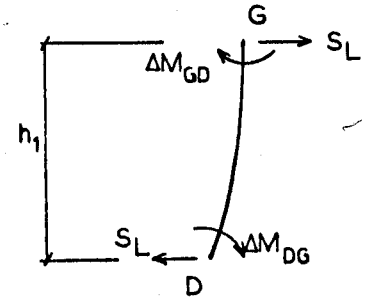

$$\therefore \quad vG = \frac{h_1\theta_D}{2} + \frac{S_L h_1^2}{12Ek_1} \qquad \text{(A10.2)}$$

Similarly for the lower leg,

$$vD = \frac{h_2}{2}\theta_D + \frac{S_L h_2^2}{12Ek_2} \qquad \text{(A10.3)}$$

Substituting (A10.2) and (A10.3) into (A10.1) and rearranging gives,

$$\theta_D = \frac{S_L}{2E}\left[\frac{h_1 + h_2}{k_1 + k_2}\right] \qquad \text{(A10.4)}$$

Hence from (A10.2) and (A10.3),

$$v_D = \frac{S_L h_2}{4E}\left[\frac{h_1 + h_2}{k_1 + k_2} + \frac{h_2}{3k_2}\right] \qquad \text{(A10.5)}$$

and

$$v_G = \frac{S_L h_1}{4E}\left[\frac{h_1 + h_2}{k_1 + k_2} + \frac{h_1}{3k_1}\right] \qquad \text{(A10.6)}$$

The total sway is given by the sum of vD and vG

$$v_L(T) = \frac{S_L}{4E}\left[\frac{h_1^2 + 2h_1 h_2 + h_2^2}{k_1 + k_2} + \frac{h_1^2}{3k_1} + \frac{h_2^2}{3k_2}\right]$$

$$= \frac{S_L}{4E}\left[\frac{(h_1 + h_2)^2}{k_1 + k_2} + \frac{h_1^2}{3k_1} + \frac{h_2^2}{3k_2}\right] \qquad \text{(A10.7)}$$

WINDWARD ASSEMBLY

Analysis of the windward assembly is similar to the leeward column except for the inclusion of the beam member,

Equilibrium of joint (B)

$$\Delta M_{BA} + \Delta M_{BF} + \Delta M_{BD} = 0$$

$$4k_1\theta_B + 4k_2\theta_B + 3k\theta_B = 6k_1(vF/h_1) + 6k_2(vB/h_2) \qquad \text{(A10.8)}$$

Sway equation (upper leg)

$$\Delta M_{BF} + \Delta M_{FB} + S_W h_1 = 0$$

$$6Ek_1\theta_B - 12Ek_1(v_F/h_1) + S_W h_1 = 0$$

$$\therefore \quad vF = \left[\frac{h_1\theta_B}{2} + \frac{S_W h_1^2}{12Ek_1}\right] \qquad \text{(A10.9)}$$

Similarly for the lower leg,

$$vB = \left[\frac{h_2\theta_B}{2} + \frac{S_W h_2^2}{12Ek_2}\right] \qquad \text{(A10.10)}$$

On substituting (A10.9) and (A10.10) into (A10.8), the rotation of joint B is obtained,

$$\theta_B = \frac{S_W}{2E}\left[\frac{h_1 + h_2}{k_1 + k_2 + 3k}\right] \qquad \text{(A10.11)}$$

and the displacements are similarly given as,

$$vF = \frac{S_W h_1}{4E}\left[\frac{h_1 + h_2}{k_1 + k_2 + 3k} + \frac{h_1}{3k_1}\right] \qquad \text{(A10.12)}$$

$$vB = \frac{S_W h_2}{4E}\left[\frac{h_1 + h_2}{k_1 + k_2 + 3k} + \frac{h_2}{3k_2}\right] \qquad \text{(A10.13)}$$

The total sway is,

$$v_W(T) = vF + vB$$

$$= \frac{S_W}{4E}\left[\frac{(h_1 + h_2)^2}{k_1 + k_2 + 3k} + \frac{h_1^2}{3k_1} + \frac{h_2^2}{3k_2}\right] \qquad \text{(A10.14)}$$

A11 INCREMENTAL ANALYSIS

(WIND LOAD)

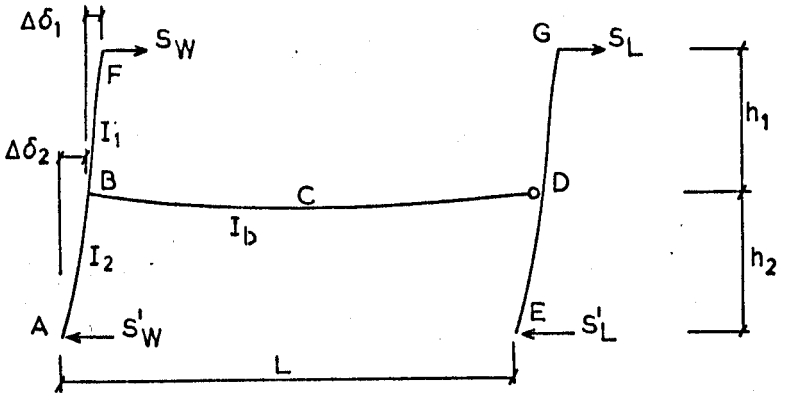

$$\Delta M_{BF} = 2E \frac{I_1}{h_1} [2\theta_B + \theta_F - \frac{3\Delta\delta_1}{h_1}] \qquad (A11.1)$$

$$\Delta M_{BA} = 2E \frac{I_2}{h_2} [2\theta_B + \theta_A - \frac{3\Delta\delta_2}{h_2}] \qquad (A11.2)$$

$$\Delta M_{DB} = 0 \qquad \therefore \quad \theta_D = -\frac{\theta_B}{2}$$

$$\therefore \quad \Delta M_{BD} = 3E \frac{I_b}{L} \theta_B \qquad (A11.3)$$

Equilibrium at joint (B)

$$4Ek_1\theta_B + 4Ek_2\theta_B + 2Ek_1\theta_F + 2Ek_2\theta_A - 6Ek_1(\Delta\delta_1/h_1) - 6Ek_2(\Delta\delta_2/h_2) + 3Ek\theta_B = 0 \qquad (A11.4)$$

Sway equation of upper leg

$$\Delta M_{BF} + \Delta M_{FB} + S_W h_1 = 0$$

$$6Ek_1\theta_B + 6Ek_1\theta_F - 12Ek_1(\Delta\delta_1/h_1) + S_W h_1 = 0$$

$$\therefore \quad \theta_F = \frac{2\Delta\delta_1}{h_1} - \theta_B - \frac{S_W h_1}{6Ek_1} \qquad (A11.5)$$

Sway equation of lower leg gives,

$$\theta_A = \frac{2\Delta\delta_2}{h_2} - \theta_B - \frac{S'_W h_2}{6Ek_2} \qquad (A11.6)$$

Substituting (A11.5) and (A11.6) into (A11.4) and rearranging gives,

$$\theta_B = \frac{2k_1(\Delta\delta_1/h_1) + 2k_2(\Delta\delta_2/h_2) + [S_W h_1 + S'_W h_2)/3E]}{2k_1 + 2k_2 + 3k} \qquad \text{(A11.7)}$$

In a similar manner, the joint rotations at D, E and G are obtained by ignoring the beam stiffness,

$$\theta_D = \frac{2k_1(\Delta\delta_1/h_1) + 2k_2(\Delta\delta_2/h_2) + [(S_L h_1 + S'_L h_2)/3E]}{2k_1 + 2k_2} \qquad \text{(A11.8)}$$

$$\theta_G = 2\frac{\Delta\delta_1}{h_1} - \theta_D - \frac{S_L h_1}{6Ek_1} \qquad \text{(A11.9)}$$

$$\theta_E = 2\frac{\Delta\delta_2}{h_2} - \theta_D - \frac{S'_L h_2}{6Ek_2} \qquad \text{(A11.10)}$$

A12 INCREMENTAL ANALYSIS OF BASE LIMITED FRAME

(MID-SPAN VERTICAL LOAD)

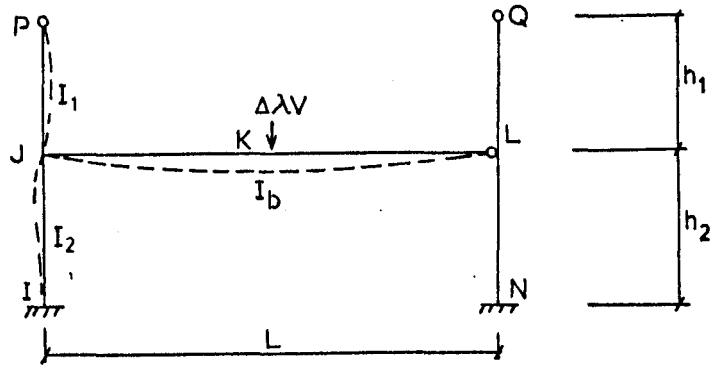

$$\Delta M_{PJ} = 0$$

$$\therefore \quad \theta_P = -\frac{\theta_J}{2}$$

$$\Delta M_{JP} = 2E \frac{I_1}{h_1} [2\theta_J + \theta_P]$$

$$= 3Ek_1\theta_J \qquad \text{(A12.1)}$$

$$\Delta M_{JI} = 2E \frac{I_2}{h_2} [2\theta_J]$$

$$= 4Ek_2\theta_J \qquad \text{(A12.2)}$$

Similarly,

$$\Delta M_{JK} = 3Ek\theta_J - \frac{3\Delta\lambda VL}{16} \qquad \text{(A12.3)}$$

Equilibrium at joint (J)

$$E\theta_J = \frac{3\Delta\lambda VL}{16} \left[\frac{1}{3k_1 + 4k_2 + 3k}\right] \qquad \text{(A12.4)}$$

Substituting (A12.4) into the slope-deflection equation above gives,

$$\Delta M_{JK} = \frac{3\Delta\lambda VL}{16} \left[\frac{3k}{3k_1 + 4k_2 + 3k} - 1\right] \qquad \text{(A12.5)}$$

$$= \Delta M_{JK}(V)$$

$$\Delta M_{JI} = \frac{3\Delta\lambda VL}{16}\left[\frac{4k_2}{3k_1 + 4k_2 + 3k}\right] \qquad \text{(A12.6)}$$

$$= \Delta M_{JI}(V)$$

and

$$\Delta MKL = \frac{\Delta\lambda VL}{4} + \frac{\Delta M_{JK}(V)}{2}$$

A13 INCREMENTAL ANALYSIS OF BASE LIMITED FRAME

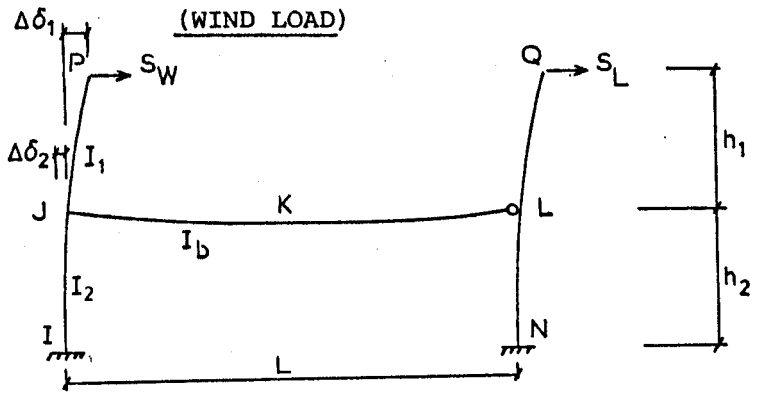

$$\Delta M_{JI} = 2Ek_2[2\theta_J - 3\Delta\delta_2/h_2] \qquad \text{(A13.1)}$$

$$\Delta M_{JP} = 2Ek_1[2\theta_J + \theta_P - 3\Delta\delta_1/h_1] \qquad \text{(A13.2)}$$

$$\Delta M_{JL} = 3Ek\theta_J \qquad \text{(A13.3)}$$

Equilibrium of joint (J)

$$\Delta M_{JP} + \Delta M_{JI} + \Delta M_{JL} = 0$$

$$4k_1\theta_J + 4k_2\theta_J + 3k\theta_J = 6k_1(\Delta\delta_1/h_1) + 6k_2(\Delta\delta_2/h_2) - 2k_1\theta_P \qquad \text{(A13.4)}$$

Sway equation of upper leg

$$\Delta M_{PJ} + \Delta M_{JP} + S_W h_1 = 0$$

$$\therefore \quad \theta_P = 2\Delta\delta_1/h_1 - \theta_J - \frac{S_W h_1}{6Ek_1} \qquad \text{(A13.5)}$$

Substitute (A13.5) into (A13.4) to solve for θ_J,

$$\theta_J[2k_1 + 4k_2 + 3k] = 2k_1(\Delta\delta_1/h_1) + 6k_2(\Delta\delta_2/h_2) + \frac{S_W h_1}{3E}$$

$$\therefore \quad \theta_J = \frac{2k_1(\Delta\delta_1/h_1) + 6k_2(\Delta\delta_2/h_2) + (S_W h_1/3E)}{(2k_1 + 4k_2 + 3k)} \qquad \text{(A13.6)}$$

The rotation at joint L of the extended leeward column is similarly obtained by ignoring the beam stiffness, k, and substituting S_L for S_W.

Equilibrium of joint (L)

$$\Delta M_{LN} + \Delta M_{LQ} = 0$$

$$4Ek_1\theta_L + 4Ek_2\theta_L + 2Ek_1\theta_Q = 6Ek_1(\Delta\delta_1/h_1) + 6Ek_2(\Delta\delta_2/h_2) \qquad \text{(A13.7)}$$

Sway equation for member NQ

$$\Delta M_{LQ} + \Delta M_{QL} + S_L h_1 = 0$$

$$\therefore \quad \theta_Q = 2\Delta\delta_1/h_1 - \theta_L - \frac{S_L h_1}{6Ek_1} \qquad \text{(A13.8)}$$

Substituting (A13.8) into (A13.7) and rearranging gives,

$$\theta_L = \frac{2k_1(\Delta\delta_1/h_1) + 6k_2(\Delta\delta_2/h_2) + (S_L h_1/3E)}{2k_1 + 4k_2} \qquad \text{(A13.9)}$$

A14 INCREMENTAL ANALYSIS OF BASE LIMITED FRAME

(VERTICAL LOAD)

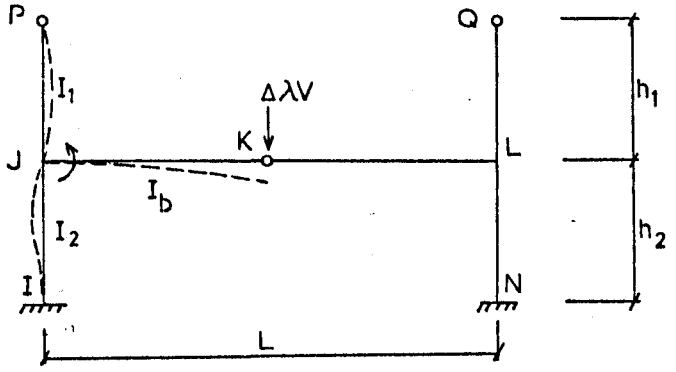

$$\Delta M_{PJ} = 0$$

$$\therefore \quad \theta_P = \frac{-\theta_J}{2}$$

$$\Delta M_{JP} = 3Ek_1\theta_J \qquad \text{(A14.1)}$$

$$\Delta M_{JI} = 4Ek_2\theta_J \qquad \text{(A14.2)}$$

and

$$\Delta M_{JK} = -\frac{\Delta\lambda VL}{4} \qquad \text{(A14.3)}$$

Equilibrium of joint (J)

$$E\theta_J = \frac{\Delta\lambda VL}{4}\left[\frac{1}{3k_1 + 4k_2}\right] \qquad \text{(A14.4)}$$

Hence from above equation,

$$\Delta M_{JI} = \frac{\Delta\lambda VL}{4}\left[\frac{4k_2}{3k_1 + 4k_2}\right] \qquad \text{(A14.5)}$$

and

$$\Delta M_{IJ} = \Delta MJI/2 \qquad \text{(A14.6)}$$

PUBLISHED WORK

The investigation described in Chapters (2) and (3) of this thesis has been published in the form of two papers, written jointly by the author and Dr. D. Anderson.

The first paper was published in "The Structural Engineer", Vol.61B, No.2, June 1983 entitled "Design Studies on Unbraced Multistorey Steel Frames".

The second paper, "An Elasto-Plastic Hand Method for Unbraced Rigid-Jointed Steel Frames" was published in the Proceedings of the Michael R. Horne Conference on "Instability and Plastic Collapse of Steel Structures", Edited by L.J. Morris, Granada, 1983.

In addition, the work presented in Chapter (2) has been included under the section "Merchant-Rankine Approach" in the European Convention for Constructional Steelwork(ECCS) Publication No.33, "Ultimate Limit State Calculation of Sway Frames with Rigid Joints", April 1984.